TRANSITION METAL CARBONYL CLUSTERS INCORPORATING SILICON

A thesis submitted to
the University of Waikato
for the degree of
Doctor of Philosophy

by

MARTIN LAMBERTUS VAN TIEL

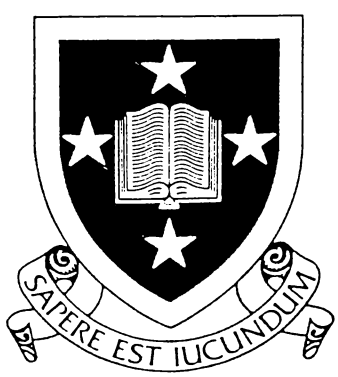

UNIVERSITY OF WAIKATO
1991

ABSTRACT

This thesis reports the reactions of silicon hydrides with the following metal carbonyls; $Fe(CO)_5$, $Fe_2(CO)_9$, $Co_2(CO)_8$ and $Co_4(CO)_{12}$. The silicon hydrides investigated include SiH_4, Si_2H_6, $PhSiH_3$, $BrSiH_3$, $ISiH_3$, $H_3SiOSiH_3$ and $H_3SiSSiH_3$.

The reaction of Si_2H_6 with $Co_2(CO)_8$ at low reactant ratios (1 : 2.5) gave the cluster $H_2Si_3Co_6(CO)_{20}$ (3.7). This is a rare example of a silicon-transition metal cluster with Si-H bonds. The structure can be regarded as $Si[Co_2(CO)_6(\mu\text{-}CO)]_2$ with both bridging carbonyls replaced by μ-Si(H)$Co(CO)_4$ groups. Further infrared evidence for the previously postulated cluster $Si_2Co_6(CO)_{20}$ was also obtained.

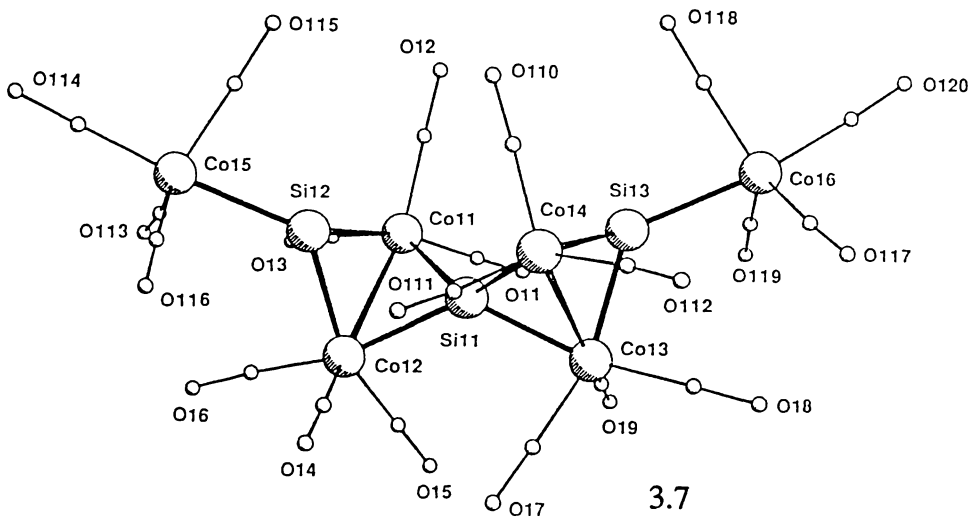

3.7

In attempts to crystallise an unknown product from the reaction of SiH_4 with $Fe(CO)_5$ and $Co_2(CO)_8$ using THF, ionic products were formed. $[FeCo_3(CO)_{12}]^-$ was isolated with $[Fe(THF)_4(H_2O)_2]^{2+}$ as the counter ion. The structure adopted by $[FeCo_3(CO)_{12}]^-$ is very similar to that found for the neutral carbonyl, $Co_4(CO)_{12}$.

$[Cp(CO)_2FeGe]_2Fe_3(CO)_9$ (3.19) was prepared for NMR and crystallographic studies for comparison with the previously reported silicon and tin analogues.

The reaction of $PhSiH_3$ with $Co_4(CO)_{12}$ resulted in the formation of the square-bipyramidal cluster $(PhSi)_2Co_4(CO)_{11}$ (4.6) in high yield. This is compared with the wide range of known $(RP)_2M_4L_x$ (R = phenyl or p-tolyl) clusters.

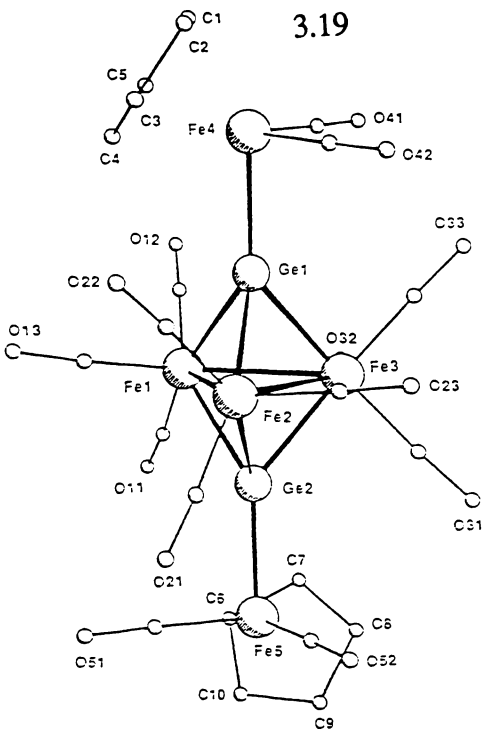

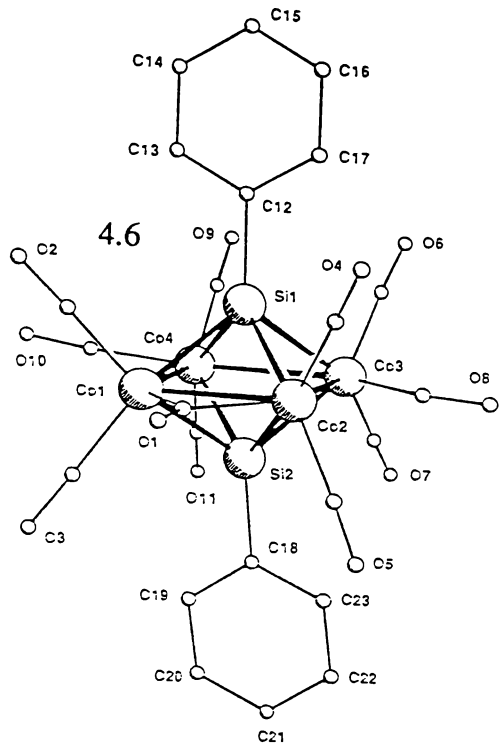

Initial investigation of $BrSiH_3$ with $Co_4(CO)_{12}$ tentatively identified a similar cluster $(BrSi)_2Co_4(CO)_{11}$, which retains a functional halogen group.

The reaction of $BrSiH_3$ or $ISiH_3$ with $Co_2(CO)_8$ shows evidence for the formation of the orange clusters $(CO)_4CoXSiCo_2(CO)_7$ (X = Br, I). These clusters also retain the halogen group via which further substitution could occur.

The reaction of $H_3SiOSiH_3$ with $Co_2(CO)_8$ proved to be very unpredictable. Tentatively identified products include two clusters which retain the Si-O-Si linkage, $O\{[Si[Co(CO)_4]Co_2(CO)_7\}_2$ and $O[SiCo_3(CO)_9]_2$. Reaction of the sulphur analogue $H_3SiSSiH_3$ with $Co_2(CO)_8$ forms the unique cluster $SSi_2Co_4(CO)_{14}$ (5.9). This cluster consists of a $Co_2(CO)_6$ unit doubly bridged by $SiCo(CO)_4$ groups. Both silicon atoms are further linked together with a sulphur atom giving rise to a very acute Si-S-Si angle of 70.3(1)°. The reaction of the analogous hydride $H_3GeSGeH_3$, with $Co_2(CO)_8$ shows no formation of a similar product.

At higher temperatures the reaction of $H_3SiSSiH_3$ with $Co_2(CO)_8$ forms the previously reported cluster $S_2Co_4(CO)_{10}$ (5.16) which consists of a rectangular cobalt plane with sulphur atoms quadruply bridging both faces. An accurate structural determination of this cluster allows for a detailed discussion.

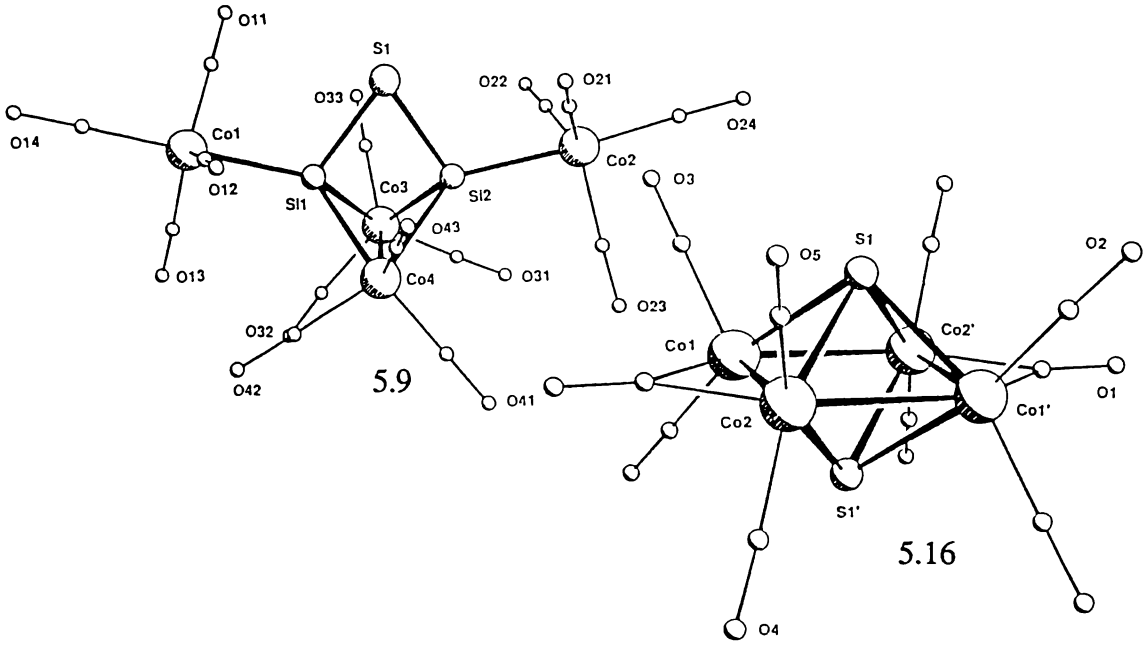

The reactions of various silicon chlorides ($SiCl_4$, Si_2Cl_6 and $Cl_3SiOSiCl_3$) with $[Co(CO)_4]^-$ were investigated. With $SiCl_4$, initial formation of the siloxy cluster $Cl_3Si\text{-}O\text{-}CCo_3(CO)_9$ was observed and further substitution resulted in the formation of $(CO)_4Co(Cl)_2SiOCCo_3(CO)_9$ (6.4, characterised crystallographically). In attempts to furthur substitute the remaining chlorine atoms the carbido cluster $[Co_6C(CO)_{15}]^{2-}$ (6.9) was formed and the structure of the $[Et_4N]^+$ salt was determined.

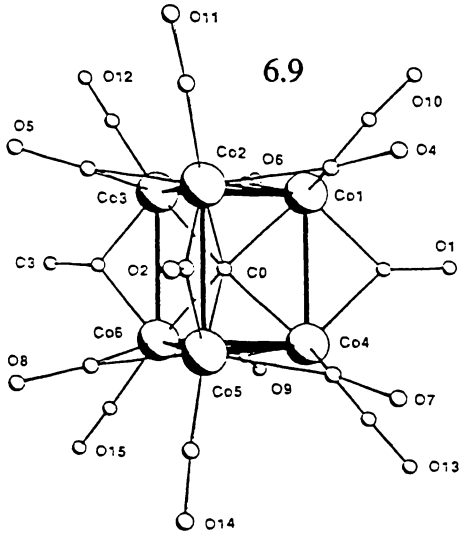

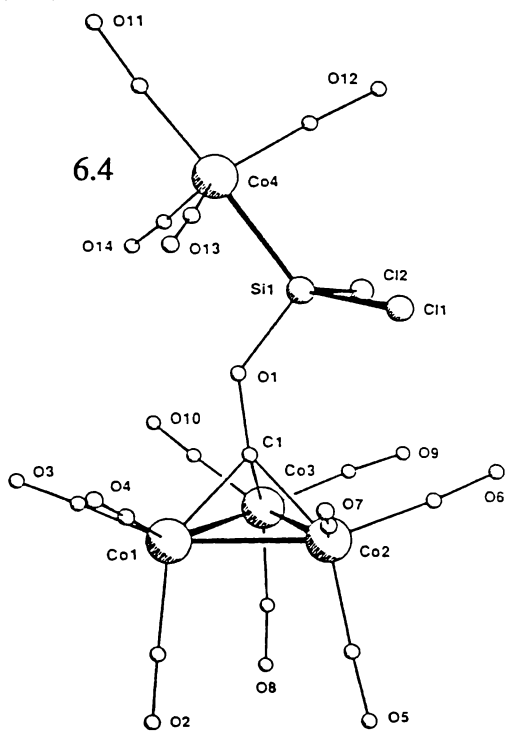

ACKNOWLEDGEMENTS

I would like to thank all the staff and students of the chemistry department for their cooperation, assistance and support during the course of this work. In particular I wish to thank the following people:

My supervisors Prof. Ken Mackay and Assoc. Prof. Brian Nicholson for their invaluable advice and encouragement.

Prof Ward T. Robinson for collecting X-ray diffraction intensity data at the University of Canterbury.

Dr Chris Adams for obtaining FABS mass spectra at the University of Adelaide.

Dr R. Thomson for obtaining NMR data.

Jannine Sims for assistance with infrared spectroscopy.

My work-mates, Dr Skelte Anema for his advice and assistance,

Les Arnold for proof reading, distractions and advice on computer matters.

I would especially like to thank Debbie Golledge for her continual encouragement and help in preparing this thesis.

Finally I would like to thank my parents and friends who have supported me through these years.

TABLE OF CONTENTS

CHAPTER TWO

EXPERIMENTAL TECHNIQUES

CHAPTER THREE

REACTIONS OF SiH_4, Si_2H_6 AND GeH_4 WITH IRON AND COBALT CARBONYL COMPOUNDS

CHAPTER FIVE

REACTIONS OF $H_3SiOSiH_3$ AND $H_3SiSSiH_3$ WITH $Co_2(CO)_8$

LIST OF FIGURES

CHAPTER ONE

CHAPTER TWO

CHAPTER THREE

CHAPTER FOUR

CHAPTER FIVE

CHAPTER SIX

LIST OF TABLES

CHAPTER ONE

CHAPTER TWO

CHAPTER THREE

CHAPTER FOUR

CHAPTER FIVE

CHAPTER SIX

ABBREVIATIONS

The following abbreviations are used in this thesis:

E	Main Group Atom
M	Transition Metal Atom
L	Ligand
R	Organic Substituent - alkyl or aryl
X	Halogen
Me	Methyl
Et	Ethyl
Bu	Butyl
Cp	Cyclopentadienyl
Ph	Phenyl
Tol	Tolyl
Cy	Cyclohexyl
dppm	Bis(diphenylphosphino)methane
acac	Acetylacetonate
THF	Tetrahydrofuran
Int	Intensity

Abbreviations used for Infrared Spectroscopy

v	very
s	strong
m	medium
w	weak
br	broad
sh	shoulder

CHAPTER ONE

CHEMISTRY OF TRANSITION METAL CLUSTERS INCORPORATING SILICON

CHEMISTRY OF TRANSITION METAL CLUSTERS INCORPORATING SILICON

1.1 INTRODUCTION

The chemistry of metal carbonyl clusters has rapidly developed into an interesting and exciting field of organometallic chemistry with the many varied structural forms that these clusters have adopted; further general information and reviews are given in references [1-6, 10, 23]. The following section is a review of the clusters so far reported which contain both silicon and transition metals.

Twenty years ago the first silicon-transition-metal clusters were reported, $(Ph_2Si)Re_2(CO)_8H_2$ [11] and $((CO)_4Co)PhSiCo_2(CO)_7$ [12], these were the precursors of an ever-expanding list. The use of X-ray crystal structure determination has become the major technique for the full identification of these clusters.

The silicon-transition-metal clusters discussed in this review are defined as having at least one metal-metal bond and at least one silicon atom directly linked to two or more metal atoms.

1.2 PREPARATIVE ROUTES TO SILICON-TRANSITION-METAL CLUSTERS

Three general preparative routes to silicon-transition-metal clusters have been employed. These are salt-elimination, silicon-hydride reaction and condensation by heat or UV irradiation with the latter two the more important.

1.2.1 SALT-ELIMINATION METHOD

This method makes use of the easily formed transition-metal anions, such as $[Co(CO)_4]^-$, $[Mn(CO)_5]^-$ and $[Fe(CO)_4]^{2-}$, reacting with a silicon halide. This method is not generally applicable to clusters but is an important route to the simpler compounds.

$$H_2SiI_2 + 2[Co(CO)_4]^- \rightarrow H_2Si[Co(CO)_4]_2 + 2I^-$$

Solvents like THF and diethylether can cause problems due to the promotion of electrophilic attack by the silicon compound on the oxygen atoms of coordinated carbonyl groups. This leads to the formation of Si-O bonded products. For example, $SiCl_4$ with $[Co(CO)_4]^-$ in diethylether solvent forms the siloxy compound $Cl_3SiOCCo_3(CO)_9$ {1} [56] in preference to any Si-Co species. With THF as the solvent, cleavage of the THF occurs to form products such as $HO(CH_2)_4CCo_3(CO)_9$. Differences in the organic or halogen substituents on the silicon atom can result in different products and a change in reaction rates (generally iodide reacts faster than the chloride).

The largest cluster directly prepared by the salt-elimination route is $(CO)_4CoSiCo_3(CO)_9$ {2}. This was prepared by Schmid and Etzrodt [46] from the reaction of SiI_4 with $[Co(CO)_4]^-$ at 50°C with n-hexane as the solvent under UV irradiation.

$$SiI_4 + 4[Co(CO)_4]^- \rightarrow (CO)4CoSiCo_3(CO)_9 + 4I^- + 3CO$$

1.2.2 REACTION OF A SILICON HYDRIDE

This preparation involves the reaction of a silicon hydride and a transition-metal carbonyl with the evolution of H_2 and CO gases. The reactions are conducted in a solvent such as hexane or benzene in sealed vessels for volatile

hydrides such as SiH_4 and Si_2H_6. Schlenk flasks or quick-fit stoppered vessels can be used for hydrides which have low volatility such as Ph_2SiH_2. The reactions involving $Co_2(CO)_8$ proceed very readily at or below room temperature, other carbonyls such as $Co_4(CO)_{12}$ may require gently heating. The equation below shows the product from the reaction of Ph_2SiH_2 with $Co_2(CO)_8$ [20, 27] at room temperature.

$$\mathbf{Ph_2SiH_2 + Co_2(CO)_8 \rightarrow Ph_2SiCo_2(CO)_7 + H_2 + CO}$$

Other metal-carbonyl derivatives such as $Fe(CO)_5$, $Fe_2(CO)_9$ and $Ru_3(CO)_{12}$ sometimes require heating to temperatures of 150°C for several hours or irradiation with UV light. Equations below are typical examples, SiH_4 with $Fe(CO)_5$ [32] and HSi_2Me_5 with $Ru_3(CO)_{12}$ [16, 19].

$$\mathbf{SiH_4 + 4Fe(CO)_5 \rightarrow Si[Fe_2(CO)_8]_2 + 2H_2 + 4CO}$$

$$\mathbf{HSi_2Me_5 + Ru_3(CO)_{12} \rightarrow (Me_2Si)_2[RuSiMe_3(CO)_3]_2 + H_2 + CO}$$

Under some reaction conditions silicon-oxygen species are formed due to attack on silicon by oxygen of coordinated carbonyl groups. For example, when excess $Co_2(CO)_8$ is reacted with Ph_2SiH_2 the siloxy cluster $[(CO)_4Co]Ph_2SiOCCo_3(CO)_9$ {1} [84] is formed. Extreme conditions decompose the cluster to the metal or metalsilicide, CO and organic material if present.

$$\mathbf{Ph_2SiCo_2(CO)_7 + Co_2(CO)_8 \rightarrow [(CO)_4Co]Ph_2SiOCCo_3(CO)_9 + CO}$$

A large number of silicon hydrides are readily available so this method has been widely used in this present work.

1.2.3 CONDENSATION BY HEAT OR UV IRRADIATION

The use of heat or irradiation by UV light on silicon-metal compounds can result in a rearrangement to clusters with an increased number of metal-metal bonds, generally with the loss of carbon monoxide. These condensations are generally reversible by addition of carbon monoxide under high pressure. Due to the smaller size of silicon compared to Ge, Sn and Pb condensation type reactions occur more readily. Cobalt carbonyl derivatives undergo condensation from a number of $Co(CO)_4$ units to $Co_2(CO)_7$ and/or to $Co_3(CO)_9$ clusters under relatively mild conditions. The loss of one carbon monoxide ligand can result in a spectacular rearrangement into a new cluster, equations below (see section 1.3.4 to 1.3.6).

$$Si[(Co_2(CO)_7]_2 \rightarrow (CO)_4CoSiCo_3(CO)_9 + CO$$

$$[(CO)_7Co_2Si]_2Co_2(CO)_6 \rightarrow [(CO)_4CoSi]_2Co_4(CO)_{11} + CO$$

1.3 REPORTED CLUSTERS

The following clusters have been reported and may be classified as in Tables 1.1 to 1.4, 1.6, 1.7 and 1.10.

* denotes those clusters that have been characterised by X-ray crystallography.

1.3.1 ONE R_2Si GROUP BRIDGING ACROSS A METAL-METAL BOND

Compounds with a single silicon atom bridging a metal-metal bond are generally formed by the reaction of the appropriate silicon hydride with a metal carbonyl. The following equations show the products formed by the reaction of the three phenylsilanes with $Co_2(CO)_8$ [1, 13, 20]. Each Si-H is replaced by Si-Co and both the di- and tri- substituted species form compounds in this class (Figure 1.1, R,R'=Ph and R=Ph, R'=$Co(CO)_4$)

$$Ph_3SiH + 0.5Co_2(CO)_8 \rightarrow Ph_3SiCo(CO)_4 + 0.5H_2$$

$$Ph_2SiH_2 + Co_2(CO)_8 \rightarrow Ph_2SiCo_2(CO)_7 + H_2 + CO$$

$$PhSiH_3 + 1.5Co_2(CO)_8 \rightarrow [(CO)_4Co]PhSiCo_2(CO)_7 + 1.5H_2 + CO$$

Other clusters have been synthesised by other methods, for example, $Me_2SiFe_2(CO)_8$ {3} [15] can be synthesised by reacting Me_2SiHCl with $Fe_2(CO)_9$ in the presence of amines to form dark red crystals in 8% yield. The compound $(Ph_2Si)Re_2(CO)_8H_2$ [11] (Figure 1.2) is produced by the ultra-violet irradiation of a solution of $Re_2(CO)_{10}$ and Ph_2SiH_2 in benzene.

Figure 1.1 $R'RSi(Metal)_2$

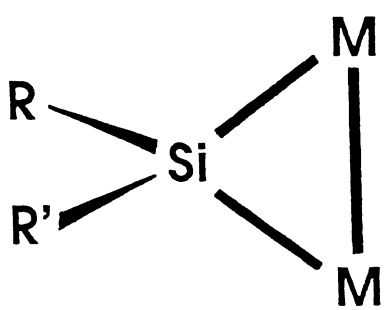

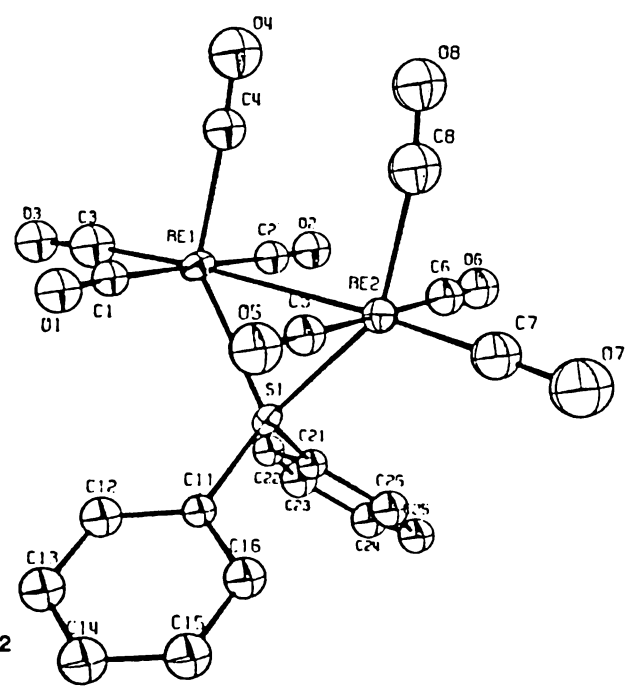

Figure 1.2 $(Ph_2Si)Re_2(CO)_8H_2$

Table 1.1

ONE R_2Si GROUP BRIDGING A METAL-METAL BOND	
COMPOUND	**REFERENCES**
$(Me_2Si)Fe_2(CO)_8$	7, 15
$(Ph_2Si)Fe_2(CO)_3Cp_2$	26
$(MeRSi)Fe_2(CO)_3Cp_2$ R = H, Cl	22
$[t\text{-}Bu(H)Si]Fe_2(CO)_3Cp_2^*$	63
$(R_2Si)Co_2(CO)_7$ R = Me, Et, Ph	20, 27
$(Cl_2Si)Co_2(CO)_7$	13
$[(CO)_4Co]PhSiCo_2(CO)_7$	12
$[(CO)_4Co]MeSiCo_2(CO)_7$	45
$[(CO)_5Mn]ClSiCo_2(CO)_7$	13
$[Cp(CO)_2Fe]RSiCo_2(CO)_7$ R = Me, Ph	79
$[Cp(CO)_3Mo]RSiCo_2(CO)_7$ R = Me, Ph	79
$[Cp(CO)_3W]RSiCo_2(CO)_7$ R = Me, Ph	79
$Me[trans\text{-}W(CO)_2(PMe_3)Cp]SiCo_2(CO)_7$	80
$cyclo\text{-}(CH_2SiMe_2)_2CH_2SiCo_2(CO)_7$	31
$(RHSi)Rh_2H_2(CO)_2(dppm)_2$ R = Ph, Et	64
$(Ph_2Si)Re_2(CO)_8H_2^*$	11
$[Me_2SiOs(CO)_3]_3$	10, 16
$(Me_2Si)Pt_2[P(cyclohexyl)_3]_2(C{\equiv}CPh)_2^*$	21

UV irradiation of $t\text{-}BuSiH_3$ with $CpFe(CO)_2SiMe_3$ in pentane produced red crystals of $Cp_2Fe_2(CO)_3SiH(t\text{-}Bu)$ [63] (Figure 1.3) in 61% yield. The crystal structure revealed the silicon group bridging an Fe-Fe bond. Two cyclopentadienyl groups are mutually *cis* and this is considered the only isomer due to the constraints imposed by attempting to place the bulky Cp and t-Bu groups on the same side of the Fe_2Si plane. The Fe-Fe distance is 2.614(1)Å which is significantly longer than that found in $Cp_2Fe_2(CO)_4$ (2.531(2)Å) [69] but

slightly shorter than that of $Cp_2Fe_2(CO)_3GeMe_2$ [70] at 2.628(1)Å. This is attributable to the size of the bridging atoms. The Fe-Si bond lengths of 2.270(1)Å and 2.272(1)Å and the Si-H bond length (1.39(4)Å) are normal.

The crystal structure of $(Ph_2Si)Re_2(CO)_8H_2$ [11] shows that the silicon atom symmetrically bridges the Re-Re bond (3.121(2)Å) with a Si-Re distance of 2.544(9)Å. The carbonyl groups are eclipsed and occupy octahedral positions about the rhenium atoms with a vacant site for the hydrogen ligand. These two hydrogen ligands as indicated by the mass spectrum are assumed to be bridging the Si-Re bonds and to lie in the ReReSi plane.

Only one silicon bridged platinum compound has been reported, $Me_2SiPt_2[P(cyclohexyl)_3]_2(C{\equiv}CPh)_2$ [21] (Figure 1.4). This was prepared from the reaction of $Si(C{\equiv}CPh)_2Me_2$ with the platinum complex $Pt(C_2H_4)_2[P(C_6H_{11})_3]$ in petroleum spirit at room temperature and involves the cleavage of a silicon-carbon bond. The crystal structure shows that the $SiMe_2$ group asymmetrically bridges the Pt-Pt bond (2.703(1)Å) at distances of 2.255(4)Å and 2.444(4)Å.

The reaction of Me_5Si_2H with the hydride $Os(CO)_4H_2$ forms a six-membered heterocyclic ring complex $[Me_2SiOs(CO)_3]_3$ [10, 16]. This probably contains three $SiOs_2$ triangular units by comparison with the germanium analogues involving ruthenium and osmium carbonyls [10, 57, 58, 59]. The structure of $[Me_2GeRu(CO)_3]_3$ [152] (Figure 1.5) has been established by X-ray crystallography and shows the symmetric arrangement of the three bridging Me_2Ge units around a triangular ruthenium core.

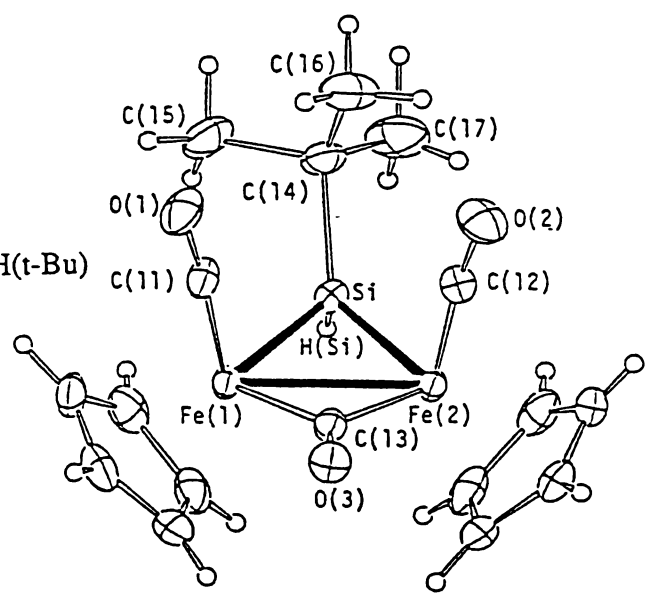

Figure 1.3 $Cp_2Fe_2(CO)_3SiH(t\text{-}Bu)$

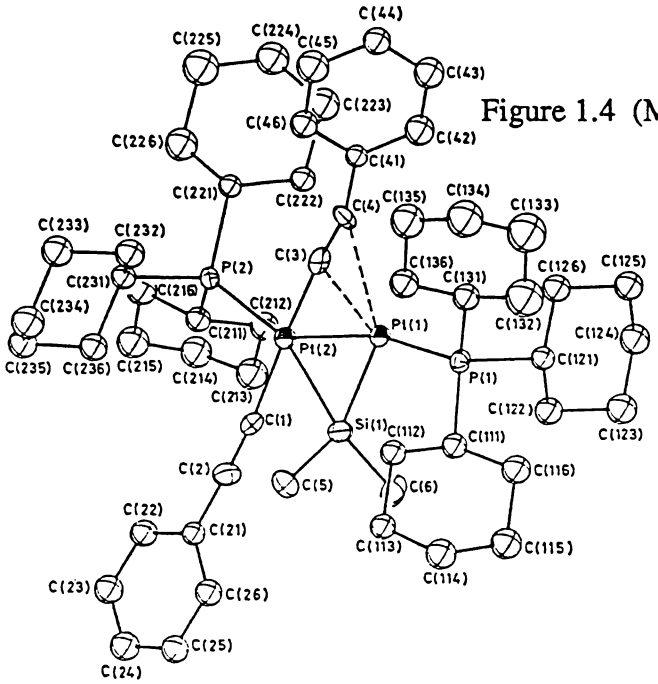

Figure 1.4 $(Me_2Si)Pt_2[P(cyclohexyl)_3]_2(C{\equiv}CPh)_2$

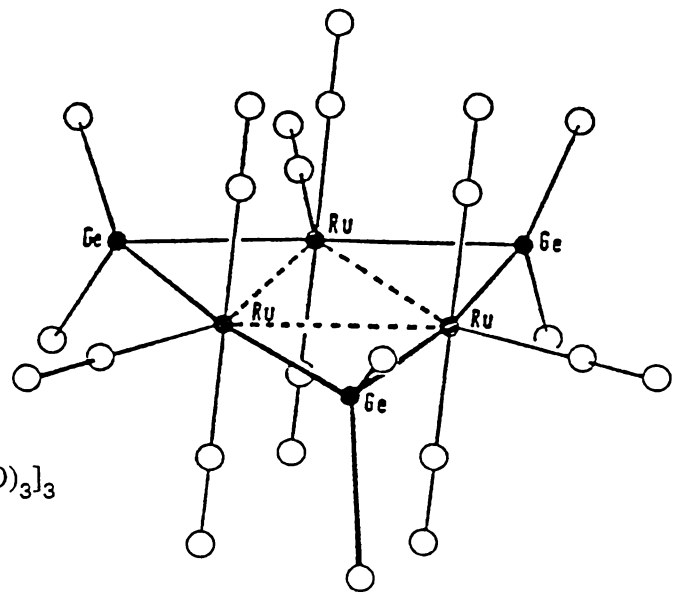

Figure 1.5 $[Me_2GeRu(CO)_3]_3$

1.3.2 TWO R_2Si GROUPS BRIDGING A METAL-METAL BOND

Clusters incorporating two silicon groups bridging the same metal-metal bond {4} are known for the elements Mn, Fe, Co, Ru, W, Re and Os. These clusters are generally formed by reacting the appropriate hydride with a metal carbonyl.

$$Me_2HSiSiHMe_2 + Fe(CO)_5 \rightarrow (Me_2Si)_2Fe_2(CO)_7 \text{ [28]}$$

$$Me_2HSiSiHMe_2 + Fe_2(CO)_9 \rightarrow (Me_2Si)_2Fe_2(CO)_7 \text{ [27]}$$

Table 1.2

TWO R_2Si GROUPS BRIDGING A METAL-METAL BOND	
COMPOUND	**REFERENCES**
$(Ph_2Si)_2Mn_2(CO)_8$	24
$(Me_2Si)_2Fe_2(CO)_7$	10, 27, 28, 29
$(ClMeSi)_2Fe_2(CO)_7$	29
$(Cl_2Si)_2Fe_2(CO)_7$	30
$(EtHSi)_2Fe_2(CO)_7$	36
$(Me_2Si)_2Co_2(CO)_6$	27
$(Me_3Si)_2(Me_2Si)_2Ru_2(CO)_6$ also Os	16, 19
$(PhHSi)_2Rh_2(CO)_2(dppm)_2$	64
$(EtHSi)_2Rh_2(CO)_2(dppm)_2$	64
$(Et_2Si)_2W_2(CO)_8H_2$	14
$(Et_2Si)_2Re_2(CO)_7H_2$	18
$(Et_2Si)_2Re_2(CO)_6H_4$	17
$(Ph_2Si)_2Re_2(CO)_8$	17, 18, 25

The structure of the manganese complex $(Ph_2Si)_2Mn_2(CO)_8$ [24] (Figure 1.6) consists of a Mn_2Si_2 rhombus, bond angles Si-Mn-Si 106.61(6)° and Mn-Si-Mn 73.39(6)°, with crystallographically-imposed planarity. Four terminal carbonyls are arranged octahedrally around each manganese atom. The Mn-Mn bond length of 2.871(2)Å is shorter than that found for $Mn_2(CO)_{10}$ (2.923(3)Å) and the bridging silicon moieties result in the sharply acute Mn-Si-Mn angle.

Derivatives with silicon in both bridging and terminal positions have been prepared from the reaction of the disilane Me_5Si_2H with $Ru_3(CO)_{12}$ or $Os_3(CO)_{12}$ [16, 19] (equation below, Figure 1.7).

$$Me_5Si_2H + Os_3(CO)_{12} \rightarrow [Me_3SiOs(CO)_3SiMe_2]_2$$

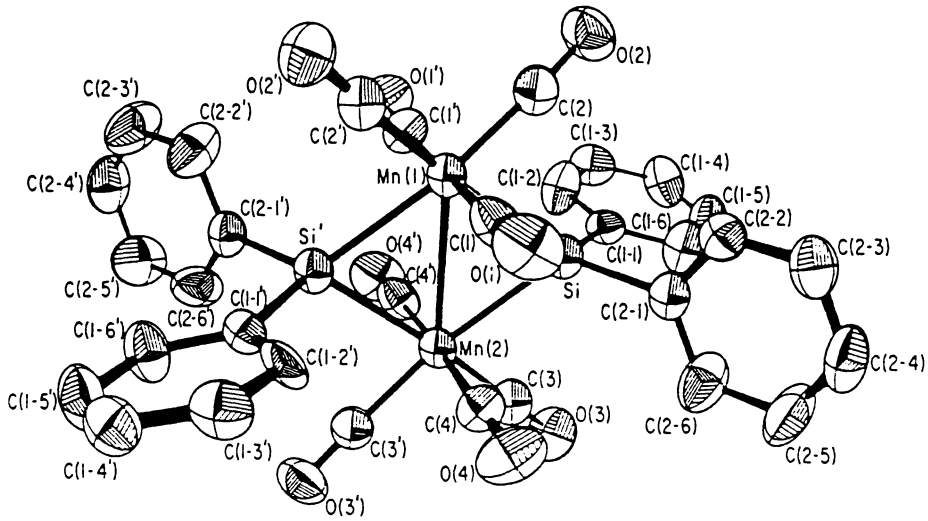

Figure 1.6 $(Ph_2Si)_2Mn_2(CO)_8$

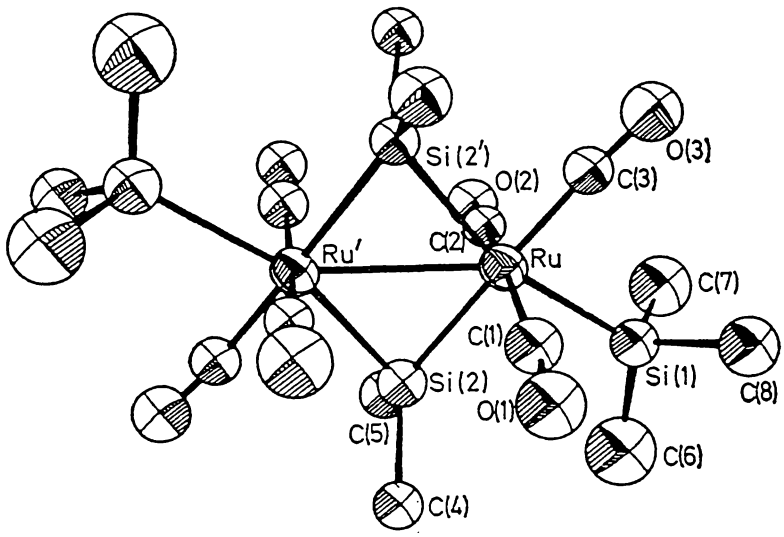

Figure 1.7 $(Me_3Si)_2(Me_2Si)_2Ru_2(CO)_6$

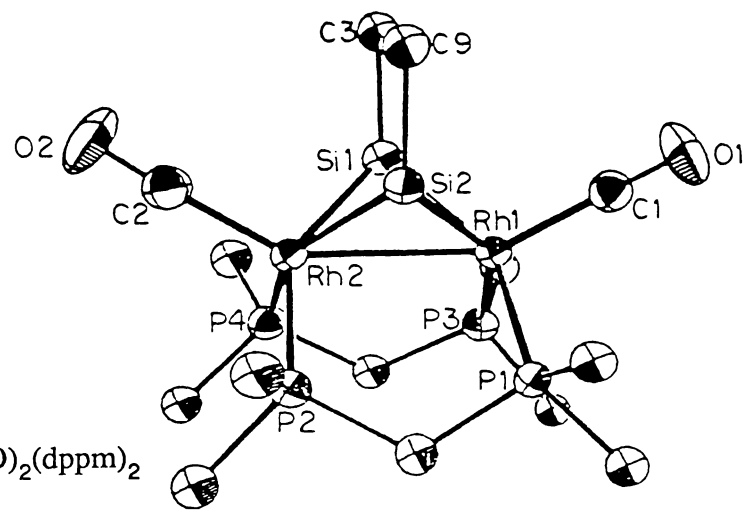

Figure 1.8 $(PhHSi)_2Rh_2(CO)_2(dppm)_2$

The ruthenium complex is obtained in 20% yield and requires UV irradiation for 40 hours, while the osmium analogue was prepared in 9% yield from a reaction at 160°C for 44 hours. The ruthenium complex can also be prepared in 44% yield from the reaction of Me_5Si_2H with $[Me_3SiRu(CO)_4]_2$ [16].

The reactions of $PhSiH_3$ and $EtSiH_3$ with the binuclear complex $Rh_2H_2(CO)_2(dppm)_2$ produces the *bis*μ-SiRH bridged complexes $(RHSi)_2Rh_2(CO)_2(dppm)_2$, (R = Ph, Et), [64]. The phenyl derivative shows a cradle like structure with two μ-SiPhH bridges (Figure 1.8), with an average Si-Rh distance of 2.35(1)Å and Rh-Rh distance of 2.813(1)Å. The Si--Si separation in the structure is 2.75Å which while longer than a Si-Si single bond is substantially shorter than the combined van der Waals radii. Also notable in the structure is the diaxial or *cis* orientation of the phenyl substituents of the silylene ligands.

The molecular structure of $(Et_2Si)_2W_2(CO)_8H_2$ [14] (Figure 1.9) shows that it contains two hydrogen-bridged tungsten-silicon bonds. Evidence for the three-centre W-H-Si bond is seen in two differing W-Si bond lengths 2.586(5)Å and 2.703(4)Å. The longer W-Si bond contains the inserted hydrogen. An acute angle of 74.0(1)° found for W-Si-W is consistent with the complex having a metal-metal bond length of 3.183(1)Å.

In contrast to the above tungsten complex the silicon-bridged rhenium hydride $(Et_2Si)_2Re_2(CO)_7H_2$ [18] (Figure 1.10) shows no hydrogen bridging between the Re-Si bond. The Re_2Si_2 core is in the shape of a rhombus, with bond angles Re-Si-Re 73.6(1)°, Si-Re-Si 106.4(2)° and a Re-Re distance of 3.052(1)Å. This Re-Re single bond distance is comparable to that of $Re_2(CO)_{10}$ at 3.02Å [60], $[Re_4(CO)_{16}]^{2-}$ ranging from 2.956(7) to 3.024(7)Å [61], and the un-bridged Re-Re bond of 3.035(7)Å in $[H_2Re_3(CO)_{12}]^-$ [62]. The four Re-Si distances are essentially identical with an average value of 2.546(5)Å. The two hydride ligands are expected to occupy terminal positions bonded only to the rhenium atoms.

$(Et_2Si)_2Re_2(CO)_6H_4$ [17] (Figure 1.11) is structurally very similar, with all the hydride ligands terminally bonded to the rhenium atoms. The Re-Re

distance is slightly longer at 3.084(1)Å compared to the dihydride above and has two independent Re-Si distances marginally shorter at 2.534(3)Å and 2.536(3)Å. For both of these structures the hydride ligand is considered to be only terminal with very little or no interaction with the Re-Si bond.

$(Ph_2Si)_2Re_2(CO)_8$ [17, 18, 25] shows a much shorter Re-Re distance of 3.001(1)Å compared to 3.121(2)Å for $Ph_2SiRe_2(CO)_8H_2$ [11] due to the presence of two silyl bridges. The Re-Si distances of 2.544(9)Å and 2.542(3)Å are very similar to the analogous distances in $(Et_2Si)_2Re_2(CO)_7H_2$ and $(Et_2Si)_2Re_2(CO)_6H_4$.

Figure 1.9 $(Et_2Si)_2W_2(CO)_8H_2$

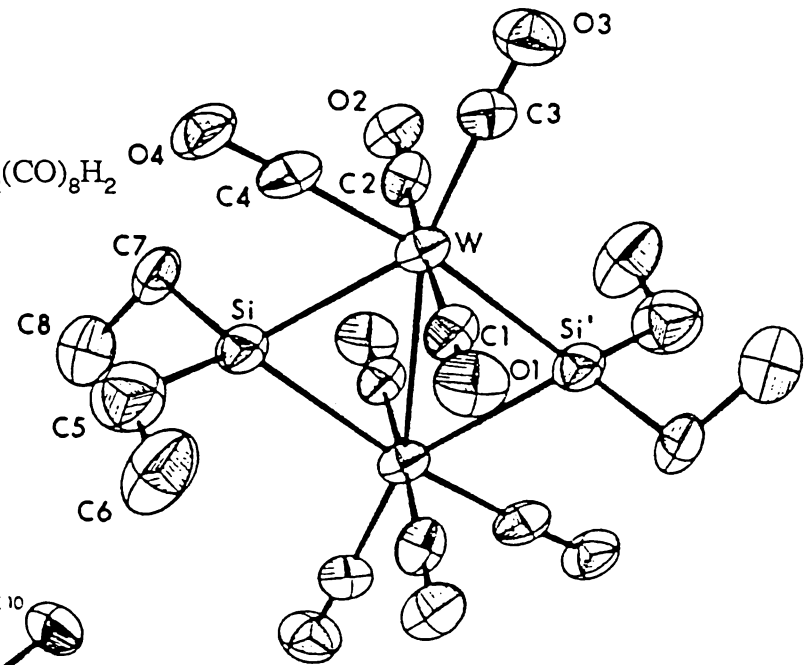

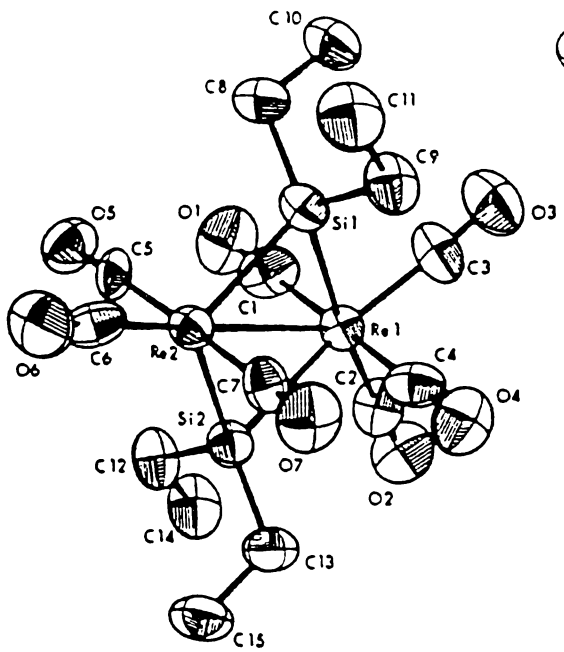

Figure 1.10 $(Et_2Si)_2Re_2(CO)_7H_2$

Figure 1.11 $(Et_2Si)_2Re_2(CO)_6H_4$

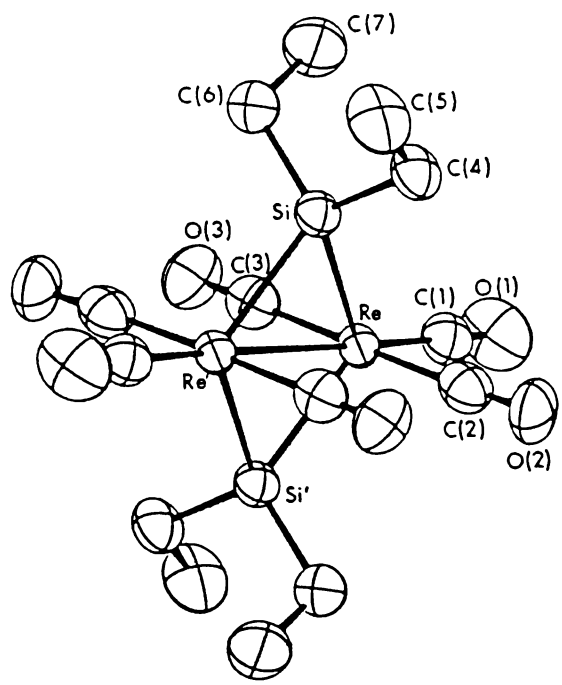

1.3.3 THREE R_2Si GROUPS BRIDGING A METAL-METAL BOND

Clusters which have three silicon groups bridging the same metal-metal bond are known only for iron and ruthenium and are related to the carbonyl compound $Fe_2(CO)_9$ which has three bridging carbonyls. The cluster $(Me_2Si)_3Fe_2(CO)_6$ [10, 36] is not synthesised by replacement of the bridging carbonyls of $Fe_2(CO)_9$ with Me_2Si groups but is synthesised from the reaction of Me_2SiH_2 with $Fe_3(CO)_{12}$. A preliminary crystallographic study showed that the structure of the yellow cluster $(Me_2Si)_3Fe_2(CO)_6$ was isomorphous to that of the germanium analogue.

Table 1.3

THREE R_2Si GROUPS BRIDGING A METAL-METAL BOND	
COMPOUND	**REFERENCES**
$(Me_2Si)_3Fe_2(CO)_6$	10, 36
$(Me_2Si)_3Ru_2(CO)_6$	10, 16

Figure 1.12 $(Me_2Ge)_3Fe_2(CO)_6$

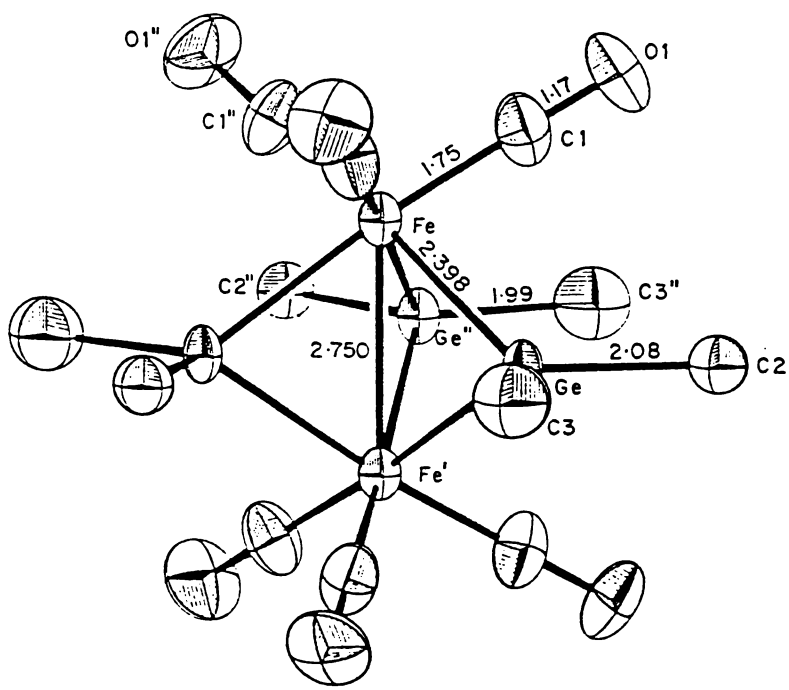

The structure of $(Me_2Ge)_3Fe_2(CO)_6$ [87, 88, 89, 90] (Figure 1.12) consists of three Me_2Ge moieties symmetrically bridging an Fe-Fe bond of length 2.750(11)Å. The three Me_2Ge groups lie on a horizontal mirror plane perpendicular to the threefold axis passing through the iron atoms. The greater size of the bridging Me_2Ge groups have increased the Fe-Fe distance by 0.3Å compared to $Fe_2(CO)_9$ and an acute Fe-Ge-Fe angle of 70.0(2)° is observed.

$(Me_2Si)_3Ru_2(CO)_6$ [10, 16] was prepared by reacting 1,1,2,2-tetramethyldisilane with $[Me_3SiRu(CO)_4]_2$ at room temperature for 12 days to obtain the cluster in 35% yield. The structure is expected to be very similar to that above.

1.3.4 SILICON BRIDGING TWO METAL-METAL BONDS

Table 1.4

SILICON BRIDGING TWO METAL-METAL BONDS	
COMPOUND	**REFERENCES**
$Si[Fe_2(CO)_8]_2^*$	32, 52
$Si[Co_2(CO)_7]_2^*$	43, 47

$Si[Fe_2(CO)_8]_2$ **{5}** [32, 52] is an orange crystalline solid which can be prepared by reacting $Fe_2(CO)_9$ with SiH_4 in hexane at 20°C to 70°C with yields varying from 15 to 70%. $Si[Fe_2(CO)_8]_2$ can also be prepared by reacting $Fe(CO)_5$ with SiH_4 at 140°C giving consistent yields of 40%.

$Si[Co_2(CO)_7]_2$ **{5}** [43, 47] is prepared in high yield from the reaction of SiH_4 with $Co_2(CO)_8$ at room temperature using hexane as the solvent. After 14 days, orange crystals can be isolated.

The structure of $Si[Fe_2(CO)_8]_2$ (Figure 1.13) consists of two mutually perpendicular $SiFe_2$ triangles sharing a silicon atom at the apex. Each iron atom has four terminal carbonyls which results in a compact structure. The Si-Fe bond lengths are all very similar (ave 2.346(4)Å), thus both $SiFe_2$ triangles are

symmetrical. The two $SiFe_2$ triangles are nearly mutually perpendicular with a dihedral angle of 89.4°. The Fe-Fe bond length of 2.793(3)Å is considerably longer than that of $Fe_2(CO)_9$ (2.523(1)Å) due to the absence of bridging carbonyls.

The isoelectronic cluster $Si[Co_2(CO)_7]_2$ (Figure 1.14) is more structurally distorted with fewer carbonyls to accommodate around the central core. There are three terminal carbonyls on each cobalt atom and one carbonyl bridging each Co-Co bond. The $SiCo_2$ triangles are scalene with Si-Co bond lengths of 2.276(1)Å and 2.301(1)Å. The dihedral angle between the two $SiCo_2$ triangles is 80.92°. The Co-Co bond length of 2.528Å is very similar to that found for $Co_2(CO)_8$ at 2.52Å.

The full range of group 14 clusters of the type $E[Fe_2(CO)_8]_2$ where E = Si [32, 52], Ge [49, 53, 54, 55], Sn [49, 50] and Pb [49, 51] has been characterised showing a general increase in E-Fe and Fe-Fe bond lengths as we proceed down Group 14 (Table 1.5). In the case of cobalt clusters of the type $E[Co_2(CO)_7]_2$, only the silicon and germanium clusters are known. Distances found in $Ge[Co_2(CO)_7]_2$ [8] are given in Table 1.5.

Figure 1.13 $Si[Fe_2(CO)_8]_2$

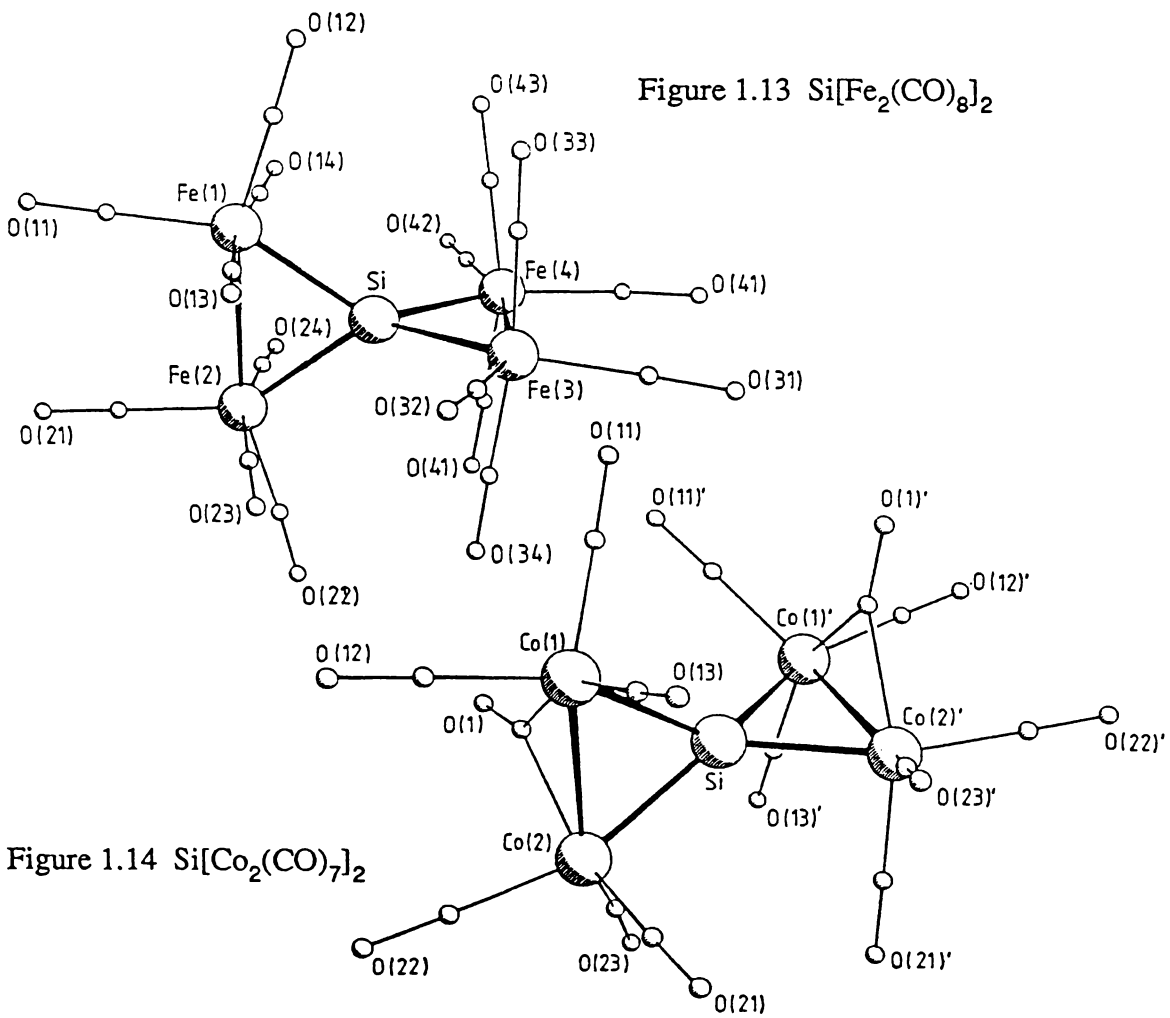

Figure 1.14 $Si[Co_2(CO)_7]_2$

Table 1.5

STRUCTURAL FEATURES OF CLUSTERS WITH A *SPIRO*-EM_4 CORE				
CLUSTER	**E-M(Å) (AVERAGE VALUES)**	**M-M(Å)**	**M-E-M(°)**	**DIHEDRAL ANGLE(°)**
$Si[Fe_2(CO)_8]_2$	2.347	2.792	73	89
$Ge[Fe_2(CO)_8]_2$	2.40	2.825	72	89
$Sn[Fe_2(CO)_8]_2$	2.54	2.87	69	87
$Pb[Fe_2(CO)_8]_2$	2.620	2.901	67	87
$Si[Co_2(CO)_7]_2$	2.288	2.528	67	81
$Ge[Co_2(CO)_7]_2$	2.361	2.56	66	84

1.3.5 SILICON BONDED TO A TRIGONAL METAL CORE

The reaction of $RSiH_3$ (R = Me, Et) with $Fe_3(CO)_{12}$ at 50°C for 14 days resulted in the formation of $(RSi)_2Fe_3(CO)_9$ **{6}** clusters. These compounds were characterised by comparing the infrared spectrum with those of the germanium analogues but further characterisation proved difficult due to decomposition.

A similar reaction using $PhSiH_3$ with $Fe(CO)_5$ at 150°C for two hours gave a product tentatively characterised as $(PhSi)_2Fe_3(CO)_9$. This cluster also decomposed readily so another capping group was needed.

A reaction of SiH_4, $Fe(CO)_5$ and $[Fe(CO)_2Cp]_2$ in petroleum spirit was conducted at 150°C for 90 minutes which resulted in a red complex in 67% yield. This was characterised by IR and X-ray crystal structure analysis as the trigonal-bipyramidal cluster $[Cp(CO)_2FeSi]_2Fe_3(CO)_9$ (Figure 1.15).

Clusters of the type $[Cp(CO)_2FeE]_2Fe_3(CO)_9$ where E = Si [38] and Sn [42] have been characterised by crystal structure analysis and show the trend of

increasing E-Fe and Fe-Fe bond lengths from silicon to tin due to the relative size increase of the atom.

Table 1.6

SILICON BONDED TO A TRIGONAL METAL CORE	
COMPOUND	**REFERENCES**
$(RSi)_2Fe_3(CO)_9$ R = Me, Et, Ph	38
$[Cp(CO)_2FeSi]_2Fe_3(CO)_9$	38
$MeSiCo_3(CO)_9$	33
$PhSiCo_3(CO)_9$	33
$H_2C{=}CHSiCo_3(CO)_9$	33
$(p\text{-Tol})SiCo_3(CO)_9$	33
$(CO)_5MnSiCo_3(CO)_9$	48
$Cp(CO)_2FeSiCo_3(CO)_9$	44
$(CO)_4CoSiCo_3(CO)_9$	23, 46, 100, 109
$MeSiIr_3(CO)_9$	65

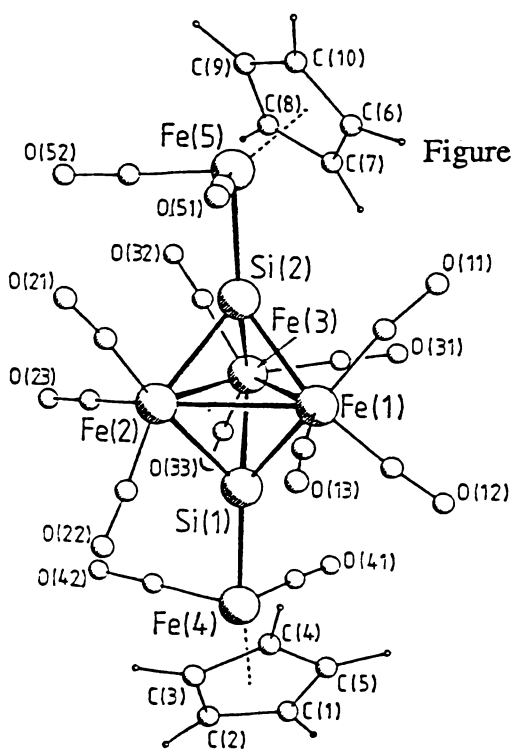

Figure 1.15 $[Cp(CO)_2FeSi]_2Fe_3(CO)_9$

The dark purple cluster $(CO)_4CoSiCo_3(CO)_9$ {2} was initially prepared in low yield by the reaction of SiI_4 with $[Co(CO)_4]^-$ in hexane [46]. A more convenient and high yielding preparation involves the reaction of SiH_4 with $Co_2(CO)_8$ at 50°C in hexane. Decarbonlyation of $Si[Co_2(CO)_7]_2$ at 50°C results in the formation of $(CO)_4CoSiCo_3(CO)_9$ in nearly quantitative yield.

$$Si[Co_2(CO)_7]_2 \rightarrow (CO)_4CoSiCo_3(CO)_9 + CO$$

The structure of $(CO)_4CoSiCo_3(CO)_9$ (Figure 1.16) consists of a pseudo-tetrahedrally coordinated silicon atom symmetrically capping the Co_3 triangular face. Si-Co bond lengths to the triangular face are short (2.218(1)Å) compared to 2.288(1)Å for the terminal Si-Co bond length. All the carbonyls are terminally bonded, four to the capping cobalt and three each to the triangular cobalt framework. The $RSiCo_3(CO)_9$ (R = Me, Ph, p-Tol, H_2C=CH) species show the same $SiCo_3$ unit.

The iridium cluster $MeSiIr_3(CO)_9$ {2} [65] was synthesised in 6% yield from the reaction of $Na[Ir(CO)_4]$ with Cl_3SiMe in THF. Comparison of the infrared spectrum in the carbonyl region matched closely those of the structurally well established methylidyne clusters $RCCo_3(CO)_9$ [66].

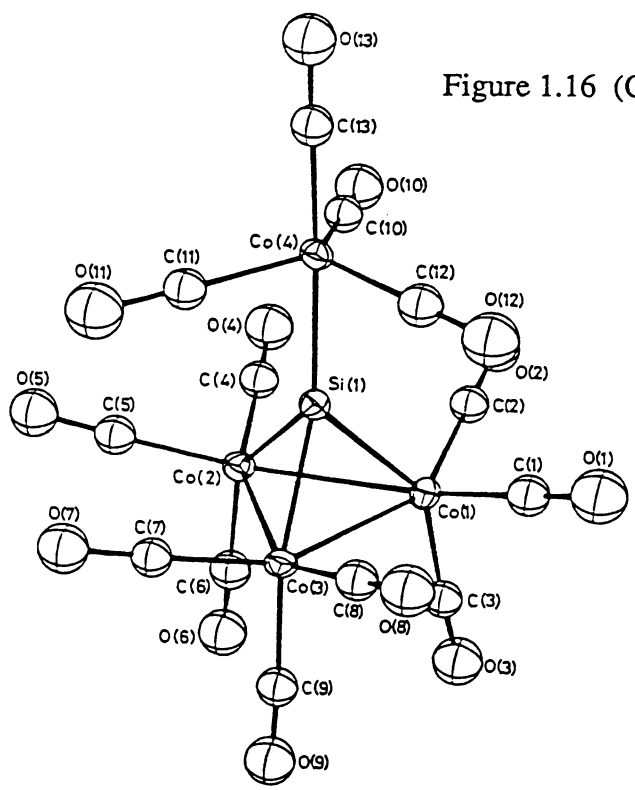

Figure 1.16 $(CO)_4CoSiCo_3(CO)_9$

1.3.6 SILICON BONDED TO A QUADRILATERAL METAL CORE

The reaction of Ge_2H_6 with $Co_2(CO)_8$ resulted in a square-bipyramidal cluster $[(CO)_4CoGe]_2Co_4(CO)_{11}$ {7} [71]. A similar reaction utilising Si_2H_6 gave similar products in which the analogous silicon cluster $[(CO)_4CoSi]_2Co_4(CO)_{11}$ [35, 45] (Figure 1.17) was synthesised. $[(CO)_4CoSi]_2Co_4(CO)_{11}$ is formed slowly at room temperature whereas the germanium equivalent requires gentle heating of the initially formed cluster $Ge_2Co_6(CO)_{20}$ {8} at 40 - 50°C. This is mainly due to the smaller size of the silicon preferring a more clustered type arrangement. There is infrared evidence for the initial formation of $[(CO)_7Co_2Si]_2Co_2(CO)_6$ {8}, which undergoes a *spiro*-cyclic rearrangement to form the cluster (see equation below for the germanium case).

$$[(CO)_7Co_2Ge]_2Co_2(CO)_6 + \text{heat} \rightarrow [(CO)_4CoGe]_2Co_4(CO)_{11} + CO$$

Table 1.7

SILICON BONDED TO A QUADRILATERAL METAL CORE	
COMPOUND	**REFERENCES**
$(MeSi)_2Co_4(CO)_{11}$*	36
$[(CO)_4CoSi]Co_4(CO)_{11}(SiMe)$*	37
$[(CO)_4CoSi]Co_4(CO)_{11}(GeR)$ R = Me, Et*	37
$[(CO)_4CoSi]_2Co_4(CO)_{11}$*	35
$(MeSi)_2Co_4(CO)_{10}(GeMe_2)$*	36

Clusters of the type $(RSi)_2Co_4(CO)_{11}$ {7} where R = Me or Et can be easily prepared from the reaction of $RSiH_3$ with $Co_4(CO)_{12}$ in hexane at 40 - 50°C.

$$RSiH_3 + Co_4(CO)_{12} \rightarrow (RSi)_2Co_4(CO)_{11} + 3H_2 + CO$$

The reaction of Me_2GeH_2 with $(MeSi)_2Co_4(CO)_{11}$ at room temperature replaces the bridging carbonyl on the cluster with a bridging Me_2Ge group to form $(MeSi)_2Co_4(CO)_{10}(GeMe_2)$ in 94% yield.

The metal core structure of the $[(CO)_4CoSi]_2Co_4(CO)_{11}$ (Figure 1.17) cluster consists of two silicon atoms quadruply bridging a distorted square-planar array of cobalt atoms with each silicon further bonded to a terminal $Co(CO)_4$ unit.

Of the 11 carbonyl ligands on the cluster core eight are distributed as purely terminal, two to each cobalt atom. The remaining three are distributed to give one unsymmetrical bridging carbonyl across the Co(1)-Co(4) bond with two semi-bridging carbonyls bonded one each to Co(2) and Co(3) facing towards the Co(1)-Co(4) bond. Therefore Co(1) and Co(4) have a total of 2.5 carbonyls with Co(2) and Co(3) having 3. Deviations that result in the semi-bridging carbonyls occur to give an overall even distribution of electrons around the core.

Figure 1.17 $[(CO)_4CoSi]_2Co_4(CO)_{11}$

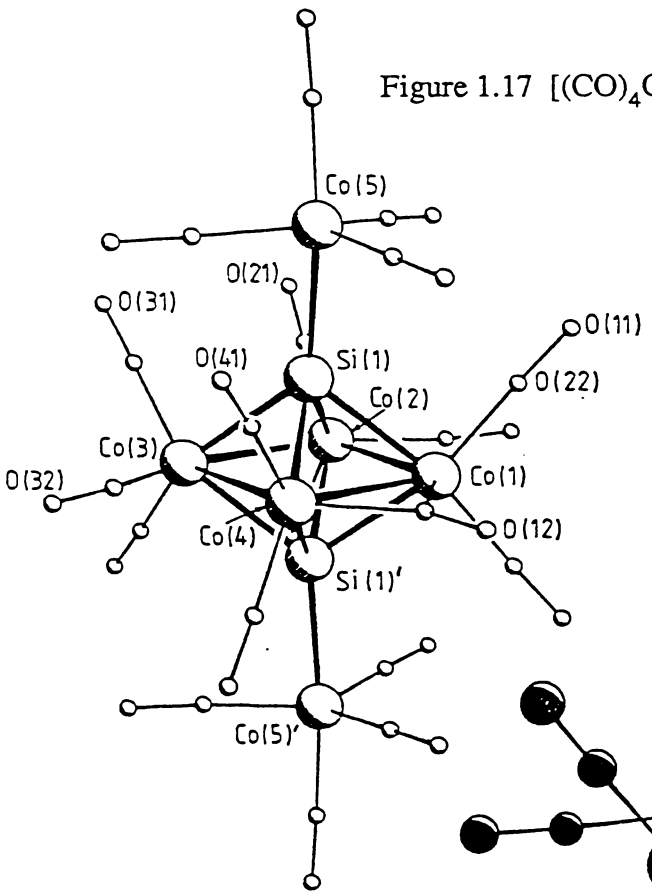

Figure 1.19 $(MeSi)_2Co_4(CO)_{11}$

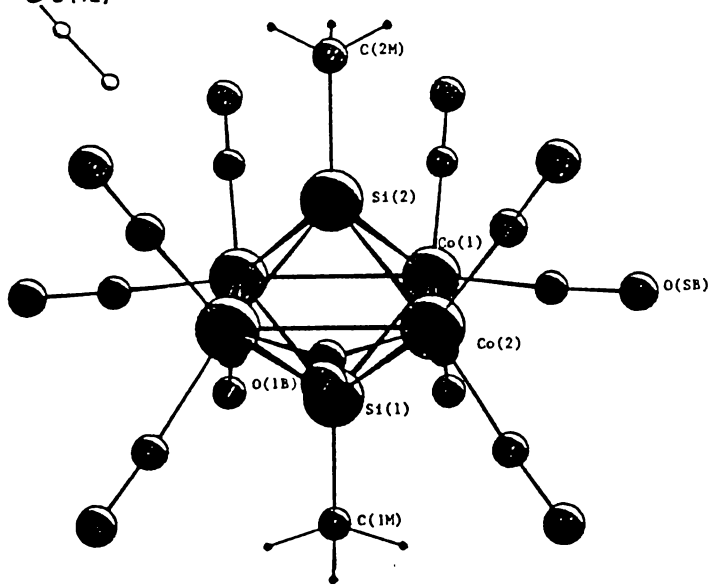

The silicon atom is shifted towards the bridged Co-Co bond (Table 1.8, Figure 1.18) with Si-Co core bond lengths of 2.308(2) and 2.330(2)Å compared to the non-bridged Co-Co with Si-Co lengths of 2.351(2)Å and 2.360(2)Å (Table 1.9). The Si-Co terminal bond length of 2.347(2)Å for this five coordinate silicon cluster is longer than the terminal bond distance of 2.288Å found in the four coordinate silicon cluster $(CO)_4CoSiCo_3(CO)_9$ as expected.

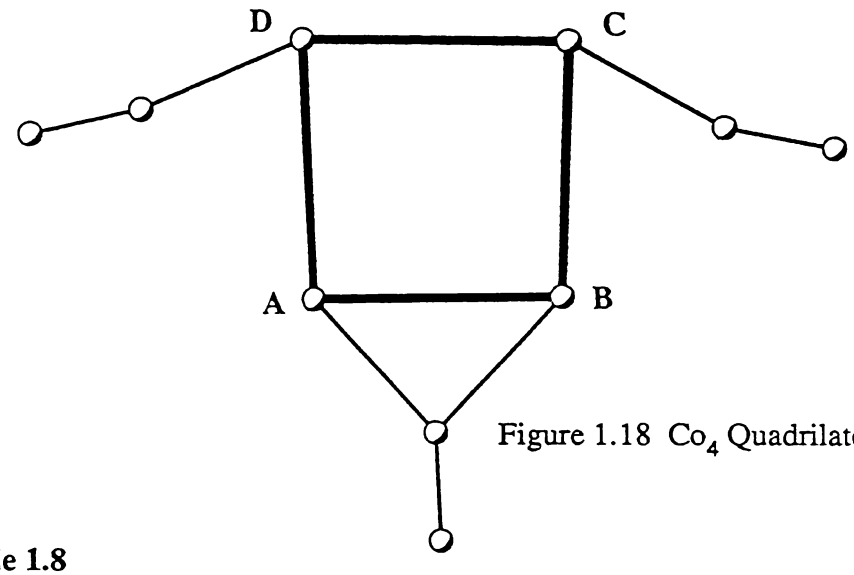

Figure 1.18 Co_4 Quadrilaterial Core

Table 1.8

COBALT-COBALT DISTANCES IN QUADRILATERAL METAL CORE CLUSTERS (Å)				
Cluster	**A - B**	**C - D**	**B - C**	**A - D**
$(MeSi)_2Co_4(CO)_{11}$	2.548	2.690	2.651	2.651
$[(CO)_4CoSi]_2Co_4(CO)_{11}$	2.569	2.653	2.623	2.696
$[(CO)_4CoSi](EtGe)Co_4(CO)_{11}$	2.581	2.697	2.668	2.696
$(MeSi)_2Co_4(CO)_{10}(GeMe_2)$	2.687	2.709	2.593	2.628

The structure of $(MeSi)_2Co_4(CO)_{11}$ (Figure 1.19) is that of a square bipyramid which consists of a quadrilateral plane of four cobalt atoms quadruply bridged on each side by SiMe groups. The quadrilateral plane contains three distinct Co-Co distances due to the degree of carbonyl bridging (Table 1.8). The

shortest Co-Co distance of 2.548(2)Å is fully bridged while the longest Co-Co distance of 2.690(2)Å is non-bridged with the remaining semi-bridged Co-Co bonds at 2.651(1)Å. These bond lengths are significantly shorter than in the isomorphous cluster $(MeGe)_2Co_4(CO)_{11}$ [9] which has distances of 2.580(2)Å, 2.721(2)Å and 2.693(2)Å respectively. These differences are due to the relative change in size between silicon and germanium.

Replacement of the bridging carbonyl greatly affects the Co-Co bond it bridges with a lengthening from 2.548(2)Å in $(MeSi)_2Co_4(CO)_{11}$ to 2.687(1)Å for $(MeSi)_2Co_4(CO)_{10}(GeMe_2)$ (Figure 1.20, Table 1.8). The non-bridged Co-Co distance of 2.709(1)Å is slightly longer compared to the same bond in $(MeSi)_2Co_4(CO)_{11}$ at 2.690(2)Å but the semi-bridged Co-Co bonds are significantly shorter in $(MeSi)_2Co_4(CO)_{10}(GeMe_2)$ at 2.593(1)Å and 2.628(1)Å compared to 2.651(1)Å. Little difference is seen in the Si-Co distances which depend more on the terminal group attached to the silicon.

Table 1.9

SILICON-COBALT DISTANCES IN QUADRILATERAL METAL CORE CLUSTERS (Å)

CLUSTER	Si - A	Si - B	Si - C	Si - D
$(MeSi)_2Co_4(CO)_{11}$	2.303	2.303	2.320	2.320
	2.302	2.302	2.311	2.311
$[(CO)_4CoSi]_2Co_4(CO)_{11}$	2.308	2.330	2.351	2.360
$[(CO)_4CoSi](EtGe)Co_4(CO)_{11}$	2.331	2.345	2.345	2.357
$(MeSi)_2Co_4(CO)_{10}(GeMe_2)$	2.294	2.320	2.301	2.316
	2.284	2.306	2.308	2.318

$[(CO)_4CoSi]Co_4(CO)_{11}(GeEt)$ (Figure 1.21) is the first cobalt cluster to incorporate both silicon and germanium within the same structure. This cluster was synthesised from the 8 month reaction of $EtGeH_3$ with $Si[Co_2(CO)_7]_2$ at room temperature. A large range of products were formed in the reaction, including $(CO)_4CoEtGeCo_2(CO)_7$, $[(CO)_4CoEtGe]_2Co_2(CO)_6$, $(EtGe)_2Co_4(CO)_{11}$ and $(CO)_4CoSiCo_3(CO)_9$ with the above cluster prepared in 16% yield.

The capping $SiCo(CO)_4$ group shows less deviation from the centre of the cobalt square compared to $[(CO)_4CoSi]_2Co_4(CO)_{11}$. Distances (Si-Co, Table 1.9) range from 2.331(2)Å to 2.357(2)Å for $[(CO)_4CoSi]Co_4(CO)_{11}(GeEt)$, compared to 2.308(2)Å through to 2.360(2)Å for $[(CO)_4CoSi]_2Co_4(CO)_{11}$. The Si-Co terminal distance of 2.357(2)Å is longer than that found for $[(CO)_4CoSi]_2Co_4(CO)_{11}$ at 2.347(2)Å.

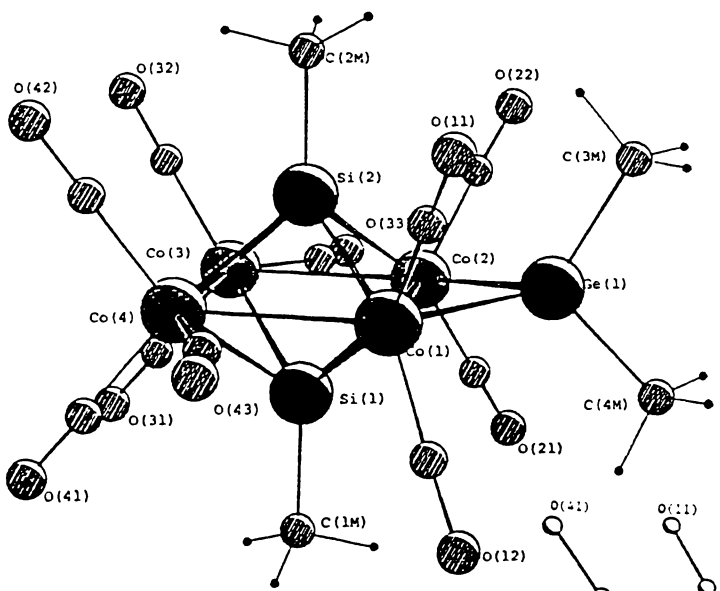

Figure 1.20 $(MeSi)_2Co_4(CO)_{10}(GeMe_2)$

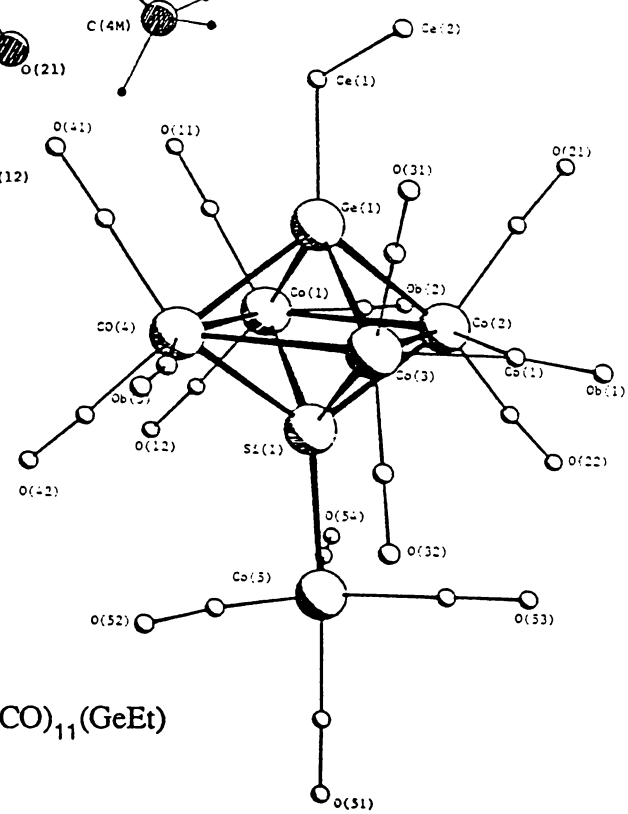

Figure 1.21 $(CO)_4CoSiCo_4(CO)_{11}(GeEt)$

1.3.7 LARGE CLUSTERS WITH ENCAPSULATED SILICON

Only two large clusters encapsulating a silicon atom are known (Table 1.10). The first is a fully encapsulated eight coordinate silicon atom found in the dianion $[\mu_8\text{-}SiCo_9(CO)_{21}]^{2-}$ (Figure 1.22) [34]. This cluster is prepared by the reaction of $Si[Co_2(CO)_7]_2$ with an excess of $[Et_4N][Co(CO)_4]$ at 40°C in CH_2Cl_2. Black crystals of formula $[Et_4N]_3[Co(CO)_4][SiCo_9(CO)_{21}]$, can be obtained in yields as high as 80% [48] which contain both the $[Co(CO)_4]^-$ anion and the $[SiCo_9(CO)_{21}]^{2-}$ dianion.

Table 1.10

LARGE CLUSTERS	
COMPOUND	**REFERENCES**
$[Et_4N]_3[Co(CO)_4][SiCo_9(CO)_{21}]^*$	34
$Cs_{0.3}Zr_6I_{14}Si^*$	67

The dianion, $[SiCo_9(CO)_{21}]^{2-}$, consists of a cage of nine cobalt atoms which structurally define a capped-tetragonal antiprism with the silicon atom occupying the cavity within the square-antiprism. There are 13 terminal carbonyls and 8 asymmetrically bridging, 4 of which occur on the Co-Co bonds of the apical cobalt atom. The apical Co--Si axis is a crystallographic four-fold rotational axis.

The cavity formed by a regular square-antiprism of cobalt atoms (r = 1.35Å) has a calculated radius of 0.85Å, compared to the silicon covalent radius of 1.12Å. This size difference is compensated for by significant expansion of the Co cage, with the Co(3)-Co(3') distance of 2.808(1)Å significantly longer than in other clusters while the Co(2)-Co(2') distance of 2.940(1)Å is exceptionally long. A comparison with the square-antiprismatic core of $[Co_8C(CO)_{18}]^{2-}$ [112] shows that the smaller carbon atom can be accommodated in the cage with Co-Co distances ranging from 2.47 to 2.59Å. Encapsulated P or As atoms in the clusters

$[Rh_9P(CO)_{21}]^{2-}$ [39] and $[Rh_{10}E(CO)_{22}]^{3-}$, E = P, As [113] similarly show significant increase in cage size.

The encapsulated silicon atom is located virtually in the centre of the anti-prism with average Si-Co distances of 2.299(2)Å, the Si-Co(1) distance (to the capping cobalt atom) being much longer at 2.527(4)Å. The overall geometry of $[SiCo_9(CO)_{21}]^{2-}$ is very similar to that of the $[Rh_9P(CO)_{21}]^{2-}$ [39] cluster.

An unusual property of the $[SiCo_9(CO)_{21}]^{2-}$ cluster is that it is paramagnetic having one electron fewer, than the expected 130 valence electrons. The only other paramagnetic clusters of this type $[Co_6C(CO)_{14}]^{-}$ [40] and $[Co_{13}C_2(CO)_{24}]^{4-}$ [41] have one electron in excess of the number expected for their structures.

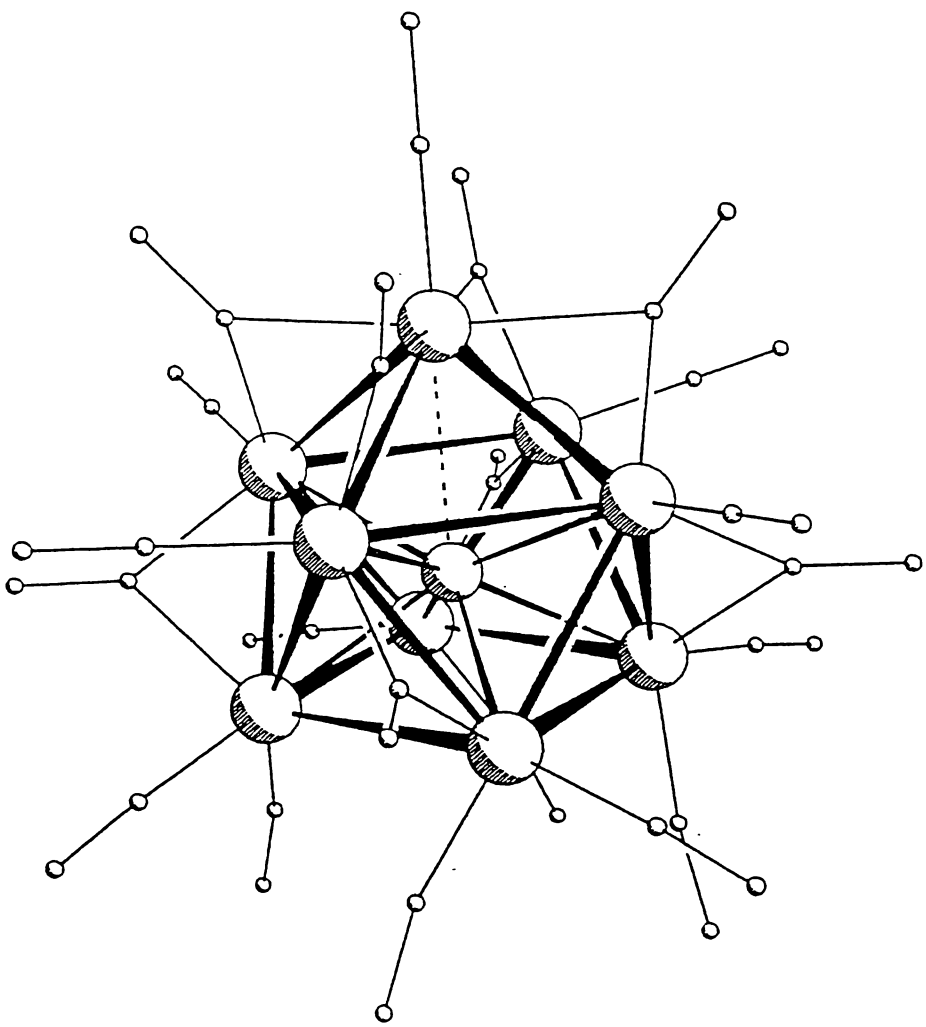

Figure 1.22 $[SiCo_9(CO)_{21}]^{2-}$

The second cluster $Cs_{0.3}Zr_6I_{14}Si$ [67] (Figure 1.23) is markedly different to the other clusters in this survey due to the external ligands consisting only of bridging and terminal iodine atoms, with a high oxidation state metal atom.

$Cs_{0.3}Zr_6I_{14}Si$ was synthesised from the reaction of a two fold excess of CsI and Zr powder with stoichiometric amounts of ZrI_4 and Si which was heated for 2 weeks at 850°C. This resulted in a 30-40% yield of well-faceted black crystals of $Cs_{0.3}Zr_6I_{14}Si$ plus ZrI_3 and $Cs_3Zr_2I_9$ as other products.

The isolated cluster in $Cs_{0.3}Zr_6I_{14}Si$ has the formula $(Zr_6I_{12}Si)I_6$ which consists of a slightly distorted octahedron of zirconium atoms with an interstitial silicon atom. Twelve iodine atoms bridge all the edges with each zirconium atom bonded terminally to one iodine atom. Each cluster is interconnected through shared iodines. The cluster has C_{2h} symmetry with an inversion centre at silicon. The slight distortion can be seen in the Si-Zr bond distances with four distances at 2.548(2)Å and two at 2.498(3)Å. Zr-Zr intralayer distances are (x2) 3.632(4)Å and (x4) 3.562(3)Å with the Zr-Zr interlayer distances (x6) 3.574(4)Å.

A range of interstitial-centered zirconium iodide clusters has been characterised, namely $Zr_6I_{14}C$, $CsZr_6I_{14}C$ and $K_{0.6}Zr_6I_{14}C$ [68], $Cs_{0.6}Zr_6I_{14}P$, $CsZr_6I_{14}B$ and $Cs_{0.7}Zr_6I_{14}Al$ [67].

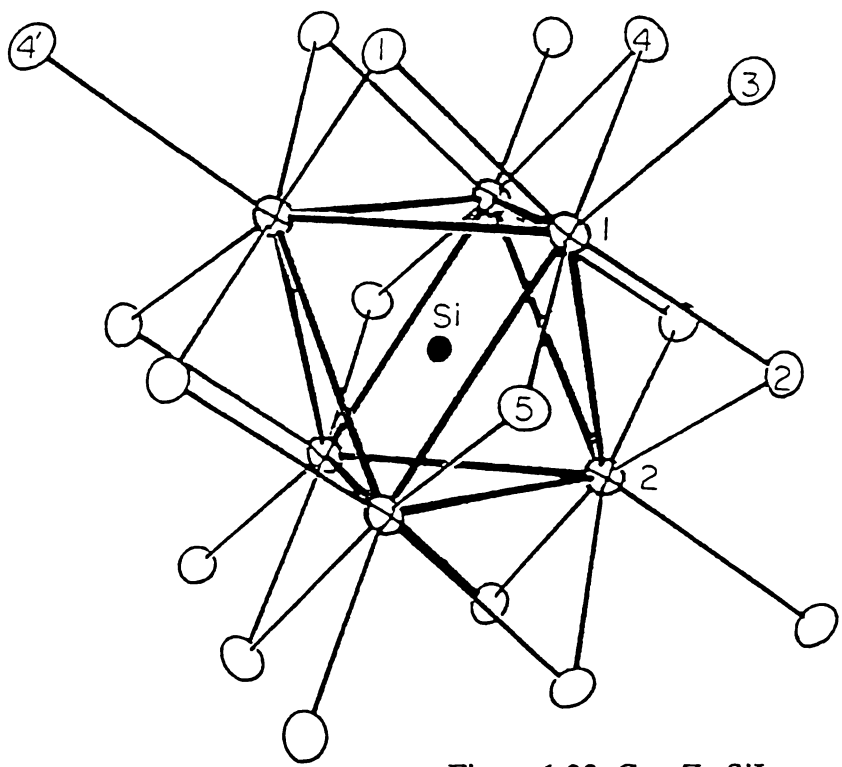

Figure 1.23 $Cs_{0.3}Zr_6SiI_{14}$

CHAPTER TWO

EXPERIMENTAL TECHNIQUES

EXPERIMENTAL TECHNIQUES

2.1 GENERAL EXPERIMENTAL TECHNIQUES

2.1.1 GENERAL MANIPULATIONS

The compounds involved in this work are unstable to varying degrees to thermal decompostion and to reaction with water, oxygen, and polar solvents. Some compounds were stable enough to handle briefly in the air, but generally all work was conducted under vacuum or under a dry nitrogen atmosphere.

All manipulations of volatile compounds were carried out on a conventional glass vacuum line fitted with mercury manometers and greased (Apiezon 'N') taps. Fractionation of the volatile components was conducted using constant temperature slush baths (Table 2.1).

Table 2.1

CONSTANT TEMPERATURE SLUSH BATHS	
CONSTITUENT	**TEMPERATURE (°C)**
Ice/Water	0
Carbon tetrachloride	-22
Chlorobenzene	-45
Chloroform	-63
Ethyl acetate	-83
Toluene	-95
n-Propanol	-127
liquid Nitrogen	-196

Reactions involving volatile gases were conducted in 50 to 200ml sealed high pressure, (8 atm maximum) glass ampoules. These sealed ampoules were opened using a thick-walled rubber tube fitted with a tap adaptor to avoid any contact with the air.

Manipulations of involatile compounds were conducted on a standard Schlenk line and reaction products stored at -25°C. When products could not be obtained pure, yields were estimated by overall weight of that fraction and by comparing species present in the infrared spectrum. Glassware was initially washed in methanolic KOH and then in chromic acid, rinsed with water and dried in an oven before use.

2.1.2 DETERMINATION OF INCONDENSABLE GASES

Incondensable gases at -196°C that are formed in the course of the reaction, generally consist of a mixture of CO and H_2. These were measured using a Toepler pump fitted with a gas burette. The proportions of CO and H_2 were determined by weighing a known pressure and volume of the gas mixture to obtain an average molecular weight. The percentage of each gas could then be calculated using the following equation.

$$\%H_2 = \frac{28 - W}{26} \times \frac{100}{1} \qquad (W = \text{average Mr of gas})$$

The accuracy of the total gas measurement was ±5% The measurement of the percentage of each gas in the sample was less accurate due to the small weight difference especially at low gas pressures, the error was generally ±10 to 20%.

2.2 INSTRUMENTAL TECHNIQUES

2.2.1 INFRARED SPECTROSCOPY

Infrared spectroscopy in the carbonyl stretching region is the major technique used to identify the compounds present. They show a characteristic pattern for each carbonyl-metal complex and can provide some information towards the symmetry of the molecule. The carbonyl region (2150-1800cm^{-1}) is particularly useful due to the high intensity and sharpness of the peaks. Absorptions due to M-C-O bends and M-C stretches occur in the region 1000-300cm^{-1} with medium to weak intensity.

The silicon hydrides show strong Si-H stretches between 2150-2050cm^{-1} and bending modes between 1000-800cm^{-1} with other M-M stretches and bending modes between 1100-300cm^{-1}.

Gas phase spectra were run on a Philips Pye Unicam PU9512 using a gas cell of 100mm pathlength with 50mm diameter KBr windows at a pressure of approximately 10mm Hg. This was generally used to check the purity of the silicon hydride gases prepared.

High resolution infrared spectra were recorded on a Digilab FTS-40 FTIR spectrophotometer. Solution spectra were obtained using a solution cell with 0.1 or 0.2mm pathlength KBr windows. Reference spectra of starting materials, solvents and known compounds were stored on disc. Subtraction of these compounds from infrared spectra of the product mixtures showed clearly the peaks due to uncharacterised compounds. All reference spectra required the same parameters and solvent before subtraction was possible. An illustration of the subtraction sequence (Figure 2.1), a mixture of $Co_2(CO)_8$, $Co_4(CO)_{12}$ and $(PhSi)_2Co_4(CO)_{11}$ in hexane is shown in diagram (X). $Co_2(CO)_8$ is subtracted resulting in diagram (Y) and subsequently $Co_4(CO)_{12}$ leaving pure $(PhSi)_2Co_4(CO)_{11}$ diagram (Z). Some subtracted infrared spectra are presented when no pure sample could be isolated.

Figure 2.1 Subtraction of Infrared Spectra

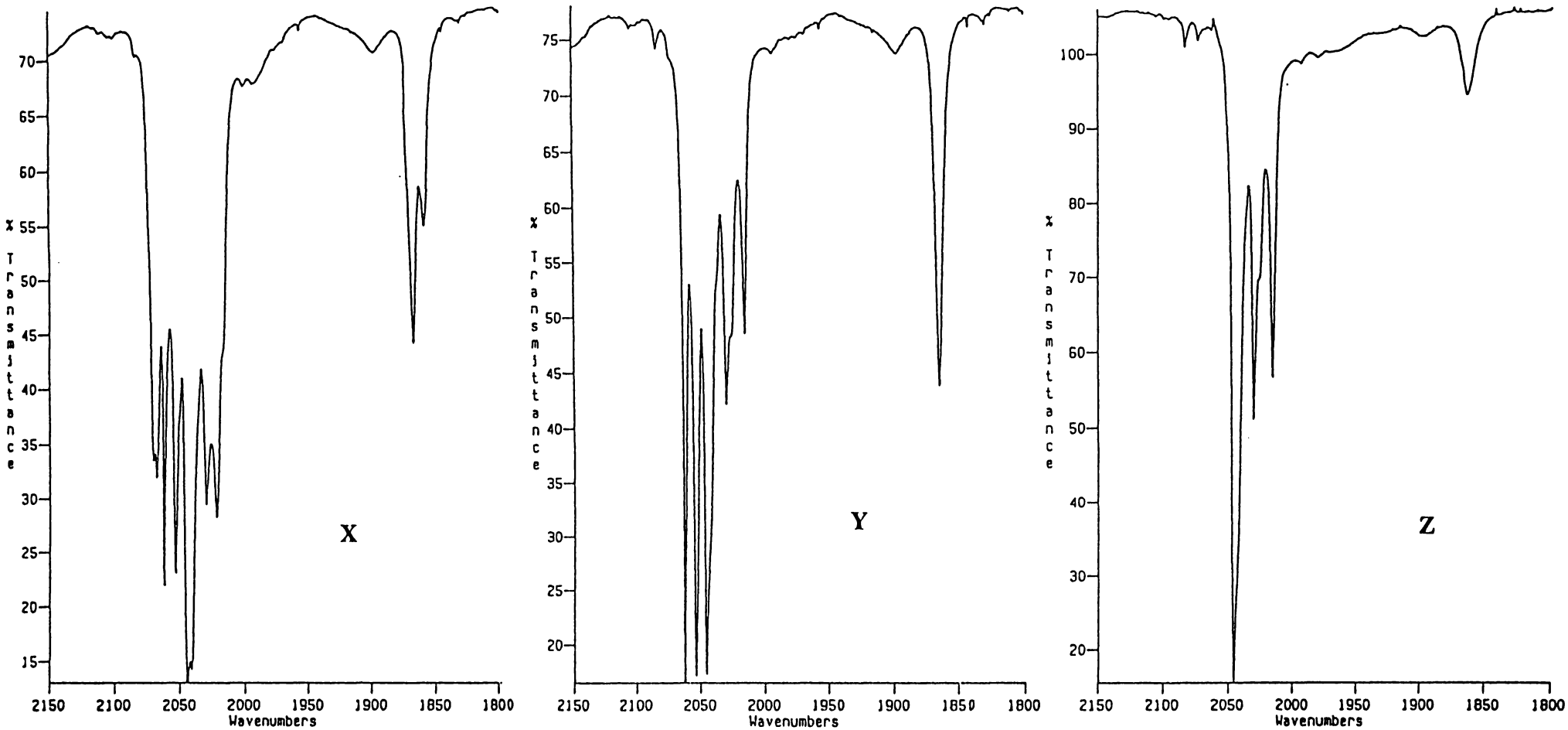

2.2.2 MASS SPECTROMETRY

Electron impact mass spectra were recorded at MAF Ruakura on a Varian CH5 mass spectrometer with a mass range of 30-1100 units. This technique is useful for identification of metal-carbonyl compounds due to clear CO losses to the metal core. From this the number of carbonyls can be deduced and a general formula for the core atoms. Chlorine gives a distinctive isotope pattern which is useful for the determination of fragments which contain one or more chlorine atoms in the molecule. Silicon and CO have the same mass units which can cause problems but generally the loss of silicon is only seen when the core breaks down.

Fast Atom Bombardment (FABS) mass spectra were collected at the University of Adelaide on a VG ZAB 2HF instrument. Only the most stable compounds arrived without significant decomposition from which mass spectra were collected. As an illustration, Figure 2.2 is part of the FAB mass spectrum of $(PhSi)_2Co_4(CO)_{11}$. This shows clearly the consecutive losses of carbon monoxide (m/e = 28).

Access to mass spectrometry was limited due to regular failure of the local aged instrument and decomposition of samples en route to the remote facility.

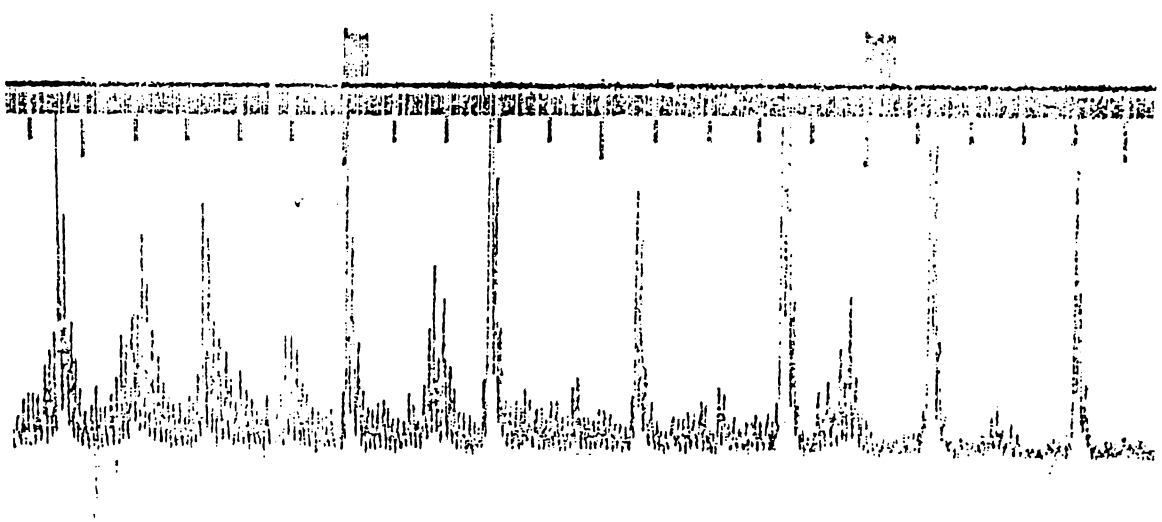

Figure 2.2 Mass Sectrum of $(PhSi)_2Co_4(CO)_{11}$

2.2.3 NUCLEAR MAGNETIC RESONANCE SPECTROSCOPY

^{1}H and ^{13}C NMR spectra were recorded on a 90MHz Jeol FX90 Multinuclear Fourier Transform spectrometer. Samples were sealed in glass tubes (5 or 10ml capacity) using deuterochloroform as the solvent.

2.2.4 ELECTRON PROBE ANALYSIS

An ORTEC Energy-dispersive X-ray Analyser was used to detect the X-ray emission from the sample when stimulated by a beam of high energy electrons directed at a small site on the sample. A JEOL JS-M35 scanning electron microscope was used to locate the area to be analysed.

Elemental idenification of small single crystals showed near quantitative results for heavier metals present (Fe, Co) in the sample. Silicon is at the limits of this technique and only semi-quantitative analysis of this element could be made.

2.2.5 X-RAY CRYSTALLOGRAPHY

X-ray crystallography is the major technique for full unambiguous characterisation of clusters. The limits of instrumental techniques to give structural information are noted above.

Suitable crystals were mounted onto a glass fibre with grease (Apiezon N) or sealed inside a thin walled glass capillary and photos were taken to align the crystal. Ni-filtered Cu-Kα X-rays were used for precession photographs from which information on unit cell dimensions, volume, crystal quality and space group were obtained.

Full crystallographic data were collected at the University of Canterbury on a Nicolet P3 four-circle automatic diffractometer. Data collected were corrected for Lorentz, polarisation and (numerical or empirical) absorption effects before solving the structure. Structures were solved and refined using the SHELX-76 and SHELXS-86 [98] series of programmes.

2.3 REAGENTS

2.3.1 SOLVENTS

To avoid decomposition of reaction products by water and dissolved oxygen, the solvents were rigorously dried under a nitrogen atmosphere.

Hexane and **Petroleum Spirit** (40°-60° fraction) - distilled from CaH_2.

Dichloromethane - distilled from phosphorus pentoxide.

Diethylether and **Tetrahydrofuran** - distilled from sodium and benzophenone.

Toluene - dried over sodium wire.

2.3.2 CHEMICALS

$SiCl_4$, Si_2Cl_6 and $(Cl_3Si)_2O$ - were stored at 0°C in glass tubes fitted with greaseless taps. Before use any HCl was pumped away and the material was distilled under vacuum. Supplied by Petrarch Systems Inc.

$LiAlH_4$ - was extracted using diethylether to obtain a pure, more reactive product.

HgS, **HgO** and **PbO** - were heated to 50°C under vacuum for 15 minutes to remove adsorbed water.

$Co_2(CO)_8$ - stored at -10°C in 10g ampoules under nitrogen. On prolonged storage decomposition to purple $CoCO_3$ takes place from the bottom up. Supplied by the Pressure Chemical Company.

$Fe(CO)_5$ - stored in the dark at room temperature.

Na, K metals - any oxide film was removed in a nitrogen filled glove-box.

Et_4NBr, 66%HI, Br_2, I_2 - used as supplied.

2.4 PREPARATION OF STARTING MATERIALS

2.4.1 PREPARATION OF SiH_4 AND Si_2H_6

SiH_4 (mp -185°C, bp -111.8°C) [116, 127] and Si_2H_6 (mp -132.6°C, bp -14.3°C) [116, 127] were prepared on a vacuum line by the reduction of the appropriate silicon chloride ($SiCl_4$, Si_2Cl_6) with $LiAlH_4$ in diethylether. An excess of $LiAlH_4$ (1.0-2.0g, 26-52mmol) was dissolved in 40mls of diethyl ether and $SiCl_4$ (2.0g, 11.8mmol) or Si_2Cl_6 (2.0g, 7.4mmol) was condensed in several increments into the flask and allowed to warm to room temperature. Each increment was condensed at -196°C until the reaction was completed.

$$2Si_2Cl_6 + 3LiAlH_4 \rightarrow 2Si_2H_6 + 3LiCl + 3AlCl_3$$

The diethylether was separated from SiH_4 using n-propanol (-127°C) slush bath and separated from Si_2H_6 using chloroform (-63°C) slush bath. To destroy unwanted silicon hydrides NaOH pellets were located in the waste trap. The purity was confirmed by infrared spectroscopy.

2.4.2 PREPARATION OF HYDROGEN IODIDE

Several methods for the preparation of HI gas were attempted. 5 grams of iodine were dissolved in 2.5 grams of hydroiodic acid (54-56%), this was added dropwise to excess red phosphorus. Nitrogen gas was used to purge the hydrogen iodide from the three necked flask. The gas was passed through a trap immersed in toluene slush to remove unwanted material.

$$5I_2 + 5H_2O + 2P \rightarrow HI + P_2O_5$$

Dehydration of concentrated hydroiodic acid using P_2O_5 proved very successful. Hydroiodic acid (66%) (5.0ml, 50mmol) was added to 10-20g phosphorus pentoxide through a dropping funnel to remove water from the acid and liberate hydrogen iodide gas. Minor amounts of iodine and water were removed by passing the gas through a toluene slush bath. This method proved to be quick, high-yielding and efficient for the preparation of hydrogen iodide.

2.4.3 PREPARATION OF IODOSILANE

In the preparation of iodosilane (mp -57°C, bp 45.6°C) [85], hydrogen iodide gas (5.12g, 40mmol) was condensed onto phenylsilane (4.33g, 40mmol) in a 200ml tube on the vacuum line. This was left to react in a chlorobenzene slush bath at -45°C for 4-12 hours. Longer reaction times provided higher yields of iodosilane.

$$C_6H_5SiH_3 + HI \rightarrow ISiH_3 + C_6H_6$$

This was fractionated for 30 minutes through traps immersed in chlorobenzene and toluene slush baths and into a trap cooled with liquid N_2. Chlorobenzene (-45°C) trapped benzene, unreacted phenylsilane and any diiodosilane formed. Iodosilane was trapped in the toluene slush (-95°C) and unreacted hydrogen iodide was condensed into liquid nitrogen cooled trap.

Synthesis was generally carried out on a 10-40mmol scale with a one to one mole ratio of reagents. The purity of $ISiH_3$ was checked by infrared spectroscopy.

2.4.4 PREPARATION OF DISILYLTHIANE

A column of mercury sulphide (10g, 43mmol) interdispersed between layers of glass wool was prepared and evacuated for 15 minutes to remove water which would result in the formation of disiloxane. Iodosilane (1.58g, 10mmol) was slowly cycled through the column at room temperature four times using liquid N_2 to cool the traps either side.

$$2ISiH_3 + HgS \rightarrow H_3SiSSiH_3 + HgI_2$$

The disilylthiane [125] was then fractionated through chlorobenzene to remove any low-volatility impurities and was retained in a toluene slush (-95°). A small amount of disiloxane was observed in the liquid nitrogen trap. The purity of disilylthiane was checked by infrared spectroscopy.

2.4.5 PREPARATION OF BROMOSILANE

A small amount of bromine (0.08g, 0.5mmol or less) was condensed into a trap containing excess silane (0.16g, 5mmol). This was allowed to warm slowly to room temperature. The red colour of the bromine rapidly disappears with the formation of $BrSiH_3$ (mp -94°C, bp 1.9°C) [85]. Repeated addition of small amounts of bromine was continued with slow warming to room temperature until approximately half of the silane has reacted. Excess silane is used to limit the formation of higher substitution products.

WARNING : As bromine and silane react readily, only small amounts are combined at any one time. If larger amounts are used the mixture begins to burn and can even lead to an explosive reaction.

$$SiH_4 + Br_2 \rightarrow BrSiH_3 + HBr$$

The bromosilane was fractionated through a trap in chlorobenzene slush bath to remove any dibromosilane. Bromosilane was held by the toluene slush (-95°C) with the hydrogen bromide and unreacted silane passing through to be trapped in liquid nitrogen.

The mixture of silane and hydrogen bromide can be converted into bromosilane at room temperature using freshly sublimed aluminium bromide as a catalyst.

$$SiH_4 + HBr \rightarrow BrSiH_3 + H_2$$

2.4.6 PREPARATION OF DISILOXANE

Several methods were used to prepare disiloxane ($H_3SiOSiH_3$, mp -145.2°C, bp -15.2°C) [127, 128, 129, 130] with varying degrees of success. Iodosilane is a readily accessible starting material so a route for the preparation of disiloxane from this halosilane was attempted.

Iodosilane was condensed onto moist lead monoxide and left to react for 10 minutes at room temperature. The products were fractionated through a toluene slush bath to give a low yield of $H_3SiOSiH_3$. The reaction of iodosilane with mercuric oxide was rather exothermic and produced water as the major product. This exothermic reaction is probably due to the oxygen being easily liberated from the mercuric oxide and lead to the combustion of the silicon hydride. Oxygen and iodine lie at opposite ends of the reactivity series which also leads to rapid reactions.

Another method used was to react iodosilane with water to form the primary unstable silanol which under-goes spontaneous condensation to produce disiloxane. The hydrogen iodide that was liberated would be absorbed into the excess water. This method was not very successful.

$$2ISiH_3 + 2H_2O \rightarrow 2H_3SiOH + 2HI \rightarrow H_3SiOSiH_3 + H_2O$$

The highest yielding preparation of disiloxane was obtained by using bromosilane which was passed several times through a column of mercuric oxide (PbO can also be used) at room temperature.

$$2BrSiH_3 + HgO \rightarrow H_3SiOSiH_3 + HgBr_2$$

This was fractionated through a toluene slush bath to give an 80% yield of disiloxane. The purity of disiloxane was checked by infrared spectroscopy. The very strong υSi-O (1106 cm^{-1}) peak was easily identified in the infrared spectrum.

2.4.7 PREPARATION OF IODOGERMANE

Monogermane (0.383-0.766g, 5-10 mmol) was condensed into a 50ml glass ampoule with iodine (1.14-2.28g, 4.5-9 mmol) in a ratio of 1 to 0.9. The reactants were left to slowly warm to room temperature upon which the vessel attained a pressure of 2.5 to 5 atm. The reaction was allowed to continue for 1 to 7 days in the dark after which the colour of the product is straw yellow.

$$GeH_4 + I_2 \rightarrow IGeH_3 + HI$$

The iodogermane ampoule [86, 123] was opened on the vacuum line and fractionated through carbon tetrachloride slush to remove higher substitution products (I_2GeH_2, I_3GeH and GeI_4) and through an ethylacetate slush to trap iodogermane. The unreacted monogermane and hydrogen iodide condensed in the liquid nitrogen trap.

2.4.8 PREPARATION OF DIGERMYL SULPHIDE

Iodogermane (1.0g, 5.0mmol) was passed several times through a column of mercury sulphide (20g) dispersed on glass-wool, similar to the preparation of disilylthiane. Small amounts of $H_3GeSGeH_3$ [86, 97] were prepared by condensing iodogermane directly onto mercury sulphide which was left to warm slowly to room temperature.

$$2IGeH_3 + HgS \rightarrow H_3GeSGeH_3 + HgI_2$$

The digermyl sulphide was condensed into a clean trap on the vacuum line and unwanted volatile compounds were removed by pumping for 30 seconds while the $H_3GeSGeH_3$ was held in a carbon tetrachloride slush. The purity of $H_3GeSGeH_3$ was checked by infrared spectroscopy [97]. Digermyl sulphide was stored at -196°C (liq N_2) and has a very distinctive foul odour.

CHAPTER THREE

REACTIONS OF SiH_4, Si_2H_6 AND GeH_4 WITH IRON AND COBALT CARBONYL COMPOUNDS

REACTIONS OF SiH_4, Si_2H_6 AND GeH_4 WITH IRON AND COBALT CARBONYL COMPOUNDS

3.1 INTRODUCTION

The reactions of germanium hydrides with $Co_2(CO)_8$ have been investigated extensively by the University of Waikato team and the products are more fully characterised than those of silicon. Monogermane, the simplest hydride, reacts with $Co_2(CO)_8$ at room temperature to form $Ge[Co_2(CO)_7]_2$ **{5}** (Figure 3.1) and upon heating this decarbonylates to the cluster $(CO)_4CoGeCo_3(CO)_9$ **{2}** [23, 100, 109, 110]. Structurally, $Ge[Co_2(CO)_7]_2$ consists of two mutually perpendicular $GeCo_2(CO)_7$ triangular units linked together at the central germanium. The analogous reaction using monosilane [43, 47] forms structurally similar products, showing little difference between the two systems.

$$GeH_4 + 2Co_2(CO)_8 \rightarrow Ge[Co_2(CO)_7]_2 + 2H_2 + 2CO$$

At room temperature the major product from the reaction of SiH_4 with $Co_2(CO)_8$ is $Si[Co_2(CO)_7]_2$ **{5}** (see section 1.3.4), but at higher temperatures (50°C) or long reaction times the purple coloured cluster $(CO)_4CoSiCo_3(CO)_9$ **{2}** (see section 1.3.5) is formed.

Digermane reacts with $Co_2(CO)_8$ to form a range of products, mainly $Ge[Co_2(CO)_7]_2$ and $Ge_2Co_6(CO)_{20}$ **{8}** [71, 73-75] with smaller amounts of $(CO)_4CoGeCo_3(CO)_9$, $[(CO)_4CoGe]_2Co_4(CO)_{11}$ [71] (Figure 3.2) and $Ge_3Co_8(CO)_{26}$ **{9}** [72, 76, 77] (Figure 3.3). From related structures, $Ge_2Co_6(CO)_{20}$ is probably an open cluster structure containing a *spiro*-cylic arrangement of $GeCo_2$ triangular units with two carbonyls bridging each of the

terminal Co-Co bonds leaving three terminal carbonyls for each cobalt atom. The heating of $Ge_2Co_6(CO)_{20}$ {8} results in decarbonylation to the closo cluster $[(CO)_4CoGe]_2Co_4(CO)_{11}$ {7}, a bicapped square pyramid.

$$Ge_2H_6 + Co_2(CO)_8 \rightarrow GeCo_4(CO)_{14} + Ge_2Co_6(CO)_{20}$$

$$Ge_2Co_6(CO)_{20} \rightarrow [(CO)_4CoGe]_2Co_4(CO)_{11} + CO$$

Preliminary investigation of the analogous reaction using disilane revealed a similar range of products, but the stability of the open cluster complexes is a lot lower compared to those of germanium. The major products from the reaction are $Si[Co_2(CO)_7]_2$ {5} [43, 47] and $[(CO)_4CoSi]_2Co_4(CO)_{11}$ {7} [35] with minor amounts of $(CO)_4CoSiCo_3(CO)_9$ {2} and other uncharacterised species depending on the conditions. Formation of the open cluster $Si_2Co_6(CO)_{20}$ {8} is likely but this readily decarbonylates at room temperature to the orange cluster $[(CO)_4CoSi]_2Co_4(CO)_{11}$ {7} (see section 1.3.6). This chapter describes further investigations into the reaction of Si_2H_6 with $Co_2(CO)_8$.

Figure 3.1 $Ge[Co_2(CO)_7]_2$

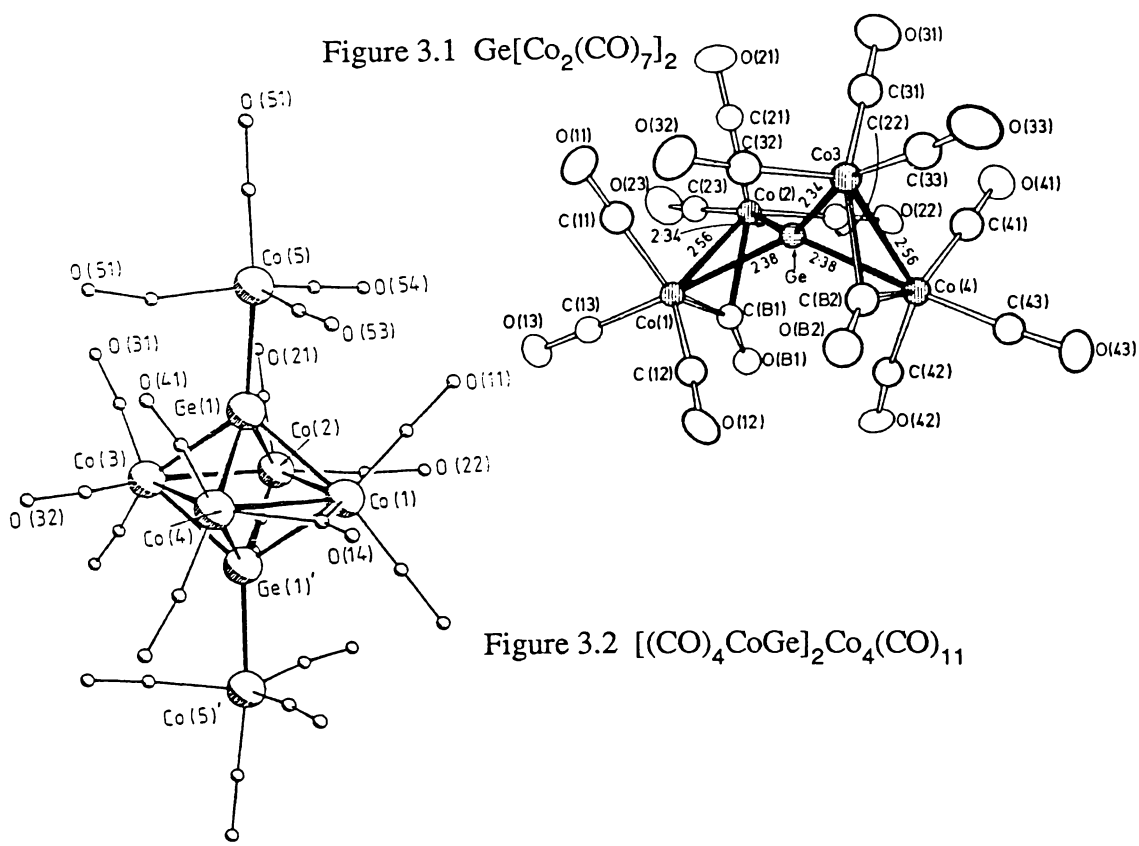

Figure 3.2 $[(CO)_4CoGe]_2Co_4(CO)_{11}$

Trigermane reacts with $Co_2(CO)_8$ to form mainly $Ge_3Co_8(CO)_{26}$ [72, 76, 77] (Figure 3.3) which has a long *spiro*-cyclic chain arrangement of $GeCo_2$ triangular fragments. Heating of this cluster results in fragmentation to the smaller germanium-cobalt carbonyl type compounds.

$$Ge_3H_8 + 4Co_2(CO)_8 \rightarrow Ge_3Co_8(CO)_{26} + 4H_2 + 6CO$$

Reaction of tetragermane (Ge_4H_{10}) with $Co_2(CO)_8$ has been investigated [111] but the expected product $Ge_4Co_{10}(CO)_{32}$ has not been isolated. The characterised products are mainly $GeCo_4(CO)_{14}$ **{5}** and $Ge_3Co_8(CO)_{26}$ **{9}** along with a smaller amount of $Ge_2Co_6(CO)_{20}$ **{8}**.

The reactions of trisilane or any higher hydrides of silicon or germanium have not been examined mainly due to the difficulty in the preparation of the pure hydrides and problems with structural isomerism.

Figure 3.3 $Ge_3Co_8(CO)_{26}$

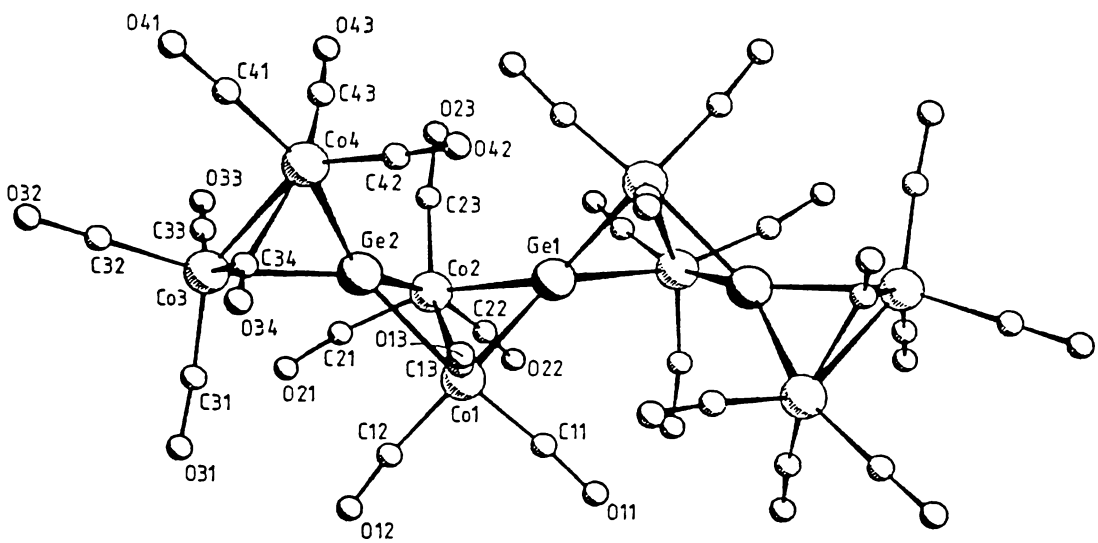

Substitution of the bridging carbonyls in the clusters $Ge[Co_2(CO)_7]_2$ **{5}**, $Ge_2Co_6(CO)_{20}$ **{8}** and $Ge_3Co_8(CO)_{26}$ **{9}** with GeRR', (where R, R' = H, Me, Et, Ph, Cl combinations) have been investigated. Characterised mono-substituted compounds include $(Me_2Ge)GeCo_4(CO)_{13}$ **{10}** [73, 74, 75],

$(MeHGe)GeCo_4(CO)_{13}$ [37] $[MeCo(CO)_4Ge]GeCo_4(CO)_{13}$ [37] with di-substituted compounds $(Me_2Ge)_2GeCo_4(CO)_{12}$ **{11}** [37] (Figure 3.4), $[(CO)_4CoMeGe]_2GeCo_4(CO)_{12}$ [37] and $(Me_2Ge)_2Ge_2Co_6(CO)_{18}$ [73, 78].

Figure 3.4 $(Me_2Ge)_2Co_4(CO)_{12}$

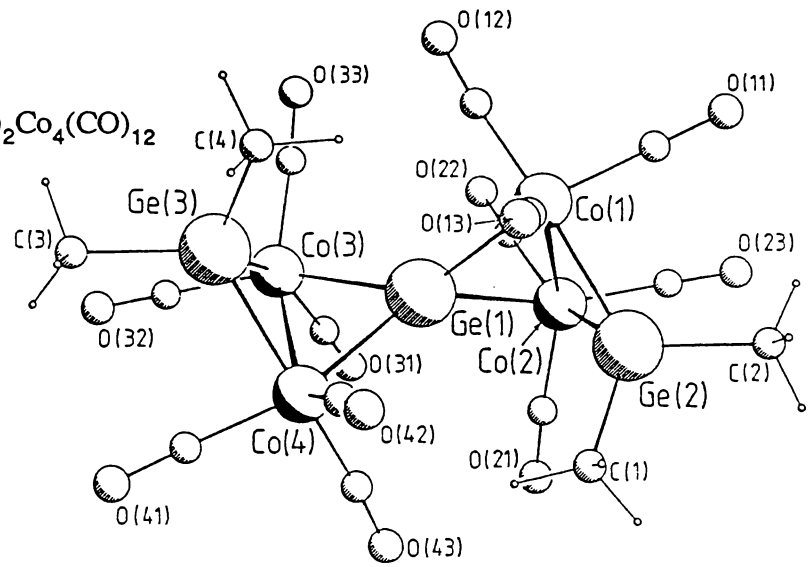

3.2 REACTION of Si_2H_6 WITH $Co_2(CO)_8$

3.2.1 EXPERIMENTAL

Si_2H_6 (0.0375g, 0.602mmol) was condensed into a 50ml high pressure ampoule with $Co_2(CO)_8$ (0.718gm, 2.10mmol) in 10ml of hexane and set aside to react for 4 years at room temperature. Reaction ratio of Si_2H_6 to $Co_2(CO)_8$ is 1 to 3.5 which is slightly higher than calculated from the equation below.

$$Si_2H_6 + 3Co_2(CO)_8 \rightarrow [(CO)_4CoSi]_2Co_4(CO)_{11} + 3H_2 + 5CO$$

After this four-year period the inside of the ampoule was coated in a light brown residue with a purple solution. The contents were transferred to a Schlenk flask using CH_2Cl_2 to wash the ampoule, and the solvents were removed. Hexane (20ml) was added and the infrared spectrum showed this fraction contained $(CO)_4CoSiCo_3(CO)_9$ **{2}** (υCO, (hexane) 2114 w, 2087 s, 2046 vs, 2030 m, cm^{-1}) and trace amounts of $Co_2(CO)_8$ and $Co_4(CO)_{12}$. The hexane

soluble fraction was completely removed from the brown solid using 3 x 10ml hexane extracts. Total weight of solids soluble in hexane was 0.462g. This represents 0.736mmol if $(CO)_4CoSiCo_3(CO)_9$ is considered as the only product with a 61% yield based on Si_2H_6.

The remaining brown solid was characterised by infrared spectroscopy to be $[(CO)_4CoSi]_2Co_4(CO)_{11}$ {7} (υCO, (CH_2Cl_2) 2102 s, 2075 w, 2054 s sh, 2043 vs, 2021 s sh, 2006 m sh, cm^{-1}). 0.203g, 0.216mmol of $[(CO)_4CoSi]_2Co_4(CO)_{11}$ was isolated which gives a yield of 36% based on Si_2H_6. Calculations show that all the available cobalt is accounted for in these two compounds. This suggests that a higher yield of $[(CO)_4CoSi]_2Co_4(CO)_{11}$ can be expected for lower ratios of Si_2H_6 to $Co_2(CO)_8$ (example: 1 to 2.5 - 3.0). This reaction also demonstrates the stability of these two clusters at room temperature.

Si_2H_6 (0.077g, 1.24mmol) was reacted with $Co_2(CO)_8$ (1.06g, 3.10mmol) (reactant ratio 1 to 2.5) in 10ml of hexane. This was left to react at 5°C in the dark for 3 weeks. Incondensable gases (CO and H_2) were measured. Total gas evolution equalled 3.45 mmol of which 32% was H_2 (1.11mmol). This amount of H_2 is only a third of that expected.

Trace amounts of SiH_4 and some $HCo(CO)_4$ were observed in the solvent which had been removed under vacuum. These hydride compounds could not be quantitatively separated from hexane but are estimated to contribute only a small portion to the overall hydrogen count.

An infrared spectrum of the initial hexane-soluble components showed very little $Co_2(CO)_8$ and $Co_4(CO)_{12}$. $Si[Co_2(CO)_7]_2$ {5} (υCO, (hexane) 2085 s, 2065 s, 2044 m, 2037 s, 2026 m, 2007 w, 1847 w br, cm^{-1}) was identified along with $H_2Si_3Co_6(CO)_{20}$ (see section 3.2.2). A third silicon-cobalt compound with a characteristic bridging carbonyl peak (see section 3.2.3) was also observed.

The later fraction contained a higher proportion of $H_2Si_3Co_6(CO)_{20}$ along with the other components above.

Approximate yields of the products: $Si[Co_2(CO)_7]_2$ 40-50%, $H_2Si_3Co_6(CO)_{20}$ 30-40%, bridging carbonyl compound 10-20%.

Si_2H_6 (0.146g, 2.34mmol) was condensed into a 100ml vessel fitted with a greaseless tap with $Co_2(CO)_8$ (2.00g, 5.85mmol) in 25ml hexane. This gives a Si_2H_6 to $Co_2(CO)_8$ reaction ratio of 1 : 2.5. This was allowed to react at a temperature of 4°C for 8 days with measurements of the incondensable gases taken after 4 hours, 24 hours and at the 8 day completion.

Initial evolution of gases consisted mainly of carbon monoxide (83%) with a small amount of hydrogen (17%). The hydrogen evolution increased as the reaction proceeded with 30% H_2 after 24 hours and 46% H_2 after 8 days. Total gas evolution amounted to 5.76mmol of which 27% was H_2 (1.56mmol). This is only a fifth of the expected hydrogen evolution. The infrared spectrum of the volatile fraction showed a small amount of SiH_4 and the formation of $HCo(CO)_4$. This accounts for another small portion of the hydrogen expected.

The contents were transferred into a Schlenk flask and the solvent and $HCo(CO)_4$ were removed under vacuum. Hexane (20ml) was added and infrared analysis showed very little unreacted $Co_2(CO)_8$ or formation of $Co_4(CO)_{12}$. Three products were identified from this reaction from which only $Si[Co_2(CO)_7]_2$ [43, 47] had been previously characterised. The remaining products are yellow to orange with slightly varying solubilities and were separated using fractional crystallisation. $H_2Si_3Co_6(CO)_{20}$ was obtained from the cooled initial hexane-soluble products as yellow rectangular crystals. After concentrating and cooling this fraction a third compound (see section 3.2.3) was obtained which formed star shaped crystals in the hexane solvent. $H_2Si_3Co_6(CO)_{20}$ was also obtained from the less hexane-soluble fraction of the

products and was soluble in a CH_2Cl_2/toluene mixed solvent. $H_2Si_3Co_6(CO)_{20}$ formed yellow quadrilateral shaped crystals from toluene. Estimated yield of $H_2Si_3Co_6(CO)_{20}$ was 40-50%.

3.2.2 INFRARED SPECTRUM OF $H_2Si_3Co_6(CO)_{20}$

The infrared spectrum of $H_2Si_3Co_6(CO)_{20}$ in hexane is shown in Figure 3.5. The spectrum exhibits seven peaks in the terminal carbonyl region with no peaks observed in the bridging carbonyl region. This is consistent with the determined structure (section 3.2.4).

The infrared spectrum of $H_2Si_3Co_6(CO)_{20}$ can be compared to the related germanium compound $Me_2Ge_3Co_6(CO)_{20}$ **{11}** [37] (see Table 3.1). This shows a very consistent shift to lower frequency of between 9 and 12cm^{-1} from the silicon to the germanium compound. The relative intensities of the infrared peaks also show a reasonable match between the two compounds.

Table 3.1

INFRARED SPECTRUM OF $H_2Si_3Co_6(CO)_{20}$ COMPARED TO $Me_2Ge_3Co_6(CO)_{20}$	
$H_2Si_3Co_6(CO)_{20}$	**$Me_2Ge_3Co_6(CO)_{20}$**
2101 w	2090 m
2082 m	2072 w
2069 s	2058 m
2054 s	2043 s
2046 m	
2030 vs	2018 m
2004 w	1995 w

Figure 3.5

INFRARED SPECTRUM OF $H_2Si_3Co_6(CO)_{20}$

HEXANE SOLUTION

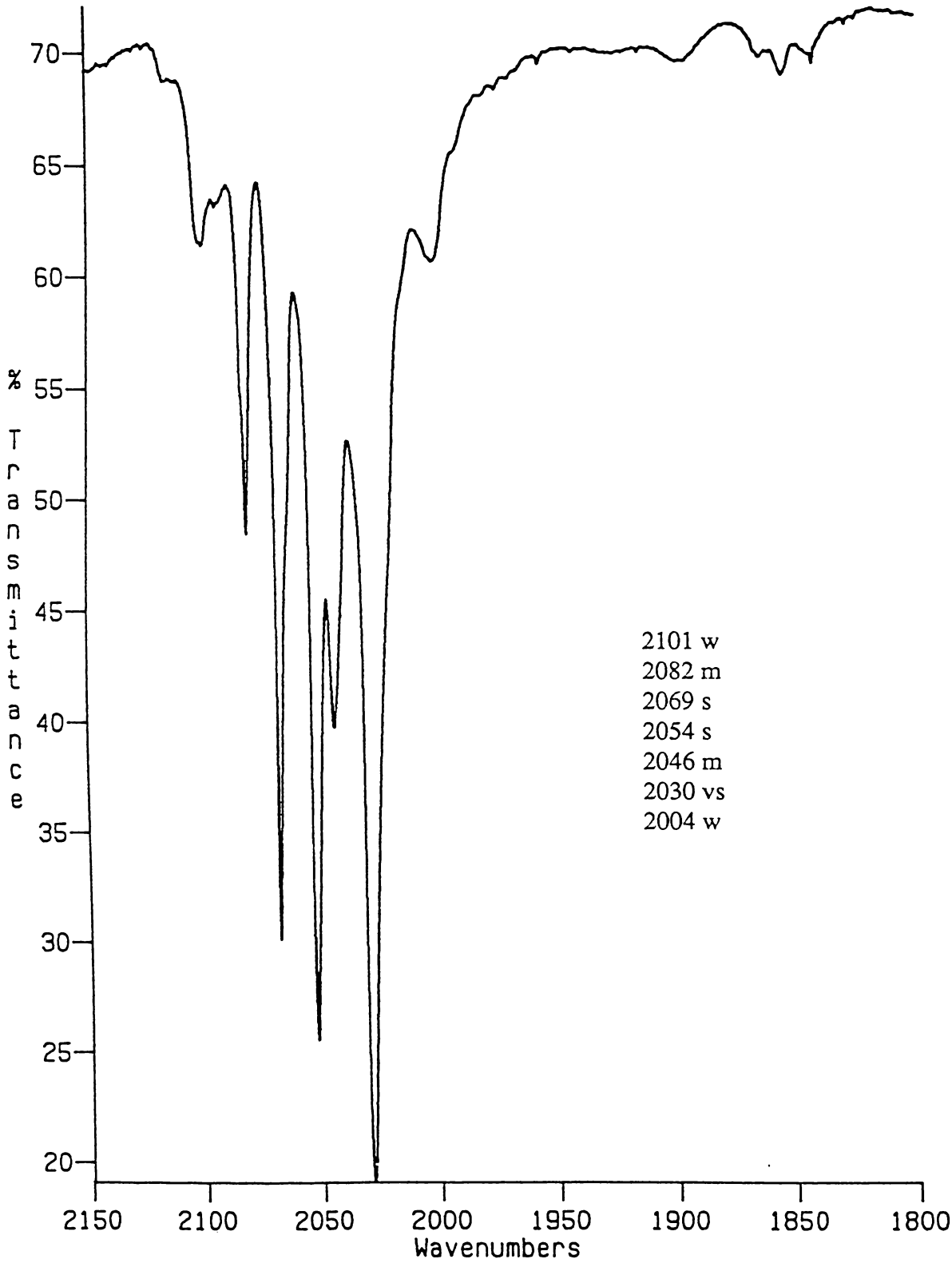

Figure 3.6

INFRARED SPECTRUM OF THIRD PRODUCT

HEXANE SOLUTION

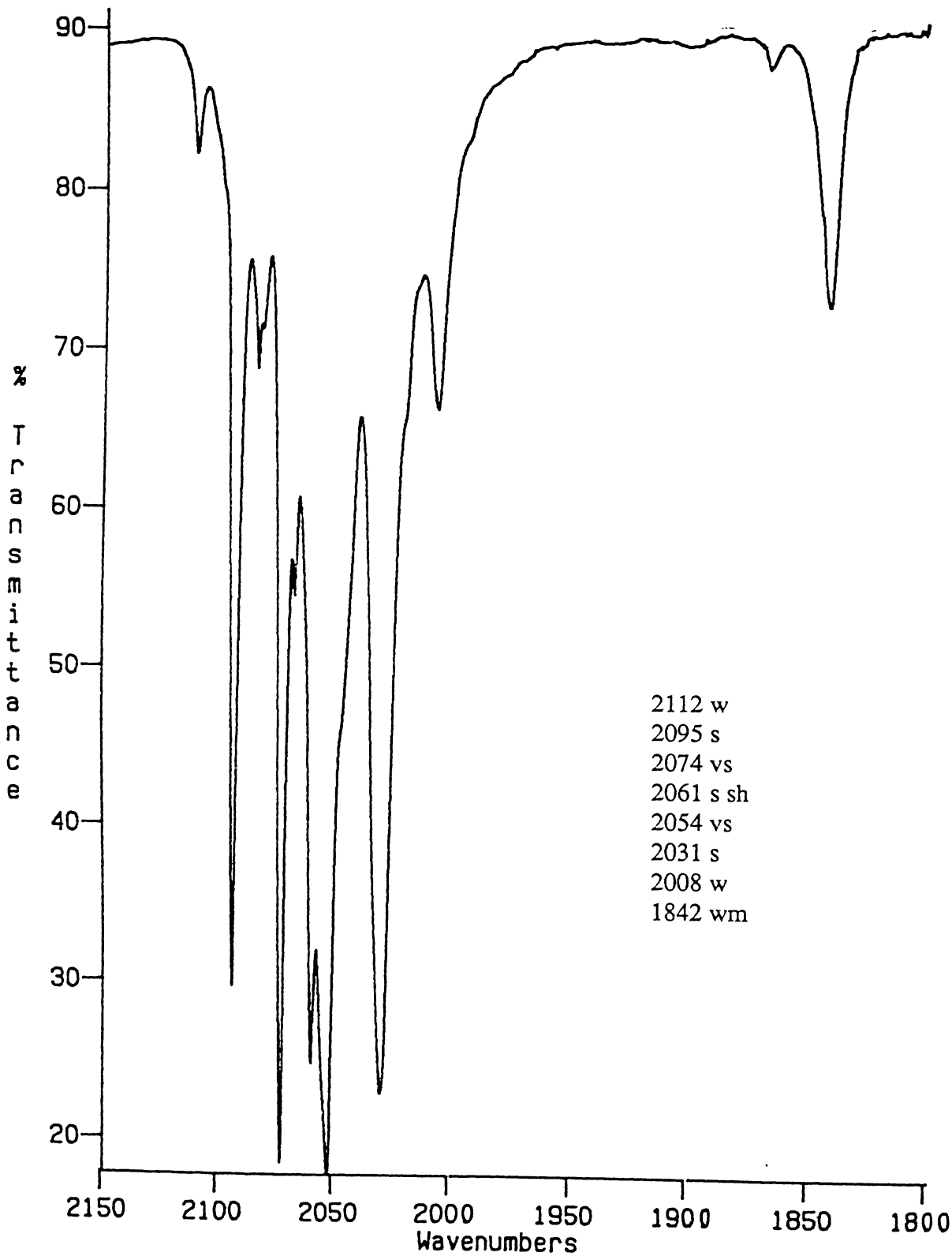

3.2.3 INFRARED SPECTRUM OF THE THIRD COMPOUND

An infrared spectrum of a yellow hexane-soluble species is shown in Figure 3.6. This is tentatively assigned to the cluster $Si_2Co_6(CO)_{20}$ {8}. The colour and solubility are similar to those observed for the germanium analogue. Comparison of the two spectra, both in hexane solvent, is shown in Table 3.2. There is good agreement between the two, with a shift to higher frequency for the silicon cluster as expected.

Table 3.2

INFRARED COMPARISON	
$Si_2Co_6(CO)_{20}$	$Ge_2Co_6(CO)_{20}$
2112 w	
2095 s	2085 s
2074 vs	2068 vs
2061 s sh	2054 s
2054 vs	2050 sh
	2040 w
	2033 wm
2031 s	2027 m
2008 w	2003 w
1842 wm	1844 wm

3.2.4 X-RAY CRYSTALLOGRAPHIC STUDY OF $H_2Si_3Co_6(CO)_{20}$

Rectangular-shaped, transparent yellow crystals were obtained from a cooled hexane solution. Preliminary precession photographs using Cu-Kα radiation showed the crystal had triclinic symmetry and was assigned to the space group $P\bar{1}$.

Intensity data were collected on a suitable crystal of dimensions 1.0 x 0.3 x 0.3 mm at the University of Canterbury on a Nicolet P3 diffractometer. A scan range of $4°<2\theta<50°$ was employed to collect 11484 unique reflections using Mo-Kα radiation. An absorption correction was applied to the data using a ϕ-scan technique with transmission factors, 0.938 maximum and 0.792 minimum. 6627 reflections with $I>3\sigma(I)$ were used for the solution and refinement of the structure. Crystal data for $H_2Si_3Co_6(CO)_{20}$ are given in Table 3.3.

Table 3.3

CRYSTAL DATA FOR $H_2Si_3Co_6(CO)_{20}$	
Formula: $C_{20}H_2Co_6O_{20}Si_3$	Mr = 1000.07
Triclinic	Space Group = $P\bar{1}$
Cryst. Colour: Yellow	
Cryst. Dimensions: 1.0 x 0.3 x 0.3 mm	
a = 10.061(7) Å	α = 69.00(7)°
b = 16.458(19) Å	β = 78.98(5)°
c = 21.592(15) Å	γ = 88.70(7)°
U = 3272(5) Å^3	Dcalc = 2.04 g cm^{-3}
Z = 4	
F(000) = 1944	Temp = 163 K
μ(Mo-Kα) = 30 cm^{-1}	
Unique Data = 11484	Range = $4°<2\theta<50°$
Refinement Data = 6627	Final R = 0.0556

For all computations, SHELXS-86 and SHELX-76 [98] crystallographic programs were used. Positions of the cobalt atoms were obtained by direct methods using TREF. A subsequent difference map located the silicon atoms and indicated the structure contained two independent molecules in the asymmetric unit. Further refinement and difference map cycles located all the

carbon and oxygen atoms. Anisotropic temperature factors were assigned to the cobalt and silicon atoms and isotropic factors for other atoms. This gives a ratio of 13.6 reflections per parameter. Attempts to locate the hydrogen atoms were not successful due to residual electron density around the carbonyl ligands which were unable to be made anisotropic due to the limited number of reflections. Final refinement (full-matrix least-squares based on F) converged to R = 0.0556, Rw = 0.0540 with $w = 1.8701[\sigma^2(F) + 0.000543F^2]^{-1}$. Largest shift/e.s.d in the final cycle was 0.0025 with the greatest electron density in the final difference of 1.20 e $Å^{-3}$ near a carbonyl group.

Positional and thermal parameters along with complete tables of bond lengths and angles are presented in Appendix One. Calculated and observed structure factors have been retained at the University of Waikato.

3.2.5 STRUCTURE OF $H_2Si_3Co_6(CO)_{20}$

Diagrams of the molecule are shown in Figures 3.7 to 3.9. Atom labelling is given in Figure 3.7 and is used throughout this discussion with the second molecule labelled similarly. Selected bond lengths and angles are given in Tables 3.4 and 3.5.

Two independent molecules were found in the asymmetric unit and will be discussed as a whole in comparison with other compounds and discussed in terms of the differences between the two molecules.

The structure of $[(CO)_4CoHSi]_2Si[Co_2(CO)_6]_2$ can be regarded as the di-substituted product of $Si[Co_2(CO)_6(\mu\text{-}CO)]_2$ **{5}** in which the two bridging carbonyls have been replaced by $SiHCo(CO)_4$ groups. The structure consists of a *spiro*-cyclic arrangement of linked $SiCo_2$ triangles with $Co(CO)_4$ and hydrogen terminal groups on the outer silicon atoms. This structure is the first to incorporate three silicon atoms into a transition metal cluster.

Figure 3.7 Perspective View of $H_2Si_3Co_6(CO)_{20}$

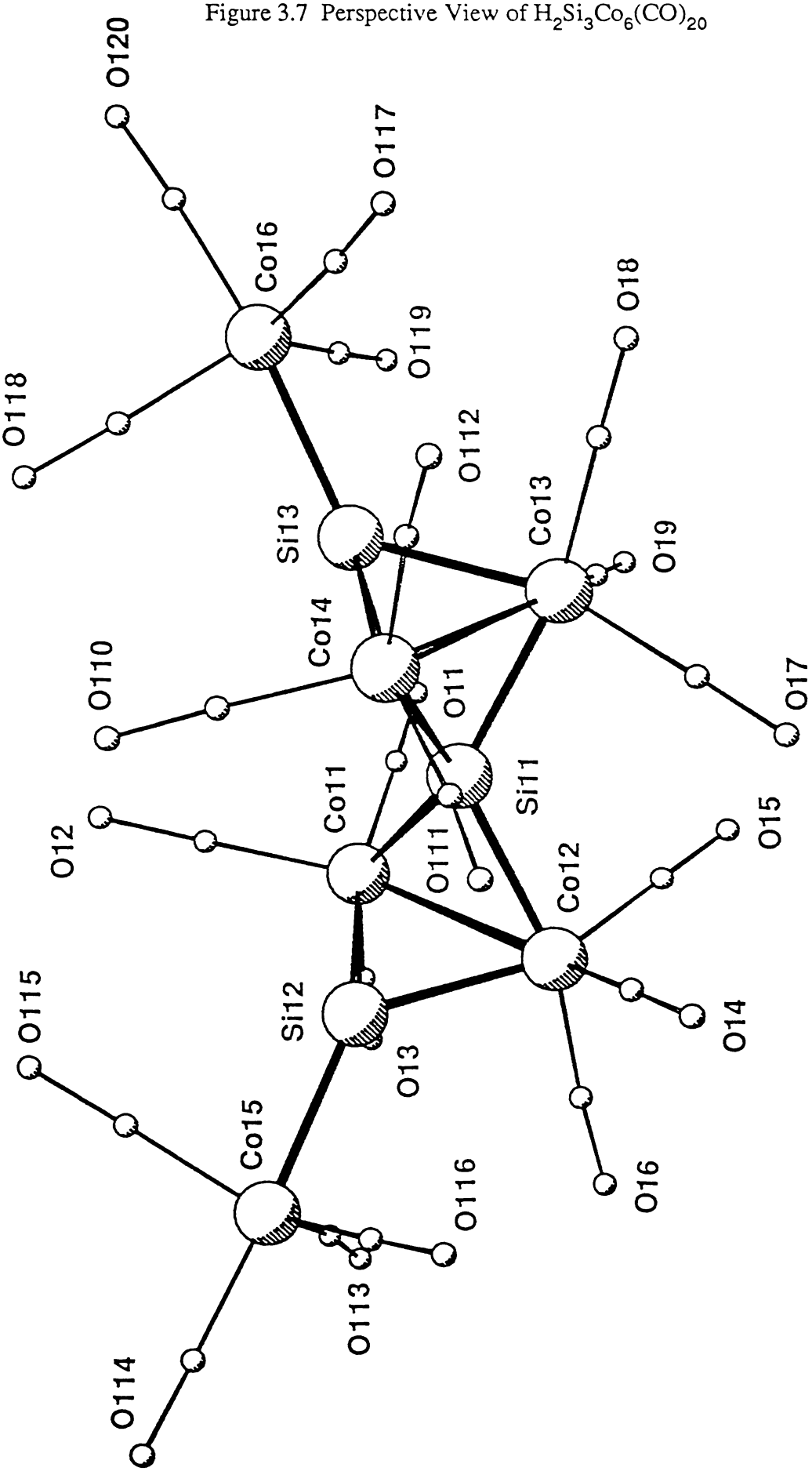

Figure 3.8 Stereo View of $H_2Si_3Co_6(CO)_{20}$

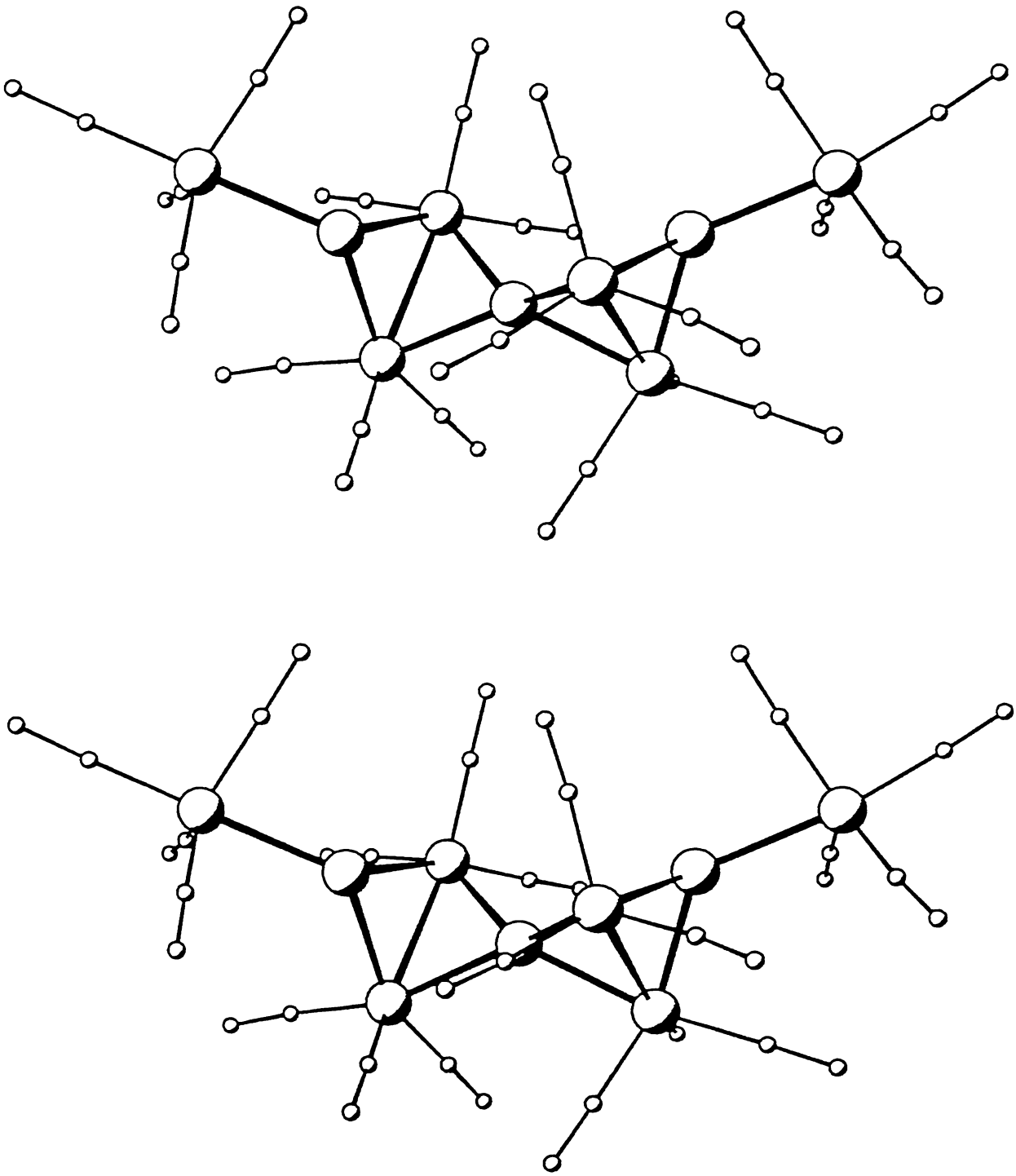

Figure 3.9 Hydrogen Atom Position in $H_2Si_3Co_6(CO)_{20}$

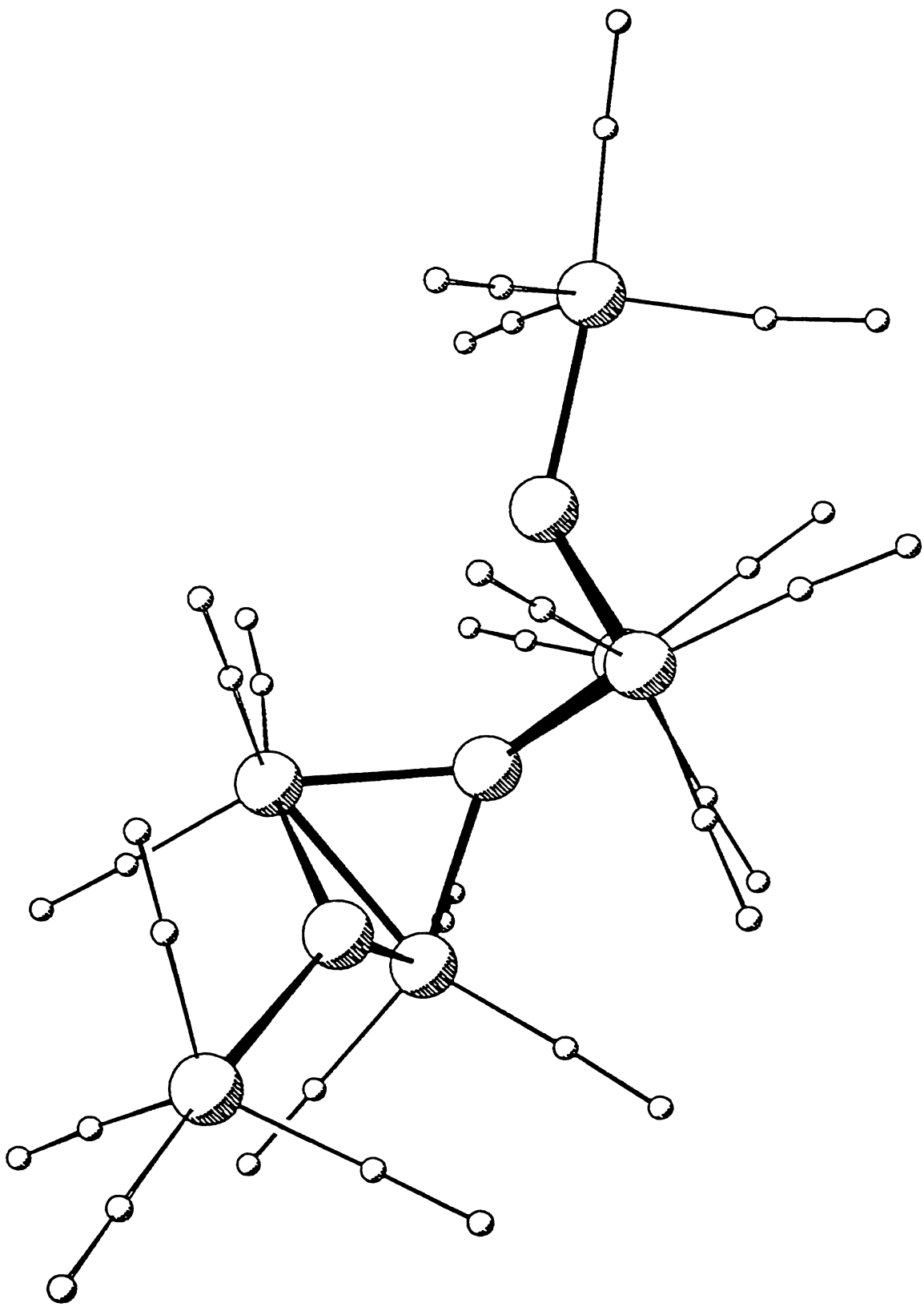

Table 3.4

SELECTED BOND LENGTHS FOR $H_2Si_3Co_6(CO)_{20}$ (Å)			
MOLECULE ONE		**MOLECULE TWO**	
Co(11)---Co(12)	2.618(2)	Co(21)---Co(22)	2.616(2)
Co(11)---Si(11)	2.281(3)	Co(21)---Si(21)	2.316(3)
Co(11)---Si(12)	2.298(3)	Co(21)---Si(22)	2.285(3)
Co(12)---Si(11)	2.322(3)	Co(22)---Si(21)	2.307(3)
Co(12)---Si(12)	2.287(3)	Co(22)---Si(22)	2.312(3)
Co(13)---Co(14)	2.614(2)	Co(23)---Co(24)	2.602(2)
Co(13)---Si(11)	2.291(3)	Co(23)---Si(21)	2.301(2)
Co(13)---Si(13)	2.281(3)	Co(23)---Si(23)	2.283(3)
Co(14)---Si(11)	2.292(3)	Co(24)---Si(21)	2.315(3)
Co(14)---Si(13)	2.314(3)	Co(24)---Si(23)	2.304(3)
Co(15)---Si(12)	2.375(3)	Co(25)---Si(22)	2.354(3)
Co(16)---Si(13)	2.371(3)	Co(26)---Si(23)	2.360(3)

The Co-Co distances in molecule (1) 2.618(2)Å and 2.614(2)Å are essentially the same, while molecule (2) with Co-Co distances of 2.616(2)Å and 2.602(2)Å shows a slight shortening in one bond. The average Co-Co distance in the cluster is 2.613Å, which is markedly longer compared to that in $Si[Co_2(CO)_7]_2$ {5} with an average Co-Co distance of 2.528Å. This can be attributed to the presence of the extra bridging Si group. A lengthening of metal-metal bonds is generally seen as the size of the bridging group increases.

Of the eight $SiCo_2$ triangles in total for both molecules only one has both Si-Co distances the same with a value of 2.291(3)Å. The most unsymmetrically bonded $SiCo_2$ triangle has a difference of 0.041Å in the Si-Co distances. The range of Si-Co distances for molecule (1), (2.281(3)Å to 2.322(3)Å, average 2.296Å) compared to molecule (2),(2.282(3)Å to 2.317(3)Å, average 2.303Å), shows that both molecules are essentially the same and any slight differences in

Table 3.5

SELECTED BOND ANGLES FOR $H_2Si_3Co_6(CO)_{20}$ (°)			
MOLECULE ONE		**MOLECULE TWO**	
Co(12)-Co(11)-Si(11)	56.1(1)	Co(22)-Co(21)-Si(21)	55.4(1)
Co(12)-Co(11)-Si(12)	55.0(1)	Co(22)-Co(21)-Si(22)	55.8(1)
Si(11)-Co(11)-Si(12)	77.4(1)	Si(21)-Co(21)-Si(22)	76.3(1)
Co(11)-Co(12)-Si(11)	54.6(1)	Co(21)-Co(22)-Si(21)	55.7(1)
Co(11)-Co(12)-Si(12)	55.4(1)	Co(21)-Co(22)-Si(22)	54.8(1)
Si(11)-Co(12)-Si(12)	76.8(1)	Si(21)-Co(22)-Si(22)	75.9(1)
Co(14)-Co(13)-Si(11)	55.3(1)	Co(24)-Co(23)-Si(21)	55.9(1)
Co(14)-Co(13)-Si(13)	55.9(1)	Co(24)-Co(23)-Si(23)	55.8(1)
Si(11)-Co(13)-Si(13)	77.0(1)	Si(21)-Co(23)-Si(23)	76.4(1)
Co(13)-Co(14)-Si(11)	55.2(1)	Co(23)-Co(24)-Si(21)	55.4(1)
Co(13)-Co(14)-Si(13)	54.7(1)	Co(23)-Co(24)-Si(23)	55.0(1)
Si(11)-Co(14)-Si(13)	76.3(1)	Si(21)-Co(24)-Si(23)	75.7(1)
Co(11)-Si(11)-Co(12)	69.3(1)	Co(21)-Si(21)-Co(22)	68.9(1)
Co(11)-Si(11)-Co(13)	137.2(1)	Co(21)-Si(21)-Co(23)	128.2(1)
Co(11)-Si(11)-Co(14)	130.4(1)	Co(21)-Si(21)-Co(24)	136.8(2)
Co(12)-Si(11)-Co(13)	126.6(1)	Co(22)-Si(21)-Co(23)	137.0(2)
Co(12)-Si(11)-Co(14)	136.4(1)	Co(22)-Si(21)-Co(24)	130.2(1)
Co(13)-Si(11)-Co(14)	69.5(1)	Co(23)-Si(21)-Co(24)	68.6(1)
Co(11)-Si(12)-Co(12)	69.6(1)	Co(21)-Si(22)-Co(22)	69.4(1)
Co(11)-Si(12)-Co(15)	128.5(1)	Co(21)-Si(22)-Co(25)	130.4(1)
Co(12)-Si(12)-Co(15)	128.1(1)	Co(22)-Si(22)-Co(25)	127.7(1)
Co(13)-Si(13)-Co(14)	69.3(1)	Co(23)-Si(23)-Co(24)	69.1(1)
Co(13)-Si(13)-Co(16)	128.8(1)	Co(23)-Si(23)-Co(26)	128.5(1)
Co(14)-Si(13)-Co(16)	129.4(2)	Co(24)-Si(23)-Co(26)	130.5(2)

Table 3.5 (continued)

DIHEDRAL ANGLES (°)	
Si(11)/Co(11)/Co(12)-Si(11)/Co(13)/Co(14)	80.53(1)
Si(21)/Co(21)/Co(22)-Si(21)/Co(23)/Co(24)	81.17(1)

bond parameters are due to crystal packing forces. Comparison of the $SiCo_2$ triangles in $H_2Si_3Co_6(CO)_{20}$ to those of $Si[Co_2(CO)_7]_2$ (Si-Co distances of 2.276(1)Å and 2.301(1)Å) shows the same scalene triangular arrangement with distances closely matching those above.

A marked increase in bond length is seen in the Si-Co distance to the terminal $Co(CO)_4$ groups. For molecule (1) the Si-Co terminal distances are 2.375(3)Å and 2.371(3)Å while for molecule (2) distances of 2.354(3)Å and 2.360(3)Å are found. This shows a significant increase compared to the central Si-Co distances average of 2.296Å. Comparison with other clusters in which silicon is bonded to a terminal $Co(CO)_4$ group, $(CO)_4CoSiCo_3(CO)_9$ {2} [23, 46] at 2.288Å or the five coordinate silicon cluster $[(CO)_4CoSi]_2Co_4(CO)_{11}$ {7} [35] at 2.347(2)Å, shows that the $H_2Si_3Co_6(CO)_{20}$ cluster contains relatively long $Si\text{-}Co(CO)_4$ terminal bond lengths.

Dihedral angles at the central silicon between the two $SiCo_2$ triangles in each molecule are 80.53° and 81.17°. The average (80.85°) compares very closely to the 80.92° found for $Si[Co_2(CO)_7]_2$ {5}.

The twenty carbonyls around the cluster are all terminally bonded. Four carbonyls are located on each of the two external cobalt atoms with the four core cobalt atoms having three each. The average bond lengths, Co-C (1.78(1)Å), C-O (1.14(1)Å) and angles Co-C-O (176±3°) are similar to those observed for other clusters.

The positions of the hydrogen atoms on silicon could not be directly located in the X-ray analysis but can be accommodated in the space left vacant as seen in Figure 3.9. The carbonyl ligands show some shielding effect around

the hydrogen atoms positions, possibly protecting them from further substitution by the bulky $Co_2(CO)_8$ reactant.

3.2.6 PROPERTIES AND DISCUSSION

$H_2Si_3Co_6(CO)_{20}$ shows little sign of change in solution or in the crystalline state at -25°C, although the crystalline solid decomposed at room temperature after one week even in the absence of air.

^1H NMR data were not collected due to the very limited quantities of $H_2Si_3Co_6(CO)_{20}$ available, therefore the existence of hydrogen has not been fully verified but far out-weights any other possibility. This compound is a rare example of a silicon cluster in which not all the hydrogen has been replaced. This probably reflects the significant steric shielding of the last Si-H by the terminal carbonyls. It should be noted also that the formation of the hydride would be favoured by the deficit of $Co_2(CO)_8$ used in the reaction (Si_2H_6 : $Co_2(CO)_8$, 1 : 2.5). The balanced equation (1) for the reaction is given below at a Si_2H_6 : $Co_2(CO)_8$ ratio of 1 to 2.

$$3Si_2H_6 + 6Co_2(CO)_8 \rightarrow 2H_2Si_3Co_6(CO)_{20} + 7H_2 + 8CO \quad (1)$$

This would suggest that a higher yield of $H_2Si_3Co_6(CO)_{20}$ could be obtained with this low reaction ratio. Other possible products are represented in the following equations (2-4).

$$Si_2H_6 + 4Co_2(CO)_8 \rightarrow 2SiCo_4(CO)_{14} + 3H_2 + 4CO \quad (2)$$

$$Si_2H_6 + 3Co_2(CO)_8 \rightarrow Si_2Co_6(CO)_{20} + 3H_2 + 4CO \quad (3)$$

$$3Si_2H_6 + 8Co_2(CO)_8 \rightarrow 2Si_3Co_8(CO)_{26} + 9H_2 + 12CO \quad (4)$$

Equation (2) represents a ratio of 1 to 4 for the formation of $SiCo_4(CO)_{14}$ **{5}** which is the smallest cluster possible. Equation (3) would indicate that a ratio of 1 to 3 would be optimum for the formation of the cluster $Si_2Co_6(CO)_{20}$

{8}. The largest cluster $Si_3Co_8(CO)_{26}$ {9}, would occur at the lowest ratio of 1 to 2.7. These equations suggest that if the ratio is lowered below this point products may form in which not all the hydrogens are replaced.

The reaction in practice forms a very complicated series of these products which is not directly related to the reaction ratio. In order to obtain these larger clusters one may conduct the reaction at low ratios initially (between 1 : 1 to 1 : 2) and then add more $Co_2(CO)_8$ later to replace the unsubstituted hydrogens, equation (5) below.

$$\mathbf{H_2Si_3Co_6(CO)_{20} + Co_2(CO)_8 \rightarrow Si_3Co_8(CO)_{26} + H_2 + 2CO} \quad (5)$$

$Ge[Co_2(CO)_7]_2$ {5} readily substitutes one or both bridging carbonyls when reacted with $RR'GeH_2$ (R, R' = H, Me, Et, Cl) [37, 73-75]. The closest related germanium compound is $Me_2Ge_3Co_6(CO)_{20}$ {11} [37] which has been characterised by infrared spectroscopy. This can be considered as the disubstituted compound of $Ge[Co_2(CO)_7]_2$ in which both bridging carbonyls have been replaced with $(CO)_4CoMeGe$ groups.

3.3 REACTION OF SiH_4 AND Si_2H_6 WITH $Co_4(CO)_{12}$

3.3.1 EXPERIMENTAL

SiH_4 (0.056g, 1.75mmol) was reacted with $Co_4(CO)_{12}$ (0.50g, 0.874mmol) at 50°C in 10ml of hexane for 2 weeks. Initially the solution was brown/black with undissolved $Co_4(CO)_{12}$, while after 2 weeks the solution was red/brown with a small black residue on the sides of the glass vessel.

The volatile fraction contained a small amount of unreacted SiH_4. An infrared spectrum of the hexane-soluble products showed $(CO)_4CoSiCo_3(CO)_9$ {2} as the major product with some unreacted $Co_4(CO)_{12}$. No other silicon-cobalt compounds were observed.

Si_2H_6 (0.0566g, 0.909mmol) was reacted with $Co_4(CO)_{12}$ (0.78g, 1.36mmol) at 40°C in 15ml of hexane for 7 days. The infrared spectrum showed

the only silicon-cobalt compound formed was $(CO)_4CoSiCo_3(CO)_9$ {2}. Black insoluble residues remained in the reaction vessel.

3.3.2 DISCUSSION

An interesting facet of the above reactions is that the starting material has 12 carbonyl ligands and forms a product ($(CO)_4CoSiCo_3(CO)_9$ {2}) which has 13. Loss of carbonyl ligands occurs readily in the formation of clusters but the addition usually requires high carbon monoxide pressures. The black residue would explain the source of carbon monoxide from the decomposition of $Co_4(CO)_{12}$.

3.4 REACTION OF SiH_4 WITH $Fe(CO)_5$

3.4.1 INTRODUCTION

Previous work has shown that this reaction provids a consistent 40% yield of the yellow-orange complex $Si[Fe_2(CO)_8]_2$ {5} and a red uncharacterised product. My initial work showed that this red compound easily decomposed on manipulation, so a more stable derivative was formed by reacting the red hexane solution with $Co_2(CO)_8$. This resulted in a red product which was easily purified and was stable enough to be easily manipulated.

3.4.2 EXPERIMENTAL

SiH_4 (0.0642g, 2.00mmol) was condensed into a 50ml ampoule with excess $Fe(CO)_5$ (3.0g, 15.3mmol) in petroleum spirit (bp 100-120°C). The solution was allowed to react at 140°C for 4 hours. This resulted in a red-brown solution with a black precipitate.

The reaction mixture was transferred into a Schlenk flask and the solvent and unreacted $Fe(CO)_5$ were removed under vacuum. Hexane (20ml) was added and the resulting red solution was filtered from the remaining solid. $Co_2(CO)_8$ (0.03g, 0.087mmol) was added to this fraction and left to react at room temperature for 24 hours. After this time small round conglomerates of a new compound were found on the sides of the flask. The supernatant was removed

and separation by thin layer chromatography showed this to contain $Si[Fe_2(CO)_8]_2$ {5} and unreacted $Co_2(CO)_8$ with a small amount of $Co_4(CO)_{12}$. The new compound left in the ampoule was washed several times with hexane and quickly washed with 2x10ml CH_2Cl_2. The solid slowly dissolved in 60ml of hot CH_2Cl_2 to form a pink solution. This solution was then slowly cooled to -25°C and very small red diamond-shaped crystals were formed.

3.4.3 INFRARED SPECTRUM OF THE RED PRODUCT

The infrared spectrum of the red product in CH_2Cl_2 is shown in Figure 3.10. The spectrum exhibits five peaks and shows no bridging carbonyl. Possible products may include $[(CO)_4CoSi]_2Fe_3(CO)_9$ {6} or $[(CO)_4CoSi]_2Fe_4(CO)_{12}$ {7}. The solubility of $[(CO)_4CoGe]_2Fe_3(CO)_9$ in CH_2Cl_2 matches that of the red product (both very slightly soluble in CH_2Cl_2) and its infrared spectrum is compared below (Table 3.6). The infrared comparison is poor but cannot be totally rejected.

Table 3.6

INFRARED SPECTRUM OF RED PRODUCT COMPARED TO $[(CO)_4CoGe]_2Fe_3(CO)_9$	
RED PRODUCT	**$[(CO)_4CoGe]_2Fe_3(CO)_9$**
2111 m	2118 vw
	2102 w
2063 w	2042 sh
2036 vs	2016 vs br
2012 m	
1976 mw	1970 m sh

Figure 3.10

INFRARED SPECTRUM OF RED PRODUCT

CH_2Cl_2 SOLUTION

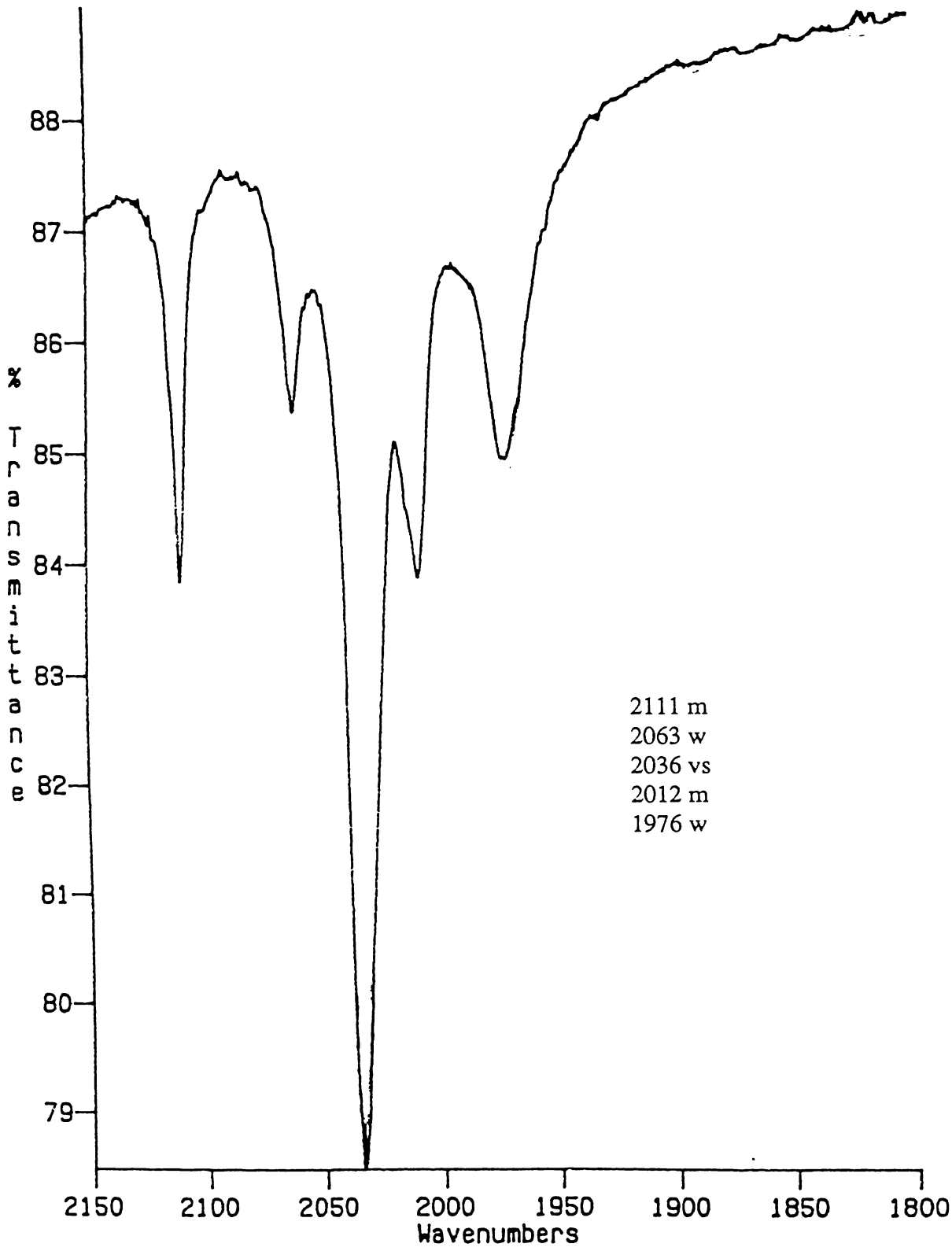

3.4.4 MASS SPECTRUM OF THE RED PRODUCT

The mass spectrum of the red product is listed in Table 3.7. The mass spectrum obtained was of low intensity due to the involatile nature of the product. From the highest ion seen (m/e = 726) there is a weak series of peaks due to the loss of ten carbonyl ligands to the ion (m/e = 446). A few very strong ions are seen at m/e = 306 and 278 which are related by the loss of one carbonyl and a strong ion at m/e = 288. The core $^{56}Fe_4{}^{59}Co$ would have m/e = 283.

Table 3.7

MASS SPECTRUM OF RED PRODUCT		
m/e	**Int**	**Assignment**
726	w	$RED(CO)_n$ n = 10
698	w	n = 9
670	w	n = 8
642	-	n = 7
614	w	n = 6
586	w	n = 5
558	-	n = 4
530	w	n = 3
502	w	n = 2
474	-	n = 1
446	w	n = 0
306	s	
278	s	
288	s	

3.4.5 ELECTRON PROBE STUDY OF THE RED PRODUCT

The electron probe analysis of several sites of the red product showed this to contain the elements iron, cobalt and silicon with a Fe to Co ratio of 1.8-2.0 to 1. The Si to Co ratio is indicated to be 1.0-2.0 to 1 but the silicon is at the lower limits of this instrument so this figure is unreliable. The overall ratio can be considered as $Fe_{2n}Co_nSi_n(CO)_m$.

3.4.6 PROPERTIES AND DISCUSSION

The red product is only slightly soluble in CH_2Cl_2 and forms a pink-red solution when hot CH_2Cl_2 is used. The red crystals are diamond shaped and are relatively air-stable.

The reaction of SiH_4 with $Fe(CO)_5$ may form $(HSi)_2Fe_3(CO)_9$ which when $Co_2(CO)_8$ is added later replaces the hydrogen forming $[(CO)_4CoSi]_2Fe_3(CO)_9$ **{6}**. This is plausible when we consider the reaction of $RSiH_3$ (R = Me, Ph) with $Fe(CO)_5$ forming clusters of the type $(RSi)_2Fe_3(CO)_9$ **{6}** (R = Me, Ph). Also Si-H bonds are readily replaced by cobalt at room temperature. The very low solubility of the compound is similar to that found for $[(CO)_4CoGe]_2Fe_3(CO)_9$.

$[(CO)_4CoSi]_2Fe_4(CO)_{12}$ **{7}** can also be considered as a possible candidate. The formation of $(HSi)_2Fe_4(CO)_{12}$ could be envisaged which would readily react with $Co_2(CO)_8$ forming $[(CO)_4CoSi]_2Fe_4(CO)_{12}$. This elemental ratio is consistent with the electron probe data. This cluster also does not contain a bridging carbonyl which is consistent with the infrared spectrum.

The mass spectrum does not support the core structure of either cluster, while the infrared spectrum shows some characteristics of both clusters. Only X-ray crystallography will determine the exact structure, but no suitable crystals have yet been obtained.

3.5 REACTION OF THE RED PRODUCT WITH TETRAHYDROFURAN

3.5.1 EXPERIMENTAL

Attempts to crystallise the red product from THF resulted in decomposition of the cluster to form an ionic product. Crystals red/black in colour were obtained from the cooled solution.

3.5.2 INFRARED SPECTRUM OF $[FeCo_3(CO)_{12}]^-$

The infrared spectrum of $[FeCo_3(CO)_{12}]^-$ in THF is shown in Figure 3.11. The infrared spectrum is dominated by a very strong peak at 1999 cm^{-1} with a number of very weak peaks which are some-what dubious. The low frequency peaks are consistent with the cluster having a negative charge.

Figure 3.11

INFRARED SPECTRUM OF $[FeCo_3(CO)_{12}]^-$

THF SOLUTION

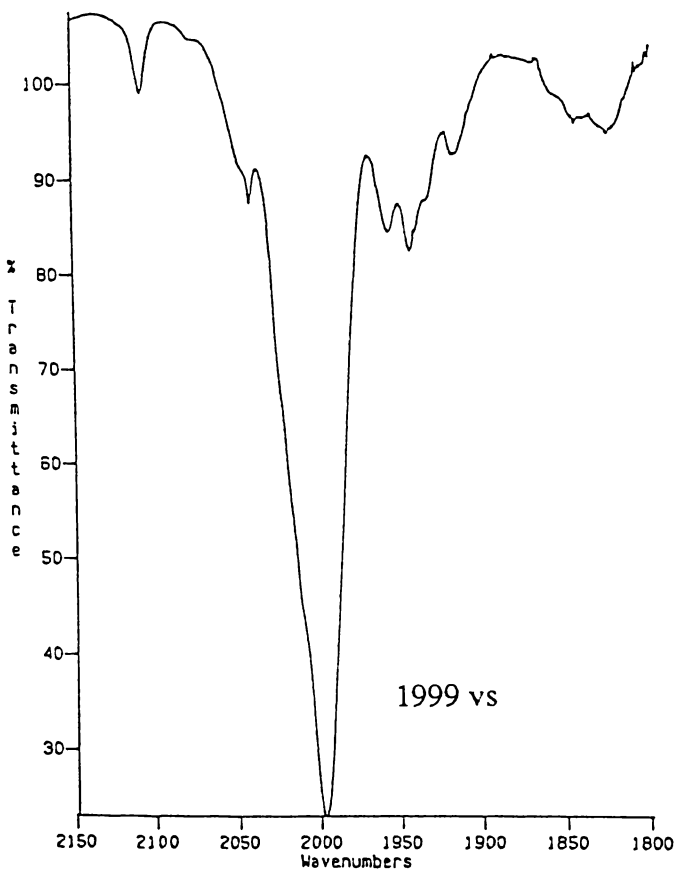

3.5.3 CRYSTALLOGRAPHIC STUDY OF $[Fe(THF)_4(H_2O)_2][FeCo_3(CO)_{12}]_2.4THF$

Dark red crystals of $[Fe(THF)_4(H_2O)_2][FeCo_3(CO)_{12}]_2.4THF$ were obtained from a cooled THF solution. Preliminary precession photographs using Cu-Kα radiation showed that the crystal had monoclinic symmetery and belonged to the space group C2/m.

Intensity data were collected on a suitable crystal at the University of Canterbury on a Nicolet P3 diffractometer. A scan range of $2°<2\theta<36°$ was employed to collect 2474 unique reflections using Mo-Kα radiation. An empirical absorption correction was applied to the data with tranmission factors, 0.739 maximum and 0.480 minimum. 1476 reflections with $I>2\sigma(I)$ were used for the solution and refinement of the structure. Crystal data for $[Fe(THF)_4(H_2O)_2][FeCo_3(CO)_{12}]_2.4THF$ are given in Table 3.8.

Table 3.8

CRYSTAL DATA FOR $[Fe(THF)_4(H_2O)_2][FeCo_3(CO)_{12}]_2.4THF$	
Formula: $C_{56}H_{68}Co_6Fe_3O_{34}$	Mr = 1806.27
Monoclinic	Space Group = C2/m
Cryst. Colour: Dark Red	
Cryst. Dimensions: 0.5 x 0.5 x 0.3 mm	
a = 20.852(7) Å	α = 90.00°
b = 13.551(6) Å	β = 92.62(1)°
c = 12.649(6) Å	γ = 90.00°
U = 3570(3) $Å^3$	Dcalc = 1.69 g cm^{-3}
Z = 2	
F(000) = 1496	Temp = 153 K
μ(Mo-Kα) = 19.7 cm^{-1}	
Unique Data = 2474	Range = $2°<2\theta<36°$
Refinement Data = 1476	Final R = 0.1186

SHELXS-86 and SHELX-76 [98] crystallographic programs were used for all computations. Positions of the heavy atoms were obtained by direct methods using TREF. Further refinement and difference map cycles located the carbonyl ligands and finally carbon atoms associated with the THF molecules. One unique THF molecule was ordered but the other showed disorder and could not be partially modelled. Anisotropic temperature factors were assigned to the cobalt and iron atoms only. Final refinement (full-matrix least-squares based on F) converged to R = 0.1186, Rw = 0.1319 with $w = 1.8698[\sigma^2(F) + 0.003928F^2]^{-1}$. Largest shift/e.s.d in the final cycle was 0.015 with 1.35 e $Å^{-3}$ electron density remaining in the final difference map.

Positional and thermal parameters along which complete tables of bond lengths and angles are presented in Appendix Two. Calculated and observed structure factors have been retained at the University of Waikato.

3.5.4 STRUCTURE OF $[Fe(THF)_4(H_2O)_2][FeCo_3(CO)_{12}]_2.4THF$

Figure 3.12 shows the overall formula and arrangement of $[Fe(THF)_4(H_2O)_2][FeCo_3(CO)_{12}]_2.4THF$. Diagrams of the individual ions, $[FeCo_3(CO)_{12}]^-$ and $[Fe(THF)_4(H_2O)_2]^{2+}$ are shown in Figures 3.13 and 3.14 respectively. Selected bond lengths and angles are given in Tables 3.9 and 3.10. Due to the poor refinement distances are less reliable and only a brief discussion will be made. The anion lies on a mirror plane with the cation lying on a mirror plane with two fold symmetry.

The structure of the anion $[FeCo_3(CO)_{12}]^-$ consists of a tetrahedral arrangement of four metal atoms with the carbonyl ligands adopting the same distribution as in $Co_4(CO)_{12}$ and $Rh_4(CO)_{12}$ [151] (Figure 3.15). This distribution consists of three carbonyl ligands bridging the edges of one triangular face with the remaining nine terminal bonded, six around the same triangular face with the capping metal atom having three. One bridging carbonyl lies on the mirror plane and is therefore constrained to be symmetrically bonded. The other bridging carbonyl is located unsymmetrically across the Co-Co bond. The remaining carbonyls have Co-C, Fe-C and C-O distances typical of terminal carbonyls.

Figure 3.12 Perspective View of $[Fe(THF)_4(H_2O)_2][FeCo_3(CO)_{12}]_2.4THF$

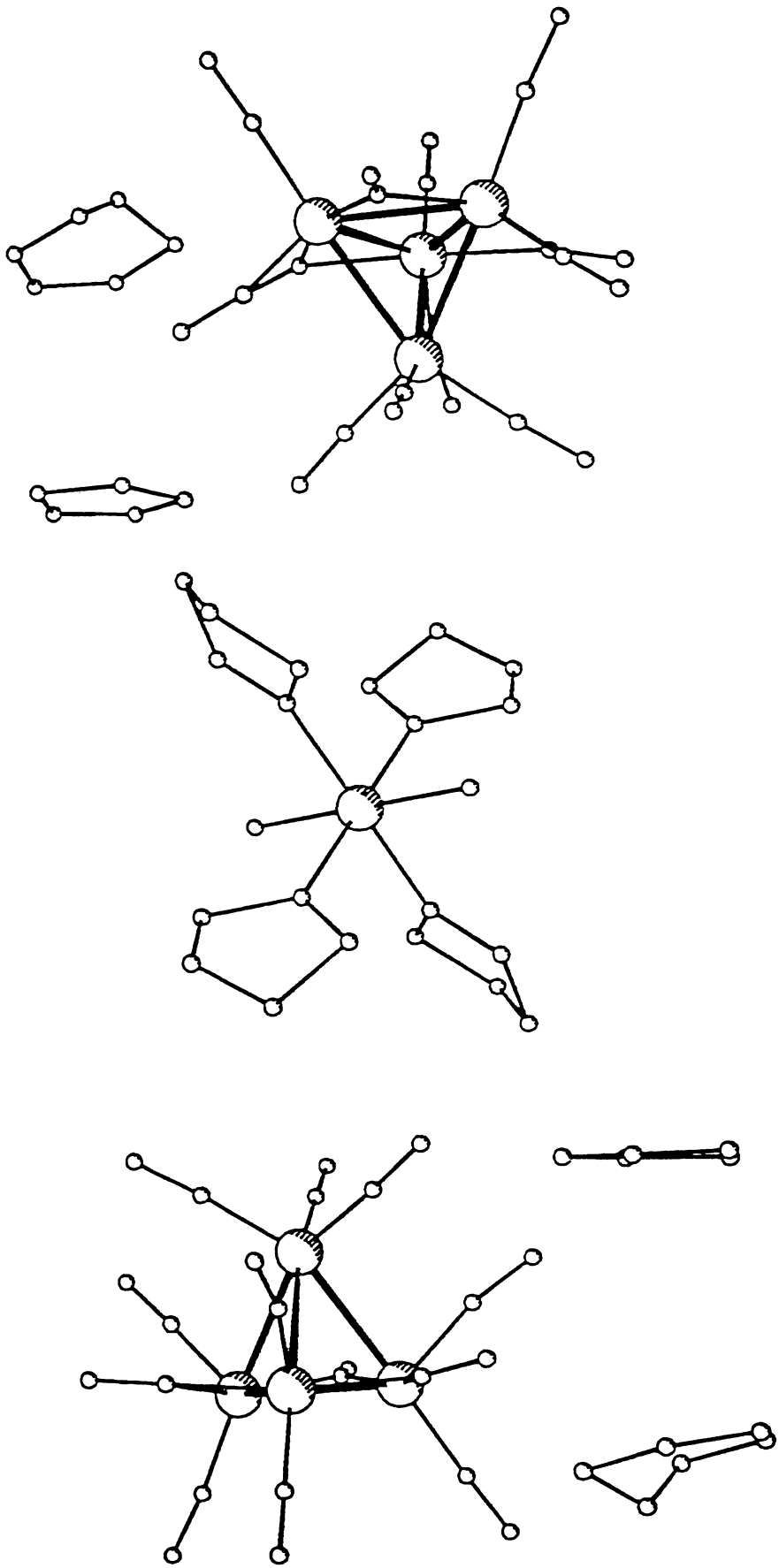

Figure 3.13 Perspective View of $[FeCo_3(CO)_{12}]^-$

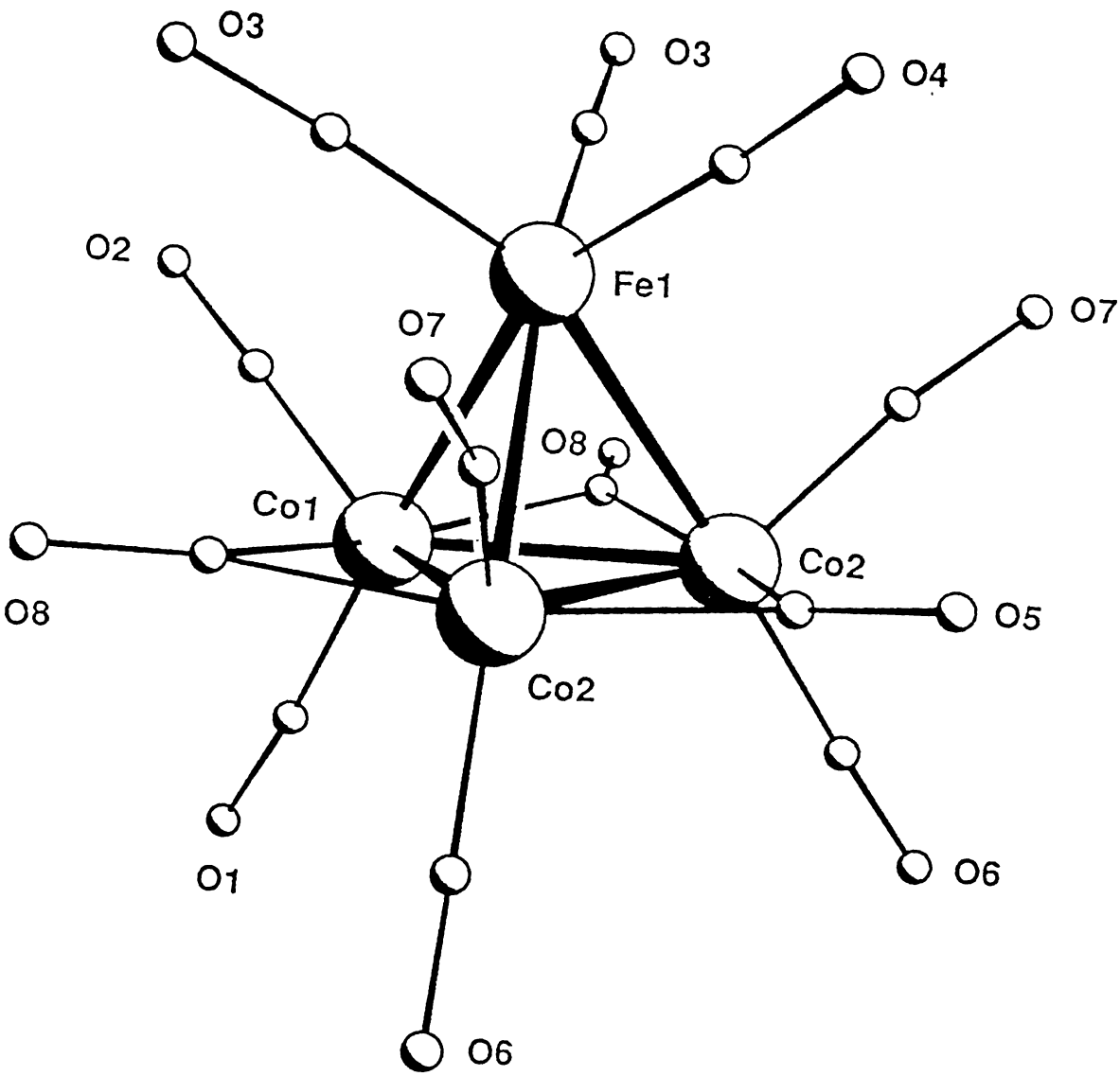

Figure 3.14 Perspective View of $[Fe(THF)_4(H_2O)_2]^{2+}$

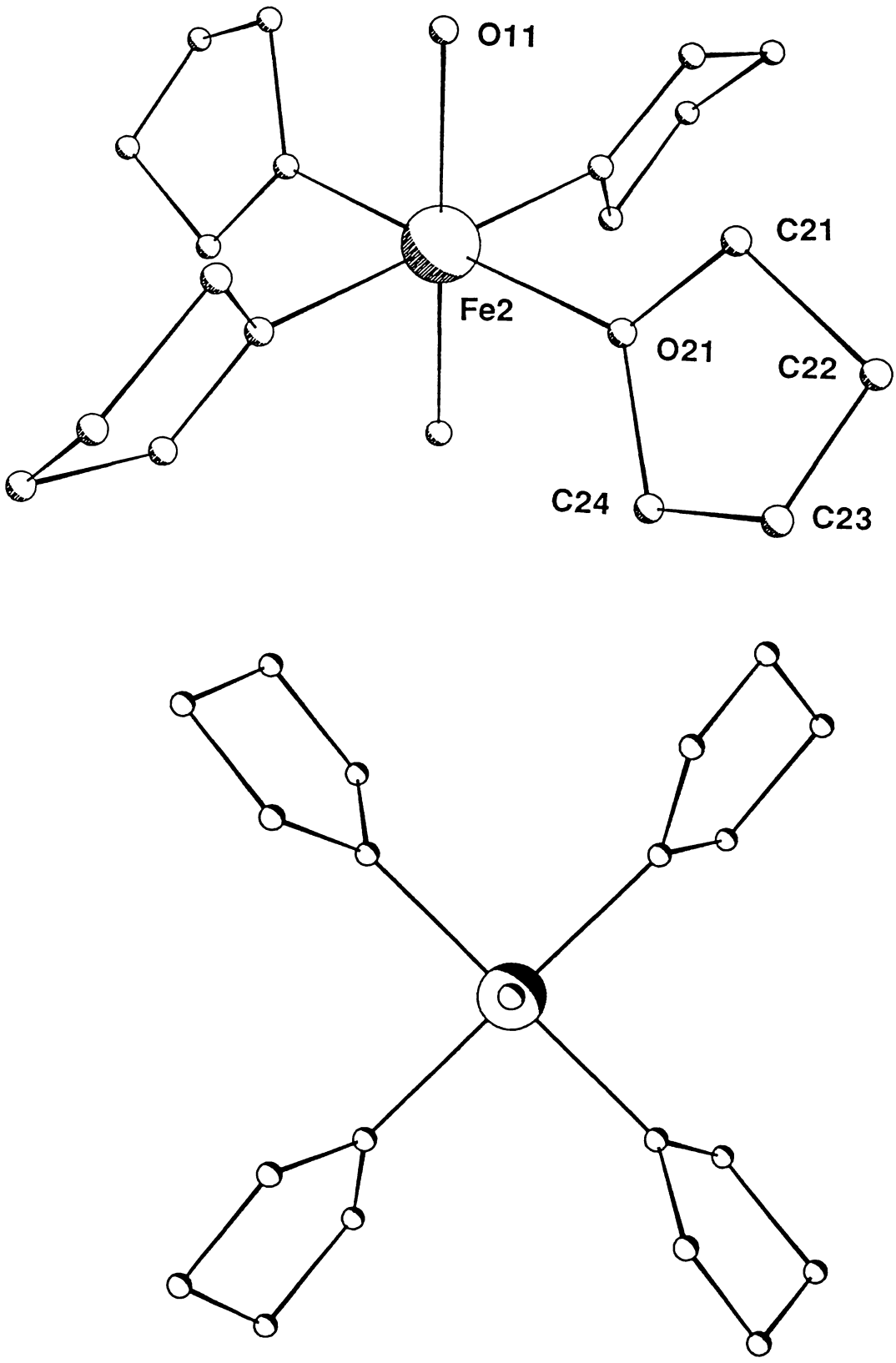

Table 3.9

SELECTED BOND LENGTHS FOR $[Fe(THF)_4(H_2O)_2][FeCo_3(CO)_{12}]_2.4THF$			
Co(1) ---Co(2)	2.502(4)	Fe(2) ---O(11)	2.10(2)
Co(1) ---Fe(1)	2.533(5)	Fe(2) ---O(21)	2.12(1)
Co(2) ---Co(2)	2.515(7)		
Co(2) ---Fe(1)	2.551(5)		

Table 3.10

SELECTED BOND ANGLES FOR $[Fe(THF)_4(H_2O)_2][FeCo_3(CO)_{12}]_2.4THF$			
Co(2) -Co(1) -Fe(1)	60.9(1)	-Fe(2) -O(21)	90.4(5)
Co(2) -Co(1) -Co(2)	60.4(2)		
Co(1) -Co(2) -Fe(1)	60.2(1)		
Co(1) -Fe(1) -Co(2)	59.0(1)		

The $[FeCo_3(CO)_{12}]^-$ core is arranged with the iron atom occupying the capping position above a cobalt triangle. The alternative position with the iron in the triangular unit is also possible. The Co(1)-Co(2) and Co(2)-Co(2') bond lengths at 2.502(4)Å and 2.515(7)Å (both carbonyl bridged) lie within the range seen for $Co_4(CO)_{12}$ (2.441(14)Å, 2.527(10)Å and 2.486(13)Å). The bond lengths to the Fe(1) atom are 2.533(5)Å and 2.551(5)Å, these bonds contain no bridging carbonyls and are therefore slightly longer.

The structure of the cation $[Fe(THF)_4(H_2O)_2]^{2+}$ (Figure 3.14) can be rationalised as four THF molecules bonded to the central metal (Fe) in a planar arrangement. Two water molecules are also bonded to the metal, above and below the THF plane.

The iron-oxygen (Fe(2)-O(21)) distance to the bonded THF molecule at 2.12(1)Å compares very closely to that found for $[Fe(THF)_6]^{2+}$ (Figure 3.16) [135] at 2.143(8)Å. Distances and angles around the ordered THF molecules are reasonable when compared to those found for $[Fe(THF)_6]^{2+}$. One THF solvent molecule shows up clearly with the other containing some disorder which could not be resolved.

The iron-oxygen (Fe(2)-O(11)) distance to the bonded water molecule at 2.10(2)Å also compares well to that of Fe-O in $[Fe(H_2O)_6]^{2+}$ [136], with an average value of 2.123(9)Å.

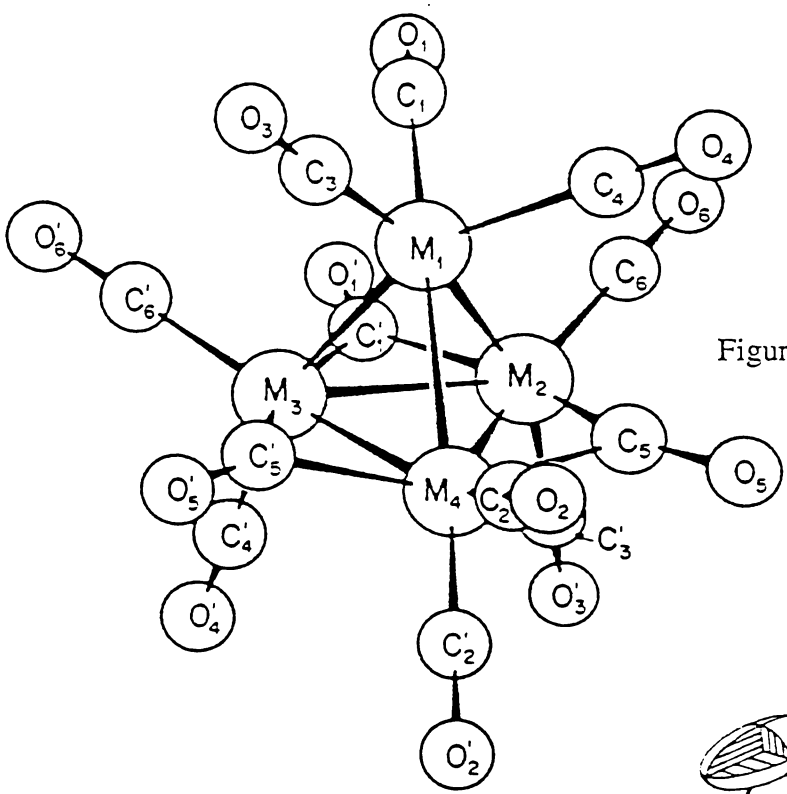

Figure 3.15 $Co_4(CO)_{12}$

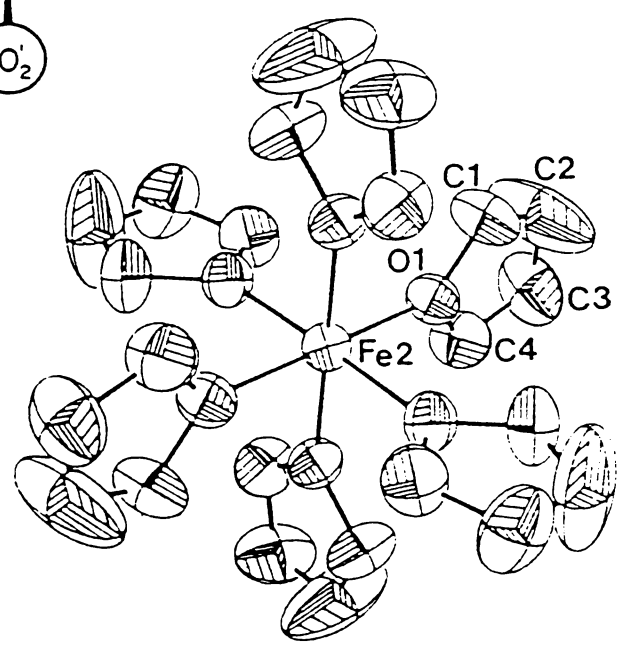

Figure 3.16 $[Fe(THF)_6]^{2+}$

3.6 REACTION OF SiH_4 AND GeH_4 WITH $Fe(CO)_5/[Fe(CO)_2Cp]_2$

3.6.1 INTRODUCTION

Previous work by S.G. Anema [38] showed that the trigonal bipyramid $[Cp(CO)_2FeSi]_2Fe_3(CO)_9$ {6} was obtained in high yields from the reaction of SiH_4 with $Fe(CO)_5$ and $[Fe(CO)_2Cp]_2$ at high temperature. This was characterised by infrared and mass spectroscopy and by X-ray crystallography. The analogous reaction using GeH_4 was conducted and the infrared spectrum indicated that the germanium-equivalent had formed. My contribution was to characterise the germanium product by X-ray crystallography and to obtain NMR spectra of these clusters.

3.6.2 PREPARATION OF $[Cp(CO)_2FeSi]_2Fe_3(CO)_9$

SiH_4 (0.0218g, 0.678mmol) was condensed into a 50ml high pressure glass ampoule with $Fe(CO)_5$ (4.73g, 22mmol) and $[Cp(CO)_2Fe]_2$ (0.120g, 0.339mmol) in 10ml of petroleum spirit (bp 100-120°C) solvent. This was heated at 150°C for 120 minutes giving a deep red solution and red/black crystals. Incondensable gases, unreacted $Fe(CO)_5$ and SiH_4, and solvent were removed under vacuum. The residue was extracted with hexane (3 x 20ml) to remove $Si[Fe_2(CO)_8]_2$ {5} (υCO, (CH_2Cl_2) 2076 m, 2050 vs, 2030 w, 2013 s, 1990 vw, cm^{-1}), together with small amounts of unidentified products.

The remaining solid was almost pure $[Cp(CO)_2FeSi]_2Fe_3(CO)_9$ with a yield of 70%.

3.6.3 INFRARED SPECTRUM OF $[Cp(CO)_2FeSi]_2Fe_3(CO)_9$

The infrared spectrum of $[Cp(CO)_2FeSi]_2Fe_3(CO)_9$ in CH_2Cl_2 is shown in Figure 3.17. Comparsion of the infrared spectrum of $[Cp(CO)_2FeSi]_2Fe_3(CO)_9$ to those of $(RSi)_2Fe_3(CO)_9$ {6} (R = Me, Ph) [38] and $(RGe)_2Fe_3(CO)_9$ (R = Me, Et) [38], which all contain the E_2Fe_3 core structure, is given in Table 3.11. This shows that the peaks at 2016 cm^{-1} and 1947 cm^{-1} could be associated with the $Fe_3(CO)_9$ core. The remaining peaks are due to the carbonyls of the capping groups and with the lower symmetry of this cluster compared to those which are

capped with an organic group, there is probably some contribution from the core carbonyls as well.

Table 3.11

INFRARED SPECTRUM OF $[Cp(CO)_2FeSi]_2Fe_3(CO)_9$ COMPARED TO THOSE OF $(RSi)_2Fe_3(CO)_9$ AND $(RGe)_2Fe_3(CO)_9$				
$[Cp(CO)_2FeSi]_2Fe_3(CO)_9$	**$(RSi)_2Fe_3(CO)_9$**		**$(RGe)_2Fe_3(CO)_9$**	
	R = Me	**R = Ph**	**R = Me**	**R = Et**
2051 m				
2031 s				
2016 s	2016 vs	2014 vs	2013 vs	2014 vs
1999 vs				
1947 m	1967 m	1965 m	1966 m	1963 m

3.6.4 NMR SPECTRUM OF $[Cp(CO)_2FeSi]_2Fe_3(CO)_9$

The ^1H and ^{13}C NMR spectra of $[Cp(CO)_2FeSi]_2Fe_3(CO)_9$ in $CDCl_3$ were obtained. The ^1H NMR spectrum gave a sharp singlet at δ 5.29 which is higher than that observed in other compounds containing cyclopentadienyl groups (e.g. $Cp(CO)_2FeGeCo_3(CO)_9$ [97] at δ 4.13). ^{13}C NMR spectrum showed three peaks, δ 85.8 corresponding to the cyclopentadienyl group, δ214.7 assigned to carbonyls of the trigonal core ($Fe_3(CO)_9$) and δ210.5 assigned to the capping carbonyls ($Fe(CO)_2$) which indicates that these carbonyls in their respective environments are in equivalent positions in solution.

No ^{29}Si NMR signal could be detected with the available instrument even with the use of $Cr(acac)_3$ as a relaxation aid.

Figure 3.17

INFRARED SPECTRUM OF $[Cp(CO)_2FeSi]_2Fe_3(CO)_9$

CH_2Cl_2 SOLUTION

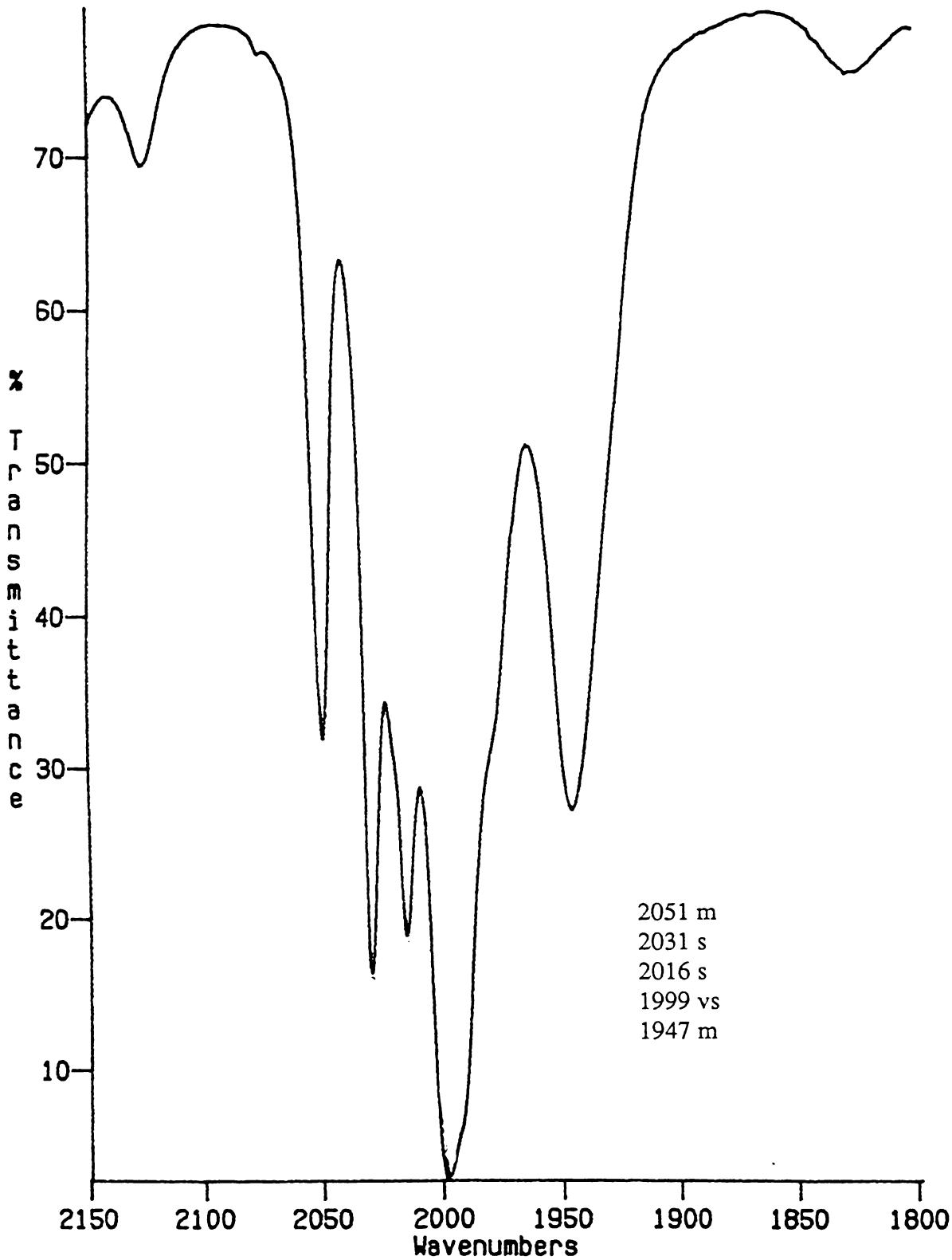

3.6.5 EXPERIMENTAL

Similarly, a mixture of $Fe(CO)_5$ (4.37g, 22mmol), $[Cp(CO)_2Fe]_2$ (0.159g, 0.45mmol), and GeH_4 (0.0766g, 1.0mmol) was heated at 145°C for 120 minutes in a petroleum spirit solvent. Black needle shaped crystals had formed with a deep red solution. The volatile components of the reaction were removed under vacuum and the hexane-soluble fraction was extracted (3 x 10ml) to remove $Ge[Fe_2(CO)_8]_2$ {5} (υCO, (CH_2Cl_2) 2078 m, 2050 vs, 2030 w, 2015 s, cm^{-1}) and another unidentified product (υCO, (hexane) 2024 s, 2001 vs cm^{-1}).

The remaining solid was dissolved in toluene (20ml), filtered and slowly cooled to crystallise the major product. Some unreacted $[Cp(CO)_2Fe]_2$ remained in this fraction with 0.268g of $[Cp(CO)_2FeGe]_2Fe_3(CO)_9$ isolated, 65% yield based on $[Cp(CO)_2Fe]_2$.

Similar preparations all produced generally the same results with high yields of $[Cp(CO)_2FeGe]_2Fe_3(CO)_9$.

3.6.6 INFRARED SPECTRUM OF $[Cp(CO)_2FeGe]_2Fe_3(CO)_9$

The infrared spectrum of $[Cp(CO)_2FeGe]_2Fe_3(CO)_9$ in CH_2Cl_2 was recorded and is shown in Figure 3.18. Comparison of this germanium cluster to that of the silicon analogue is shown in Table 3.12. The two spectra are very similar and show only a small shift to higher frequency for the silicon cluster.

Table 3.12

INFRARED SPECTRUM OF $[Cp(CO)_2FeGe]_2Fe_3(CO)_9$	
$[Cp(CO)_2FeE]_2Fe_3(CO)_9$	
E = Ge	**E = Si**
2048 w	2051 m
2030 m	2031 s
2021 w	2016 s
1997 vs	1999 vs
1942 mw	1947 m

Figure 3.18

INFRARED SPECTRUM OF $[Cp(CO)_2FeGe]_2Fe_3(CO)_9$

TOLUENE SOLUTION

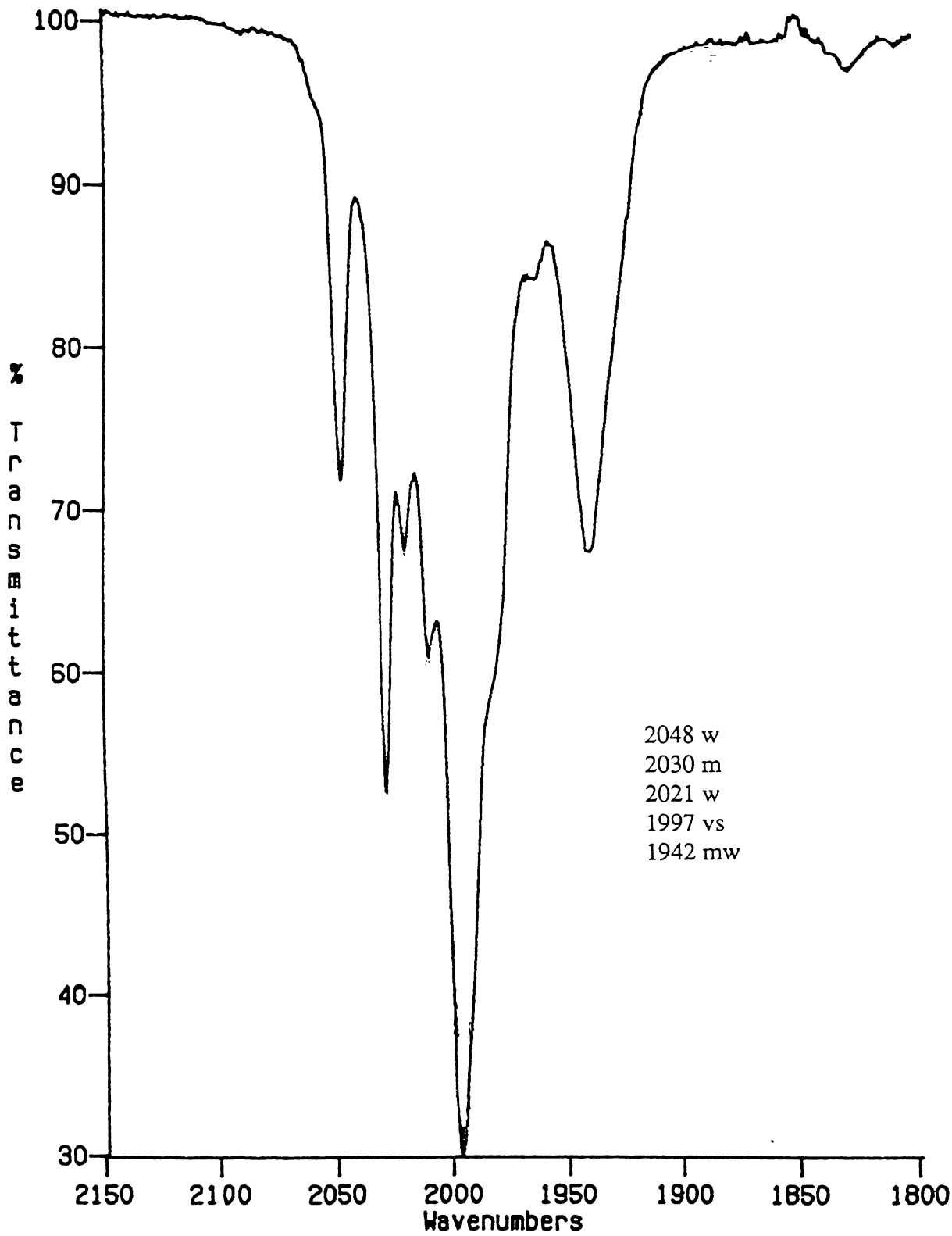

3.6.7 NMR SPECTRUM OF $[Cp(CO)_2FeGe]_2Fe_3(CO)_9$

The ^1H and ^{13}C NMR spectra of $[Cp(CO)_2FeGe]_2Fe_3(CO)_9$ in $CDCl_3$ were very similar to those of the silicon analogue. The ^1H NMR spectrum gave a singlet at δ 5.32 which corresponds closely to that seen for the cyclopentadienyl group in the silicon analogue. An increase in the δ value is seen for the clusters $[Cp(CO)_2FeE]_2Fe_3(CO)_9$ {6}, E = Si [38], Ge [38] and Sn [42] with δ values of 5.29, 5.32 and 5.68 respectively. The ^{13}C NMR spectrum is nearly identical to that of the silicon analogue with signals at δ84.8 due to C_5H_5, δ214.6 due to the $Fe_3(CO)_9$ core and at δ210.0 due to the $Fe(CO)_2$ capping group.

3.6.8 X-RAY CRYSTALLOGRAPHIC STUDY OF $[Cp(CO)_2FeGe]_2Fe_3(CO)_9$

Dark-red rectangular crystals of $[Cp(CO)_2FeGe]_2Fe_3(CO)_9$ were obtained from a slowly cooled toluene solution. Preliminary precession photographs using Cu-Kα radiation indicated that the crystal had monoclinic symmetry and belonged to the space group $P2_1/n$.

Intensity data were collected on a suitable crystal of dimensions 0.34 x 0.21 x 0.2 mm for 5036 unique reflections , in the range $3°<2\theta<50°$, at the University of Canterbury on a Nicolet P3 diffractometer. Graphite-monochromated Mo-Kα X-rays (0.71069Å) were used as a starting point. For structure solution and refinement, 3187 reflections were used with $I>2.5\sigma(I)$. Absorption corrections were based on the empirical ϕ-scan technique with transmission factors, 0.95 maximum and 0.65 minimum. Crystal data for $[Cp(CO)_2FeGe]_2Fe_3(CO)_9$ are given in Table 3.13.

The positional coordinates of the isomorphous silicon analogue $[Cp(CO)_2FeSi]_2Fe_3(CO)_9$ were used. These were refined by full-matrix least-squares using SHELX-76 [98] programs. Anisotropic temperature factors were assigned to the Fe, Ge, C and O atoms with the hydrogen atoms included in calculated positions with common temperature factors. Final refinement converged to R = 0.0551, Rw = 0.0543 with $w = 1.2442[\sigma^2(F) + 0.001131F^2]^{-1}$. Final difference map showed no electron density greater than 0.8 e $Å^{-3}$ and the largest shift/e.s.d of 0.011.

Table 3.13

CRYSTAL DATA FOR $[Cp(CO)_2FeGe]_2Fe_3(CO)_9$	
Formula: $C_{23}H_{10}Fe_5Ge_2O_{13}$	Mr = 918.78
Monoclinic	Space Group = $P2_1/n$
Cryst. Colour: Dark Red	
Cryst. Dimensions: 0.34 x 0.21 x 0.20 mm	
a = 10.125(3) Å	$\alpha = 90.00°$
b = 10.024(3) Å	$\beta = 92.53(3)°$
c = 28.308(9) Å	$\gamma = 90.00°$
U = 2870(1) $Å^3$	Dcalc = 2.13 g cm^{-3}
Z = 4	
F(000) = 1784	Temp = 153 K
μ(Mo-Kα) = 47 cm^{-1}	
Unique Data = 5036	Range = $3°<2\theta<50°$
Refinement Data = 3187	Final R = 0.0551

Positional and thermal parameters along with complete tables of bond lengths and angles are presented in Appendix Three. Calculated and observed structure factors have been retained at the University of Waikato.

3.6.9 STRUCTURE OF $[Cp(CO)_2FeGe]_2Fe_3(CO)_9$

Diagrams of the molecule are shown in Figure 3.19 and 3.20 with selected bond lengths and angles given in Table 3.14 and 3.15. Atom labelling is shown in Figure 3.19 and is used throughout this discussion.

The structure of $[Cp(CO)_2FeGe]_2Fe_3(CO)_9$ consists of a triangle of iron atoms capped on either face by a $GeFe(CO)_2Cp$ group. This trigonal bipyramidal cluster is isomorphous with the silicon analogue $[Cp(CO)_2FeSi]_2Fe_3(CO)_9$ [38] and is structurally similar to the tin analogue $[Cp(CO)_2FeSn]_2Fe_3(CO)_9$ [42], which was reported in 1977.

Figure 3.19 Perspective View of $[Cp(CO)_2FeGe]_2Fe_3(CO)_9$

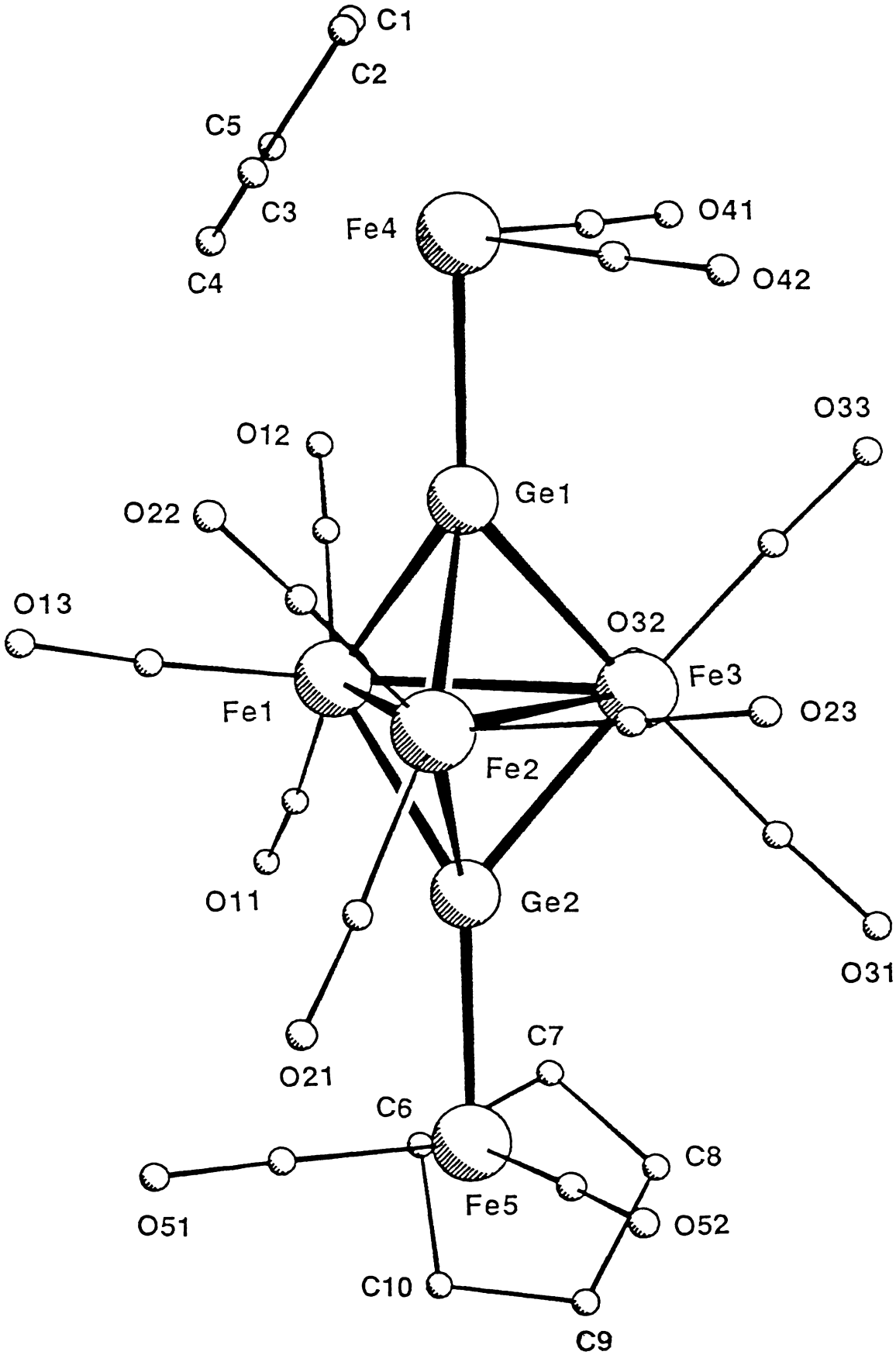

Figure 3.20 Stereo View of $[Cp(CO)_2FeGe]_2Fe_3(CO)_9$

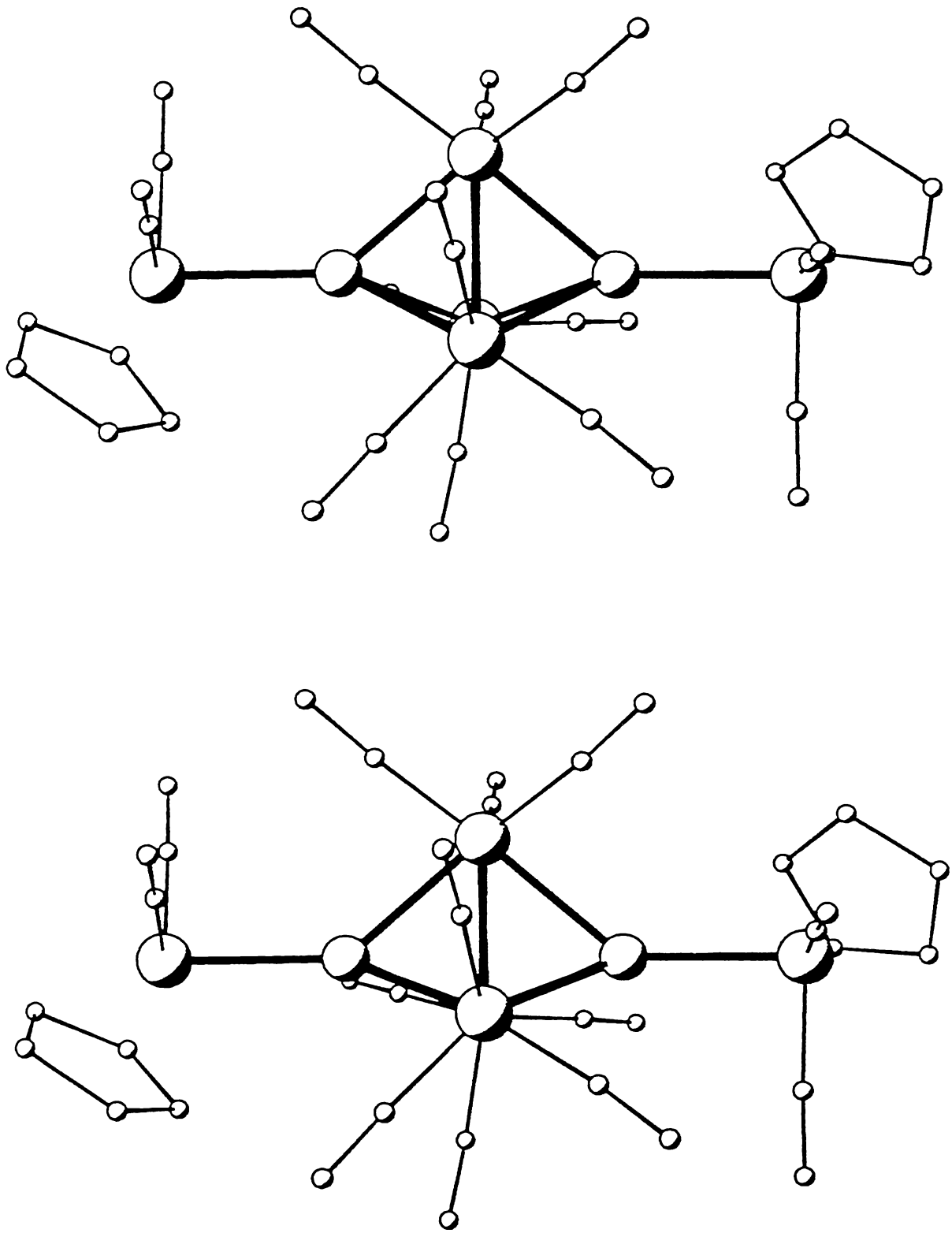

Table 3.14

SELECTED BOND LENGTHS FOR $[Cp(CO)_2FeGe]_2Fe_3(CO)_9$ (Å)			
Ge(1) ---Fe(1)	2.367(2)	Ge(1) ---Fe(2)	2.365(2)
Ge(1) ---Fe(3)	2.391(2)	Ge(1) ---Fe(4)	2.316(2)
Ge(2) ---Fe(1)	2.382(2)	Ge(2) ---Fe(2)	2.380(2)
Ge(2) ---Fe(3)	2.383(2)	Ge(2) ---Fe(5)	2.319(2)
Fe(1) ---Fe(2)	2.742(2)	Fe(1) ---Fe(3)	2.717(2)
Fe(2) ---Fe(3)	2.719(2)		

Table 3.15

SELECTED BOND ANGLES FOR $[Cp(CO)_2FeGe]_2Fe_3(CO)_9$ (°)			
Fe(1) -Ge(1) -Fe(2)	70.8(1)	Fe(1) -Ge(1) -Fe(3)	69.6(1)
Fe(1) -Ge(1) -Fe(4)	139.8(1)	Fe(2) -Ge(1) -Fe(3)	69.7(1)
Fe(2) -Ge(1) -Fe(4)	136.2(1)	Fe(3) -Ge(1) -Fe(4)	139.4(1)
Fe(1) -Ge(2) -Fe(2)	70.3(1)	Fe(1) -Ge(2) -Fe(3)	69.5(1)
Fe(1) -Ge(2) -Fe(5)	140.3(1)	Fe(2) -Ge(2) -Fe(3)	69.6(1)
Fe(2) -Ge(2) -Fe(5)	137.4(1)	Fe(3) -Ge(2) -Fe(5)	138.1(1)
Ge(1) -Fe(1) -Ge(2)	97.3(1)	Ge(1) -Fe(1) -Fe(2)	54.6(1)
Ge(1) -Fe(1) -Fe(3)	55.6(1)	Ge(2) -Fe(1) -Fe(2)	54.8(1)
Ge(2) -Fe(1) -Fe(3)	55.3(1)	Fe(2) -Fe(1) -Fe(3)	59.7(1)
Ge(1) -Fe(2) -Ge(2)	97.4(1)	Ge(1) -Fe(2) -Fe(1)	54.6(1)
Ge(1) -Fe(2) -Fe(3)	55.6(1)	Ge(2) -Fe(2) -Fe(1)	54.9(1)
Ge(2) -Fe(2) -Fe(3)	55.2(1)	Fe(1) -Fe(2) -Fe(3)	59.7(1)
Ge(1) -Fe(3) -Ge(2)	96.6(1)	Ge(1) -Fe(3) -Fe(1)	54.8(1)
Ge(1) -Fe(3) -Fe(2)	54.7(1)	Ge(2) -Fe(3) -Fe(1)	55.2(1)
Ge(2) -Fe(3) -Fe(2)	55.1(1)	Fe(1) -Fe(3) -Fe(2)	60.6(1)

The triangular iron core is in the shape of an isosceles triangle with the two equal distances, Fe(1)-Fe(3) at 2.717(2)Å and Fe(2)-Fe(3) at 2.719(2)Å. The longer Fe(1)-Fe(2) distance 2.742(2)Å is probably due to one germanium atom which is bonded closer to this edge. These bond lengths (ave 2.726Å), as expected, are longer than those of the silicon cluster, ave Fe-Fe 2.666Å and are shorter than those of the tin cluster, ave Fe-Fe distance of 2.792Å (Table 3.16). This shows that as the capping atom changes from Si to Ge to Sn, the Fe-Fe bond lengths increase reflecting the relative size change.

Ge(1) is not symmetrically placed above the triangle but is bonded closer to the Fe(1)-Fe(2) edge, with a distances of 2.367(2)Å to Fe(1) and 2.365(2)Å to Fe(2). The Ge(1)-Fe(3) distance of 2.391(2)Å is significantly longer. In contrast Ge(2) is symmetrically placed above the iron triangle with distances of 2.382(2)Å, 2.380(2)Å and 2.383(2)Å to Fe(1), Fe(2) and Fe(3) respectively. Both apical substituents have the same low symmetry therefore this deviation from the most symmetrical site is due to crystal-packing effects.

The average Ge-Fe distance of 2.378(±13)Å can be compared to similar Ge_2Fe_3 core structures such as $[(CO)_4CoGe]_2Fe_3(CO)_9$ [36] ave 2.342(±32)Å and $(EtGe)_2Fe_3(CO)_9$ **{6}** [38] ave 2.321(±19)Å which are shorter, but compared to $[(CO)_5ReGe]_2Fe_3(CO)_9$ **{6}** [115] ave 2.379Å is the same.

Ge-Fe distances to the apical $Fe(CO)_2Cp$ groups are markedly shorter than to the core with lengths, Ge(1)-Fe(4) 2.316(2)Å and Ge(2)-Fe(5) 2.319(2)Å. This effect is also seen for the analogous silicon cluster, with Si-Fe core ave 2.306Å, compared to Si-Fe apical ave 2.250Å and for the tin analogue [42] with the longer distance to the core, Sn-Fe ave 2.537(4)Å compared to Sn-Fe apical ave 2.471(5)Å (Table 3.16).

The cyclopentadienyl group on Fe(4) lies over the Fe(1)-Fe(2) edge which has the longest distance. The two terminal carbonyl ligands of Fe(4) lie between the axial carbonyls of the core over the Fe(1)-Fe(3) and Fe(2)-Fe(3) edges. The cyclopentadienyl group on Fe(5) though lies above the Fe(1)-Fe(3) edge with the two terminal carbonyls lying over the other two Fe-Fe edges between the axial core carbonyls.

Table 3.16

AVERAGE BOND LENGTHS FOR $[Cp(CO)_2FeE]_2Fe_3(CO)_9$			
BOND	**E = Si**	**E = Ge**	**E = Sn**
Fe-Fe (core)	2.666	2.726	2.792
E-Fe (core)	2.306	2.378	2.537
E-Fe (apical)	2.250	2.318	2.471

Each of the iron atoms in the trigonal core is bonded to three carbonyl ligands, two axial (up and down configuration) and one equatorial. The equatorial carbonyl ligands are all orientated in the same direction towards the next iron atom in the trigonal plane. The distances and angles are such that these carbonyl ligands should not be regarded as semibridging, although only a small rotation of the core would change this.

The terminal carbonyl ligands on the iron atoms adopt the same general arrangement described above for silicon and germanium clusters suggesting that this is determined by intramolecular rather than crystal-packing interactions.

Overall this structure completes the Si, Ge, Sn series for this cluster and it should be noted that there are only a few clusters where the Si, Ge, Sn, Pb set is available for comparison (example $E[Fe_2(CO)_8]_2$ **{5}**, E = Si, Ge, Sn, Pb, see section 1.3.4). Preparation of the silicon and germanium clusters proceeds in good yields from the reaction of SiH_4 or GeH_4 with $Fe(CO)_5$ and $[Cp(CO)_2Fe]_2$ at 150°C in petroleum spirit solvent. The only other known route to trigonal-bipyramidal clusters of this type is the reaction of $SnCl_2$ or $GeCl_4$/Ge with $Fe(CO)_5$ and $MnRe(CO)_{10}$ to prepare $[(CO)_5ReSn]_2Fe_3(CO)_9$ [114] or the germanium analogue [115].

CHAPTER FOUR

REACTIONS OF $PhSiH_3$, $BrSiH_3$ AND $ISiH_3$ WITH $Co_2(CO)_8$ AND $Co_4(CO)_{12}$

REACTIONS OF $PhSiH_3$, $BrSiH_3$ AND $ISiH_3$ WITH $Co_2(CO)_8$ AND $Co_4(CO)_{12}$

4.1 INTRODUCTION

Reactions of $Co_2(CO)_8$ with mono-organo substituted silanes such as $MeSiH_3$, $EtSiH_3$ and $PhSiH_3$ have been investigated and result in the formation of $(CO)_4CoRSiCo_2(CO)_7$ (R = Me, Et, Ph) compounds in high yields [12, 45]. Similar results are seen with mono-organo germanes, for example $PhGeH_3$ with $Co_2(CO)_8$ forms the cluster $(CO)_4CoPhGeCo_2(CO)_7$ {3} [12] (Figure 4.1) according to the equation below.

$$PhGeH_3 + 1.5Co_2(CO)_8 \rightarrow (CO)_4CoPhGeCo_2(CO)_7 + 1.5H_2 + CO$$

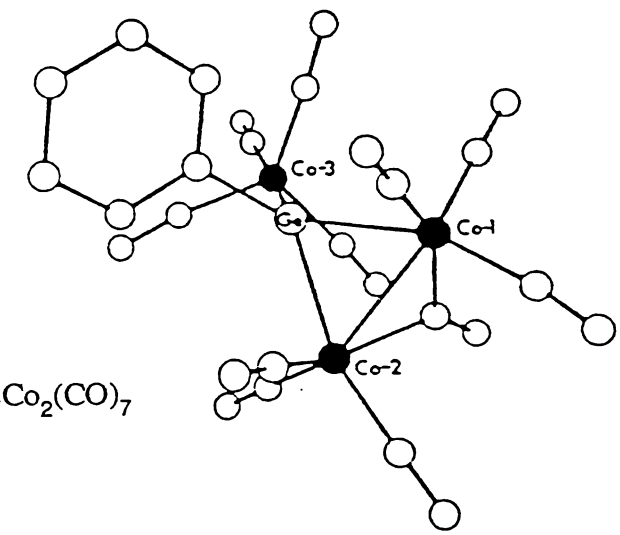

Figure 4.1 $(CO)_4CoPhGeCo_2(CO)_7$

When $(CO)_4CoPhGeCo_2(CO)_7$ (one Co-Co and 3Co-Ge bonds) is refluxed in hexane for several hours, it undergoes rearrangement with the loss of two carbonyl ligands to form the closed cluster $PhGeCo_3(CO)_9$ {2}, with three Co-Co bonds. At high carbon monoxide pressures (300 atm), $(CO)_4CoPhGeCo_2(CO)_7$ adds carbon monoxide to form the fully open compound $PhGe(Co(CO)_4)_3$, which contains no cobalt-cobalt bonds. On heating, this open arrangement of

cobalt groups, reforms first the semi-open, then the closed clusters with the loss of carbon monoxide according to the steps in the equation below.

$$\mathbf{PhGe(Co(CO)_4)_3 \rightarrow (CO)_4CoPhGeCo_2(CO)_7 \rightarrow PhGeCo_3(CO)_9}$$

$GeBr_4$ reacts with $Na[Co(CO)_4]$ under mild conditions to form the cluster $(CO)_4CoBrGeCo_2(CO)_7$ {3} [82] in which one halogen atom has not been substituted forming an analogous product to that described above. In contrast to such organic substituents, this bromine group can now undergo a further reaction with anionic groups such as $[Co(CO)_4]^-$, $[Mn(CO)_5]^-$, $[Fe_2(CO)_8]^{2-}$, etc, with the possibility of forming new clusters.

This chapter describes the initial investigation of the reaction of $BrSiH_3$ and $ISiH_3$ with $Co_2(CO)_8$ for the purpose of synthesising clusters which retain the functional halogen group. Investigation of the reactions of $PhSiH_3$ and $BrSiH_3$ with $Co_4(CO)_{12}$ is also reported.

4.2 REACTION OF $PhSiH_3$ WITH $Co_4(CO)_{12}$

4.2.1 INTRODUCTION

Clusters of the type $(RGe)_2Co_4(CO)_{11}$ (R = t-Bu, Ph) {7} have been prepared in low yield from the reaction of $RGeX_3$ with $K[Co(CO)_4]$ [122]. Other methods for preparing clusters of this type with Si or Ge include the reaction of Si_2H_6 or Ge_2H_6 with $Co_2(CO)_8$ to form $[(CO)_4CoE]_2Co_4(CO)_{11}$ (E = Si, Ge) {7} [35, 71], but this method is not applicable to the formation of any clusters without $Co(CO)_4$ moieties on the apical group. Another route is the reaction of $Fe(CO)_4(GeH_2Me)_2$ with $Co_2(CO)_8$ [120] to give $Me_2Ge_2Co_4(CO)_{14}$ which decarbonylates to form $(MeGe)_2Co_4(CO)_{11}$. This is generally more

applicable to a wider range of terminal groups but the synthesis of $Fe(CO)_4(GeH_2Me)_2$ is complex.

A more general and direct method involves the reaction of $RSiH_3$ or $RGeH_3$ with $Co_4(CO)_{12}$ to directly form E_2Co_4 clusters in high yield. $MeSiH_3$ reacts with $Co_4(CO)_{12}$ to form the square bipyramidal cluster $(MeSi)_2Co_4(CO)_{11}$ [36] in high yields according to the equation below.

$$2MeSiH_3 + Co_4(CO)_{12} \rightarrow (MeSi)_2Co_4(CO)_{11} + CO + 3H_2$$

An analogous reaction using $MeGeH_3$ with $Co_4(CO)_{12}$ also forms a square bipyramidal cluster, $(MeGe)_2Co_4(CO)_{11}$ [9, 119]. Similar germanium-cobalt clusters with ethyl and phenyl groups [37] have also been prepared by this route. To show further the generality of this reaction, $PhSiH_3$ was reacted with $Co_4(CO)_{12}$ and the product was fully characterised.

4.2.2 EXPERIMENTAL

$PhSiH_3$ (0.265g, 2.45mmol) was condensed into a 50ml high pressure ampoule with $Co_4(CO)_{12}$ (0.70g, 1.23mmol) in 10ml of hexane. The reaction was conducted at 40°C for 2 months which resulted in a dark red/brown solution with black crystals.

The contents were transferred to a Schlenk flask using CH_2Cl_2 and the solvent removed under vacuum. Hexane (15ml) was used to wash the solid free from the small amount of unreacted $Co_4(CO)_{12}$. Another 5ml of hexane was used to ensure the removal. The red/black solid was recrystallised from toluene by slowly cooling from 30°C to -25°. The isolated weight of $(PhSi)_2Co_4(CO)_{11}$ (0.792g, 1.05mmol) represents an 86% yield based on $PhSiH_3$. The cluster is slightly soluble in hexane with increasing solublity in toluene and CH_2Cl_2.

The yield can be increased to almost 100% by using a slight excess of the silicon hydride. A temperature of 40-60°C may be employed and/or a better solvent such as benzene or toluene may be used to reduce the reaction time substantially.

4.2.3 INFRARED SPECTRUM OF $(PhSi)_2Co_4(CO)_{11}$

The infrared spectrum of $(PhSi)_2Co_4(CO)_{11}$ in hexane and CH_2Cl_2 is shown in Figures 4.2 and 4.3 respectively. Table 4.1 shows the frequencies for $(PhSi)_2Co_4(CO)_{11}$ as compared to the analogous clusters $(MeSi)_2Co_4(CO)_{11}$ {7} [36] and $(PhGe)_2Co_4(CO)_{11}$ {7} [122].

Table 4.1

INFRARED SPECTRUM OF $(PhSi)_2Co_4(CO)_{11}$ COMPARED WITH $(MeSi)_2Co_4(CO)_{11}$ AND $(PhGe)_2Co_4(CO)_{11}$

$(PhSi)_2Co_4(CO)_{11}$		$(MeSi)_2Co_4(CO)_{11}$	$(PhGe)_2Co_4(CO)_{11}$
Hexane	**CH_2Cl_2**	**Hexane/CH_2Cl_2**	**Cyclohexane**
2085 vw	2086 w	2061 w sh	2069 vw
2075 vw		2048 m sh	
2047 s	2046 s	2039 vs	2032 vs
2032 m	2030 m	2022 m	2018 m
2028 m sh			
2018 m	2016 m	2009 mw	2006 m
1866 w br	1855 w br	1855 w	1858 w br

Figure 4.2

INFRARED SPECTRUM OF $(PhSi)_2Co_4(CO)_{11}$

HEXANE SOLUTION

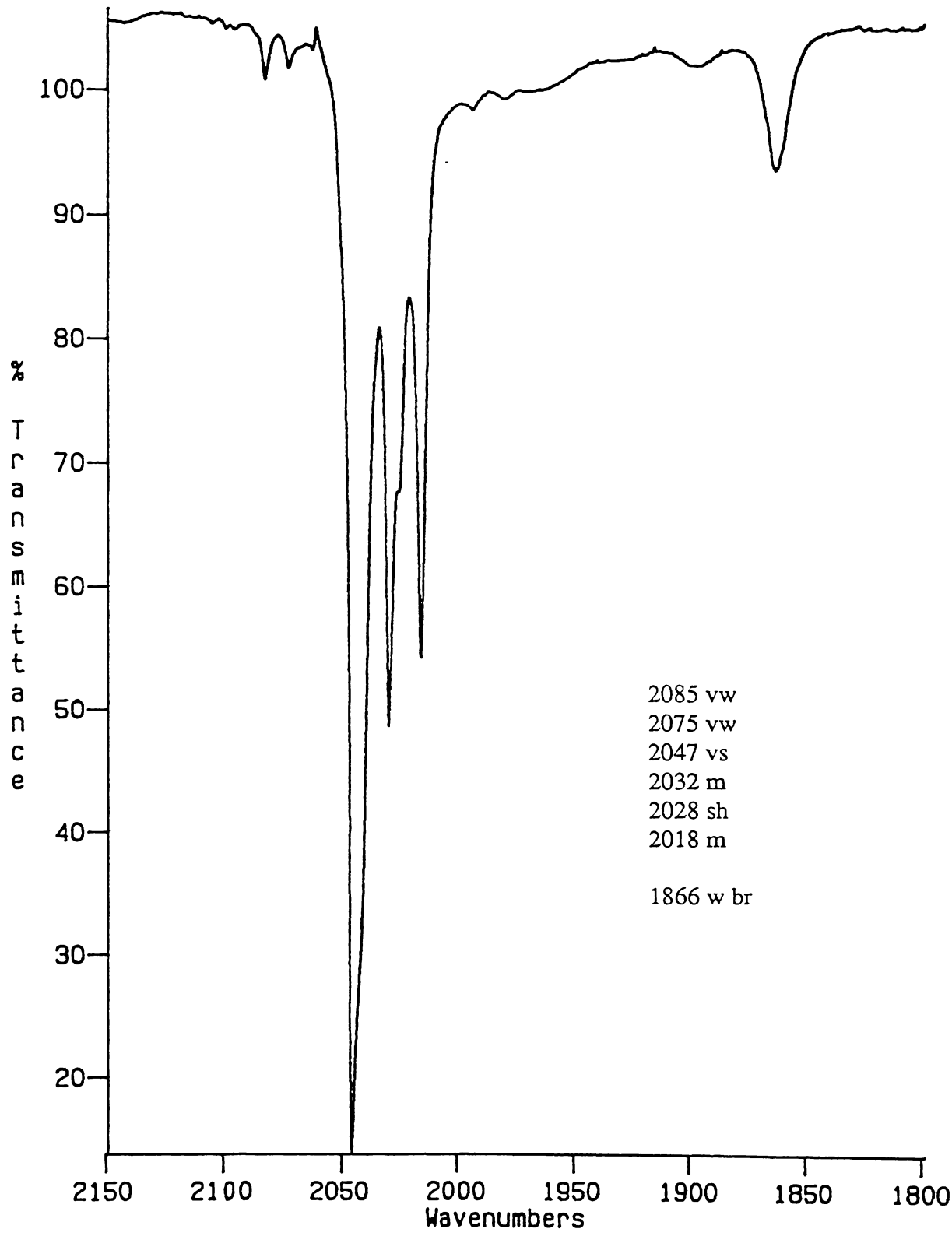

Figure 4.3

INFRARED SPECTRUM OF $(PhSi)_2Co_4(CO)_{11}$

CH_2Cl_2 SOLUTION

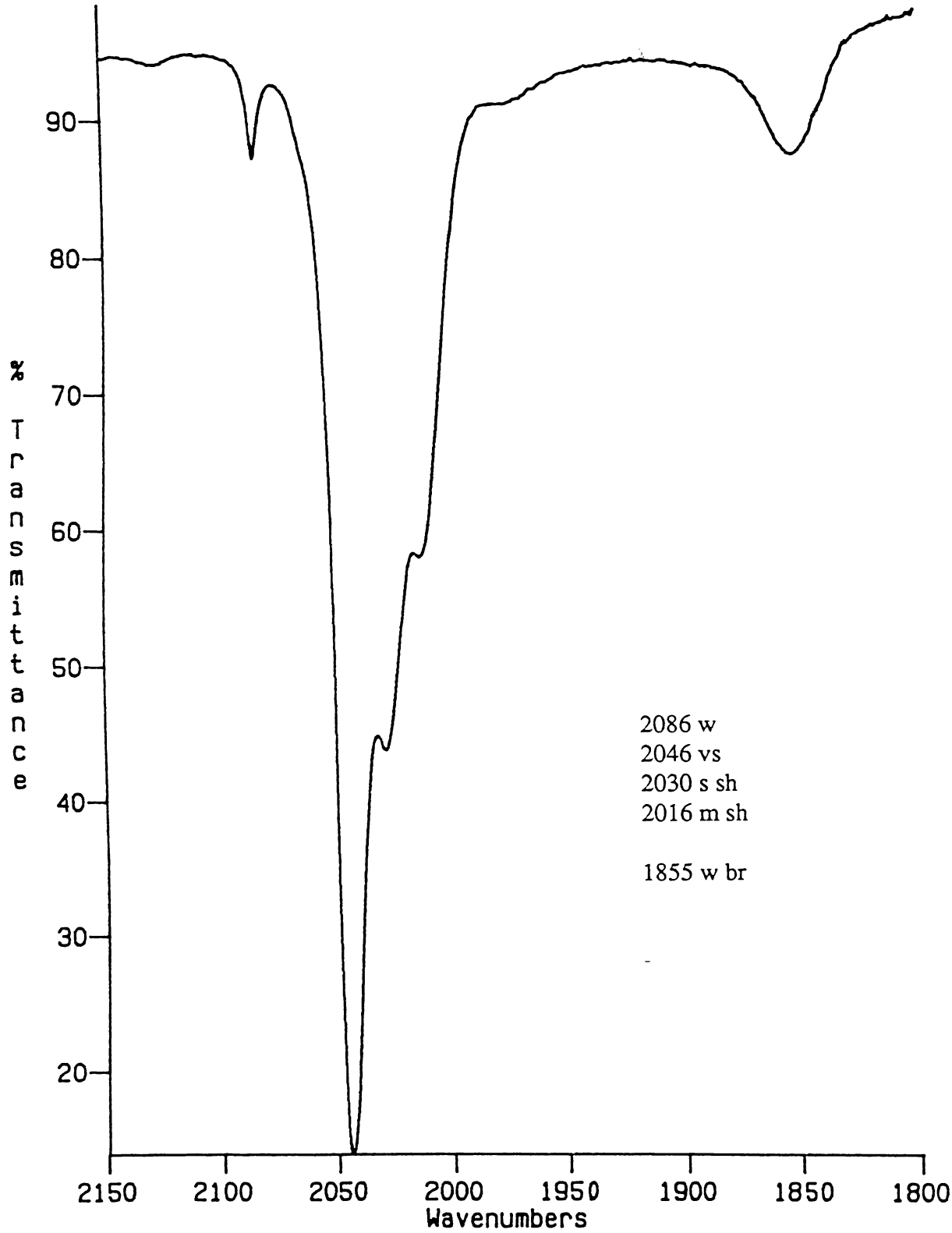

A good correlation exists between the hexane spectrum of $(PhSi)_2Co_4(CO)_{11}$ and the cyclohexane spectrum of $(PhGe)_2Co_4(CO)_{11}$ with a shift of 10-17 cm^{-1} to higher frequency for the silicon cluster. The bridging carbonyl occurs at a high value of 1866 cm^{-1} for the silicon cluster in hexane compared to 1855 cm^{-1} in CH_2Cl_2 and 1858 cm^{-1} for the germanium cluster. The significant shifts to higher frequency exhibited in going from $(MeSi)_2Co_4(CO)_{11}$ to the analogous phenyl cluster are generally not seen, to such an extent, with changes in organic groups.

A total of eight infrared peaks ($3A_1 + 3B_1 + 2B_2$) (bridging carbonyl peak, A_1) are expected for $(PhSi)_2Co_4(CO)_{11}$ assuming C_{2V} symmetry. The infrared spectrum of $(PhSi)_2Co_4(CO)_{11}$ in hexane shows a maximum of six terminal carbonyl peaks with a weak bridging peak at 1866 cm^{-1}, which is rather high. In CH_2Cl_2 only four terminal carbonyl peaks are observed in the infrared spectrum of $(PhSi)_2Co_4(CO)_{11}$ with the bridging peak shifted to lower frequency, 11 cm^{-1} to 1855 cm^{-1}.

4.2.4 MASS SPECTRUM OF $(PhSi)_2Co_2(CO)_{11}$

The FAB mass spectrum of $(PhSi)_2Co_4(CO)_{11}$ is listed in Table 4.2. The mass spectrum shows the parent ion $[(PhSi)_2Co_4(CO)_{11}]^+$ (m/e = 754) with a clear loss of all eleven carbonyl ligands to m/e = 446 ($[(PhSi)_2Co_4]^+$ ion). This series dominates the whole spectrum. A weak series of ions are seen with the loss of m/e = 2 x 77 or 2 x 105 which corresponds to phenyl or Si-phenyl groups. This cannot be distinguished due to Si and CO having the same m/e of 28. This weak series shows the loss of several carbonyls from m/e = 516 down to 460.

The mass spectrum compares well with that of $(MeSi)_2Co_4(CO)_{11}$ [36]. $(MeSi)_2Co_4(CO)_{11}$ shows no parent ion but ions due to the consecutive loss of the remaining ten carbonyls were observed along with losses of the Me groups and Si atoms leaving the Co_4 core.

Table 4.2

MASS SPECTRUM OF $(PhSi)_2Co_4(CO)_{11}$			
m/e	**Int**	**Assignment**	
754	w	$[(PhSi)_2Co_4(CO)_n]^+$	n = 11
726	m		n = 10
698	s		n = 9
670	s		n = 8
642	w		n = 7
614	m		n = 6
586	m		n = 5
558	w		n = 4
530	m		n = 3
502	w		n = 2
474	w		n = 1
446	w		n = 0
516	w	$[Co_4(CO)_n]^+$	n = 10
488	w		n = 9
460	w		n = 8

4.2.5. X-RAY CRYSTALLOGRAPHIC STUDY OF $(PhSi)_2Co_4(CO)_{11}$

Large black rectangular shaped crystals were obtained from a slowly cooled toluene solution. Preliminary precession photographs using Cu-Kα radiation indicated that the crystal had monoclinic symmetry and was assigned to the non-standard space group $P2_1/n$ despite the β angle of almost 90°. Loss of crystallinity was observed over a period of 4-5 days which suggested that a loss of solvent of crystallisation was occurring. Initial density calculations were low, supporting this observation.

Intensity data were collected on a suitable crystal of dimensions 0.7 x 0.7 x 0.3 mm at the University of Canterbury on a Nicolet P3 diffractometer. A scan range of $3°<2\theta<52°$ was employed obtaining 5960 unique reflections using Mo-Kα radiation. An absorption correction was applied to the data using an empirical ϕ-scan technique with transmission factors, 0.710 maximum and 0.503 minimum values. For the solution and refinement of the structure, 4328 reflections were used with $I>3\sigma(I)$. Crystal data for $(PhSi)_2Co_4(CO)_{11}$ are given in Table 4.3.

Table 4.3

CRYSTAL DATA FOR $(PhSi)_2Co_4(CO)_{11}$	
Formula: $C_{23}H_{10}Co_4O_{11}Si_2$	Mr = 754.23
Monoclinic	Space Group = $P2_1/n$
Cryst. Colour: Black	
Cryst. Dimensions: 0.7 x 0.7 x 0.3 mm	
a = 9.46(1) Å	$\alpha = 90.00°$
b = 21.58(1) Å	$\beta = 90.09(1)°$
c = 14.85(1) Å	$\gamma = 90.00°$
U = 3031.6(5) Å^3	Dcalc = 1.76 g cm^{-3}
Z = 4	
F(000) = 1587.9	Temp = 173 K
μ(Mo-Kα) = 22 cm^{-1}	
Unique Data = 5960	Range = $3°<2\theta<52°$
Refinement Data = 4328	Final R = 0.0343

Heavy atom positions for four cobalt and two silicon atoms were obtained using TREF in the SHELX-76 and SHELXS-86 [98] package of crystallographic programs. These positions were used and refined yielding the coordinates of the carbon atoms of the phenyl rings and the carbonyl ligands. Refinement of these atoms showed residual electron density due to a disordered (toluene) solvent

molecule. These positions were located and refined. All atoms were made anisotropic with the phenyl carbons assigned as rigid hexagons and the hydrogen atoms in calculated positions. The hydrogen atoms on the toluene solvent molecule were not located. In the final refinement, R = 0.0343, R_w = 0.0371 with w = $0.8874[\sigma^2(F) + 0.000500F^2]^{-1}$. Largest shift/e.s.d in the final refinement cycle was 0.03 with the greatest electron density at 0.88 e $Å^{-3}$.

Positional and thermal parameters along with complete tables of bond lengths and angles are given in Appendix Four. Tables of calculated and observed structure factors have been retained at the University of Waikato.

4.2.6 STRUCTURE OF $(PhSi)_2Co_4(CO)_{11}$

Views of the cluster $(PhSi)_2Co_4(CO)_{11}$ are shown in Figures 4.4, 4.5 and 4.6. Atom labelling as shown in Figure 4.6 is used throughout the following discussion. Selected bond lengths and angles are given in Tables 4.4 and 4.5.

Table 4.4

SELECTED BOND LENGTHS FOR $(PhSi)_2Co_4(CO)_{11}$ (Å)			
Co(1) ---Si(1)	2.315(1)	Co(1) ---Co(2)	2.565(1)
Co(1) ---Si(2)	2.312(1)	Co(1) ---Co(4)	2.685(1)
Co(2) ---Si(1)	2.312(1)	Co(2) ---Co(3)	2.647(1)
Co(2) ---Si(2)	2.327(1)	Co(3) ---Co(4)	2.726(1)
Co(3) ---Si(1)	2.310(1)		
Co(3) ---Si(2)	2.312(1)		
Co(4) ---Si(1)	2.312(1)		
Co(4) ---Si(2)	2.316(1)	Si(1) ...Si(2)	2.705(2)

Figure 4.4 Top and Side View of $(PhSi)_2Co_4(CO)_{11}$

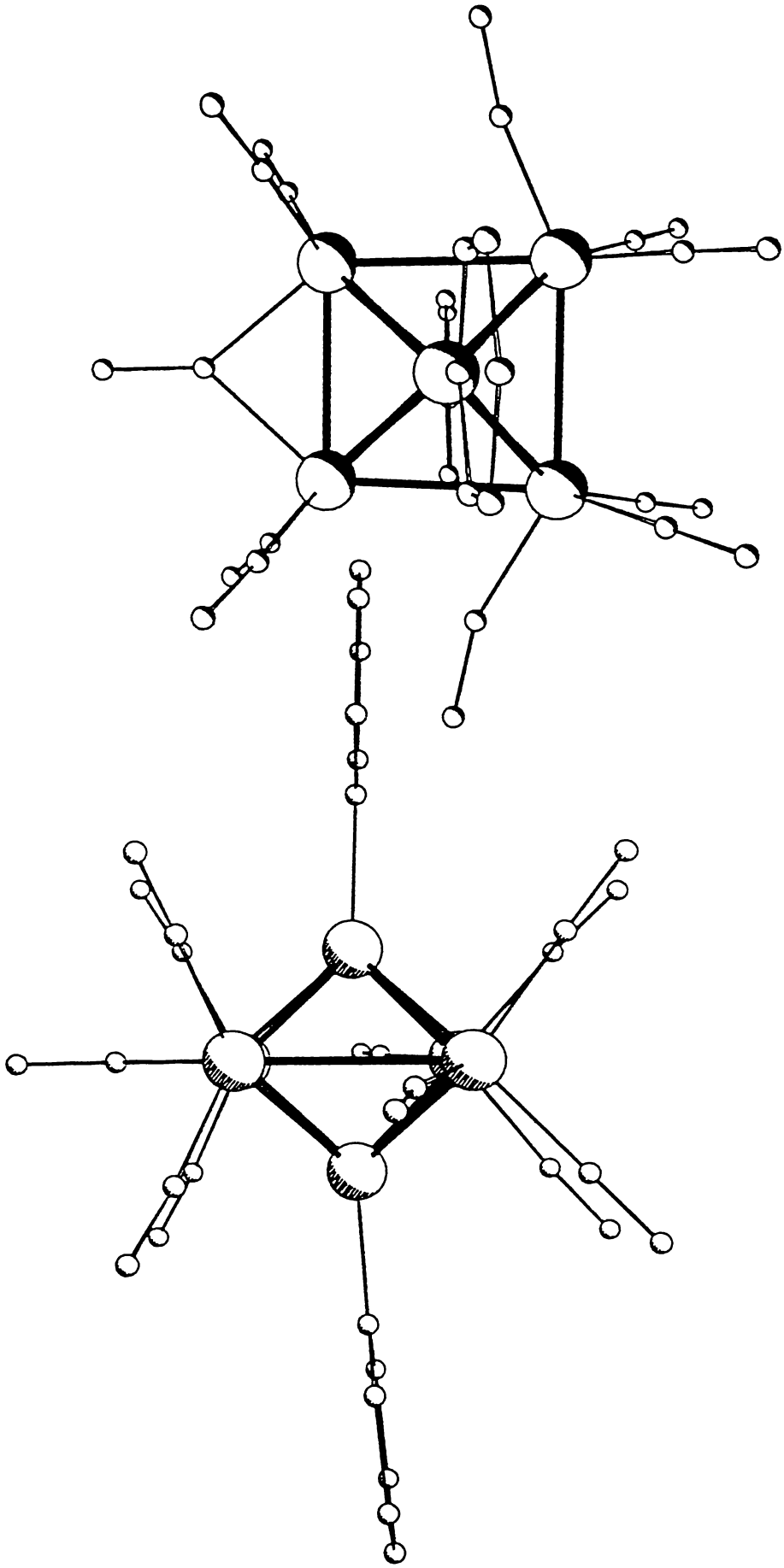

Figure 4.5 Stereo View of $(PhSi)_2Co_4(CO)_{11}$

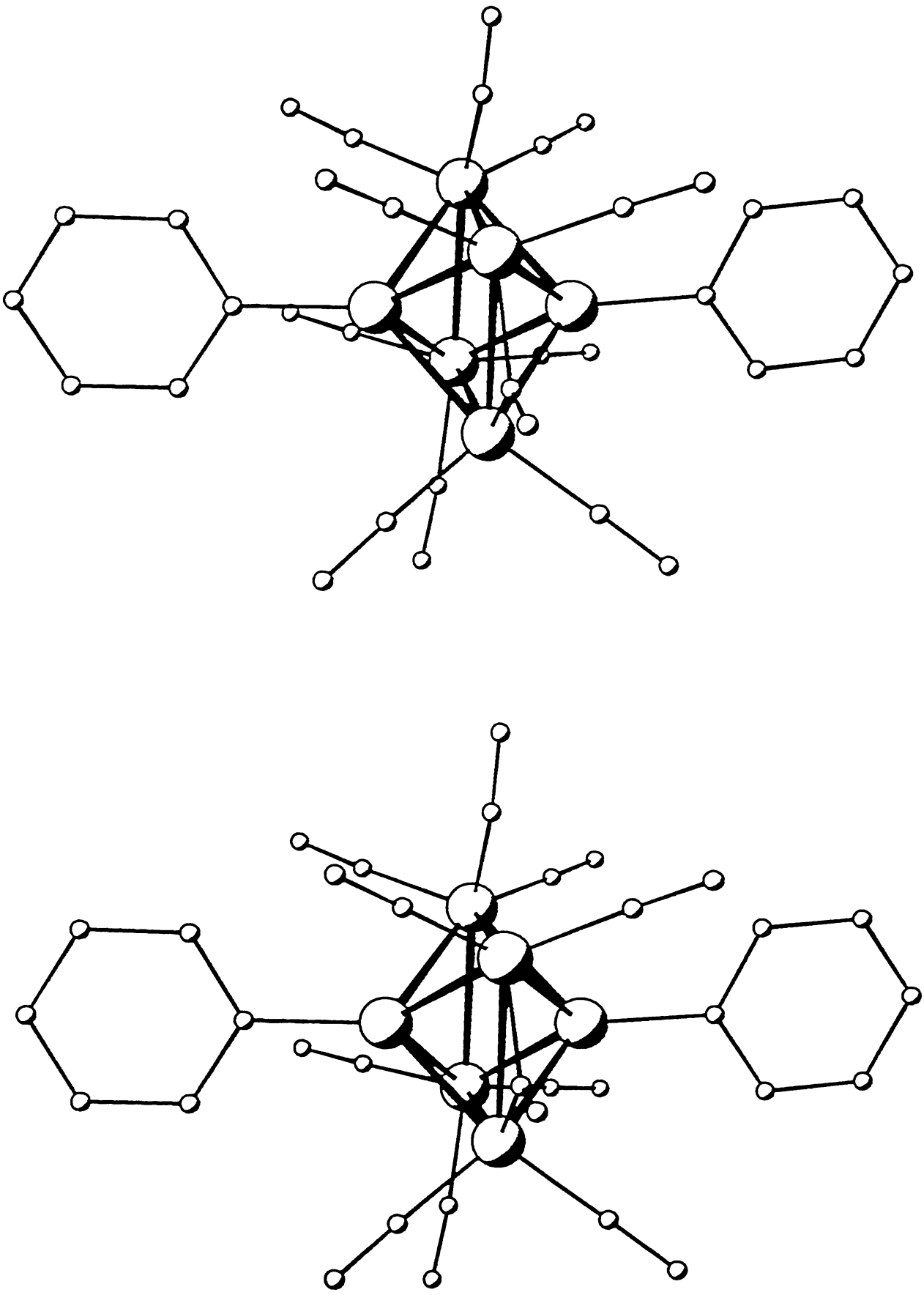

Figure 4.6 Perspective View of $(PhSi)_2Co_4(CO)_{11}$

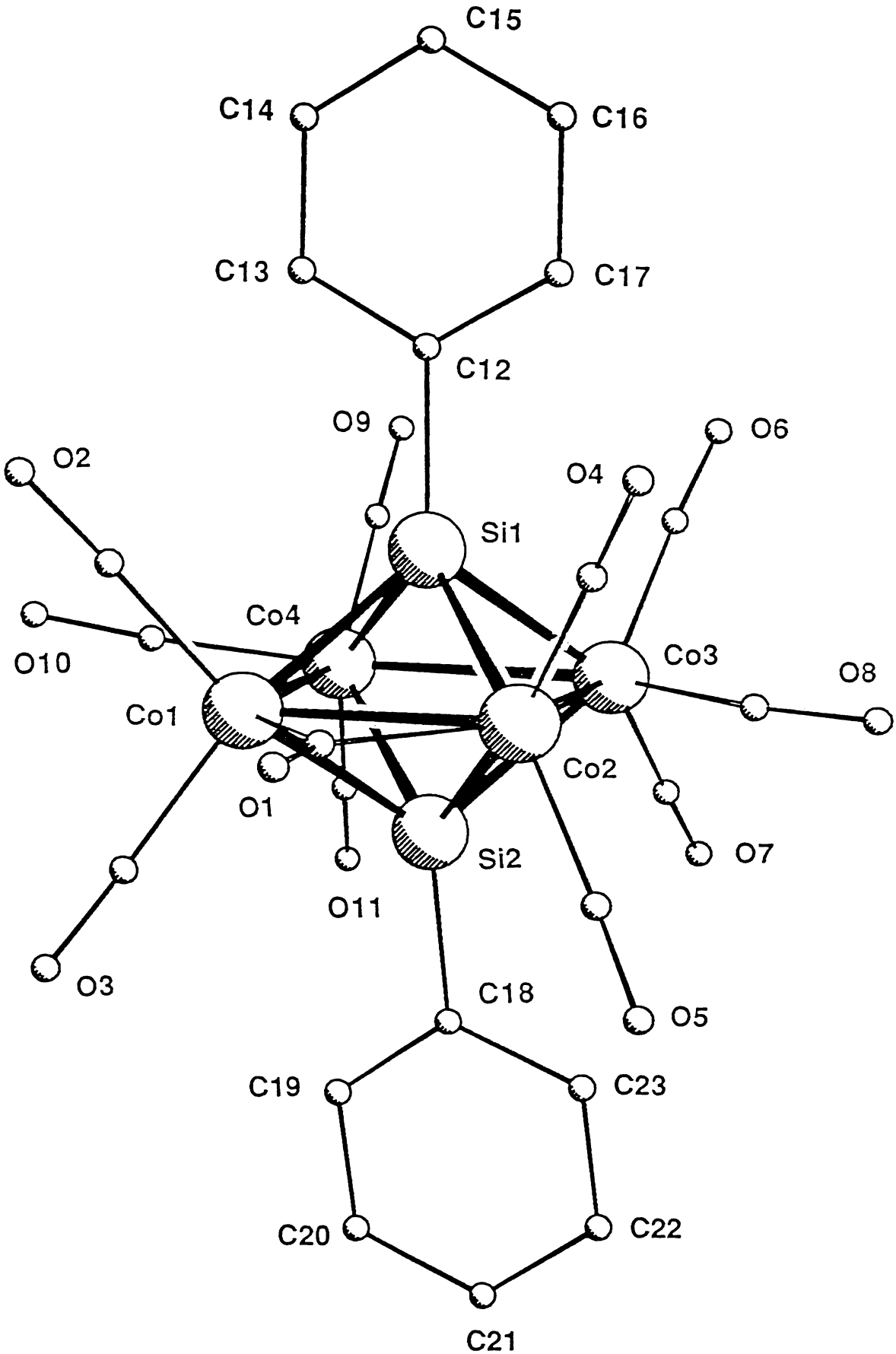

Table 4.5

SELECTED BOND ANGLES FOR $(PhSi)_2Co_4(CO)_{11}$ (°)			
Co(2) -Co(1) -Co(4)	91.5(1)	Co(1) -Co(4) -Co(3)	87.7(1)
Co(2) -Co(1) -Si(1)	56.3(1)	Co(1) -Co(4) -Si(1)	54.6(1)
Co(2) -Co(1) -Si(2)	56.7(1)	Co(1) -Co(4) -Si(2)	54.5(1)
Co(4) -Co(1) -Si(1)	54.5(1)	Co(3) -Co(4) -Si(1)	53.8(1)
Co(4) -Co(1) -Si(2)	54.6(1)	Co(3) -Co(4) -Si(2)	53.8(1)
Si(1) -Co(1) -Si(2)	71.5(1)	Si(1) -Co(4) -Si(2)	71.5(1)
Co(1) -Co(2) -Co(3)	92.0(1)	Co(1) -Si(1) -Co(2)	67.3(1)
Co(1) -Co(2) -Si(1)	56.4(1)	Co(1) -Si(1) -Co(3)	108.3(1)
Co(1) -Co(2) -Si(2)	56.2(1)	Co(1) -Si(1) -Co(4)	70.9(1)
Co(3) -Co(2) -Si(1)	55.0(1)	Co(2) -Si(1) -Co(3)	69.9(1)
Co(3) -Co(2) -Si(2)	54.9(1)	Co(2) -Si(1) -Co(4)	108.8(1)
Si(1) -Co(2) -Si(2)	71.3(1)	Co(3) -Si(1) -Co(4)	72.3(1)
Co(2) -Co(3) -Co(4)	88.8(1)	Co(1) -Si(2) -Co(2)	67.1(1)
Co(2) -Co(3) -Si(1)	55.1(1)	Co(1) -Si(2) -Co(3)	108.3(1)
Co(2) -Co(3) -Si(2)	55.5(1)	Co(1) -Si(2) -Co(4)	70.9(1)
Co(4) -Co(3) -Si(1)	53.9(1)	Co(2) -Si(2) -Co(3)	69.6(1)
Co(4) -Co(3) -Si(2)	54.0(1)	Co(2) -Si(2) -Co(4)	108.2(1)
Si(1) -Co(3) -Si(2)	71.6(1)	Co(3) -Si(2) -Co(4)	72.2(1)

The structure of $(PhSi)_2Co_4(CO)_{11}$ consists of a quadrilateral plane of four cobalt atoms which is quadruply bridged on each side by SiPh groups. This is the first example of a group 14 cluster of this type in which a capping phenyl group has been crystallographically characterised. This gives a unique comparison with other clusters which also contain a capping phenyl or p-Tol group such as those listed in Table 4.6 and a direct comparison to the methyl analogue $(MeSi)_2Co_4(CO)_{11}$ [36].

Table 4.6

E_2M_4 CLUSTERS WHICH CONTAIN PHENYL OR p-TOL CAPPING GROUPS		
CLUSTER	**REF**	**$(\mu\text{-CO})_n$**
$(PhGe)_2Co_4(CO)_{11}$	122	1
$(PhP)_2Co_4(CO)_{10}$	93	2
$(PhP)_2Co_4(CO)_9(PCy_3)$	142	2
$(PhP)_2Co_4(CO)_8(PPh_3)_2$	143	2
$[(PhP)_2Co_4(CO)_9(\mu\text{-H})]^-$	143	1
$(PhP)_2Co_4(CO)_6[P(OMe)_3]_4$	146, 147	2
$(PhP)_2Co_4(CO)_8[PPh_2(CH_2)_2Ph_2P]$	147	2
$(p\text{-TolP})_2Fe_4(CO)_{11}$ also Ph	140	1
$(PhP)_2Fe_4(CO)_{12}$ also p-Tol	140	0
$(p\text{-TolP})_2Fe_4(CO)_{10}[P(OMe)_3]$	144	1
$(p\text{-TolP})_2Fe_4(CO)_{11}[P(OMe)_3]$	144	0
$(PhP)_2Fe_2Co_2(CO)_{11}$	145	1

An interesting comparison can be made with this large range of phenyl or p-Tol capping groups (Table 4.6) with respect to the position adopted above and below the quadrilateral plane. The position adopted seems to be based purely on steric considerations. The phenyl groups in $(PhSi)_2Co_4(CO)_{11}$ (see Figure 4.6) lie perpendicular to the bridging carbonyl where the largest gap exists due to the positions of the terminal carbonyls.

Comparison of $(PhSi)_2Co_4(CO)_{11}$ with the cluster $(p\text{-TolP})_2Fe_4(CO)_{11}$ [140] (Figure 4.7) shows that they are structurally very similar with the p-Tol group orientated in the same position above the Fe_4 plane and with the carbonyls orientated in a very similar fashion around the core. In the cluster $(PhP)_2Co_4(CO)_{10}$ [93] (Figure 4.8) the phenyl group lies parallel with the bridging carbonyls which minimises the steric interaction with the terminal

carbonyls orientated above and below the rectangular plane. With the substitution of one carbonyl ligand in $(PhP)_2Co_4(CO)_{10}$ for the bulky PCy_3 group ($(PhP)_2Co_4(CO)_9(PCy_3)$ [142]), the phenyl group which encounters this ligand rotates 77.3(8)° with respect to the other phenyl group (Figure 4.9). This then minimises the steric interaction of the phenyl group with respect to the bulky PCy_3 ligand, there is also a tipping of the phenyl group away from the PCy_3 ligand. For the clusters $(p\text{-}TolP)_2Fe_4(CO)_{10}[P(OMe)_3]$ [144] (Figure 4.10), $(p\text{-}TolP)_2Fe_4(CO)_{11}[P(OMe)_3]$ [144] (Figure 4.11) and $(PhP)_2Co_4(CO)_8(PPh_3)_2$ (Figure 4.12) the p-Tol or phenyl groups all rotate to minimise steric interaction with the phosphine ligands.

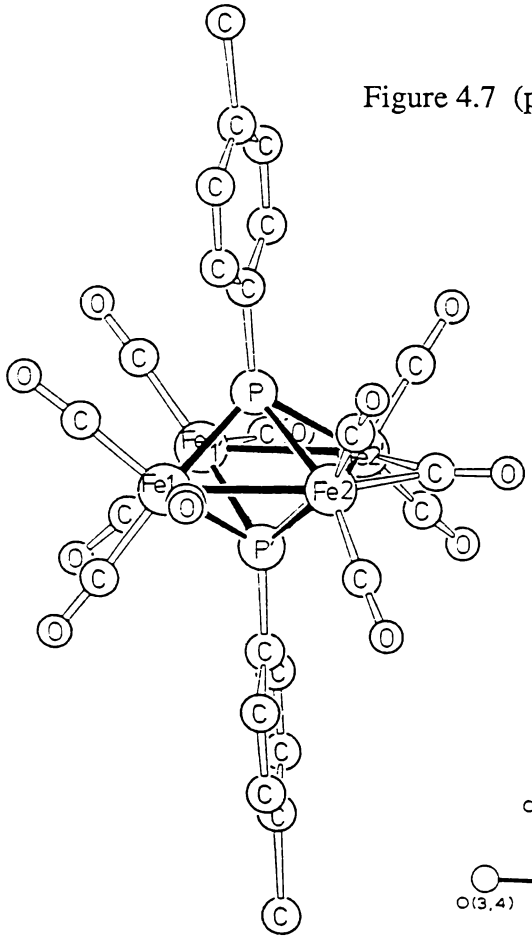

Figure 4.7 $(p\text{-}TolP)_2Fe_4(CO)_{11}$

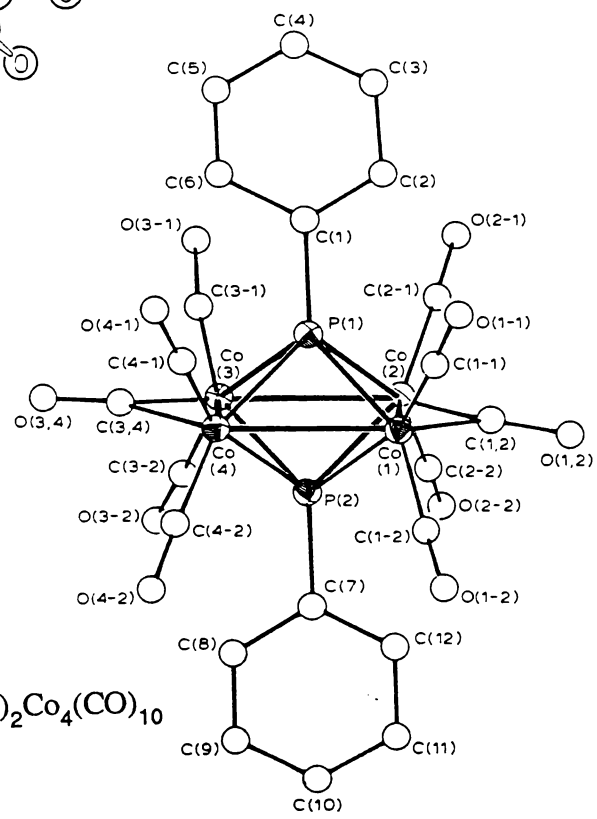

Figure 4.8 $(PhP)_2Co_4(CO)_{10}$

Figure 4.10 $(p\text{-TolP})_2Fe_4(CO)_{10}P(OMe)_3$

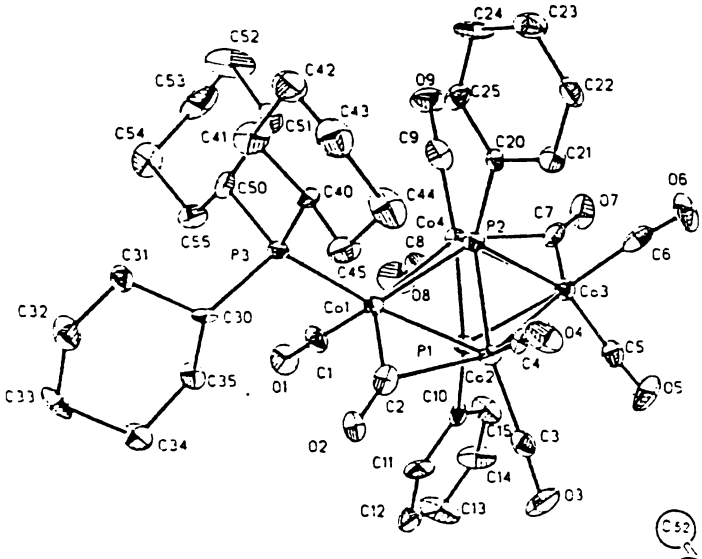

Figure 4.9 $(PhP)_2Co_4(CO)_9PCy_3$

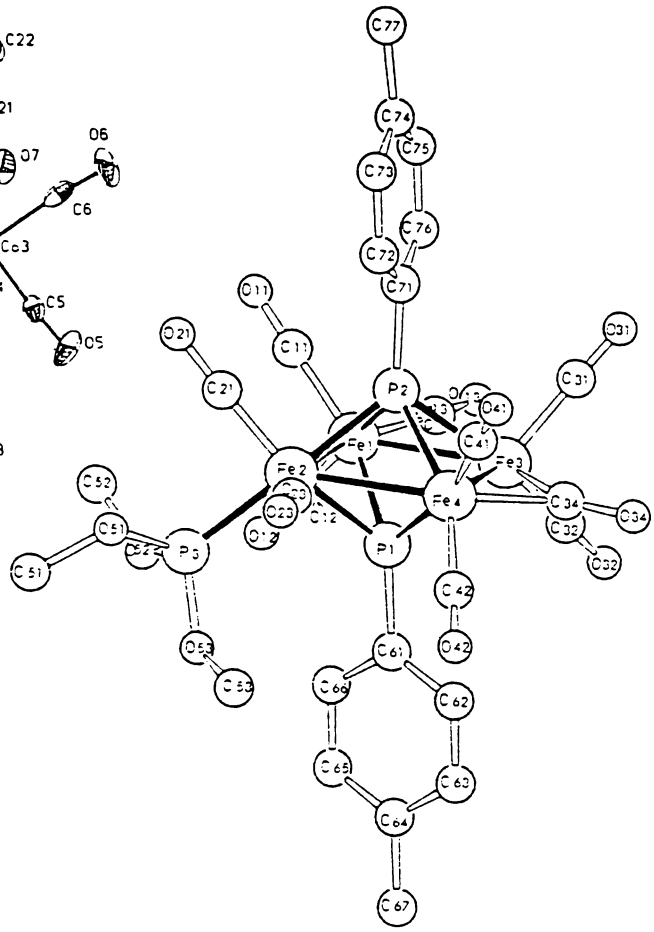

Figure 4.11 $(p\text{-TolP})_2Fe_4(CO)_{11}P(OMe)_3$

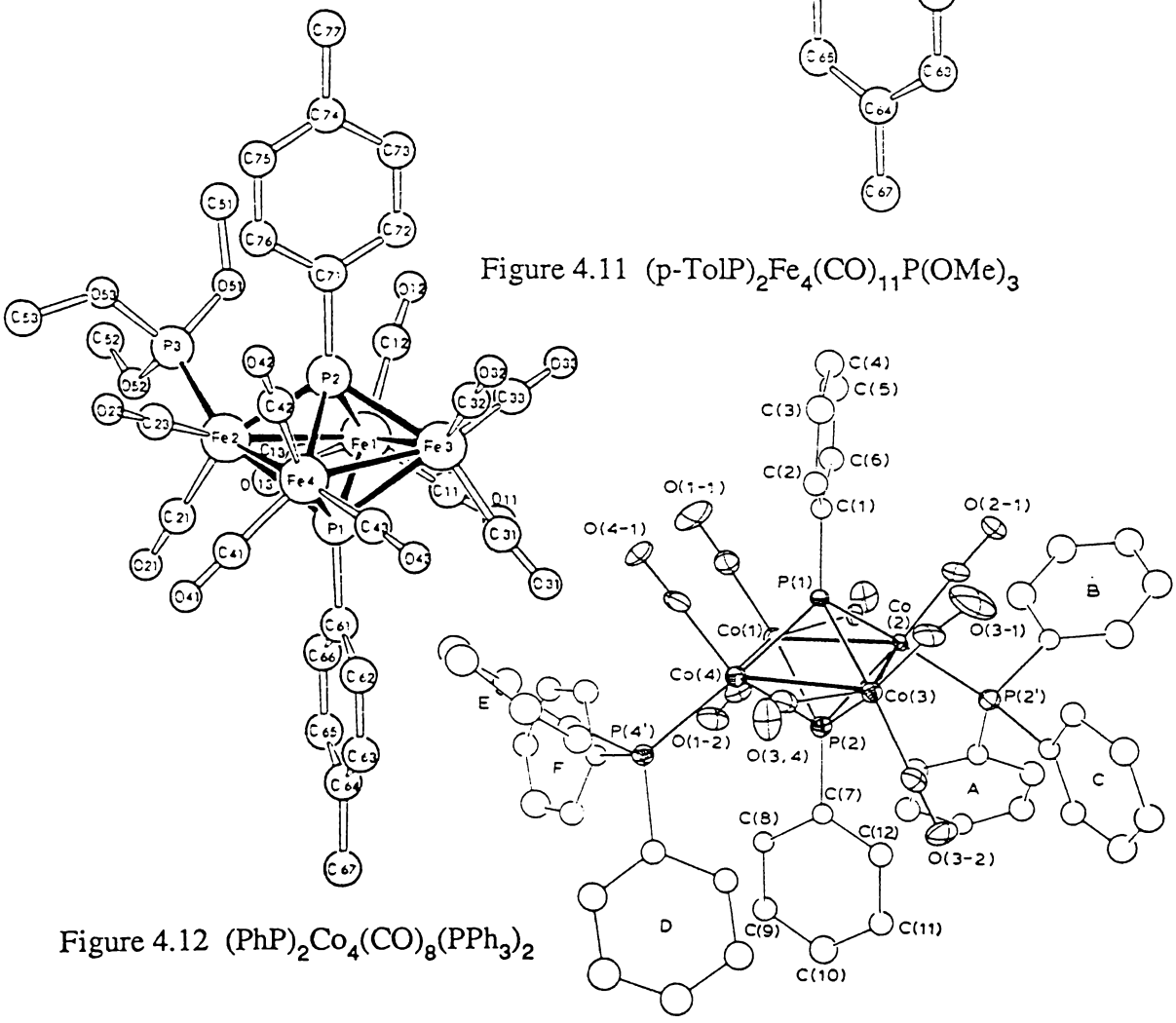

Figure 4.12 $(PhP)_2Co_4(CO)_8(PPh_3)_2$

The quadrilateral plane in $(PhSi)_2Co_4(CO)_{11}$ exhibits three distinct Co-Co distances which are determined by the degree of carbonyl bridging (Figure 4.13). The Co(1)-Co(2) bond is the shortest at 2.565(1)Å in which a carbonyl group fully bridges the bond. The unbridged Co(3)-Co(4) bond is the longest at 2.726(1)Å with two intermediate bond lengths of Co(1)-Co(4) at 2.685(1)Å and Co(2)-Co(3) at 2.647(1)Å due to semi-bridging carbonyls. These observations are consistent with a shortening of a metal-metal bond when bridged by a carbonyl ligand. Table 4.7 shows the core distances found in similar structures.

Comparison to $(MeSi)_2Co_4(CO)_{11}$ [36], with respect to the Co-Co, bonds shows that the carbonyl bridged bond is the shortest at 2.548Å and the non-bridged bond at 2.690Å is the longest. The same effect is seen for $(MeGe)_2Co_4(CO)_{11}$.

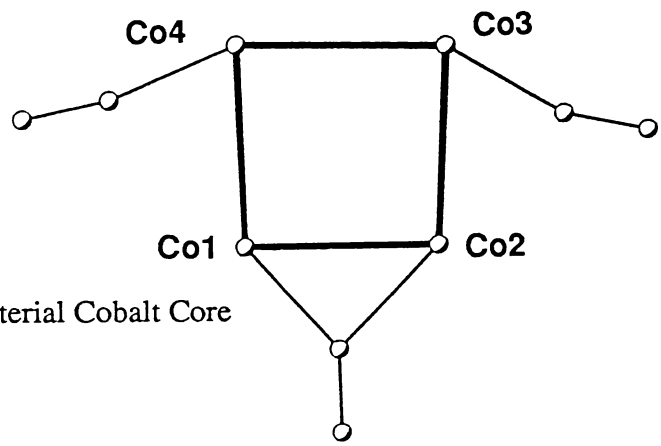

Figure 4.13 Quadrilaterial Cobalt Core

Table 4.7

DISTANCES IN Si_2Co_4 AND Ge_2Co_4 QUADRILATERAL CORES				
CLUSTER	**COBALT-COBALT DISTANCES (Å)**			
	1 - 2	3 - 4	1 - 4	2 - 3
$(PhSi)_2Co_4(CO)_{11}$	2.565	2.726	2.685	2.647
$(MeSi)_2Co_4(CO)_{11}$	2.548	2.690	2.651	2.651
$(MeGe)_2Co_4(CO)_{11}$	2.580	2.721	2.692	2.692
$[(CO)_4CoSi]_2Co_4(CO)_{11}$	2.569	2.653	2.696	2.623
$[(CO)_4CoGe]_2Co_4(CO)_{11}$	2.604	2.693	2.735	2.671

The iron cluster $(p\text{-TolP})_2Fe_4(CO)_{11}$ [140] (Figure 4.7) has a similar carbonyl arrangement, with the bridging carbonyl across the shortest Fe-Fe bond (2.440(3)Å), two semi-bridging carbonyls across Fe-Fe bonds of length 2.685(2)Å and a non-bridged Fe-Fe bond of length 2.694(3)Å. The bridged Fe-Fe bond shows a marked shortening compared to the non-bridged bond with the two semi-bridging carbonyls having a weak effect on the remaining Fe-Fe bonds. In contrast $(PhSi)_2Co_4(CO)_{11}$ shows a gradual change in Co-Co bond lengths from non-bridged to semi-bridged to fully bridged.

The silicon atoms lie very symmetrically above and below the cobalt plane. Co-Si(1) distances range from 2.310(1)Å to 2.315(1)Å (average 2.312Å) and those of Si(2) have three Co-Si distances very similar at 2.312(1)Å, 2.312(1)Å and 2.316(1)Å. The Co(2)-Si(2) bond length is the only deviation from symmetrical capping at 2.327(1)Å.

Comparison with the Si-Co distances in $(MeSi)_2Co_4(CO)_{11}$ show that the length of the Co-Co bond effects the length of the Si-Co bond. The shortest Co-Co bond has the shortest Si-Co bond lengths of 2.303(2)Å and 2.302(2)Å. The longest Co-Co bond has Si-Co distances of 2.311(2)Å and 2.320(2)Å. The average Si-Co distance in $(MeSi)_2Co_4(CO)_{11}$ is 2.309Å compared with the average Si-Co distance in $(PhSi)_2Co_4(CO)_{11}$ of 2.315Å, this shows a slight lengthening.

The Si--Si non-bonded distance of 2.705(2)Å is slightly shorter than that found in $(MeSi)_2Co_4(CO)_{11}$ [36] at 2.726Å and that found for $((CO)_4CoSi)_2Co_4(CO)_{11}$ [35, 45] at 2.817Å. This distance is only slightly greater than the longest known Si-Si bond found in $(t\text{-Bu})_3Si\text{-}Si(t\text{-Bu})_3$ [139] at 2.697Å.

The Si(1)-C distance of 1.878(2)Å and that of Si(2)-C at 1.883(2)Å to the phenyl groups is very similar to the values (1.87(2)Å and 1.88(2)Å) found in the rhenium cluster $Ph_2SiH_2Re_2(CO)_8$ [11].

The bridging carbonyl does not symmetrically bridge the shortest Co-Co bond. Co(1)-C(1) is the shorter distance at 1.899(3)Å with the Co(2)-C(1) distance extended to 1.954(4)Å. These Co-C distances are significantly longer than any other in this cluster. Two more carbonyls adopt a semi-bridging position along the intermediate Co-Co bonds. These have noticeably shorter

Co-C distances of 1.798(4)Å and 1.790(4)Å with less obtuse Co-C-O angles of 161.8(3)° and 168.9(3)°. The remaining carbonyls have Co-C distances ranging from 1.804(4)Å to 1.834(4)Å (average 1.815Å) with the least obtuse Co-C-O angle at 175.3(3)°.

4.2.7 PROPERTIES

This cluster is thermally stable for long periods at 40°C and is moderately air sensitive, although a lot less than other compounds in this work.

4.3 REACTION OF $BrSiH_3$ WITH $Co_4(CO)_{12}$ (AN INITIAL STUDY)

4.3.1 EXPERIMENTAL

$BrSiH_3$ (0.194g, 1.75mmol) was condensed into a 50ml ampoule with $Co_4(CO)_{12}$ (0.500g, 0.874mmol) in 10ml of hexane. This was left to react at 40°C for two months. The ampoule contained large black crystals of unreacted $Co_4(CO)_{12}$ and some very small brown needle-shaped crystals. The ampoule was opened, all the contents were transferred into a Schlenk flask and evacuated to dryness, 40ml of hexane cooled to 0°C was used to extract the product and the residue of $Co_4(CO)_{12}$ remained in the flask along with a small amount of $CoBr_2$. Estimated yield of the new product was 20-30%. Handling properties of the product: air-sensitive, hexane soluble and stable at a temperature of 40°C.

4.3.2 INFRARED SPECTRUM OF $(BrSi)_2Co_4(CO)_{11}$

An infrared spectrum of the product is consistent with the formulation $(BrSi)_2Co_4(CO)_{11}$ {7}. The spectrum in hexane is shown in Figure 4.14. This can be compared to $(MeSi)_2Co_4(CO)_{11}$ [36] and $(PhSi)_2Co_4(CO)_{11}$ which show some similar features (Table 4.8). Due to the bromine groups, the carbonyl peaks of $(BrSi)_2Co_4(CO)_{11}$ have shifted to higher frequency which is common for halogen substituents. This is illustrated by the strongest peak of 2039 cm^{-1} (Methyl) and 2047 cm^{-1} (Phenyl) shifting to 2061 cm^{-1} in the bromine cluster.

Figure 4.14

INFRARED SPECTRUM OF $(BrSi)_2Co_4(CO)_{11}$

HEXANE SOLUTION

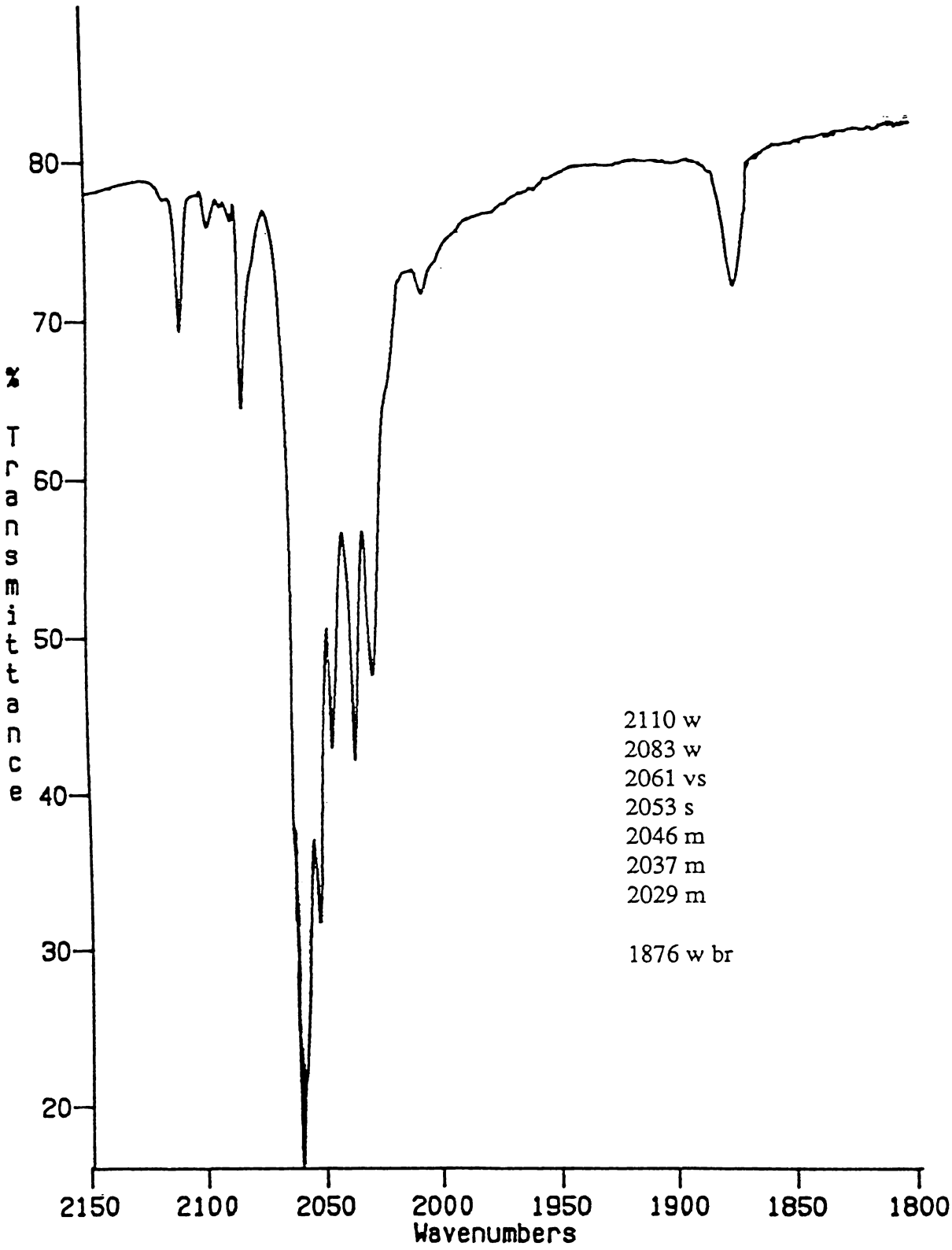

Table 4.8

INFRARED SPECTRUM OF $(BrSi)_2Co_4(CO)_{11}$ COMPARED TO $(PhSi)_2Co_4(CO)_{11}$ AND $(MeSi)_2Co_4(CO)_{11}$		
$(BrSi)_2Co_4(CO)_{11}$	$(PhSi)_2Co_4(CO)_{11}$	$(MeSi)_2Co_4(CO)_{11}$
2110 w	2085 vw	2061 w sh
2083 w	2075 vw	2048 m sh
2061 s	2047 vs	2039 vs
2053 m	2032 m	
2047 m	2028 w sh	2022 ms
2037 m		
2029 m	2018 m	2009 mw
1876 br w	1866 w	1855 w

The bridging carbonyl peak at 1876 cm^{-1} is extremely high compared to other cobalt compounds and shows a marked shift to higher frequency compared to the bridging carbonyls of the other clusters in Table 4.8.

4.3.3 PROPERTIES AND DISCUSSION

The tentative product $(BrSi)_2Co_4(CO)_{11}$, shows little decomposition at temperatures of 40°C but is sensitive to air decomposition. $(BrSi)_2Co_4(CO)_{11}$ forms black needle-shaped crystals from hexane.

If this product is indeed $(BrSi)_2Co_4(CO)_{11}$, this further demonstrates the generality of the reaction of $XSiH_3$ (X = Br, organic) with $Co_4(CO)_{12}$ to form the pseudo-octahedral core clusters $(XSi)_2Co_4(CO)_{11}$ (see equation below).

$$2BrSiH_3 + Co_4(CO)_{12} \rightarrow (BrSi)_2Co_4(CO)_{11} + 3H_2 + CO$$

Such a cluster lends itself to further substitution by anionic reagents such as $[Co(CO)_4]^-$, $[Mn(CO)_5]^-$, $[Fe_2(CO)_8]^{2-}$, etc. This could replace one or both bromine groups depending on reactant ratio. With $[Fe_2(CO)_8]^{2-}$ the possibility of linking two or more Si_2Co_4 cores together exists.

4.4 REACTION OF $BrSiH_3$ WITH $Co_2(CO)_8$

4.4.1 EXPERIMENTAL

$BrSiH_3$ (0.216g, 1.95mmol) was condensed into a 50ml ampoule with $Co_2(CO)_8$ (1.00g, 2.92mmol) in 10ml of hexane. The reaction was conducted in the dark for three days at room temperature resulting in an orange-brown solution with some green precipitate. On storage of the products at -25°C orange crystals were formed. The reaction products were transferred to a Schlenk flask which was evacuated to remove the hexane solvent and a quantity of $HCo(CO)_4$. Hexane was added to dissolve the products and this was filtered away from the green $CoBr_2$. The infrared spectrum showed only a small amount of unreacted $Co_2(CO)_8$ and $Co_4(CO)_{12}$ giving a yield of 80-90% of the orange product. Crystals are obtained by cooling the saturated hexane solution.

A similar experiment was conducted at room temperature for two weeks. $BrSiH_3$ (0.222g, 2.00mmol) was reacted with $Co_2(CO)_8$ (1.00g, 2.92mmol) in 10ml of hexane giving a reaction ratio of 1 to 1.5. After two weeks the solution was an orange colour with some green precipitate.

On work-up only the green precipitate was not hexane soluble. The green precipitate was dissolved in water to give a light pink solution. The addition of a silver nitrate solution immediately gave a white precipitate. These observations are all consistent with the green precipitate being $CoBr_2$.

The hexane soluble fraction was shown to contain a small amount of unreacted $Co_2(CO)_8$ and the formation of a trace amount of $Co_4(CO)_{12}$. The major product was tentatively identified as $(CO)_4CoBrSiCo_2(CO)_7$ {3} and is formed in approximately 80-90% yield.

4.4.2 PROPERTIES AND INFRARED SPECTRUM OF $(CO)_4CoBrSiCo_2(CO)_7$

The suggested product $(CO)_4CoBrSiCo_2(CO)_7$ {3}, is very hexane soluble, even more so than $Co_2(CO)_8$. The solution is rapidly decomposed in air with the solid only briefly air-stable. The solution or solid can be indefinitely stored at -25°C in the dark.

The infrared spectrum of $(CO)_4CoBrSiCo_2(CO)_7$ in hexane is shown in Figure 4.15. Table 4.9 compares the infrared spectrum in the carbonyl region of $(CO)_4CoBrSiCo_2(CO)_7$ with the analogous germanium compound $(CO)_4CoBrGeCo_2(CO)_7$ [82] and $(CO)_4CoPhGeCo_2(CO)_7$ [141].

Table 4.9

COMPARISON OF THE INFRARED SPECTRA OF $(CO)_4CoBrECo_2(CO)_7$ (E = Si, Ge) AND $(CO)_4CoPhGeCo_2(CO)_7$

$(CO)_4CoBrSiCo_2(CO)_7$	$(CO)_4CoBrGeCo_2(CO)_7$	$(CO)_4CoPhGeCo_2(CO)_7$
2113 w	2113 w	2104 w
	2099 w	
2092 m	2090 s	2082 s
	2080 w	
2065 s	2064 s	2056 s
2055 w		2044 w
2047 s	2048 m	2036 s
2038 w		
2030 m	2033 sh	2025 m
2028 sh		2014 m
	2004 w	1998 w
1852 w	1856 w	1850 w
1846 w	1846 w	1835 w

Figure 4.15

INFRARED SPECTRUM OF $(CO)_4CoBrSiCo_2(CO)_7$

HEXANE SOLUTION

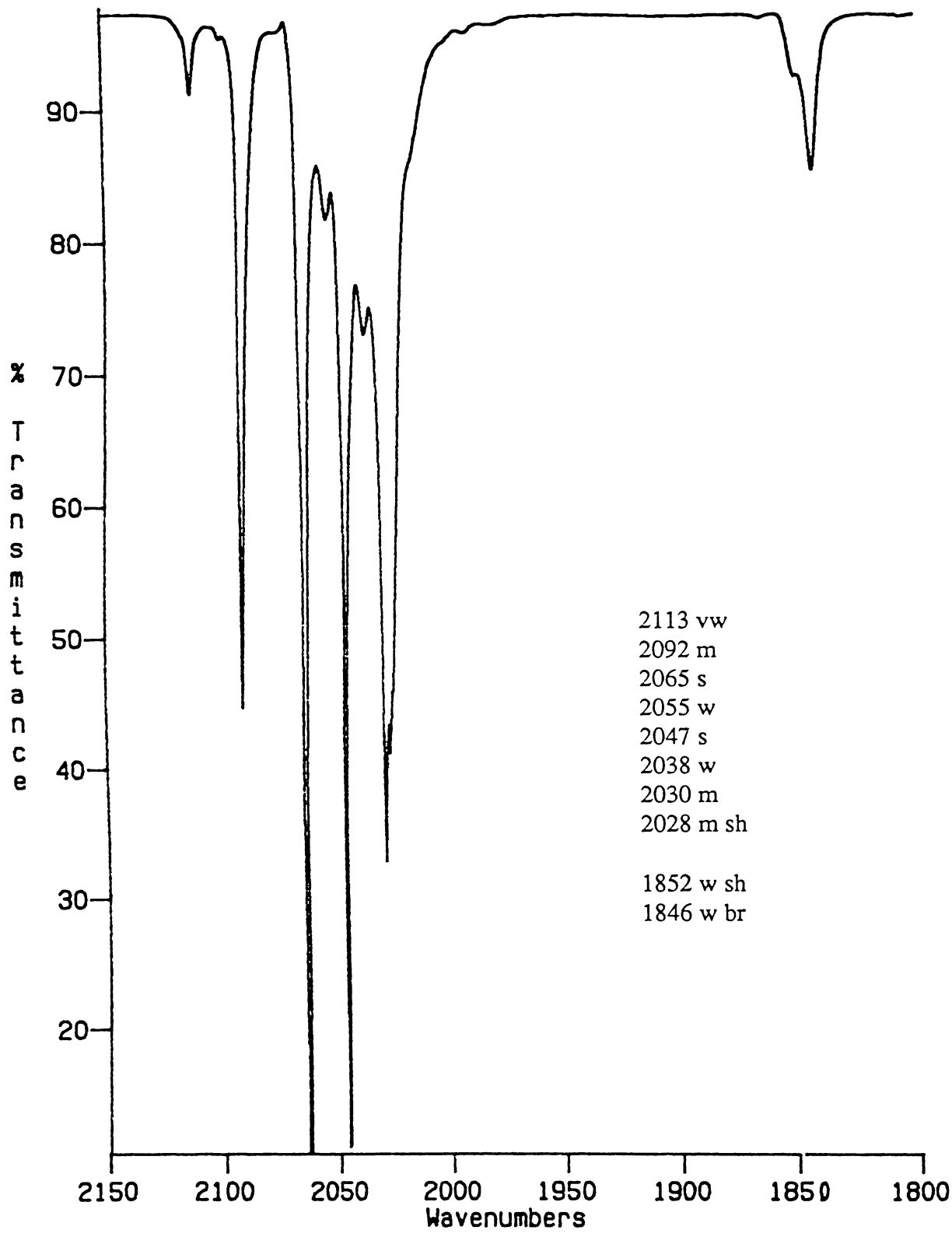

This comparison shows clearly a very high correlation between the two bromine compounds. Only a small shift in frequency is seen with a close match in intensity of the peaks. On comparison with $(CO)_4CoPhGeCo_2(CO)_7$ [141] we see a greater shift in the peaks mainly due to the halogen substituent as expected. A reasonable correlation in the number of peaks and intensity is observed.

4.5 REACTION OF $ISiH_3$ WITH $Co_2(CO)_8$

4.5.1 EXPERIMENTAL

$ISiH_3$ (0.308g, 1.95mmol) was condensed into a 50ml high pressure ampoule containing $Co_2(CO)_8$ (1.00g, 2.92mmol) in 10ml of hexane. This was left to react at room temperature for 12 months which resulted in a red/black coloured solution.

The volatile components were removed under vacuum and the remaining solid was completely soluble in hexane. The infrared spectrum of the hexane-soluble fraction showed it to contain unreacted $Co_2(CO)_8$ and $Co_4(CO)_{12}$ formed in the reaction. The products containing silicon were $(CO)_4CoSiCo_3(CO)_9$ (υCO, (hexane), 2114 w, 2087 m, 2046 vs, 2030 m, cm^{-1}) and a new product tentatively assigned as $ISiCo_3(CO)_9$ (υCO, (hexane) 2099 m, 2045 s, cm^{-1}).

Estimated percentage yields of the various solid species, $Co_2(CO)_8$ 30%, $Co_4(CO)_{12}$ 20%, $(CO)_4CoSiCo_3(CO)_9$ 30% and new product 20-30%.

$ISiH_3$ (0.826g, 5.23mmol) was condensed into a 150ml high pressure ampoule with $Co_2(CO)_8$ (2.50g, 7.32mmol) in 20ml of hexane. This gives a reaction ratio of 1 to 1.4 slightly less than the predicted ratio of 1 to 1.5. The reaction was conducted for one week at a temperature of 0°C to minimise decomposition of the product. After this time the ampoule was stored at -25°C until work-up. Initially the solution was dark brown due to $Co_2(CO)_8$ which changed to orange after one week and on cooling to -25°C large orange crystals formed.

On work-up these orange crystals were separated from the other components. The infrared spectrum revealed these crystals to be a mixture of $Co_2(CO)_8$ and a new orange product. All the solid products were combined and the solvent removed. The solid material was completely soluble in hexane and the infrared spectrum showed this to contain $Co_2(CO)_8$ 20-30%, $Co_4(CO)_{12}$ 5% and an orange product tentatively assigned to $(CO)_4CoISiCo_2(CO)_7$ {3} 60-70% (section 4.5.2).

Iodine analysis of a clean fraction of the suggested product $(CO)_4CoISiCo_2(CO)_7$ was carried out. The solid (1.943g, 3.04mmol) was dissolved in ethanol which started decomposing immediately as the solvent was added. An excess of NaOH in water was added and the solution was left to decompose. This was then neutralised and made slightly acidic with nitric acid, then filtered. Silver nitrate solution was added until no more creamy coloured precipitate formed. This was then filtered, dried and weighed. The isolated weight of AgI was 0.736g, 3.15mmol. This compares very well to the expected number of moles above of 3.04mmol.

4.5.2 INFRARED SPECTRUM OF $(CO)_4CoISiCo_2(CO)_7$

The infrared spectrum of $(CO)_4CoISiCo_2(CO)_7$ {3} in hexane is shown in Figure 4.16. This infrared spectrum was obtained from a relatively pure sample. Subtraction of the known compounds in the sample leaves the infrared spectrum with a pattern differing slightly from that of $(CO)_4CoBrSiCo_2(CO)_7$. Table 4.10 compares the infrared spectrum of $(CO)_4CoISiCo_2(CO)_7$ with $(CO)_4CoBrSiCo_2(CO)_7$ (see section 4.4.2) and $(CO)_4CoBrGeCo_2(CO)_7$ [82] in the carbonyl region.

The infrared spectrum of $(CO)_4CoISiCo_2(CO)_7$ matches exactly to the bromine analogue in frequency and intensity. A close match to the related germanium cluster, $(CO)_4CoBrGeCo_2(CO)_7$ is also seen. A very slight drop in frequency is observed, generally only 1 cm^{-1}, in going from the bromine to the iodine cluster.

Figure 4.16

INFRARED SPECTRUM OF $(CO)_4CoISiCo_2(CO)_7$

HEXANE SOLUTION

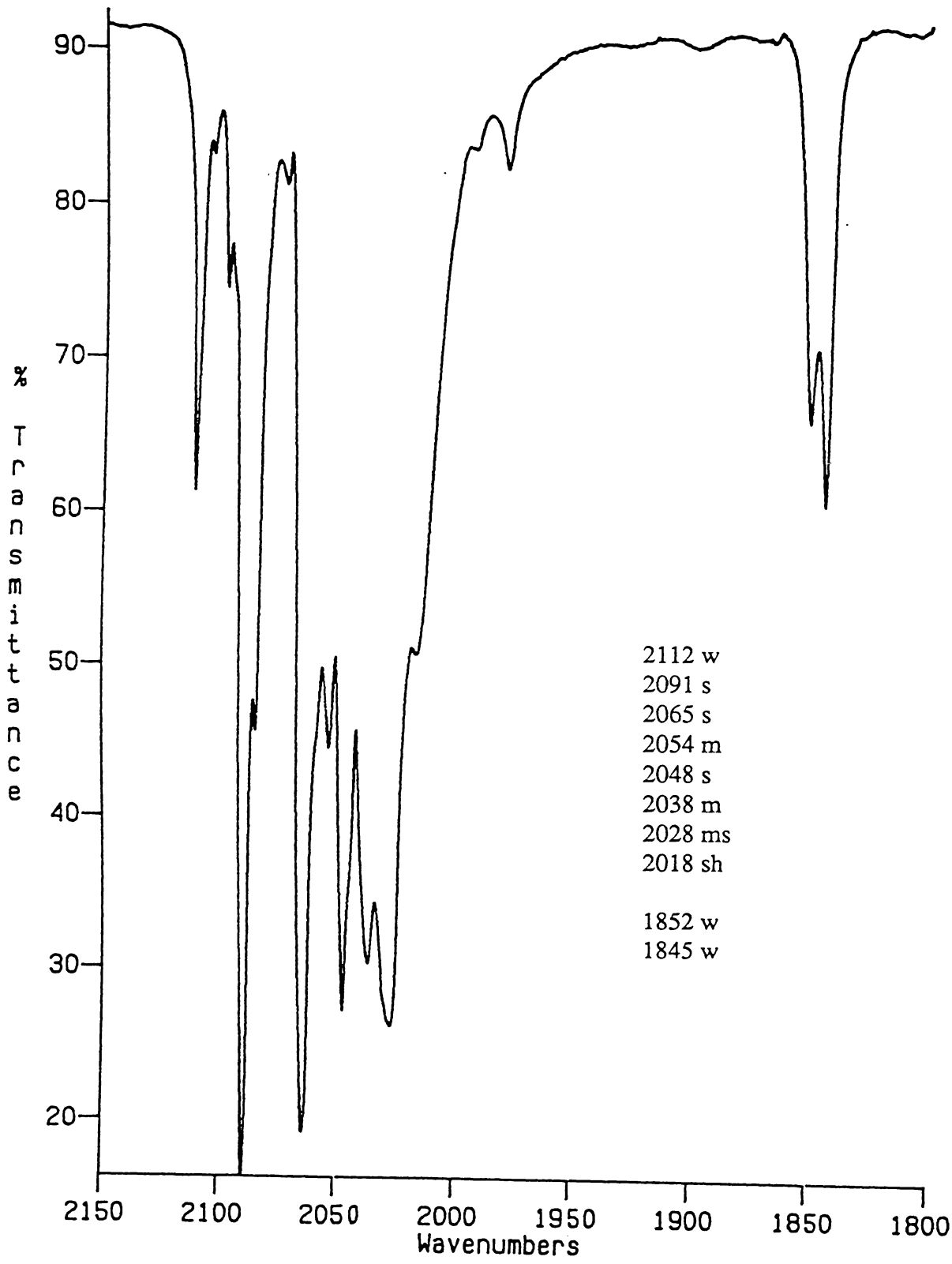

Table 4.10

INFRARED SPECTRUM OF $(CO)_4CoISiCo_2(CO)_7$ COMPARED WITH THOSE OF $(CO)_4CoBrSiCo_2(CO)_7$ AND $(CO)_4CoBrGeCo_2(CO)_7$		
$(CO)_4CoISiCo_2(CO)_7$	$(CO)_4CoBrSiCo_2(CO)_7$	$(CO)_4CoBrGeCo_2(CO)_7$
2112 w	2113 w	2113 w
		2099 w
2091 s	2092 m	2090 s
		2080 w
2065 s	2065 s	2064 s
2054 m	2055 w	
2048 s	2047 s	2048 m
2038 m	2038 w	
2028 ms	2030 m	2033 sh
	2028 sh	
2018 sh		2004 w
1852 w	1852 w	1856 w
1845 w	1846 w	1846 w

4.6 PROPERTIES AND DISCUSSION

The suggested products $(CO)_4CoBrSiCo_2(CO)_7$ {3} and $(CO)_4CoISiCo_2(CO)_7$ {3} are very hexane soluble. The solutions and, to a slightly lesser extent, the solids are air sensitive, but the solutions or solids can be stored for long periods at -25°C in the dark. Decomposition in polar solvents readily occurs.

Characterisation is limited due to the unavailability of mass spectrometry facilities and the very limited stability of the compounds. Single crystals of both clusters were difficult to obtain from hexane which gave small bundles of needle

shaped crystals. Toluene provided better shaped crystals but time did not permit further crystallographic study. The iodine analysis is consistent with the formulation given for the product.

Reactions of $RSiH_3$ or $RGeH_3$ (R = organic) [12, 45, 82, 83] with $Co_2(CO)_8$ form the products $(CO)_4CoRSiCo_2(CO)_7$ {3} or the analogous germanium products. Therefore $(CO)_4CoBrSiCo_2(CO)_7$ and $(CO)_4CoISiCo_2(CO)_7$ are the expected products from the reaction of $BrSiH_3$ or $ISiH_3$ with $Co_2(CO)_8$. Suggesting that the halogen substituent acts in a similar manner to the organic substituent is reasonable for this system. The reaction goes to completion in 3 days at room temperature (20°C). The orange cluster $(CO)_4CoISiCo_2(CO)_7$ undergoes further reaction at room temperature to form a dark red solution. The more stable bromine analogue requires gentle heating (40- 50°C) to promote the same reaction.

Examination of the dark red solution above by infrared spectroscopy indicated the major species present was $(CO)_4CoSiCo_3(CO)_9$ {2}. The formation of $(CO)_4CoSiCo_3(CO)_9$ can be envisaged to arise from the decarbonylation of $(CO)_4CoISiCo_2(CO)_7$ to initially form the unstable cluster $ISiCo_3(CO)_9$ (infrared peaks possibly due to this were seen). This then is readily attacked by unreacted cobalt carbonyl species in the reaction vessel. This Si-I bond is rather weak and could easily leave as I_2 or HI.

In contrast to the $BrSiH_3$ reaction no CoI_2 was observed in the reaction vessel, even at long reaction times. Therefore the small amount observed in the $BrSiH_3$ reaction may be due to an HBr impurity in the reactant gas. This would explain the small amount of unreacted $Co_2(CO)_8$ since the remaining reaction is very specific forming only $(CO)_4CoBrSiCo_2(CO)_7$ in high yields.

4.7 FURTHER WORK

Full characterisation of these halogen clusters needs to be undertaken with an extension to cover the available mono-halosilanes ($ClSiH_3$, $BrSiH_3$ and $ISiH_3$) with $Co_2(CO)_8$ and $Co_4(CO)_{12}$.

Substitution of the functional halogen containing clusters could be undertaken to form a wide range of mixed metal or organic clusters. The possibility of linking two or more of these clusters together with group 15 and 16 elements would open-up a whole new range of clusters.

CHAPTER FIVE

REACTIONS OF $H_3SiOSiH_3$ AND $H_3SiSSiH_3$ WITH $Co_2(CO)_8$

REACTIONS OF $H_3SiOSiH_3$ AND $H_3SiSSiH_3$ WITH $Co_2(CO)_8$

5.1 INTRODUCTION

The results of the reactions of disiloxane ($H_3SiOSiH_3$) and disilylthiane ($H_3SiSSiH_3$) with $Co_2(CO)_8$, $Co_4(CO)_{12}$, $Fe(CO)_5$ and $Fe_2(CO)_9$ are reported in this chapter. Also the reaction of digermylsulphide ($H_3GeSGeH_3$) with $Co_2(CO)_8$ was investigated.

Previous work shows that a monosubstituted silane ($RSiH_3$ where R = organic) [12, 33, 45] reacting with $Co_2(CO)_8$, will replace the three hydrogens by metal-carbonyl groups giving two possible structures, firstly $(CO)_4CoRSiCo_2(CO)_7$ {3}, or with longer reaction times or heating, $RSiCo_3(CO)_9$ {2}.

$$MeSiH_3 + 1.5Co_2(CO)_8 \rightarrow (CO)_4CoMeSiCo_2(CO)_7$$

We could consider the above hydrides as two monosubstituted silanes linked together by the oxygen or sulphur atom. Therefore we would predict that the products formed could consist of the same type of structures but linked together giving $E[SiCo(CO)_4Co_2(CO)_7]_2$ and $E[SiCo_3(CO)_9]_2$ clusters where E = O or S. These structures would be expected to occur in pairs although a very interesting comparison could be made if a cluster could be isolated with one of each unit linked together. In this chapter we examine whether such structures form, or whether the Si-O-Si and Si-S-Si linkages break and rearrange.

5.2 REACTION OF $H_3SiOSiH_3$ WITH $Co_2(CO)_8$

5.2.1 EXPERIMENTAL

$H_3SiOSiH_3$ (0.0763g, 0.975mmol) was condensed into a 50ml high pressure ampoule with $Co_2(CO)_8$ (1.00g, 2.92mmol) in 10ml of hexane giving a ratio of 1 to 3. The reaction was left in the dark at room temperature for four

months resulting in a dark brown solution with a brown precipitate. The contents were transferred to a Schlenk flask and the residue in the ampoule washed out using CH_2Cl_2. The solvents and any $HCo(CO)_4$ were removed under vacuum and unreacted $Co_2(CO)_8$ was sublimed onto a cold finger. The remaining solid was dissolved in hexane and the infrared spectrum showed it to contain $Co_2(CO)_8$ at (υCO, (hexane) 2069, 2043, 2031, 2024 and 1858cm^{-1}), $Co_4(CO)_{12}$ at (υCO, (hexane) 2064, 2055 and 1867cm^{-1}), approximately 5-10% $Si[Co_2(CO)_7]_2$ {5} at (υCO, (hexane) 2085 s, 2065 s, 2044 m, 2037 s, 2026 m, 2007 w, 1847 br w, cm^{-1}) and a new product in approximately 20-30% yield (see section 5.2.2 for characterisation as $O[SiCo(CO)_4Co_2(CO)_7]_2$).

$H_3SiOSiH_3$ (0.0572g, 0.731mmol) was reacted with $Co_2(CO)_8$ (0.50g, 1.46mmol) at room temperature using 10ml of hexane as solvent with a reaction ratio of 1 to 2. The reaction was allowed to proceed for 2 days after which a brown precipitate had formed with the solution still a brown colour.

Infrared spectra of the volatile components showed only a trace of Si-H species remaining. The hexane soluble fraction contained unreacted $Co_2(CO)_8$ with a small amount of $Co_4(CO)_{12}$ and some $Si[Co_2(CO)_7]_2$.

Extraction with CH_2Cl_2 gave a yellow/brown solution of a new product (υCO, (CH_2Cl_2) 2101 w, 2072 s, 2042 vs, 2028 s, 1848 br w, cm^{-1}, Figure 5.3) in a yield of approximately 10-20%.

$H_3SiOSiH_3$ (0.114g, 1.46mmol) was reacted with $Co_2(CO)_8$ (0.75g, 2.19mmol) at room temperature in the dark for six months using 10ml of hexane as solvent. This reaction ratio of 1 to 1.5 was used to see if the $Co_2(CO)_8$ would completely react. After two days the colour in the reaction vessel had changed from dark brown to orange brown with the formation of a brown precipitate. After six months the solution was red/brown with a brown precipitate.

Work-up of the reaction revealed six hexane soluble products. Smaller amounts of $Co_2(CO)_8$ and $Co_4(CO)_{12}$ were identified compared to previous reactions (20% of solids). $Si[Co_2(CO)_7]_2$ {5} and $(CO)_4CoSiCo_3(CO)_9$ {2} were

the major products (50-60% of solids). The remaining 20-30% of the solids contained two products (1) with a strong 2030 cm^{-1} infrared peak and (2) a product with a bridging carbonyl peak at 1846 cm^{-1} (see section 5.2.2).

This hexane-soluble fraction was gently refluxed in petroleum spirit (approximately 50°C) for 30 minutes. After heating, the colour of the solution had noticeably changed to a deeper red. Infrared spectra showed that the amount of the brown product (1846 cm^{-1}) had decreased with the formation of a greater proportion of the red 2030 cm^{-1} compound.

A higher temperature reaction of $H_3SiOSiH_3$ (0.0763g, 0.975mmol) with $Co_2(CO)_8$ (1.00g, 2.92mmol) was carried out in a sealed vessel. Hexane (10ml) was used as the solvent with a reaction temperature of 50°C for 2 weeks. After heating the solution had formed a black precipitate with a dark red/brown solution.

Infrared spectra of the hexane-soluble fraction showed it to contain some $Co_2(CO)_8$, a large amount of $Co_4(CO)_{12}$, $(CO)_4CoSiCo_3(CO)_9$ and a small amount of the new product with the 2030 cm^{-1} peak. A minor quantity of solid, was not soluble in hexane, this gave a red/brown CH_2Cl_2 solution which was not characterised.

A similar reaction using a ratio of $H_3SiOSiH_3$ to $Co_2(CO)_8$ of 1 to 2 gave essentially the same product distribution.

A large scale reaction was prepared, $H_3SiOSiH_3$ (0.260g, 3.33mmol) was condensed into a 250ml high pressure ampoule with $Co_2(CO)_8$ (3.00g, 8.77mmol) in 30ml of hexane giving a reaction ratio of 1 to 2.6. Small bubbleswere observed in the initially vigorous reaction which was left to proceed at room temperature for two weeks.

On work-up only a very small amount of silicon containing compounds were observed (less than 5%). The majority of the solid fraction contained unreacted $Co_2(CO)_8$ with the formation of some $Co_4(CO)_{12}$. For this reason extraction of the products containing silicon was not attempted. An insoluble residue remained which may have contain the decomposed disiloxane products.

5.2.2 INFRARED SPECTRA OF PRODUCTS

An infrared spectrum of the red hexane-soluble product is shown in Figure 5.1. The very simple spectrum with only two major peaks (υCO, (hexane) 2054 m, 2030 vs, cm^{-1}) together with a number of very weak peaks (which are possibly due to trace impurities) suggests that the product has high symmetry. When this spectrum is compared with those of $MeCCo_3(CO)_9$ [118] and $MeGeCo_3(CO)_9$ [82] (Table 5.1) we see similar two peak spectra but with the intensities reversed.

Table 5.1

INFRARED SPECTRA OF -$Co_3(CO)_9$ GROUPS		
RED	**$MeCCo_3(CO)_9$**	**$MeGeCo_3(CO)_9$**
	2103 w	2108 m
2054 m	2052 vs	2055 vs
2030 vs	2039 m	2045 s
	2018 w	2018 m
	1990 vw	1992 w

The red colour and hexane solubility are found for compounds of the type $XSiCo_3(CO)_9$ (X = metal-carbonyl, organic) while other hexane-soluble silicon-cobalt compounds are generally yellow, orange or brown in colour. The product is tentatively assigned as $O[SiCo_3(CO)_9]_2$ for the following reasons: (1) red colour, (2) hexane solubility which is slightly less than the related $(CO)_4CoSiCo_3(CO)_9$ {2} compound, (3) very simple infrared spectrum, (4) sensible possible product from the reaction. In terms of $O[SiCo_3(CO)_9]_2$ with a linear Si-O-Si bond (or local symmetry at each end) we would predict for C_{3V} symmetry, $2A_1 + A_2 + 3E$ which gives 5 infrared active modes ($2A_1 + 3E$). As can be seen above for $MeCCo_3(CO)_9$ and $MeGeCo_3(CO)_9$ this number of peaks are observed but only two are prominent. Two strong infrared peaks are

observed for this red product along with other possible weak peaks as predicted from the symmetry.

An infrared spectrum of the brown hexane-soluble compound is shown in Figure 5.2. This infrared spectrum is compared to $(CO)_4CoPhGeCo_2(CO)_7$ {3} [141] for the tentative assignment of the compound thought to be $O[SiCo(CO)_4Co_2(CO)_7]_2$ (Table 5.2). This comparison shows a very reasonable match in wavenumber and intensity with the 1846 cm^{-1} bridging carbonyl peak very characteristic of a $Co_2(CO)_7$ group. Peaks at the top end of this infrared spectrum are indicative of a terminal $Co(CO)_4$ group. The yellow/brown colouration is consistent with the -$SiCo(CO)_4Co_2(CO)_7$ group.

Table 5.2

INFRARED SPECTRUM OF BROWN PRODUCT COMPARED WITH $(CO)_4CoPhGeCo_2(CO)_7$	
BROWN PRODUCT hexane	**$(CO)_4CoPhGeCo_2(CO)_7$ cyclohexane**
2110 w	
2101 w	2104 w
2089 s	2082 s
2061 s	2056 s
	2044 w
2037 s	2036 s
2021 s	2025 m
2015 m sh	2014 m
	1998 w
1846 m	1850 w
	1835 sh

Figure 5.1

INFRARED SPECTRUM OF $H_3SiOSiH_3$ WITH $Co_2(CO)_8$

HEXANE SOLUTION (RED)

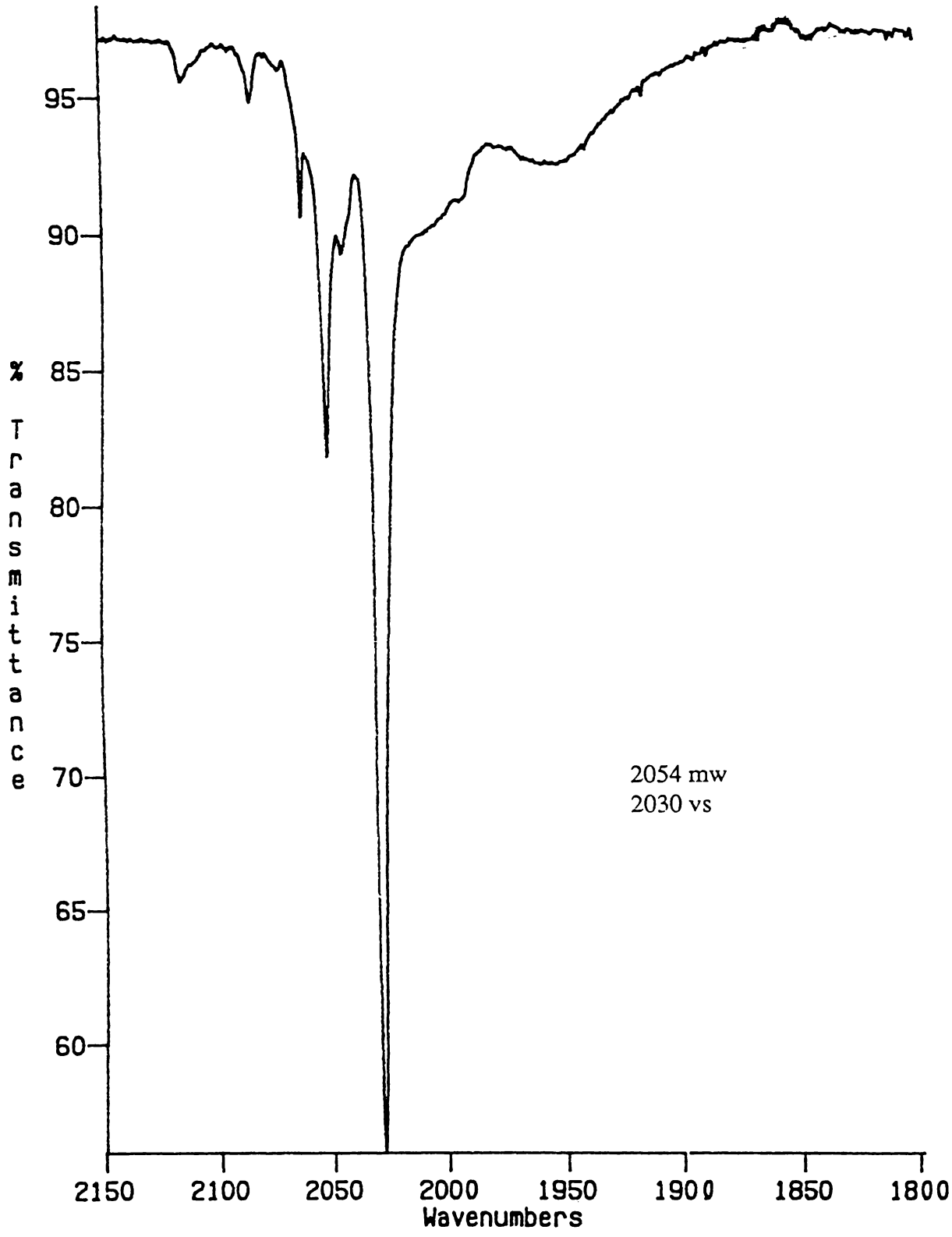

Figure 5.2

INFRARED SPECTRUM OF $H_3SiOSiH_3$ WITH $Co_2(CO)_8$

HEXANE SOLUTION (BROWN)

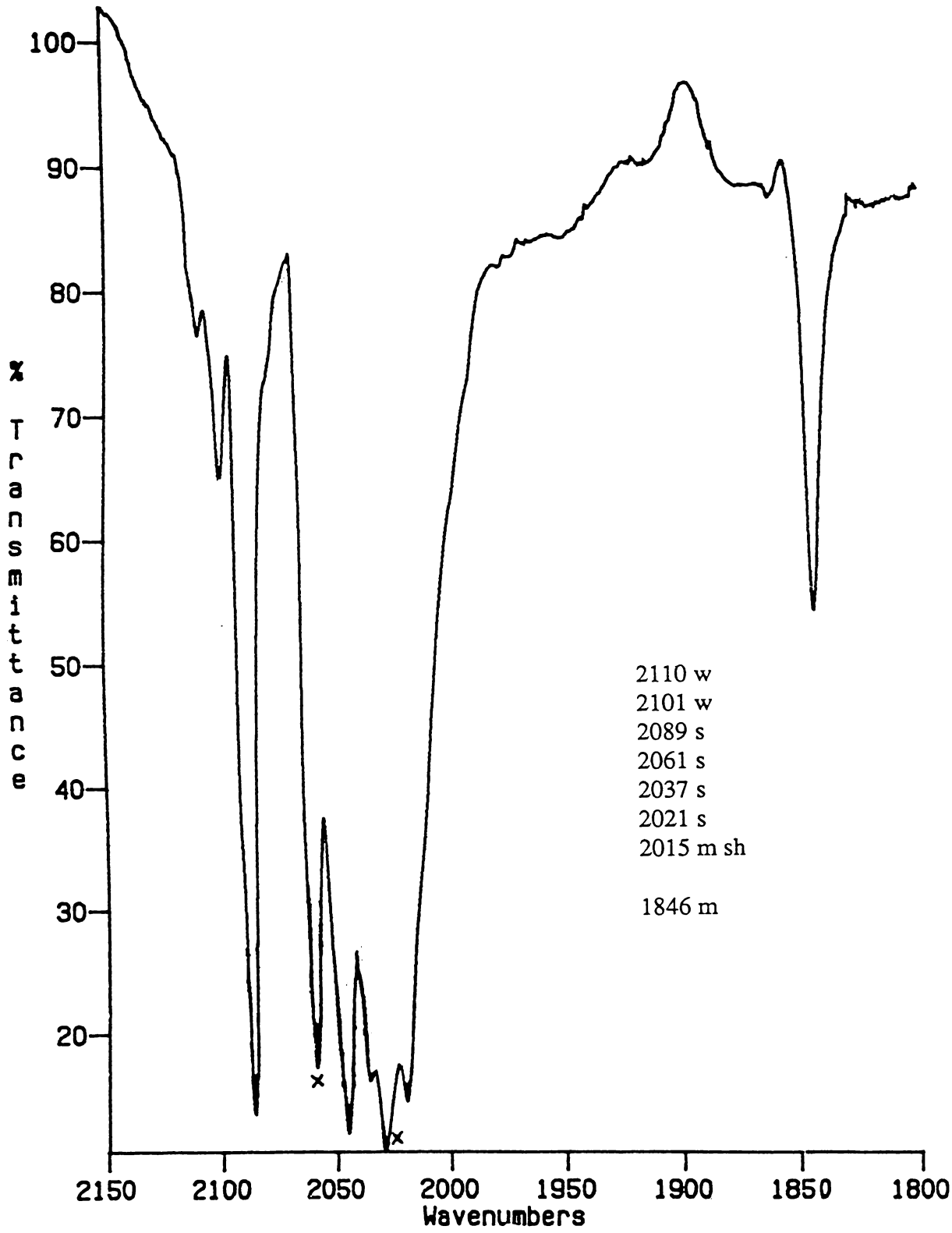

Figure 5.3

INFRARED SPECTRUM OF $H_3SiOSiH_3$ WITH $Co_2(CO)_8$

CH_2Cl_2 SOLUTION (YELLOW/BROWN)

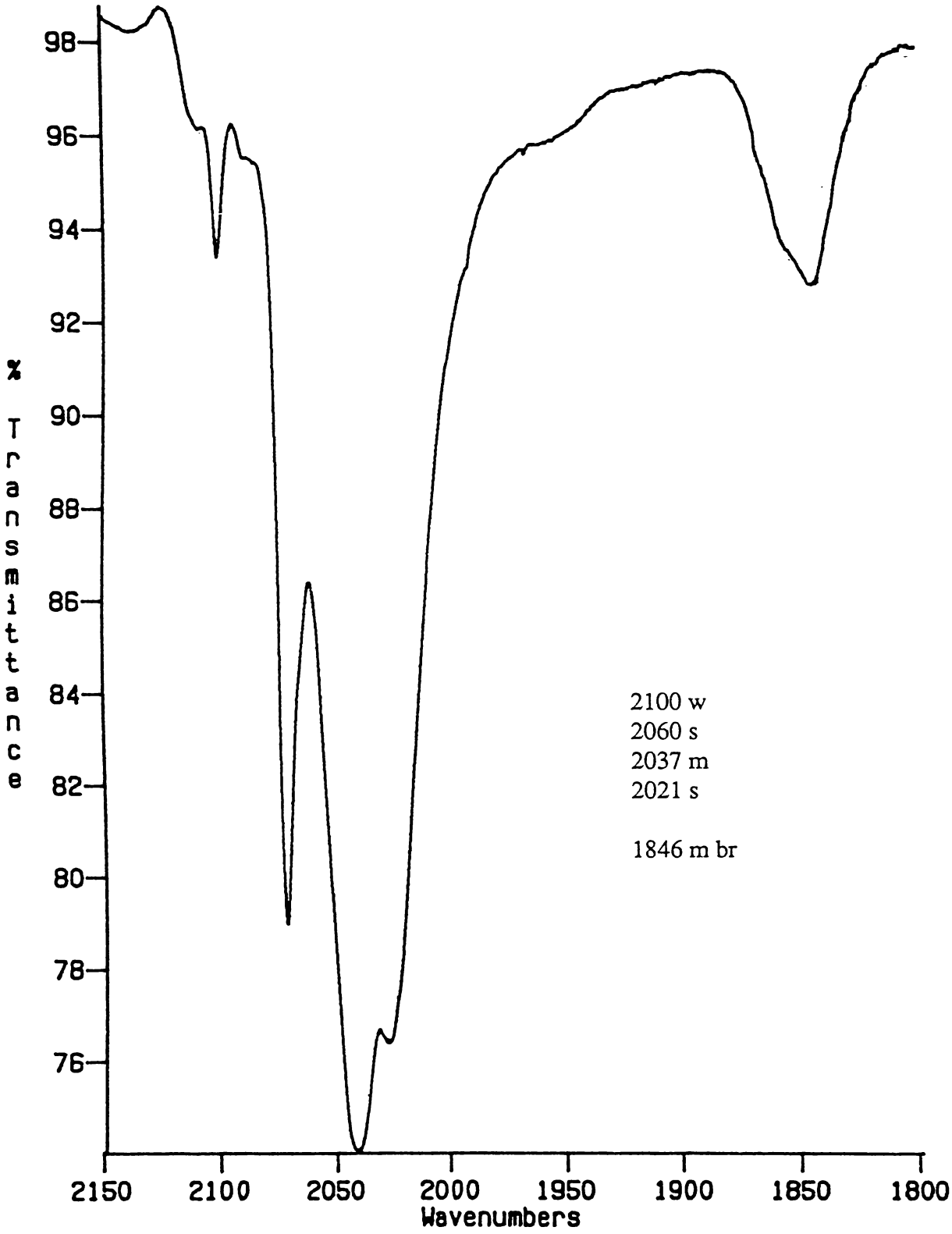

The infrared spectrum of the yellow/brown CH_2Cl_2 soluble product is shown in Figure 5.3. As expected the CH_2Cl_2 infrared spectrum is simplified due to solvent effects. This effect is also demonstrated in the case of $(PhSi)_2Co_4(CO)_{11}$ in which the spectra in both the hexane and CH_2Cl_2 are shown (section 4.2.3). This yellow/brown compound contains a characteristic bridging carbonyl which is generally associated with the $Co_2(CO)_7$ group. This infrared spectrum has some similarities to the above brown compound but remains uncharacterised.

5.2.3 DISCUSSION

These reactions of $H_3SiOSiH_3$ with $Co_2(CO)_8$ showed great inconsistency with respect to the products formed and the often large and variable amount of unreacted $Co_2(CO)_8$. The products observed arose mainly from the breaking of the strong Si-O-Si linkage to form $Si[Co_2(CO)_7]_2$ {5} and $(CO)_4CoSiCo_3(CO)_9$ {2}. These range from 5 to 60% of the solid fraction. Products which retain the Si-O-Si linkage, $O[SiCo(CO)_4Co_2(CO)_7]_2$ (Figure 5.4) and $O[SiCo_3(CO)_9]_2$ (Figure 5.5), may indeed be formed but these are only minor components.

Some evidence for these products is seen in the decarbonylation experiment above, which was monitored by infrared spectroscopy. $Si[Co_2(CO)_7]_2$ and the tentatively assigned compound $O[SiCo(CO)_4Co_2(CO)_7]_2$, were both present in the reaction mixture. On heating carbon monoxide was evolved which formed the decarbonylated products $(CO)_4CoSiCo_3(CO)_9$ and $O[SiCo_3(CO)_9]_2$ (tentatively assigned) respectively (see equations below). The red colouration of the solution is characteristic of the $-Co_3(CO)_9$ group.

$$Si[Co_2(CO)_7]_2 \rightarrow (CO)_4CoSiCo_3(CO)_9 + CO$$

$$O[SiCo(CO)_4Co_2(CO)_7]_2 \rightarrow O[SiCo_3(CO)_9]_2 + 4CO$$

Only a minor proportion of the Si-O links are found intact in the products (maximum 20% of solids), and there is an overall deficiency in recovered

silicon. This suggests that a variable amount of the disiloxane ends up as involatile products, presumably Si-O, Si-O-Co, or even Co-Si-O polymeric products.

Figure 5.4 $O[SiCo(CO)_4Co_2(CO)_7]_2$

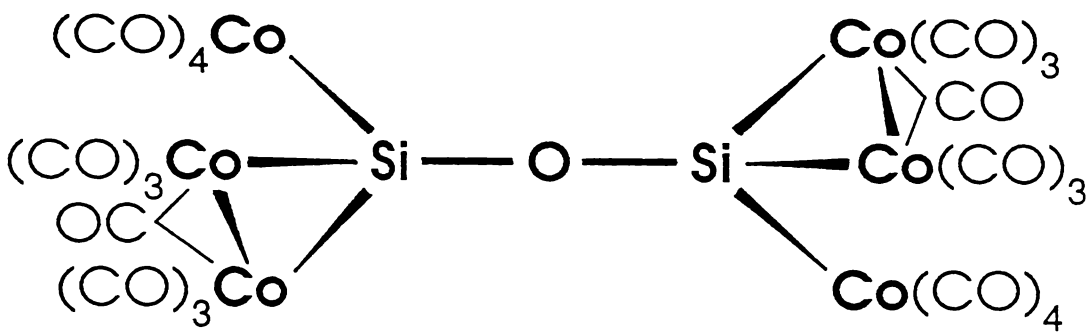

Figure 5.5 $O[SiCo_3(CO)_9]_2$

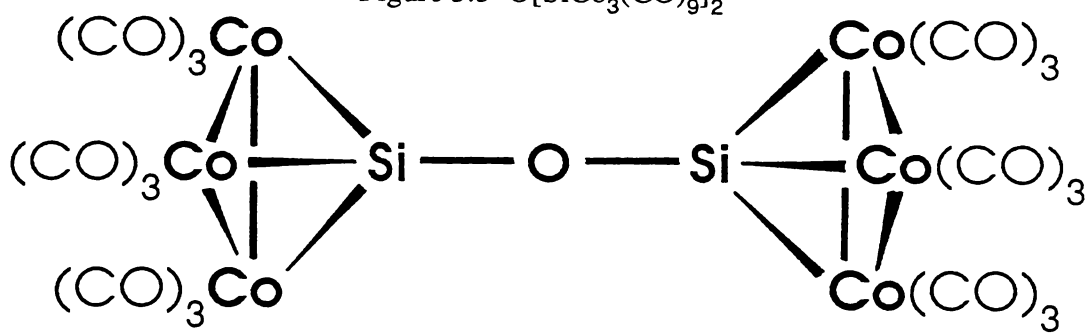

5.3 REACTION OF $H_3SiOSiH_3$ WITH $Co_4(CO)_{12}$

5.3.1 INTRODUCTION

This reaction was investigated for comparison with those above which utilise $Co_2(CO)_8$. The advantage of using $Co_4(CO)_{12}$ is that the range of products is markedly smaller making separation and identification easier. The reason for this is that generally the more clustered products are formed, for example the products formed from the reaction between SiH_4 and $Co_2(CO)_8$ are $Co_2(CO)_8$, $Co_4(CO)_{12}$, $Si[Co_2(CO)_7]_2$ {5} and $(CO)_4CoSiCo_3(CO)_9$ {2} while SiH_4 with $Co_4(CO)_{12}$ gives only $Co_4(CO)_{12}$ and $(CO)_4CoSiCo_3(CO)_9$. One possible disadvantage is that $Co_4(CO)_{12}$ reacts more slowly requiring longer times or higher reaction temperatures which may decompose wanted products.

5.3.2 EXPERIMENTAL

$H_3SiOSiH_3$ (0.142g, 1.82mmol) was condensed into a 50ml high pressure ampoule with $Co_4(CO)_{12}$ (1.04g, 1.82mmol) in 10mls of hexane to give a ratio of 1 to 1. The reaction was left at room temperature for 6 months to give a red/brown solution with black crystals.

The contents were transferred to a Schlenk flask and the hexane (20 ml) soluble fraction was extracted. The infrared spectrum showed this to contain unreacted $Co_4(CO)_{12}$ and the silicon cluster $(CO)_4CoSiCo_3(CO)_9$ (υCO, (hexane) 2114 w, 2087 s, 2046 vs, 2030 m, cm^{-1}) in approximately 10-20% yield. No new products were isolated. The CH_2Cl_2 soluble fraction contained only unreacted $Co_4(CO)_{12}$. A small amount of light brown insoluble material remained.

5.3.3 DISCUSSION

Only a small proportion of the silicon is accounted for in the products. $(CO)_4CoSiCo_3(CO)_9$ {2} is readily formed, presumably as a byproduct via rearrangement of the $H_3SiOSiH_3$. The remaining silicon may form Si-O species which are not soluble.

Formation of the possible cluster $O[SiCo_3(CO)_9]_2$ (see equation below) would require $Co_4(CO)_{12}$ to undergo substantial rearrangement.

$$H_3SiOSiH_3 + 1.5Co_4(CO)_{12} \rightarrow O[SiCo_3(CO)_9]_2 + 3H_2$$

Contrary to the above equation the reaction forms $(CO)_4CoSiCo_3(CO)_9$. This requires both the breaking of strong Si-O bonds and the scavenging of one more carbonyl ligand. This situation is also seen in the reaction of SiH_4 with $Co_4(CO)_{12}$ which requires an extra carbonyl ligand and rearrangement of the Co_4 core. The great stability of the $(CO)_4CoSiCo_3(CO)_9$ cluster may be the driving force. The formation of a polymeric structure such as $-O-[-Si-Co_4(CO)_{11}-Si-O-]_n-Si-$ in the insoluble residue is possible.

5.4 REACTION OF $H_3SiOSiH_3$ WITH $Fe(CO)_5$

5.4.1 EXPERIMENTAL

$H_3SiOSiH_3$ (0.0599g, 0.766mmol) was condensed into a 50ml high pressure ampoule with a large excess of $Fe(CO)_5$ (2.9g, 15mmol) in 5ml petroleum spirit (80-100°C). The contents were heated for 4 hours at 150°C resulting in a yellow/brown solution with a black precipitate and a metallic coating. The contents were transferred to a Schlenk flask and the solvent and unreacted $Fe(CO)_5$ were pumped away. Extraction of the solid with hexane (3 x 10ml) gave a light yellow solution. This was characterised by infrared spectroscopy and shown to contain only $Si[Fe_2(CO)_8]_2$ **{5}** (υCO, (hexane) 2076 m, 2050 vs, 2030 w, 2013 m, cm^{-1}). Further extracts with CH_2Cl_2 (2 x 20ml) also contained $Si[Fe_2(CO)_8]_2$ and these were removed from the remaining black solid, estimated yield 40-50%.

After removal of the $Si[Fe_2(CO)_8]_2$ a solution of $[Et_4N]Br$ in CH_2Cl_2 was added to the black solid. This resulted in a red/brown solution with an infrared spectrum of (υCO, (CH_2Cl_2) 2050 w, 2034 sh, 2020 sh, 1989 s br, 1922 m, 1887 w, cm^{-1}). This shift to lower frequency is characteristic of an anionic species but the compound remains uncharacterised.

An experiment at lower temperature (120°C for 3 hours) produced less decomposition of the $Fe(CO)_5$ with the major product being $Si[Fe_2(CO)_8]_2$.

5.4.2 DISCUSSION

The high temperature reaction of SiH_4 or Si_2H_6 with $Fe(CO)_5$ [36] forms $Si[Fe_2(CO)_8]_2$ as the major product. $H_3SiOSiH_3$ with $Fe(CO)_5$ also results in the formation of the same product. Generally, the reaction of silicon hydrides with $Fe(CO)_5$, $Fe_2(CO)_9$ or $Fe_3(CO)_{12}$ form $Si[Fe_2(CO)_8]_2$ as the major product. Reactions of other related hydrides such as GeH_4, Ge_2H_6 and SnH_4 with $Fe(CO)_5$, $Fe_2(CO)_9$ or $Fe_3(CO)_{12}$ [36] give a much wider range of products which include $[(CO)_8Fe_2Ge]_2Fe_2(CO)_7$ **{8}** and the Sn analogue,

$[(CO)_8Fe_2Ge]_2Fe_3(CO)_{10}$ and the Sn analogue, $[(CO)_8Fe_2Sn]Fe_3(CO)_{11}$ along with the Ge and Sn analogues of $Si[Fe_2(CO)_8]_2$ {5}.

Therefore the above reaction does conform to what is generally found for the silicon hydrides but does involve the breaking of strong Si-O bonds.

5.5 REACTION OF $H_3SiSSiH_3$ WITH $Co_2(CO)_8$

5.5.1 INTRODUCTION

This reaction was conducted to see if silicon-cobalt carbonyl products could be isolated which retain the Si-S-Si linkage. This is the most convenient silicon hydride to prepare which is linked by a group 16 element other than oxygen.

5.5.2 EXPERIMENTAL

$H_3SiSSiH_3$ (0.0979g, 1.04mmol) was condensed into a 50ml ampoule with $Co_2(CO)_8$ (1.00g, 2.92mmol) in 10ml of hexane. Bubbles appeared as the reaction started and the mixture was left to react in the dark at room temperature for three weeks. A brown solution with a black precipitate formed and on opening the ampoule only a trace of silicon hydrides was detected.

The contents of the ampoule were transferred to a Schlenk flask and extracted using 3 x 10ml hexane, leaving a black precipitate. The infrared spectrum of the hexane solubles showed unreacted $Co_2(CO)_8$ at (2069, 2043, 2031, 2024 and 1858 cm^{-1}), $Co_4(CO)_{12}$ at (2064, 2055 and 1867 cm^{-1}) and a new orange compound, shown below to be $SSi_2Co_4(CO)_{14}$ (see section 5.5.5). This hexane solution was slowly cooled to -25°C whereupon yellow/orange feather-like crystals formed. These crystals were dissolved in toluene (10ml) and slowly cooled to -25°C which resulted in yellow/orange diamond-shaped crystals suitable for X-ray crystallography. The weight of $SSi_2Co_4(CO)_{14}$ isolated amounted to 0.32g (0.45mmol). This represents a 43% yield based on $H_3SiSSiH_3$.

The black precipitate was soluble in CH_2Cl_2 and was characterised by its infrared spectrum as $S_2Co_4(CO)_{10}$ which has a strong peak at 2050 cm^{-1} (see section 5.5.9), together with a small amount of $Co_4(CO)_{12}$.

A similar reaction which was left for a longer period of time was investigated. $H_3SiSSiH_3$ (0.0979g, 1.04mmol) was sealed with $Co_2(CO)_8$ (1.00g, 2.92mmol) in 10ml of hexane giving a reaction ratio of 1 to 2.8. This was left to react at room temperature in the dark for two years. Initially the solution was orange/brown, but on completion the solution was brown/black with a large amount of brown/black solid.

Work-up showed the products to comprise unreacted $Co_2(CO)_8$ (10-20%) and $Co_4(CO)_{12}$ (30-40%). The yield of the orange hexane-soluble product ($SSi_2Co_4(CO)_{14}$) had decreased to 10%. The black CH_2Cl_2 soluble product, $S_2Co_4(CO)_{10}$, was obtained in an estimated yield of 30-40%.

A reaction at low temperature was investigated. $H_3SiSSiH_3$ (0.0919g, 0.975mmol) with $Co_2(CO)_8$ (1.00g, 2.92mmol) was reacted at 5°C for 2 months using 10ml of hexane solvent. The reaction solution was orange/brown in colour with some orange crystals and a small amount of black precipitate.

Work-up of initial hexane-solubles (2 x 20ml) showed unreacted $Co_2(CO)_8$, a small amount of $Co_4(CO)_{12}$ and $SSi_2Co_4(CO)_{14}$ together with an uncharacterised compound with infrared peaks at (υCO, (hexane) 2050 s, 2030 s, cm^{-1}). The next 3 x 20ml hexane extracts contained only $SSi_2Co_4(CO)_{14}$ in a moderate yield of 40-50%. The CH_2Cl_2 soluble fraction contained a small amount of $S_2Co_4(CO)_{10}$.

A reaction at higher temperature was investigated. $H_3SiSSiH_3$ (0.0979g, 1.04mmol) was sealed with $Co_2(CO)_8$ (1.00g, 2.92mmol) in 10ml of hexane giving a reaction ratio of 1 to 2.8. This was heated to 50°C for 10 days which resulted in a brown/black solution with a black solid.

Extraction using hexane (4 x 10ml) showed it to contain a small amount of unreacted $Co_2(CO)_8$ together with $Co_4(CO)_{12}$. The silicon cluster $(CO)_4CoSiCo_3(CO)_9$ formed in minor quantities from Si-S bond cleavage.

The remaining $Co_4(CO)_{12}$ was removed with 3 x 10ml hexane. CH_2Cl_2 was added to dissolve the black solid, which an infrared spectrum showed to be almost pure $S_2Co_4(CO)_{10}$ with a very strong peak at 2050 cm^{-1} (see section 5.5.6). The isolated weight (0.283g 0.488mmol), represents a 47% yield based on $H_3SiSSiH_3$.

5.5.3 INFRARED SPECTRUM OF $SSi_2Co_4(CO)_{14}$

The infrared spectrum of $SSi_2Co_4(CO)_{14}$ in the carbonyl region in hexane is shown in Figure 5.6. The spectrum exhibits seven peaks. From the crystal structure, the idealised molecular symmetry is C_{2V}, while the Si-$Co(CO)_4$ units have local C_{3V} symmetry. Other molecules with $ECo(CO)_4$ units bridging $Co_2(CO)_6$ show little or no mixing between $Co(CO)_4$ and $Co_2(CO)_6$ modes [37,78]. If further, we assume little interaction between the $Co(CO)_4$ units, then we might expect to see three bands ($2A_1 + E$) in C_{3V} for these superimposed on a Bor [121] spectrum of up to 5 bands ($2A_1 + A_2 + 2B_1 + B_2$ in C_{2V}) for $Co_2(CO)_6$ (Note, A_2 is infrared inactive).

Table 5.3

INFRARED SPECTRUM OF $SSi_2Co_4(CO)_{14}$ COMPARED TO $(Me_2Si)_2Co_2(CO)_6$ AND $[(CO)_4CoMeGe]_2Co_2(CO)_6$

$SSi_2Co_4(CO)_{14}$	$(Me_2Si)_2Co_2(CO)_6$	$[(CO)_4CoMeGe]_2Co_2(CO)_6$
2104 s		2097w
2072 s	2087 s	2087 s
2056 m		2067 mw
2046 vs		2039 s
2038 s	2030 s	2029 s
2024 m	2005 s	2017 vs
2014 w	1995 s	2002 mw
	1993 sh	1970 w

Figure 5.6

INFRARED SPECTRUM OF $SSi_2Co_4(CO)_{14}$

HEXANE SOLUTION

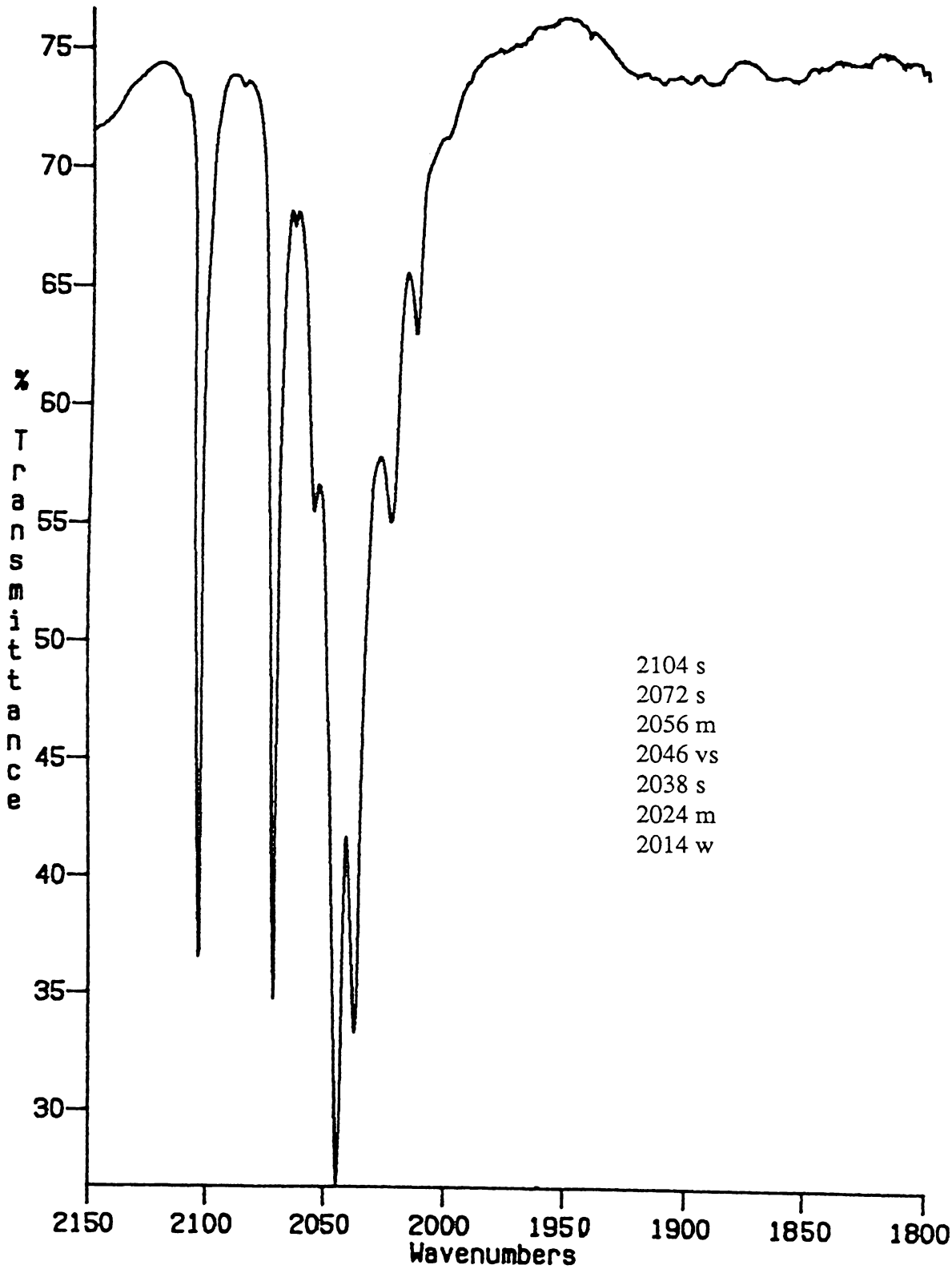

The comparison of infrared spectra containing the $Co_2(CO)_6$ unit $(Me_2Si)_2Co_2(CO)_6$ {4} [27] and $[(CO)_4CoMeGe]_2Co_2(CO)_6$ {4} [37, 120] is shown in Table 5.3. A reasonable match with the closely related compound $[(CO)_4CoMeGe]_2Co_2(CO)_6$ is difficult to see. This is due to the new bonding arrangement adopted in $SSi_2Co_4(CO)_{14}$ (see section 5.5.5) in which the terminal $Co(CO)_4$ groups are constrained diffrently than in $[(CO)_4CoMeGe]_2Co_2(CO)_6$. This could result in the differences seen in the infrared spectra. On comparison with $(Me_2Si)_2Co_2(CO)_6$ even the central $Co_2(CO)_6$ unit is hard to recognise with mixing between the two. The higher peaks would generally be due to the terminal $Co(CO)_4$ group.

5.5.4 X-RAY CRYSTALLOGRAPHIC STUDY OF $SSi_2Co_4(CO)_{14}$

Yellow/orange diamond shaped crystals were obtained from a slowly cooled toluene solution. Preliminary precession photographs using Cu-Kα radiation indicated that the crystal had orthorhombic symmetry and was originally thought to belong to the space group Pnma.

Intensity data were collected in the space group Pnma on a suitable crystal of dimensions 0.7 x 0.5 x 0.4 mm at the University of Canterbury on a Nicolet P3 diffractometer. A scan range of $4°<2\theta<52°$ was employed to obtain 4575 unique reflections using Mo-Kα radiation. No significant decay was observed. An absorption correction was applied to the data using an empirical ϕ-scan technique with transmission factors, 0.962 maximum and 0.497 minimum. For the solution of the structure and refinement, 3107 reflections were used with $I>3\sigma(I)$. Crystal data for $SSi_2Co_4(CO)_{14}$ are given in Table 5.4.

For all computations the SHELX-76 and SHELXS-86 [98] package of crystallographic programs were used. Attempts to locate sensible positions for the heavy atoms could not be achieved for the space group Pnma. Another examination of the preliminary precession photographs showed Pbcn to be the correct space group. So the data were transposed from Pnma to Pbcn using the matrix 0 1 0/0 0 1/1 0 0. Heavy atom position were located using TREF and subsequent refinement and difference maps easily located the carbon and oxygen atoms. All atoms were assigned anisotropic temperature factors with 9.8

reflections per parameter. Final refinement converged to R = 0.0350, Rw = 0.0398 with $w = 1.1003[\sigma^2(F) + 0.00300F^2]^{-1}$. Largest shift/e.s.d in the final refinement cycle was 0.003 with the greatest electron density at 0.8 e $Å^{-3}$.

Positional and thermal parameters along with complete tables of bond lengths and angles are given in Appendix Five. Tables of calculated and observed structure factors have been retained by the University of Waikato.

Table 5.4

CRYSTAL DATA FOR $SSi_2Co_4(CO)_{14}$	
Formula: $C_{14}Co_4O_{14}SSi_2$	Mr = 715.96
Orthorhombic	Space Group = Pbcn
Cryst. Colour: yellow/orange	
Cryst. Dimensions: 0.7 x 0.5 x 0.4 mm	
a = 20.834(6) Å	$\alpha = 90.00°$
b = 12.345(3) Å	$\beta = 90.00°$
c = 18.147(11) Å	$\gamma = 90.00°$
U = 4667(3) $Å^3$	Dcalc = 2.04 g cm^{-3}
Z = 8	
F(000) = 2784	Temp = 173 K
μ(Mo-Kα) = 29 cm^{-1}	
Unique Data = 4575	Range = $4° < 2\theta < 52°$
Refinement Data = 3107	Final R = 0.035

5.5.5 STRUCTURE OF $SSi_2Co_4(CO)_{14}$

Prespective views of the cluster $SSi_2Co_4(CO)_{14}$ are shown in Figures 5.7, 5.8 and 5.9. Atom labelling is shown in Figure 5.9 and is used throughout the following discussion. Selected bond lengths and angles are given in Tables 5.5 and 5.6.

Figure 5.7 Top and Side View of $SSi_2Co_4(CO)_{14}$

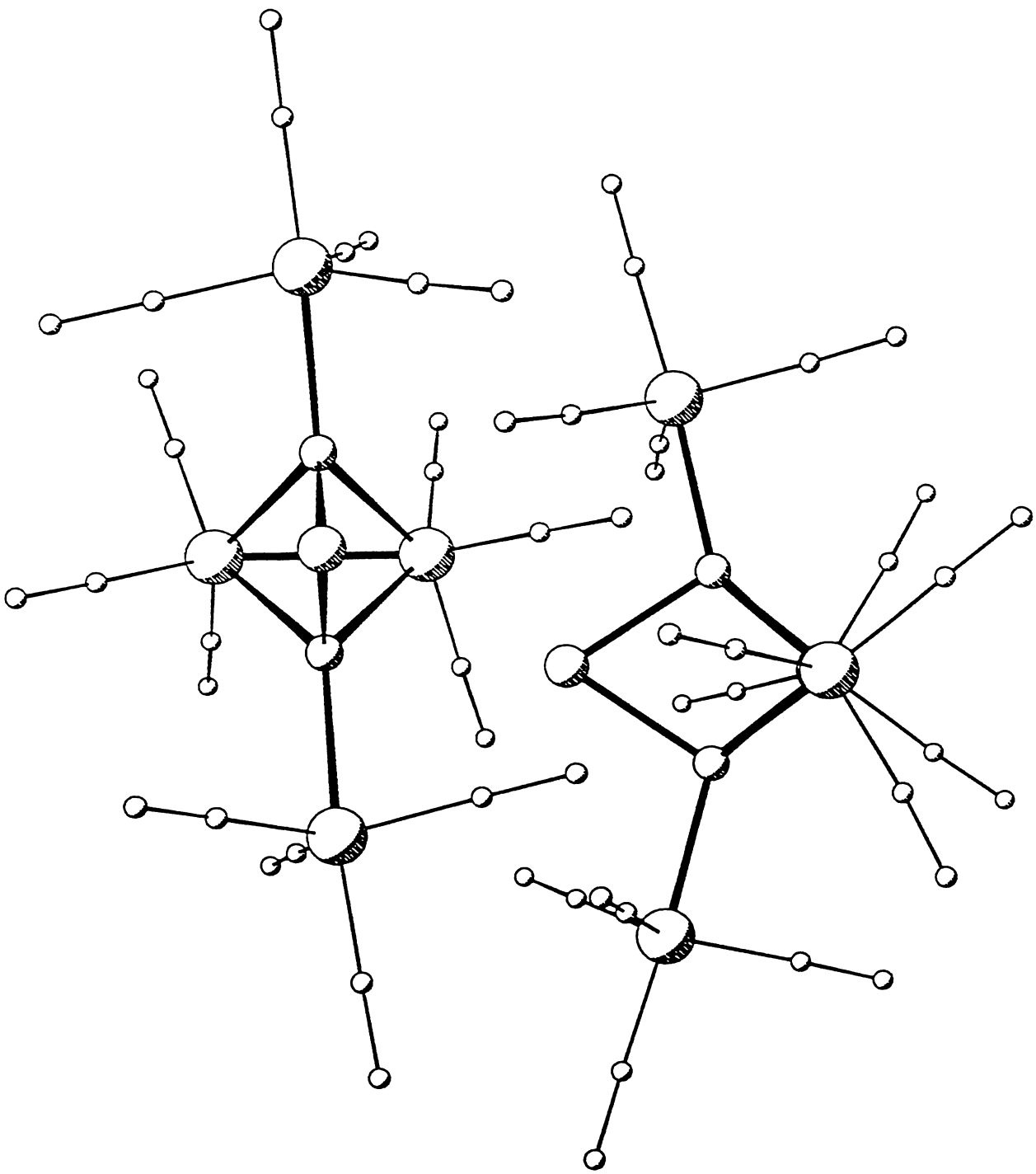

Figure 5.8 Stereo View of $SSi_2Co_4(CO)_{14}$

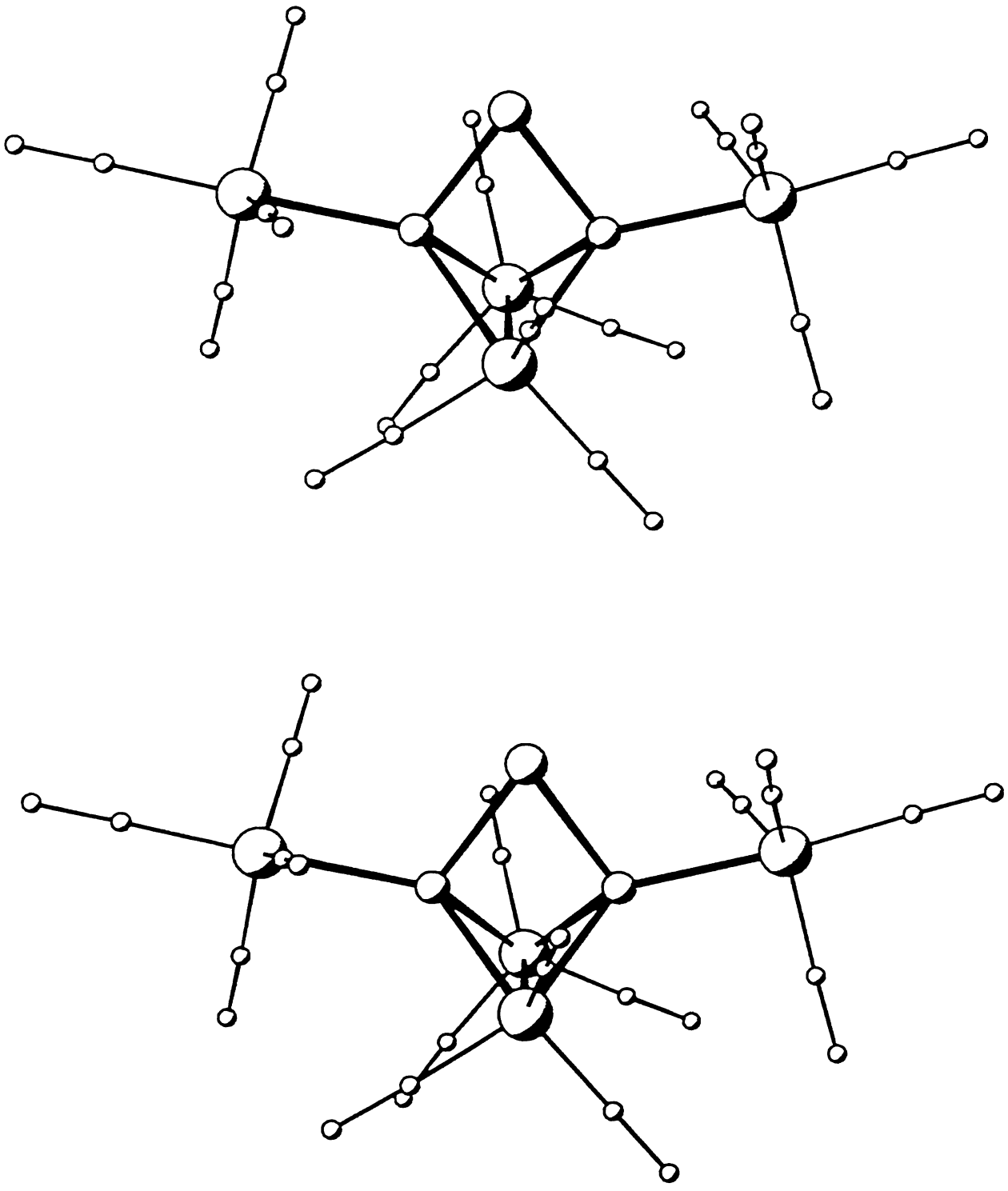

Figure 5.9 Labelled Perspective View of $SSi_2Co_4(CO)_{14}$

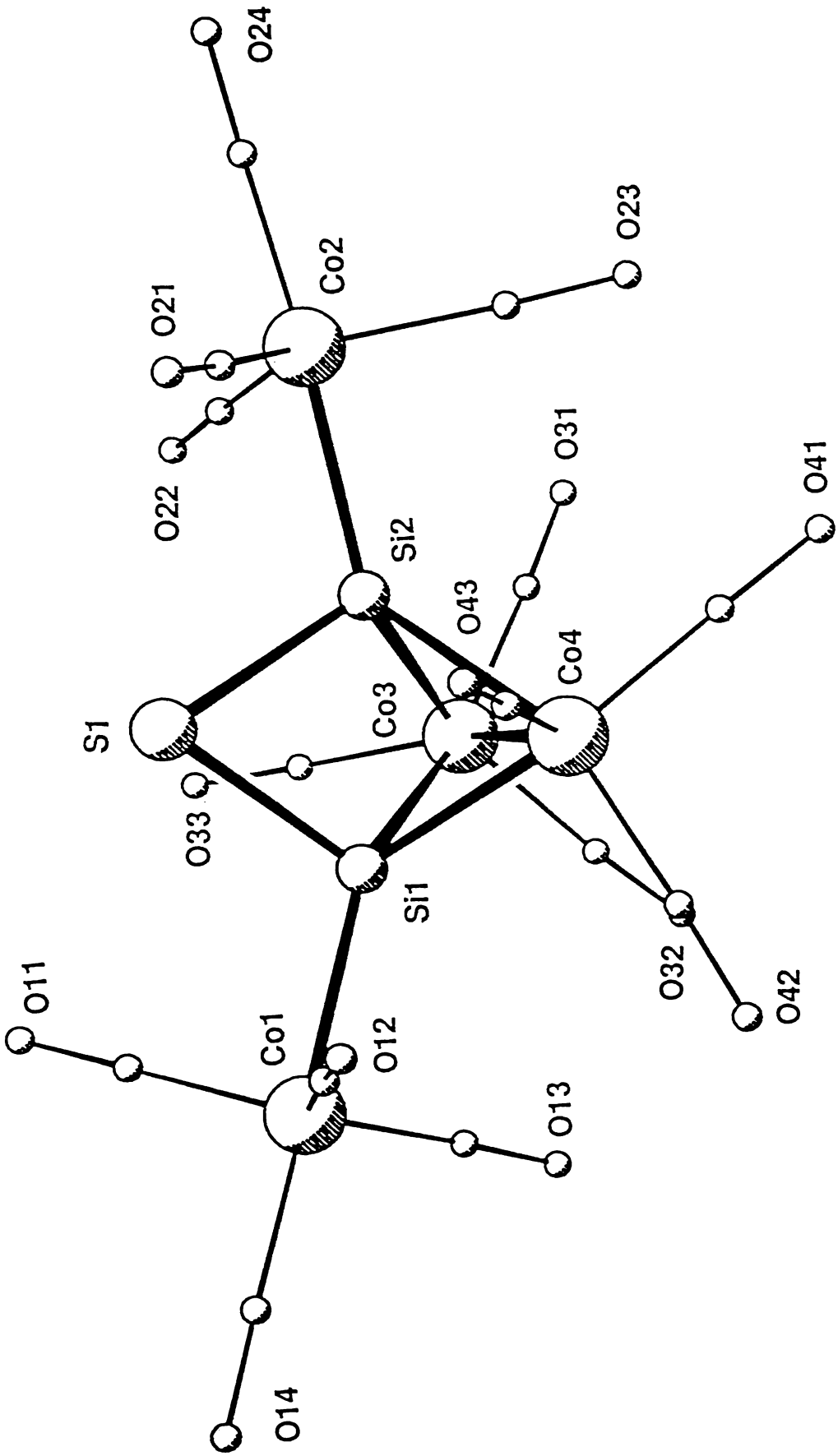

Table 5.5

SELECTED BOND LENGTHS FOR $SSi_2Co_4(CO)_{14}$ (Å)			
Co(1) ---Si(1)	2.295(1)	Co(2) ---Si(2)	2.299(1)
Co(3) ---Co(4)	2.623(1)	Co(3) ---Si(1)	2.309(1)
Co(3) ---Si(2)	2.297(1)	Co(4) ---Si(1)	2.291(1)
Co(4) ---Si(2)	2.309(1)	Si(1) ---S(1)	2.169(2)
Si(2) ---S(1)	2.174(2)		
Si(1) ...Si(2)	2.499(2)		

Table 5.6

SELECTED BOND ANGLES FOR $SSi_2Co_4(CO)_{14}$ (°)			
Co(4) -Co(3) -Si(1)	54.9(1)	Co(4) -Si(1) -S(1)	101.3(1)
Co(4) -Co(3) -Si(2)	55.5(1)	Si(2) -Si(1) -S(1)	55.0(1)
Si(1) -Co(3) -Si(2)	65.7(1)	Co(2) -Si(2) -Co(3)	129.5(1)
Co(3) -Co(4) -Si(1)	55.5(1)	Co(2) -Si(2) -Co(4)	134.3(1)
Co(3) -Co(4) -Si(2)	55.1(1)	Co(2) -Si(2) -Si(1)	166.7(1)
Si(1) -Co(4) -Si(2)	65.8(1)	Co(2) -Si(2) -S(1)	112.2(1)
Co(1) -Si(1) -Co(3)	133.8(1)	Co(3) -Si(2) -Co(4)	69.4(1)
Co(1) -Si(1) -Co(4)	130.2(1)	Co(3) -Si(2) -Si(1)	57.4(1)
Co(1) -Si(1) -Si(2)	166.5(1)	Co(3) -Si(2) -S(1)	101.3(1)
Co(1) -Si(1) -S(1)	111.7(1)	Co(4) -Si(2) -Si(1)	56.8(1)
Co(3) -Si(1) -Co(4)	69.5(1)	Co(4) -Si(2) -S(1)	100.6(1)
Co(3) -Si(1) -Si(2)	56.9(1)	Si(1) -Si(2) -S(1)	54.8(1)
Co(3) -Si(1) -S(1)	101.1(1)	Si(1) -S(1) -Si(2)	70.3(1)
Co(4) -Si(1) -Si(2)	57.4(1)		

The structure of $SSi_2Co_4(CO)_{14}$ consists of a $Co_2(CO)_6$ unit in which the Co-Co bond is bridged by two $SiCo(CO)_4$ groups which are linked to a sulphur atom. This structure retains the Si-S-Si linkage of the parent hydride. This is the first cluster in which such a linked bridging arrangement occurs across a metal-metal bond.

Arrangement of the fourteen carbonyls around the cluster consists of four each to the two terminal $Co(CO)_4$ groups and three terminally bonded to each cobalt in the central $Co_2(CO)_6$ unit. The two $Co(CO)_4$ groups have their carbonyls arranged in an almost fully staggered configuration whereas those on the $Co_2(CO)_6$ unit deviate only slightly from the eclipsed formation with respect to each other. This may be due to the packing arrangement in the crystal.

The very acute Si-S-Si angle of 70.3(1)° seen in the cluster $SSi_2Co_4(CO)_{14}$, is markedly smaller than the 97.4° of the parent hydride ($H_3SiSSiH_3$) [131, 132] and 92° in H_2S. Sterically crowded disilylthianes such as $Ph_3SiSSiPh_3$ [147] (Figure 5.10) and $(t\text{-}BuO)_3SiSSi(t\text{-}BuO)_3$ [148] (Figure 5.11) have Si-S-Si angles of 112.0° and 110.5° respectively. This shows an opening of the angle due to steric crowding of the bulky R groups. The angles in tetramethylcyclodisilylthiane [149] (Figure 5.12) are constrained into a planar Si_2S_2 tetracycle with the Si-S-Si angle at 82.46(6)°, this is still well away from the acute angle found in the cluster $SSi_2Co_4(CO)_{14}$.

Figure 5.10 $Ph_3SiSSiPh_3$

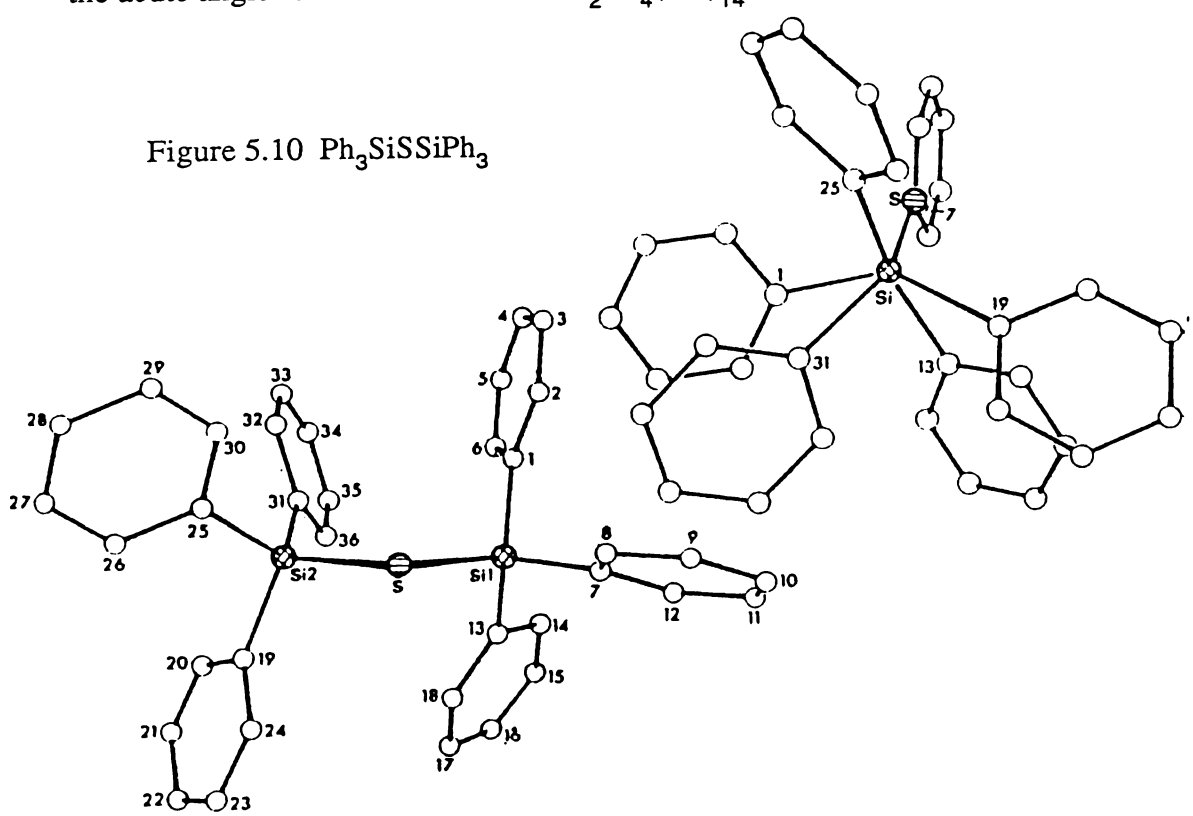

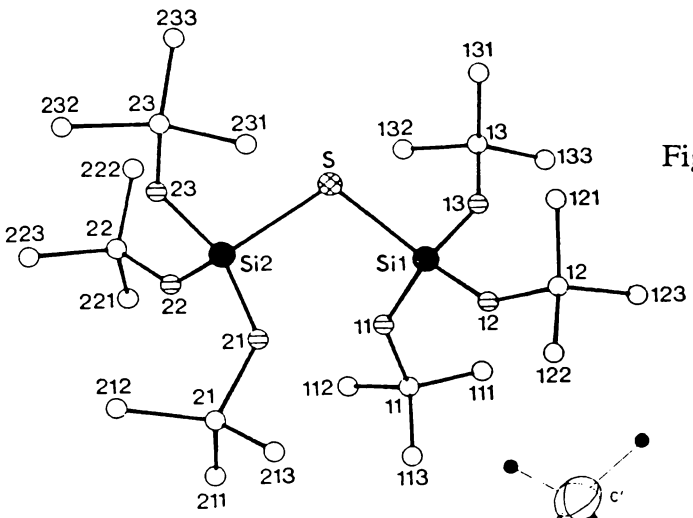

Figure 5.11 $(t\text{-}BuO)_3SiSSi(t\text{-}BuO)_3$

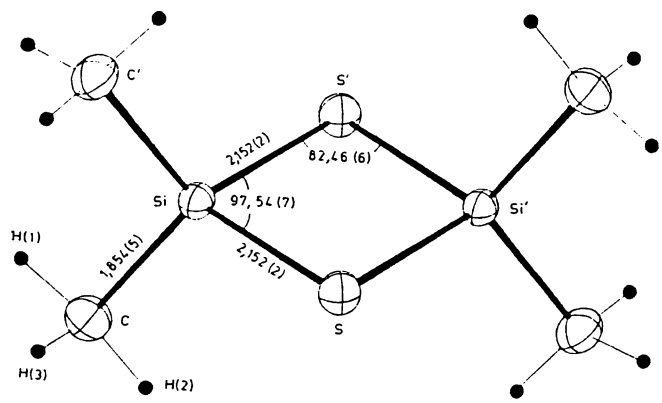

Figure 5.12 $Me_2SiS_2SiMe_2$

The Si-S distances of 2.169(2)Å and 2.174(2)Å can be compared to $Ph_3SiSSiPh_3$ at 2.152(1)Å, $(t\text{-}BuO)_3SiSSi(t\text{-}BuO)_3$ at 2.152(3)Å and tetramethylcyclodisilylthiane at 2.152(2)Å. This shows some lengthening of the Si-S bond in the cluster.

The di-bridged Co-Co distance of 2.623(1)Å is markedly longer than that of $Co_2(CO)_8$ at 2.52Å or that of $Si[Co_2(CO)_7]_2$ [43, 47] at 2.528Å. No structures containing a $(\mu\text{-}Si)_2$ analogue such as $(Me_2Si)_2Co_2(CO)_6$ [27] have yet been characterised by X-ray crystallography. Comparison with the di-bridged Co-Co distance in $[(CO)_4CoMeGe]_2Co_2(CO)_6$ [37, 120] at 2.733(2)Å shows the effect of the increased size of the bridging substituents on this Co-Co bond.

The silicon atoms do not symmetrically bridge the Co-Co bond but are mutually askew with Si(1)-Co distances of 2.291(1)Å and 2.309(1)Å and Si(2)-Co distances of 2.297(1)Å and 2.309(1)Å with an overall average value of 2.301Å. Comparison with $Si[Co_2(CO)_7]_2$, average 2.288Å shows a slightly longer Si-Co bond in this cluster.

The Si-Co distances to the terminal $Co(CO)_4$ groups are 2.295(1)Å and 2.299(1)Å. These can be compared to $(CO)_4CoSiCo_3(CO)_9$ {2} with a Si-Co terminal distance of 2.288Å and 2.347(2)Å for the five coordinate silicon cluster

$[(CO)_4CoSi]_2Co_4(CO)_{11}$ {7} [35]. These terminal groups are bent away from the $SiCo_2$ triangular face towards the sulphur atom at an angle of 144.4° with S-Si-Co angles to the terminal $Co(CO)_4$ groups of 111.7(1)° and 112.2(1)°.

The silicon-silicon distance of 2.499(2)Å is short enough to suggest a bonding interaction. This value can be compared to 2.32Å for Si_2H_6 [131, 138] and to the longest known single Si-Si bond, that of $(t\text{-}Bu)_3Si\text{-}Si(t\text{-}Bu)_3$ [139] at 2.679Å. This shows that the Si(1)-Si(2) distance is well within the range of known Si-Si single bond lengths. It would therefore be possible to regard the Si_2S unit as a triangle with a weak Si-Si bond, giving a rationalisation of the acute Si-S-Si angle. Clusters such as $[(CO)_4CoSi]_2Co_4(CO)_{11}$ {7} [35, 45] and $(RSi)_2Co_4(CO)_{11}$ {7} (R = Me, Ph, section 4.2.6) [36] have Si-Si non-bonded distances of 2.817(2)Å, 2.726(2)Å and 2.705(1)Å respectively. These distances are shorter than their combined Van der Waals radii of 4.2Å but just outside of the range of a Si-Si single bond.

The average Co-C and C-O distances for the terminal $Co(CO)_4$ groups are 1.805Å (range 1.786(6)Å to 1.826(6)Å) and 1.133Å (range 1.116(7)Å to 1.144(7)Å). Carbonyl distances in the $Co_2(CO)_6$ group show a slight shortening in the Co-C bonds with an average value of 1.788Å (range 1.762(6)Å to 1.825(6)Å) and a slight lengthening in the C-O bonds with an average value of 1.144Å (range 1.125(7)Å to 1.154(7)Å). Overall these terminal carbonyl distances lie well within the expected range.

5.5.6 INFRARED SPECTRUM OF $S_2Co_4(CO)_{10}$

The infrared spectrum of $S_2Co_4(CO)_{10}$ in CH_2Cl_2 is shown in Figure 5.13. The spectrum is dominated by a very strong peak at 2050 cm^{-1}. The symmetry of the molecule is D_{2h} with an overall representation for the carbonyl stretches of $2A_g + B_{1g} + B_{2g} + B_{3g} + A_u + B_{1u} + 2B_{2u} + B_{3u}$. Infrared active modes are $B_{1u} + 2B_{2u} + B_{3u}$, therefore we predict four infrared peaks (three terminal, one bridging). The infrared spectrum is consistent with this; we see three terminal peaks at (υCO, (CH_2Cl_2) 2050 vs, 2038 m, 2024 w, cm^{-1}) and a bridging peak at 1862 cm^{-1}.

Figure 5.13

INFRARED SPECTRUM OF $S_2Co_4(CO)_{10}$

CH_2Cl_2 SOLUTION

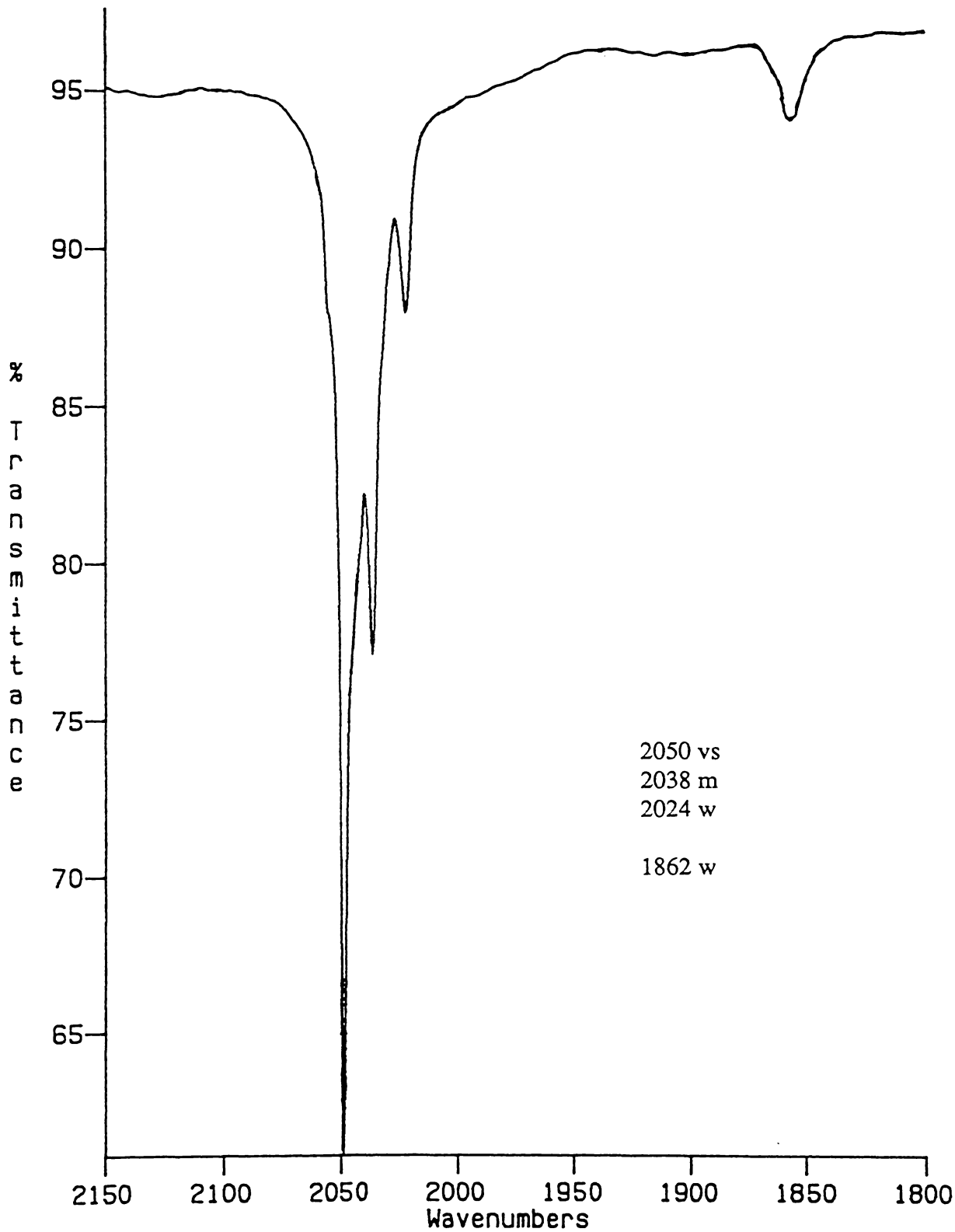

5.5.7 MASS SPECTRUM OF $S_2Co_4(CO)_{10}$

A FAB mass spectrum of $S_2Co_4(CO)_{10}$ is listed in Table 5.7. A very simple spectrum resulted with only one series of ions due to the sequential loss of all the carbonyls. The parent ion $[S_2Co_4(CO)_{10}]^+$ was very weak at m/e = 580. Following this a consecutive loss of ten carbonyls to the m/e = 300 (ion $[S_2Co_4]^+$) was observed with generally weak intensity. A very strong peak at m/e = 384 was observed corresponding to the ion $[S_2Co_4(CO)_3]^+$.

Table 5.7

MASS SPECTRUM OF $S_2Co_4(CO)_{10}$

m/e	Int	Assignment	
580	vw	$[S_2Co_4(CO)_n]^+$	n = 10
552	w		n = 9
524	w		n = 8
496	vw		n = 7
468	vw		n = 6
440	w		n = 5
412	w		n = 4
384	vs		n = 3
356	m		n = 2
328	w		n = 1
300	w		n = 0

5.5.8 X-RAY CRYSTALLOGRAPHIC STUDY OF $S_2Co_4(CO)_{10}$

Black diamond-shaped crystals were obtained from a cooled CH_2Cl_2 solution. Preliminary precession photographs using Cu-Kα radiation on a suitable crystal showed that the crystal had monoclinic symmetry and was found to belong to the space group $P2_1/n$.

Intensity data was collected on a high quality crystal of dimensions 0.74 x 0.3 x 0.08 mm at the University of Canterbury on a Nicolet P3 diffractometer. A scan range of $4°<2\theta<52°$ was employed resulting in 1617 unique reflections using Mo-Kα radiation. Standard reflections were measured at regular intervals with no significant decay observed. An absorption correction was applied to the data using an empirical ϕ-scan technique with transmission factors, 0.800 maximum and 0.681 minimum. For the solution and refinement of the structure, 1312 reflections were used with $I>3\sigma(I)$. Crystal data for $S_2Co_4(CO)_{10}$ are given in Table 5.8.

Table 5.8

CRYSTAL DATA FOR $S_2Co_4(CO)_{10}$	
Formula: $C_{10}Co_4O_{10}S_2$	Mr = 579.86
Monoclinic	Space Group = $P2_1/n$
Cryst. Colour: Black	
Cryst. Dimensions: 0.74 x 0.3 x 0.08 mm	
a = 9.962(4) Å	$\alpha = 90.00°$
b = 6.711(2) Å	$\beta = 96.76(3)°$
c = 12.339(5) Å	$\gamma = 90.00°$
U = 819.1(5) Å^3	Dcalc = 2.35 g cm^{-3}
Z = 2	
F(000) = 527.9	Temp = 173 K
μ(Mo-Kα) = 40 cm^{-1}	
Unique Data = 1617	Range = $4°<2\theta<52°$
Refinement Data = 1312	Final R = 0.0212

For all computations the SHELX-76 and SHELXS-86 [98] package of crystallographic programs were used. The positions of the heavy atoms were obtained using TREF and several carbonyls were located from a subsequent refinement and difference map. This showed the structure to contain a square

planar array of cobalt atoms bicapped with sulphur. Since this structure had been previously reported [92] the published coordinates were used for all the atoms. This refined well but showed residual electron density around the oxygen atoms. All the atoms were assigned anisotropic temperature factors giving 11.1 reflections per parameter which after final refinement converged to R = 0.0212, Rw = 0.0216 with $w = 1.2498[\sigma^2(F) + 0.000205F^2]^{-1}$. Largest shift/e.s.d in the final cycle was 0.001 with 0.36 e $Å^{-3}$electron density near a cobalt atom.

Positional and thermal parameters along with complete tables of bond lengths and angles are given in Appendix Six. Tables of calculated and observed structure factors have been retained by the University of Waikato.

5.5.9 STRUCTURE OF $S_2Co_4(CO)_{10}$

This structure has been previously reported by C.H. Wei and L.F. Dahl [92] in which photographic data was visually estimated with the structure refined to a final R value of 0.092. Some significant changes in the overall values have been found in the present determination. The high precision of this refinement makes for a more detailed discussion. Examples of the accuracy and standard deviations between the two structures are Co-Co 2.598(10)Å compared to 2.605(1)Å and a marked difference in the S-Co 2.244(11)Å as compared to 2.270(1)Å.

Perspective views of the cluster $S_2Co_4(CO)_{10}$ are shown in Figures 5.14, 5.15 and 5.16. Atom labelling is shown in Figure 5.16 and is used throughout the following discussion. Selected bond lengths and angles are given in Tables 5.9 and 5.10.

The molecule lies about a crystallographic inversion centre and therefore the overall structure consists of two sulphur atoms coordinated to four cobalt atoms in a rectangular bipyramidal configuration. The sulphur atom is situated 1.391Å above the rectangular cobalt plane. Two distinct S-Co distances are seen to each of the shortest Co-Co edges. The shorter lengths, S(1)-Co(1) and S(1)-Co(2) at 2.270(1)Å and 2.271(1)Å can be compared to S(1)-Co(1') and S(1)-Co(2') at 2.279(1)Å and 2.283(1)Å. The second sulphur atom is located in the opposite position under the plane due to the centre of inversion symmetry.

Figure 5.14 Top and Side View of $S_2Co_4(CO)_{10}$

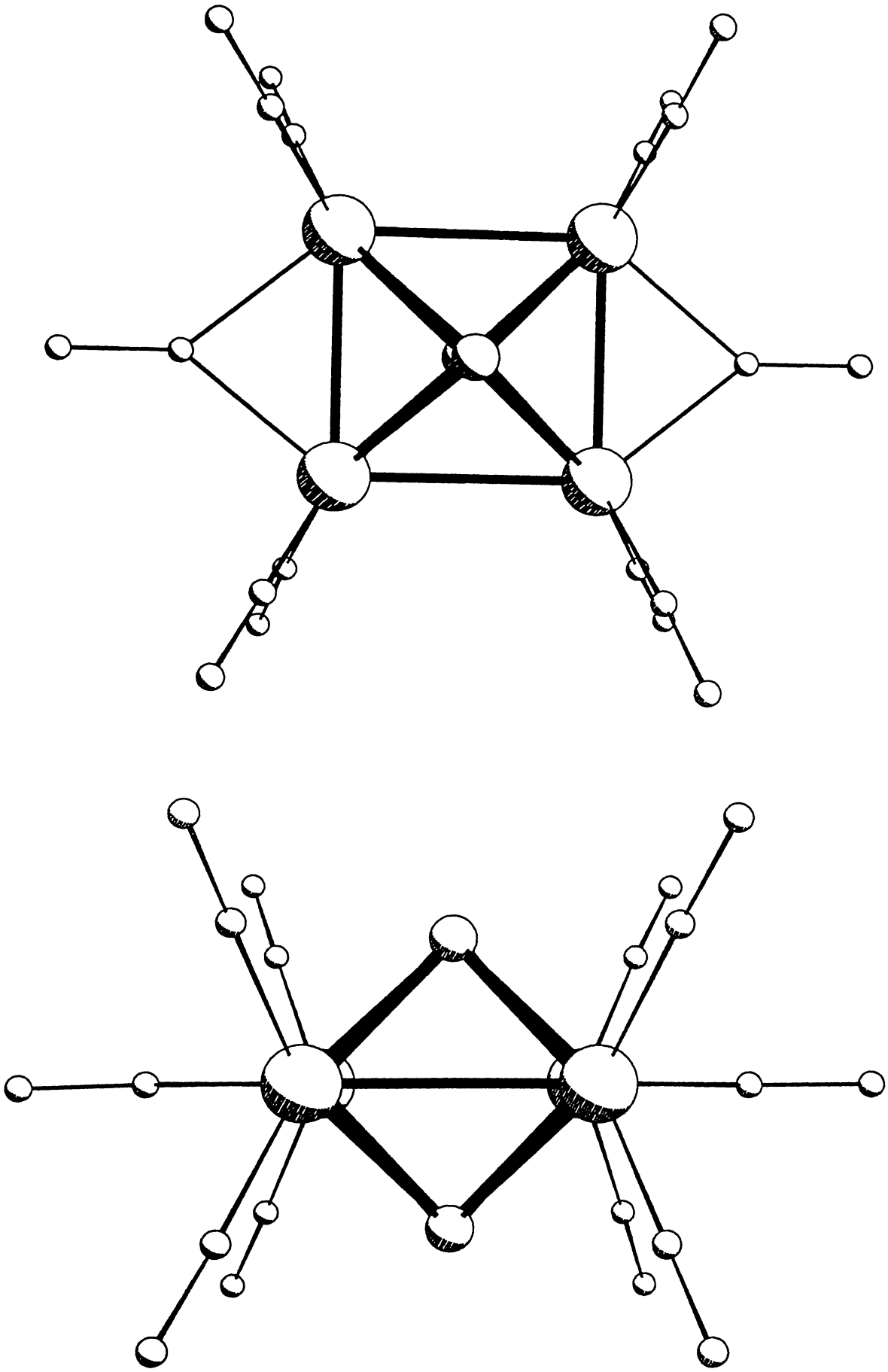

Figure 5.15 Stereo View of $S_2Co_4(CO)_{10}$

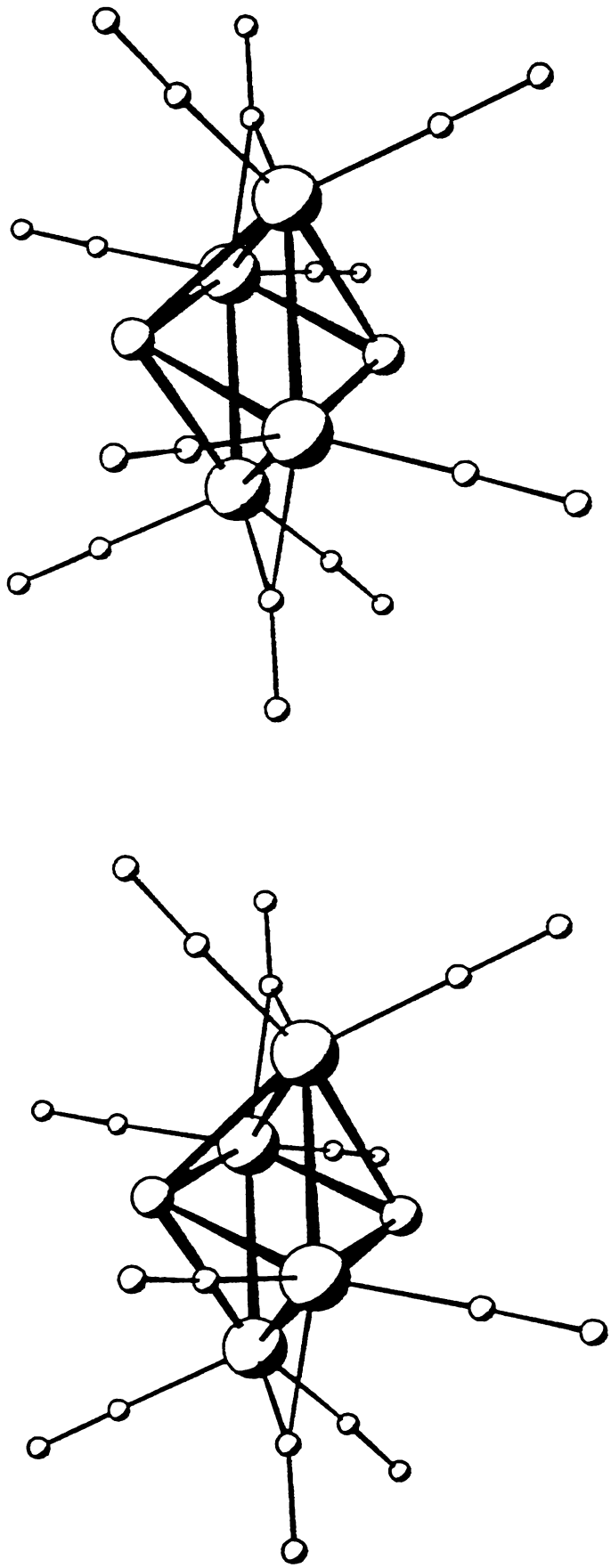

Figure 5.16 Labelled Perspective View of $S_2Co_4(CO)_{10}$

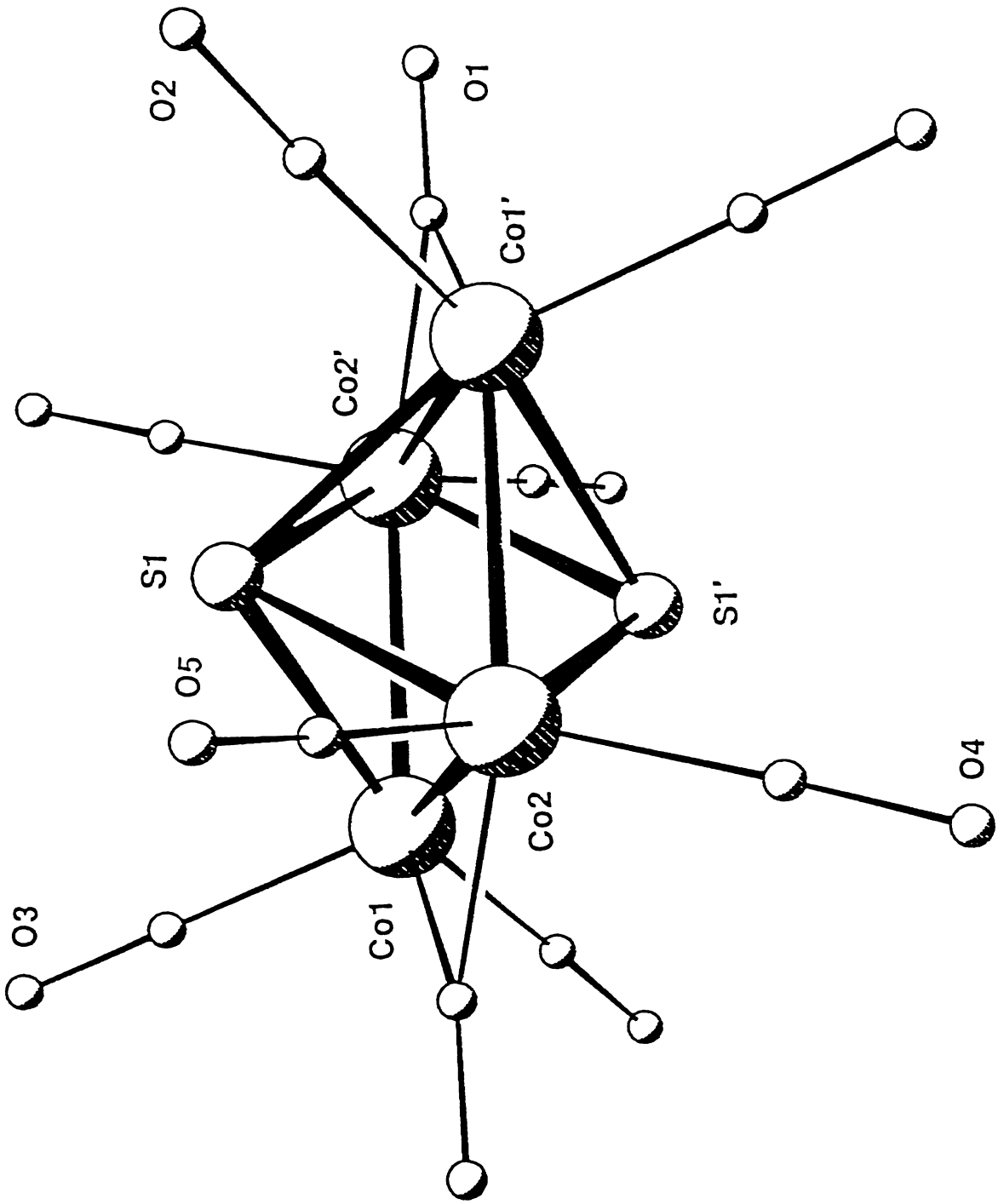

Table 5.9

SELECTED BOND LENGTHS FOR $S_2Co_4(CO)_{10}$ (Å)			
Co(1) ---Co(2)	2.488(1)	Co(1) ---Co(2')	2.605(1)
Co(1) ---S(1)	2.270(1)	Co(1')---S(1)	2.278(1)
Co(2) ---S(1)	2.271(1)	Co(2')---S(1)	2.283(1)
Co(1) ---C(1)	1.953(3)	Co(1) ---C(2)	1.811(3)
Co(1) ---C(3)	1.814(3)	Co(2) ---C(1)	1.947(3)
Co(2) ---C(4)	1.818(3)	Co(2) ---C(5)	1.814(3)
C(1) ---O(1)	1.154(4)	C(2) ---O(2)	1.137(4)
C(3) ---O(3)	1.128(4)	C(4) ---O(4)	1.134(3)
C(5) ---O(5)	1.133(4)		
S(1) ...S(1')	2.782(1)		

Table 5.10

SELECTED BOND ANGLES FOR $S_2Co_4(CO)_{10}$ (°)			
Co(1) -Co(2) -Co(1')	89.9(1)	Co(2) -Co(1')-Co(2')	90.1(1)
Co(1) -S(1) -Co(2)	66.4(1)	Co(1')-S(1) -Co(2')	66.1(1)
Co(1) -S(1) -Co(2')	69.8(1)	Co(2) -S(1) -Co(1')	69.9(1)
Co(1) -S(1) -Co(1')	104.6(1)	Co(2) -S(1) -Co(2')	104.7(1)
S(1) -Co(1) -S(1')	75.4(1)	S(1) -Co(2) -S(1')	75.3(1)
S(1) -Co(1) -Co(2)	56.8(1)	S(1) -Co(2) -Co(1)	56.8(1)
S(1) -Co(1')-Co(2')	57.1(1)	S(1) -Co(2')-Co(1')	56.9(1)
S(1) -Co(2) -Co(1')	55.2(1)	S(1) -Co(1')-Co(2)	54.9(1)
S(1) -Co(2')-Co(1)	54.8(1)	S(1) -Co(1) -Co(2')	55.3(1)

The carbonyl bridged Co-Co bond lengths at 2.488(1)Å are markedly shorter than the non-bridged Co-Co bond lengths at 2.605(1)Å. Shortening of Co-Co bonds due to bridging carbonyls is well documented. This can be compared with other pseudo-square planar cobalt clusters like $[(CO)_4CoSi]_2Co_4(CO)_{11}$ [35] Co-Co(bridged) at 2.569(2)Å, Co-Co (non-bridged) at 2.653(2)Å, $(MeSi)_2Co_4(CO)_{11}$ [36] at 2.548(2)Å and 2.690(2)Å and $(PhP)_2Co_4(CO)_{10}$ [96] at 2.520(4)Å and 2.698(4)Å respectively. The smaller size of the sulphur atom allows for the shorter Co-Co distance of 2.488(1)Å and 2.605(1)Å as compared with the tellurium analogue $Te_2Co_4(CO)_{10}$ [93] with average Co-Co distances of 2.58(2)Å and 2.88(2)Å respectively. Analogous distances in the phosphorus and silicon E_2Co_4 clusters show the same size relationship in which Co-Co bond lengths decrease in going across the period, Si > P > S .

The S--S non bonded distance of 2.782(1)Å is shorter than that found in $S_2Fe_4(CO)_{11}$ [108] with S--S at 2.911(4)Å. Both size and electronic factors contribute to the existence of short E--E contacts in closo M_4E_2 clusters [155].

Eight terminally bonded carbonyls are distributed very symmetrically with two per cobalt atom. The average Co-C distance is 1.814Å with a very small range of 1.811(3)Å to 1.818(3)Å. This is attributed to each carbonyl having essentially the same environment. Average C-O distance of 1.133Å (range 1.128(4)Å to 1.137(4)Å) and Co-C-O angles between 177.3(3)° and 178.1(3)° also indicate that each terminal carbonyl is nearly identical. The bridging carbonyls symmetrically bridge the Co-Co bonds with Co-C distances of 1.947(3)Å and 1.953(3)Å and a C-O distance of 1.154(4)Å.

Recently reported was the structure of $S_2Co_4Cp_4$ [94] (Figure 5.17). This was isolated from the reaction between $CoCp(PPh_3)_2$ and Li_2S at 60°C. The structure consists of the four cobalt atoms at the corners of a regular square which is capped by two quadruply-bridging sulphur atoms. The Co-Co distance of 2.438(1)Å is shorter than those of the isoelectronic E_2Co_4 clusters above. The Co-S distances range from 2.225(1)Å to 2.233(1)Å (ave 2.229Å) which are shorter than in $S_2Co_4(CO)_{10}$ or in $S_2Co_3Cp_3$ [95].

Figure 5.17 $S_2Co_4Cp_4$

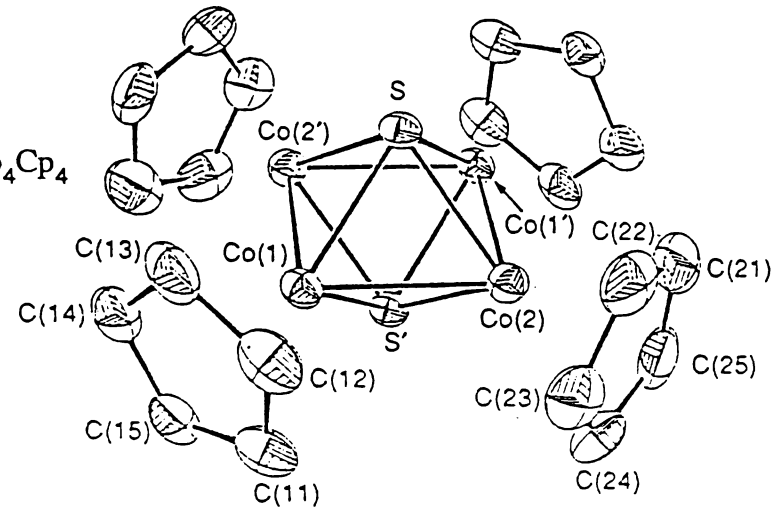

Table 5.11 lists the clusters in which sulphur or tellurium quadruply bridges both sides of a square-planar array of four metal atoms. No selenium clusters of this type have been reported. This is probably due to the lack of investigation rather than to any other factors.

Table 5.11

E_2M_4 CLUSTERS OF SULPHUR AND TELLURIUM	
CLUSTER	**REF**
$S_2Fe_4(CO)_{10}(\mu\text{-}CO)$	108
$S_2Fe_2Co_2(CO)_{10}(\mu\text{-}CO)$	104
$S_2Co_4(CO)_8(\mu\text{-}CO)_2$	92, 93
$S_2Co_4(Cp)_4$	94
$S_2Ru_4(CO)_9(\mu\text{-}CO)_2$	105
$S_2Ru_4(CO)_7(PMe_2Ph)_2(\mu\text{-}CO)_2$	105
$Te_2Fe_2Ru_2(CO)_{10}(\mu\text{-}CO)$	106
$Te_2Co_4(CO)_8(\mu\text{-}CO)_2$	93
$Te_2Ru_4(CO)_{10}(\mu\text{-}CO)$	107
$Te_2Ru_4(CO)_8(PPh_3)(\mu\text{-}CO)_2$	107
$Te_2Ru_4(CO)_8(\mu\text{-}Ph_2PCH_2PPh_2)(\mu\text{-}CO)$	107

5.5.10 DISCUSSION

The reaction of $H_3SiSSiH_3$ with $Co_2(CO)_8$ produces two major products, $SSi_2Co_4(CO)_{14}$ which retains the parent hydride backbone, and $S_2Co_4(CO)_{10}$ in which the sulphur has been extracted.

The cluster $SSi_2Co_4(CO)_{14}$ probably results due to the Si-S-Si angle of 97.4° [131, 132] in the hydride which holds the two silicon atoms in a position close enough so that the Co-Co bond is simultaneously bridged twice (Figure 5.18) instead of reacting on either end to form a six metal species of the type $S(SiCo(CO)_4Co_2(CO)_7)_2$. The Si-S-Si angle remains relatively acute even when bulky organic groups are placed on the silicon atoms (see below).

Figure 5.18
Reaction of $H_3SiSSiH_3$ with $Co_2(CO)_8$

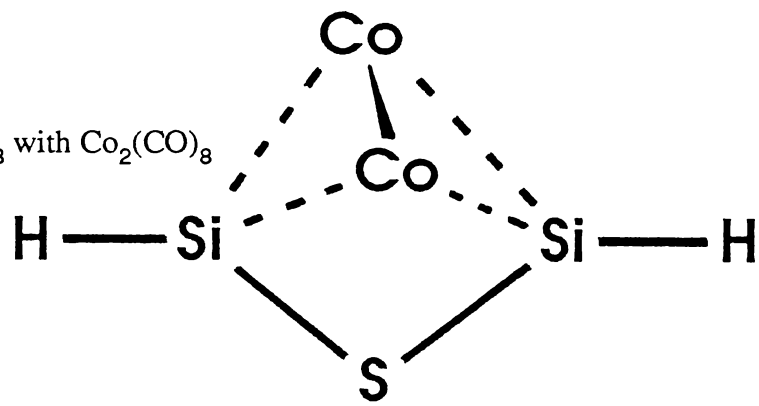

Further reaction of the remaining hydrogen with $Co_2(CO)_8$ can occur in the following ways (equations below).

$$\text{Si-H} + Co_2(CO)_8 \rightarrow \text{Si-Co}(CO)_4 + HCo(CO)_4$$

$$\text{Si-H} + HCo(CO)_4 \rightarrow \text{Si-Co}(CO)_4 + H_2$$

There is no indication that $H_3SiOSiH_3$ with a Si-O-Si angle of 142.2(3)° [133, 137] forms the similar compound $OSi_2Co_4(CO)_{14}$. This is probably due to the Si-O-Si angle being linear (or nearly so) when bulky groups are bonded to the silicon. For example, $(t\text{-}BuO)_3SiOSi(t\text{-}BuO)_3$ [148] (Figure 5.19) appears to be linear although strong anisotropic ellipsoids around the oxygen suggest that

the corrected angle is more probably about 144°. A review of Si-O-Si structures [153] and the structures of $Ph_3SiOSiPh_3$ [154] (Figure 5.20) and $[(Me_3Si)_3C]Cl_2SiOSiCl_2[C(SiMe_3)_3]$ [150] show that generally any bulky group will give a linear Si-O-Si bond. This would prevent the situation in which both sides of $Co_2(CO)_8$ could be bridged because any initial bond to the silicon would cause the Si-O-Si linkage to straighten forcing the free silicon atom away from the Co-Co bond.

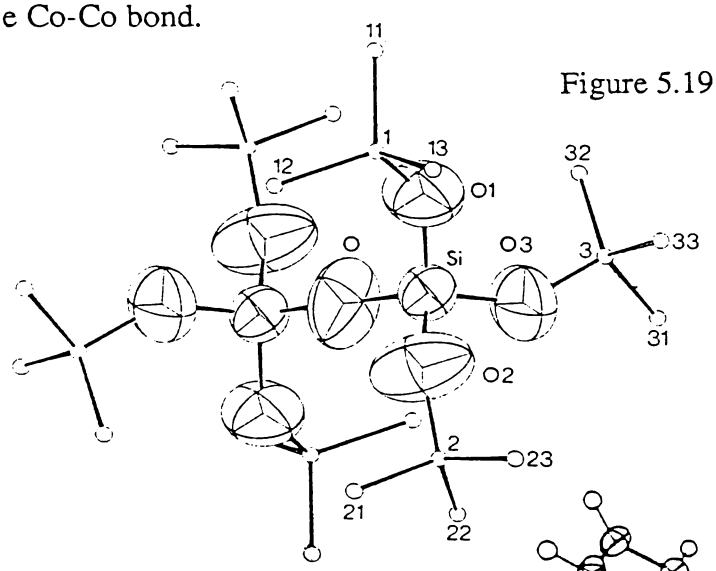

Figure 5.19 $(t\text{-}BuO)_3SiOSi(t\text{-}BuO)_3$

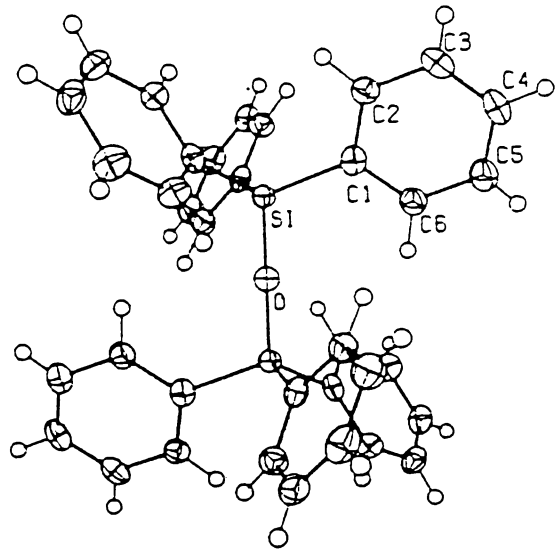

Figure 5.20 $Ph_3SiOSiPh_3$

$S_2Co_4(CO)_{10}$ was initially prepared by reacting sulphur with $Co_2(CO)_8$ in heptane at 30°C [92]. At higher temperatures the disilylthiane decomposes into silicon hydrides and sulphur or H_2S which can then react to form $S_2Co_4(CO)_{10}$. When the reaction of $H_3SiSSiH_3$ and $Co_2(CO)_8$ was conducted at higher temperature the yield of $S_2Co_4(CO)_{10}$ increased due to the greater availability of the sulphur. No sign of $O_2Co_4(CO)_{10}$ was seen in the reaction of $H_3SiOSiH_3$ with $Co_2(CO)_8$.

In the reactions of $H_3SiSSiH_3$ with $Co_2(CO)_8$, generally $SSi_2Co_4(CO)_{14}$ and $S_2Co_4(CO)_{10}$ account together for 50-60% of the sulphur but only 10-30% of the silicon. Minor amounts of silicon hydrides are detected in the volatile fraction with the fate of the remaining silicon unknown.

5.6. REACTION OF $H_3SiSSiH_3$ WITH $Fe_2(CO)_9$

5.6.1 EXPERIMENTAL

$H_3SiSSiH_3$ (0.0452g, 0.479mmol) was added to $Fe_2(CO)_9$ (0.50g, 1.37mmol) in 10ml of hexane solvent. This was heated to 50°C for 4 days after which the colour had changed from the insoluble yellow $Fe_2(CO)_9$ to a green solution with a black precipitate.

The contents were transferred to a Schlenk flask and the solvent and other volatile compounds removed. The solid was extracted using 3 x 10ml of hexane. A small portion was chromatographed and shown to contain four mobile compounds. The first compound was red/brown with an infrared spectrum consistent with the formation of $S_2Fe_3(CO)_9$ [81] (υCO, (hexane) 2062, 2045, 2024, 1985, cm^{-1}), 5-10%. The second green compound was characterised as $Fe_3(CO)_{12}$ (υCO, (hexane) 2046 vs, 2023 m, 2013 sh, 1867 vw, 1835 vw, cm^{-1}), 20-40%. The third compound, yellow in colour, was characterised as $Si[Fe_2(CO)_8]_2$ **{5}** (υCO, (hexane) 2076 m, 2050 vs, 2030 w, 2013 m, cm^{-1}), 20-30%. The fourth compound, brown in colour, is as yet uncharacterised with an infrared spectrum (υCO, (hexane) 2067 m, 2061 m, 2046 s, cm^{-1}).

5.7 REACTION OF $H_3GeSGeH_3$ WITH $Co_2(CO)_8$

5.7.1 INTRODUCTION

Investigation of the reaction of digermylsulphide with $Co_2(CO)_8$ was conducted to see if the products obtained would be similar to those of the analogous silicon hydride, $H_3SiSSiH_3$. $SSi_2Co_4(CO)_{14}$ has a characteristic infrared pattern and therefore the formation of $SGe_2Co_4(CO)_{14}$ could be easily identified.

5.7.2 EXPERIMENTAL

$H_3GeSGeH_3$ (0.180g, 0.982mmol) was sealed in a 50ml ampoule with $Co_2(CO)_8$ (1.00g, 2.92mmol) in 10ml of hexane giving a 1 : 3 ratio. A rapid initial reaction proceeded and a brown precipitate started to form after 30 minutes. The reaction was allowed to proceed at 5°C for two months which resulted in the formation of a large amount of black precipitate.

The contents were transferred to a Schlenk flask using CH_2Cl_2 to wash the residue inside the ampoule. The solvents and $HCo(CO)_4$ were removed under vacuum to give a dark brown residue. Hexane was added and the infrared spectrum of the extract showed peaks due to unreacted $Co_2(CO)_8$ at (υCO, (hexane) 2069, 2043, 2031, 2024, 1858cm^{-1}), $Co_4(CO)_{12}$ at (υCO, (hexane) 2064, 2055, 1867cm^{-1}), $Ge[Co_2(CO)_7]_2$ {5} at (υCO, (hexane) 2080, 2063, 2042, 2033, 2024, 1850cm^{-1}) and a small amount of $(CO)_4CoGeCo_3(CO)_9$ (υCO, (hexane) 2112 w, 2083 s, 2045 vs, 2029 m, 2008 vw, cm^{-1}). Further hexane and CH_2Cl_2 fractions only contained pure $Ge[Co_2(CO)_7]_2$ which was the major product (60-70% yield).

No new products with the Ge-S-Ge linkage intact were obtained from the reaction.

An experiment was attempted in which a reaction ratio of 1 to 2 of the hydride $H_3GeSGeH_3$ to $Co_2(CO)_8$ was used. $H_3GeSGeH_3$ (0.228g, 1.46mmol) was reacted with $Co_2(CO)_8$ (1.00g, 2.92mmol) in 10ml of hexane. A rapid initial reaction was observed with the formation of small bubbles. The reaction was left to proceed at 5°C in the dark for 2 weeks. After this time the solution was a brown colour and contained a black precipitate.

On work-up the infrared spectrum of the first 10ml hexane soluble fraction showed a very small amount of unreacted $Co_2(CO)_8$, with the remaining fraction consisting of $Ge[Co_2(CO)_7]_2$. Further extractions using hexane and CH_2Cl_2 contained only $Ge[Co_2(CO)_7]_2$.

5.7.3 DISCUSSION

Digermylsulphide does not form the analogue of the silicon compound $SGe_2Co_4(CO)_{14}$. In the reaction of $H_3GeSGeH_3$ with $Co_2(CO)_8$ the products observed were those which resulted from the breaking of the Ge-S bonds in the parent hydride. The bond strength of the Ge-S bond at 551(3)kJ mol^{-1} is substantially less than that of Si-S at 619(13)kJ mol^{-1}, but this is only one of several factors affecting the formation of products. The Ge-S-Ge angle of 98.9° in the hydride $H_3GeSGeH_3$ [131, 134] is very similar to that of $H_3SiSSiH_3$ at 97.4° [131, 132] so this consideration would suggest that the compound $SGe_2Co_4(CO)_{14}$ could form. Digermylsulphide is markedly less stable than the corresponding disilylthiane [86, 97] which is another factor to consider. This stability difference is also seen for $H_3SiOSiH_3$, which can be stored at room temperature indefinitely compared to $H_3GeOGeH_3$ which decomposes when allowed to warm above 0°C.

At the reaction temperature of 5°C no $S_2Co_4(CO)_{10}$ was isolated. The decomposition of $H_3GeSGeH_3$ occurs more readily when compared to $H_3SiSSiH_3$. Therefore more sulphur is available but the lower temperature will reduce the reaction rate between the sulphur and $Co_2(CO)_8$.

$$H_3GeSGeH_3 + 4Co_2(CO)_8 \rightarrow 2Ge[Co_2(CO)_7]_2 + S + 3H_2 + 4CO$$

This unreacted sulphur would remain in the insoluble fraction.

5.8. OVERALL DISCUSSION

The reactions of $H_3SiOSiH_3$, $H_3SiSSiH_3$ and $H_3GeSGeH_3$ with $Co_2(CO)_8$ do not readily form products which retain the parent framework. This is rather surprising, especially in the reactions of $H_3SiOSiH_3$ which involve the breaking of very strong Si-O bonds. Possibly the cobalt catalyses the decomposition of these hydrides according to the equation below.

$$2H_3SiOSiH_3 \rightarrow 3SiH_4 + SiO_2$$

The SiH_4 formed can react with $Co_2(CO)_8$ to form the compounds observed above (eg. $Si[Co_2(CO)_7]_2$ and $(CO)_4CoSiCo_3(CO)_9$).

$H_3SiSSiH_3$ and $H_3GeSGeH_3$ form similar products arising from the decomposition of the hydride with the only exception being the fully characterised cluster $SSi_2Co_4(CO)_{14}$.

5.9 FURTHER WORK

The reactions of mono- or di-substituted disilylthiane ($RH_2SiSSiH_2R$, R = organic) may form $R_2SSi_2Co_2(CO)_6$ type compounds. Further work on the reaction of $H_3SiOSiH_3$ with $Co_2(CO)_8$ at different ratios and temperatures may lead to crystallographic characterisation of the products. Reactions of $H_3SiSeSiH_3$ or $H_3SiTeSiH_3$ with $Co_2(CO)_8$ may form interesting analogues of $SSi_2Co_4(CO)_{14}$.

Reactions of $N(SiH_3)_3$ or H_3SiPH_2 with $Co_2(CO)_8$ may prove interesting with the possible formation of $N[SiCo_3(CO)_9]_3$ and a mixed silicon-phosphorus square-bipyramid cluster respectively.

CHAPTER SIX

REACTIONS OF SILICON CHLORIDES WITH $[Co(CO)_4]^-$

REACTIONS OF SILICON CHLORIDES WITH $[Co(CO)_4]^-$

6.1 INTRODUCTION

This chapter describes the reactions of various silicon chlorides with $[Co(CO)_4]^-$. Earlier work by B.K. Nicholson and J. Simpson [56] showed that the reaction of $SiCl_4$ with $Na[Co(CO)_4]$ in diethylether gave good yields (52%) of the siloxy cluster $Cl_3SiOCCo_3(CO)_9$ **{1}**. Short reaction times (30 minutes) and low $SiCl_4$: $Na[Co(CO)_4]$ ratios (1 to 1) were used which limited the formation of larger clusters.

Other chlorosilanes (Me_nSiCl_{4-n} (n = 1-3)) were also studied [56] with $Na[Co(CO)_4]$ in diethylether and tetrahydrofuran solvents. Results for $MeSiCl_3$ were similar with the formation of the siloxy cluster $MeCl_2SiOCCo_3(CO)_9$ **{1}**. However Me_3SiCl under-went salt-elimination to form $Me_3SiCo(CO)_4$. Me_2SiCl_2 was intermediate in nature forming a wide range of uncharacterised products.

$$Me_3SiCl + Na[Co(CO)_4] \rightarrow Me_3SiCo(CO)_4 + NaCl$$

This chapter extends this work using various silicon chlorides ($SiCl_4$, Si_2Cl_6 and $Cl_3SiOSiCl_3$) with the K^+ and Et_4N^+ salts of $[Co(CO)_4]^-$. The longer reaction times employed may result in the formation of larger clusters.

6.2 REACTION OF $SiCl_4$ WITH $K[Co(CO)_4]$

6.2.1 INTRODUCTION

The reaction of SiI_4 with $Na[Co(CO)_4]$ in n-hexane at 50°C under UV irradiation was conducted by G. Schmid and G. Etzrodt [46], which formed the cluster $(CO)_4CoSiCo_3(CO)_9$ (Figure 6.1) in low yield. This method generally does not yield the larger clusters.

The following experiment was conducted with the readily available silicon tetrachloride and the anion $[Co(CO)_4]^-$ in an attempt to form new clusters of the

type $(CO)_9Co_3SiOCCo_3(CO)_9$. Initially the cluster $Cl_3SiOCCo_3(CO)_9$ is rapidly formed and therefore substitution of the remaining Si-Cl for Si-Co groups should result in the formation of such a cluster.

Figure 6.1 $(CO)_4CoSiCo_3(CO)_9$

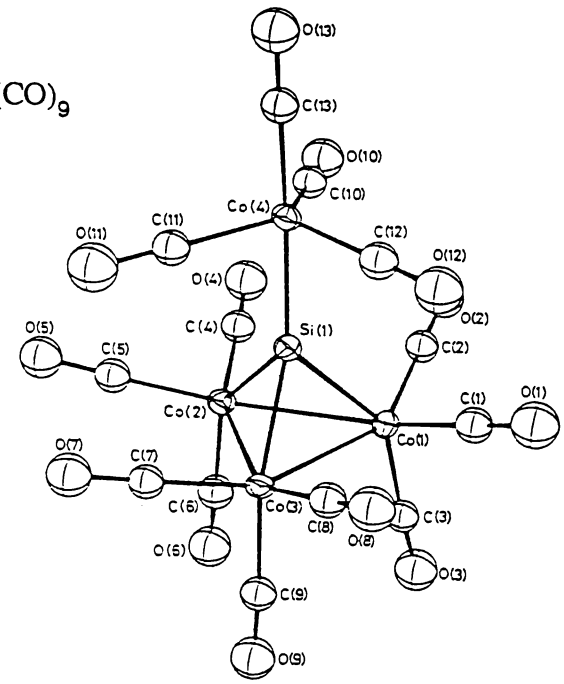

6.2.2 EXPERIMENTAL

$K[Co(CO)_4]$ (1.47g, 7.00mmol) was dissolved in 10ml of dry diethylether in a 50ml high pressure ampoule and $SiCl_4$ (0.15g, 0.882mmol) was condensed into this giving a ratio of 8 to 1. The reaction was allowed to proceed at 30°C for 7 days which resulted in a dark red-black solution. Incondensable CO gas was measured giving a total of 1.41mmol which indicates the formation of cluster type compounds rather than straight substitution of the chlorine for $Co(CO)_4$. The contents of the ampoule were transferred to a Schlenk flask and the diethylether was recovered. Hexane was used to extract the non-ionic products giving a deep red solution containing 0.26g of products shown below to be $(CO)_4Co(Cl)_2SiOCCo_3(CO)_9$. An infrared spectrum showed a small amount of $Co_2(CO)_8$ and $Co_4(CO)_{12}$ along with a new dark-red compound in 40% yield.

A solution of Et_4NBr in CH_2Cl_2 was added to the remaining residue resulting in a black solution which was filtered from the KBr and KCl. Concentrating and cooling this solution resulted in black crystals slightly soluble in CH_2Cl_2 and more soluble in THF (see section 6.4.3).

A similar experiment using $SiCl_4$ (0.068g, 0.40mmol) with $K[Co(CO)_4]$ (0.84g, 4.0mmol) in 20ml of diethylether was conducted. This reaction was left for 20 days at room temperature in which time the reaction colour went from colourless through red to red/black. A hexane extract contained $Co_2(CO)_8$ and $Co_4(CO)_{12}$ as minor products along with the new red product in 40-50% yield. The remaining black solid was worked up as above and shown to contain the anion $[Co(CO)_4]^-$ and a black cluster (see section 6.4.3).

This experiment was conducted for a very long period of time (3 years). $SiCl_4$ (0.263g, 1.55mmol) was sealed with $K[Co(CO)_4]$ (1.60g, 7.62mmol) in 10ml of diethylether and left to react at room temperature. The ampoule contained large amounts of a black solid with a red/black solution.

On work-up 1.71g of solid was isolated, of this 0.42g was extracted using (2 x 15ml) hexane. The infrared spectrum showed the hexane extract to contain small amounts of $Co_2(CO)_8$ and $Co_4(CO)_{12}$ along with the siloxy cluster $Cl_3SiOCCo_3(CO)_9$ which has previously been characterised [56].

The remaining black solid (1.29g) contained anionic compounds; $[Co(CO)_4]^-$ (minor) along with a black cluster (see section 6.4.3).

6.3 CHARACTERISATION OF $(CO)_4CoCl_2SiOCCo_3(CO)_9$

6.3.1 INFRARED SPECTRUM OF $(CO)_4CoCl_2SiOCCo_3(CO)_9$

The infrared spectrum of $(CO)_4CoCl_2SiOCCo_3(CO)_9$ in hexane (shown in Figure 6.2) exhibits six peaks in the carbonyl stretching region. This spectrum can be compared to similar siloxy clusters $Cl_3SiOCCo_3(CO)_9$ **{1}** [56] and $MeCl_2SiOCCo_3(CO)_9$ **{1}** [56] (Table 6.1). The carbonyl peaks due to the $OCCo_3(CO)_9$ moiety at (υCO, 2105 w, 2057 s, 2042 m, cm^{-1}) match very closely to those seen for $Cl_3SiOCCo_3(CO)_9$ at (υCO, 2104 w, 2056 vs, 2040 s, 2020 sh w, cm^{-1}) and $MeCl_2SiOCCo_3(CO)_9$ at (υCO, 2104 w, 2053 s, 2039 s, 2020 w, cm^{-1}).

Figure 6.2

INFRARED SPECTRUM OF $(CO)_4CoCl_2SiOCCo_3(CO)_9$

HEXANE SOLUTION

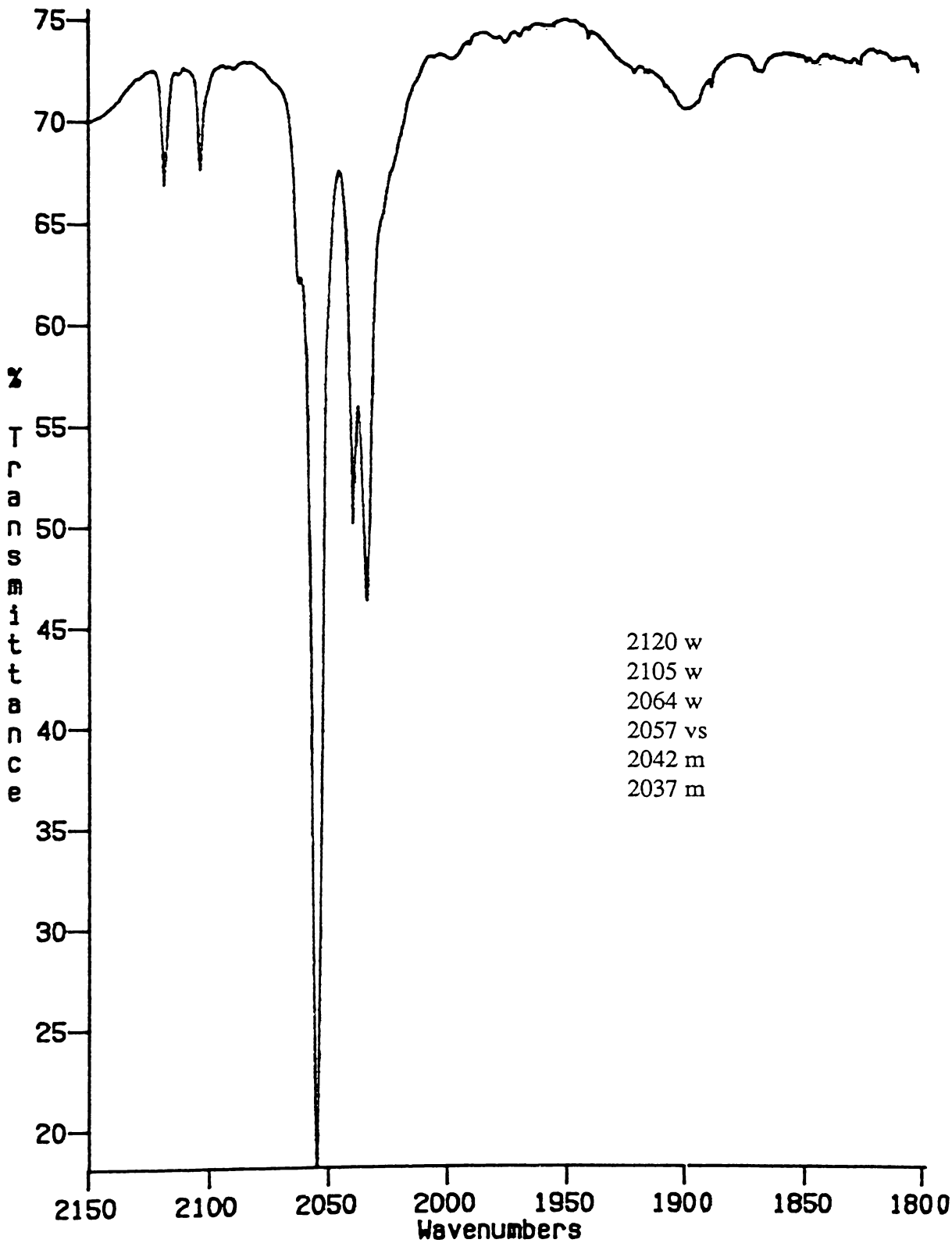

For the local symmetry, C_{3V}, of the terminal $Co(CO)_4$ group, we would predict three infrared active modes for the carbonyl stretches ($2A_1 + E$). Three peaks are seen at (υCO, 2120 w, 2064 w, 2037 m cm^{-1}) which match very closely those seen for $Cl_3SiCo(CO)_4$ at (υCO, 2118 s, 2066 s, 2039 vs, 1999 w cm^{-1}) (Table 6.1). The first two peaks at 2120 and 2064cm^{-1} can be assigned as the A_1 modes with the E mode at 2037cm^{-1}.

This shows little coupling of carbonyl vibrations between the $Co(CO)_4$ and $OCCo_3(CO)_9$ groups across the silicon-oxgyen-carbon bridge.

Table 6.1

INFRARED SPECTRUM OF $(CO)_4CoCl_2SiOCCo_3(CO)_9$ COMPARED TO SIMILAR SPECIES

	Y = $-OCCo_3(CO)_9$		
$(CO)_4CoCl_2Si$-Y	Cl_3Si-Y	$MeCl_2Si$-Y	$Cl_3SiCo(CO)_4$
2120 w			2118 s
2105 w	2104 w	2104 w	
2064 w			2066 s
2057 vs	2056 vs	2053 s	
2042 m	2040 s	2039 s	
2037 m			2039 vs
	2020 sh w	2020 w	
			1999 w

6.3.2 MASS SPECTRUM OF $(CO)_4CoCl_2SiOCCo_3(CO)_9$

A mass spectrum assigned to $(CO)_4CoCl_2SiOCCo_3(CO)_9$ was obtained (Table 6.2). The parent ion is not observed, the highest mass (m/e = 698) is assigned to $[P\text{-}CO]^+$. A series corresponding to the loss of all carbonyls is observed, $[Cl_2SiCo_4(CO)_n]^+$ (n = 1-13). This can be compared to the mass

spectrum of $Cl_3SiOCCo_3(CO)_9$ which shows a weak parent ion and fragments due to $[Cl_3SiOCCo_3(CO)_n]^+$ (n = 9-0) [56]. The fragment ion at m/e 334 would involve some rearrangement of the core with the loss of silicon (fragment = $[Cl_2Co_4CO]^+$) or the loss of CO (fragment = $[Cl_2SiCo_4]^+$). Since the difference in m/e is 28 in both cases we can suggest that the loss of CO is more probable. The mass spectrum of $Cl_3SiOCCo_3(CO)_9$ [56] shows the same loss of all nine carbonyls, with another loss of m/e = 28 after this series.

Other ions include a series due to $[Cl_2SiCo_3(CO)_n]^+$ (n = 0-6) which is due to the loss of the terminal $Co(CO)_4$ moiety. Ions assigned to the series $[Co_3(CO)_n]^+$ (n = 0-9) are also observed. The Cl_2 isotope pattern is seen for the first two series in the mass spectrum. At the strong fragment ion m/e = 530, the Cl_2 isotope pattern corresponds very closely to that expected.

Table 6.2

MASS SPECTRUM OF $(CO)_4CoCl_2SiOCCo_3(CO)_9$

m/e	Int	Assignment	
698	w	$[Cl_2SiCo_4(CO)_n]^+$	n = 13
670	w		n = 12
642	-		n = 11
614	w		n = 10
586	w		n = 9
558	m		n = 8
530	s		n = 7
502	s		n = 6
474	m		n = 5
446	s		n = 4
418	m		n = 3
390	m		n = 2

Table 6.2 (continued)

m/e	Int	Assignment	
362	m		n = 1
334	s	$[Cl_2SiCo_4]^+$ or $[Cl_2Co_4CO]^+$	
443	w	$[Cl_2SiCo_3(CO)_n]^+$	n = 6
415	w		n = 5
387	w		n = 4
359	w		n = 3
331	m		n = 2
303	m		n = 1
275	m		n = 0
429	m	$[Co_3(CO)_n]^+$	n = 9
401	m		n = 8
373	w		n = 7
345	m		n = 6
317	s		n = 5
289	s		n = 4
261	s		n = 3
233	s		n = 2
205	s		n = 1
177	s		n = 0
189	w	$[Co_3C]^+$	

6.3.3 X-RAY CRYSTALLOGRAPHIC STUDY OF $(CO)_4CoCl_2SiOCCo_3(CO)_9$

Dark red crystals of $(CO)_4CoCl_2SiOCCo_3(CO)_9$ were obtained from a hexane solution cooled slowly from room temperature to -30°C. A rectangular plate-like crystal was mounted inside a fine capillary tube and sealed. Preliminary precession photographs using Cu-Kα radiation indicated that the crystal class was triclinic and belonged to the space group $P\bar{1}$.

Intensity data were collected at the University of Canterbury on a Nicolet P3 diffractometer for 2830 unique reflections in the range $4°<2\theta<45°$. Of these 1595 reflections were used in the final refinement with $I>3\sigma(I)$. An empirical absorption correction was applied using a ϕ-scan technique with transmission factors 0.81 maximum and 0.24 minimum. Crystal data for $(CO)_4CoCl_2SiOCCo_3(CO)_9$ are presented in Table 6.3.

Table 6.3

CRYSTAL DATA FOR $(CO)_4CoCl_2SiOCCo_3(CO)_9$	
Formula: $C_{14}Cl_2Co_4O_{14}Si$	Mr = 726.72
Triclinic	Space Group = $P\bar{1}$
Cryst. Colour: Dark Red	
Cryst. Dimensions: 1.5 x 0.5 x 0.05 mm	
a = 7.785(22) Å	α = 67.23(11)°
b = 8.798(15) Å	β = 68.92(16)°
c = 20.546(28) Å	γ = 67.77(16)°
U = 1163(4) $Å^3$	Dcalc = 2.08 g cm^{-3}
Z = 2	
F(000) = 704	Temp = 173 K
μ(Mo-Kα) = 30 cm^{-1}	
Unique Data = 2830	Range = $4°<2\theta<45°$
Refinement Data = 1595	Final R = 0.1003

The coordinates of the cobalt atoms were obtained using the TREF direct methods routine. Refinement and difference map cycles using SHELX-76 [98] located the remaining Cl, Si, C and O atoms. The Co, Cl and Si atoms were assigned anisotropic temperatures factors with other atoms treated isotropically. The final least squares refinement converged to R = 0.1003, R_w = 0.1079, $w = 1.1423[\sigma^2(F) + 0.0156F^2]^{-1}$ with 9.06 reflections per parameter. This poor refinement can be attributed to the very thin plate-like crystal (dimensions 1.5 x 0.5 x 0.05 mm) giving a large absorption correction, and poor mosaicity which required wide scan widths. The highest electron density peak found in the final difference map was 1.4 e $Å^{-3}$.

Positional and thermal parameters along with tables of complete bond lengths and angles are given in Appendix Seven. Tables of calculated and observed structure factors have been retained at the University of Waikato.

6.3.4 STRUCTURE OF $(CO)_4CoCl_2SiOCCo_3(CO)_9$

The structure of $(CO)_4CoCl_2SiOCCo_3(CO)_9$ consists of a Si-O-C unit in which the carbon atom triply bridges a $Co_3(CO)_9$ moiety. The silicon is bonded to two chlorine atoms and to a terminal $Co(CO)_4$ group. Stereo view and perspective diagram of the cluster are shown in Figures 6.3 and 6.4. A labelled atom diagram of $(CO)_4CoCl_2SiOCCo_3(CO)_9$ (Figure 6.4) is used throughout this discussion. Selected bond lengths and bond angles are presented in Tables 6.4 and 6.5 respectively.

The silicon atom is essentially tetrahedral, with the Co(4)-Si(1)-O(1) angle of 108.9(6)° slightly opened due to the bulky $Co(CO)_4$ group compared to the closing in of the Cl(1)-Si(1)-Cl(2) angle at 104.2(5)°. The analogous angles in the cluster $[Et_4N][(CO)_{11}Co_4Cl_2SiOCCo_3(CO)_9]$ [48] (Figure 6.5) at 111.2(4)° and 101.8(3)° respectively show a greater deviation due to the greater bulk of the $Co_4(CO)_{11}$ group. The other tetrahedral angles are slightly distorted to accommodate the more significant deviations.

The Si-Cl distances in this cluster, 2.065(10)Å and 2.054(10)Å, are slightly shorter than those found in $[Et_4N][(CO)_{11}Co_4Cl_2SiOCCo_3(CO)_9]$ at 2.088(6)Å and 2.099(7)Å.

Figure 6.3 Stereo View of $(CO)_4CoCl_2SiOCCo_3(CO)_9$

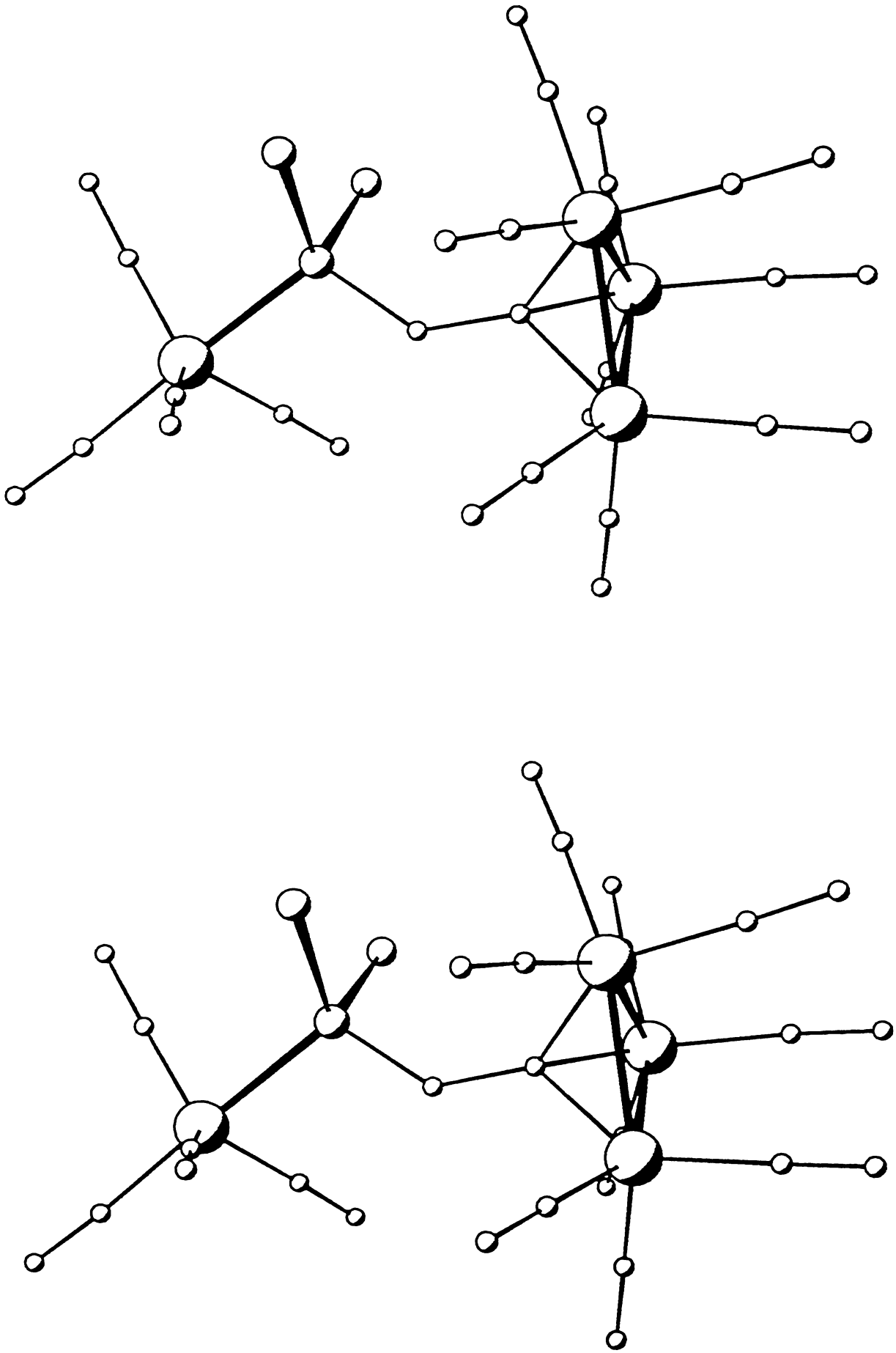

Figure 6.4 Labelled Perspective View of $(CO)_4CoCl_2SiOCCo_3(CO)_9$

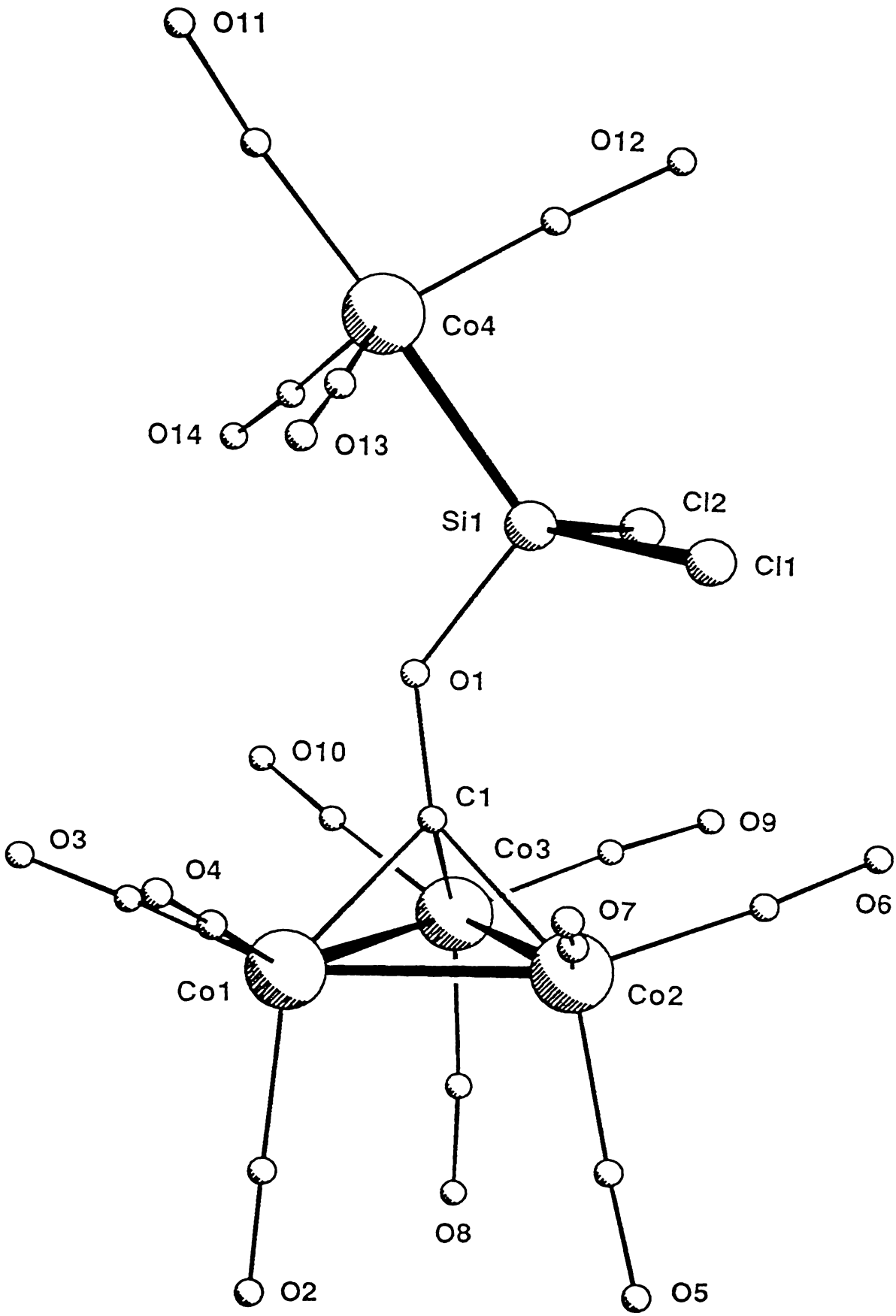

Table 6.4

SELECTED BOND LENGTHS FOR $(CO)_4CoCl_2SiOCCo_3(CO)_9$ (Å)			
Co(1) ---Co(2)	2.478(5)	Co(1) ---Co(3)	2.472(5)
Co(1) ---C(1)	1.90(3)	Co(2) ---Co(3)	2.486(4)
Co(2) ---C(1)	1.90(2)	Co(3) ---C(1)	1.87(2)
Co(4) ---Si(1)	2.249(8	Si(1) ---Cl(1)	2.07(1)
Si(1) ---Cl(2)	2.05(1)	Si(1) ---O(1)	1.67(2)
C(1) ---O(1)	1.36(3)		

Table 6.5

SELECTED BOND ANGLES FOR $(CO)_4CoCl_2SiOCCo_3(CO)_9$ (°)			
Co(2) -Co(1) -Co(3)	60.3(1)	Co(2) -Co(1) -C(1)	49.4(7)
Co(3) -Co(1) -C(1)	48.5(6)	Co(1) -Co(2) -Co(3)	59.7(1)
Co(1) -Co(2) -C(1)	49.3(8)	Co(3) -Co(2) -C(1)	48.2(6)
Co(1) -Co(3) -Co(2)	60.0(1)	Co(1) -Co(3) -C(1)	49.6(8)
Co(2) -Co(3) -C(1)	49.3(7)	Co(4) -Si(1) -Cl(1)	114.2(4)
Co(4) -Si(1) -Cl(2)	114.3(4)	Co(4) -Si(1) -O(1)	108.9(6)
Cl(1) -Si(1) -Cl(2)	104.2(5)	Cl(1) -Si(1) -O(1)	107.0(7)
Cl(2) -Si(1) -O(1)	107.8(6)	Co(1) -C(1) -Co(2)	81.0(1)
Co(1) -C(1) -Co(3)	81.9(9)	Co(1) -C(1) -O(1)	124.0(2)
Co(2) -C(1) -Co(3)	82.0(1)	Co(2) -C(1) -O(1)	132.0(2)
Co(3) -C(1) -O(1)	134.0(2)	Si(1) -O(1) -C(1)	135.0(2)

The Si(1)-Co(4) bond length of 2.249(8)Å is similar to that found for $(CO)_4CoSiCl_3$ at 2.254(3)Å but significantly shorter than those found for the Si-Co terminal distances in $(CO)_4CoSiCo_3(CO)_9$ (2.288(1)Å) and in the five coordinate silicon cluster $[(CO)_4CoSi]_2Co_4(CO)_{11}$ {7} at 2.347Å. This shortening is due more to the larger electronegativity of the chlorine atoms.

The Si(1)-O(1) (1.67(2)Å) and O(1)-C(1) (1.36(3)Å) bonds are very similar to those found for $[Et_4N][(CO)_{11}Co_4Cl_2SiOCCo_3(CO)_9]$ at 1.67(1)Å and 1.30(2)Å. Both are relatively short which suggests some form of delocalised π-bonding. Due to some steric repulsion between the $Co(CO)_4$ and the $Co_3(CO)_9$ groups the Si(1)-O(1)-C(1) angle is rather large at 135.6(1.5)°. This is also seen to a greater extent for $[Et_4N][(CO)_{11}Co_4Cl_2SiOCCo_3(CO)_9]$ with greater deviation due to the larger group. This results in an angle of 140(1)°. Any Si-O-C delocalised π-bonding would also contribute to the opening of this angle.

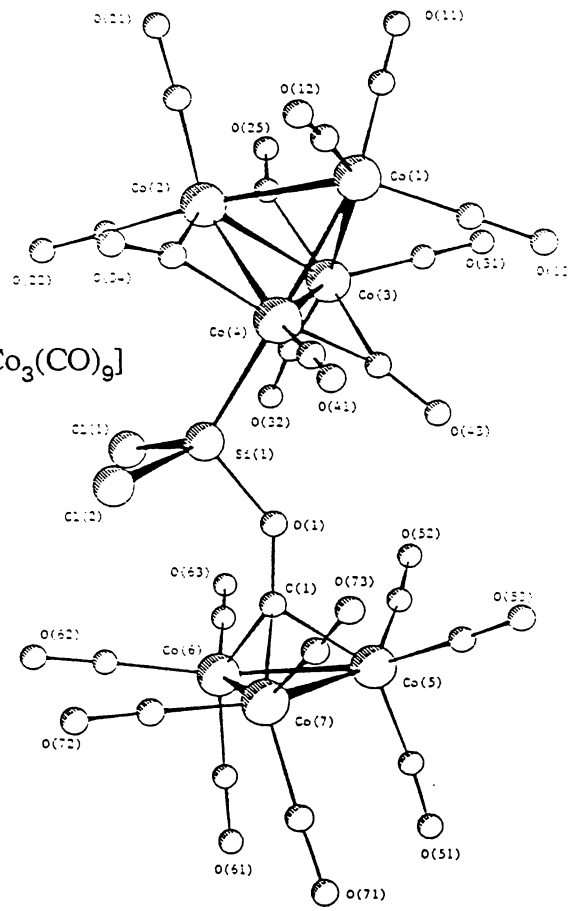

Figure 6.5

$[Et_4N][(CO)_{11}Co_4Cl_2SiOCCo_3(CO)_9]$

The oxymethylidine cluster ($-OCCo_3(CO)_9$) end of the molecule has similar angles and distances to those found for $[Et_4N][(CO)_{11}Co_4Cl_2SiOCCo_3(CO)_9]$ [48], $Cp_2ClTiOCCo_3(CO)_9$ [101], $Et_3NCl_2BOCCo_3(CO)_9$ [102] and $Et_3NH_2BOCCo_3(CO)_9$ [103]. The three cobalt atoms form an almost regular triangle with distances of 2.472(5)Å, 2.478(5)Å and 2.486(4)Å between them. The carbon atom symmetrically bridges the cobalt triangle with C(1)-Co distances of 1.87(2)Å and 1.90(2)Å for the remaining two. The structure shows that the $Co(CO)_4$ group is located over the Co(1)-Co(2) bond.

Four carbonyl ligands are terminally bonded to Co(4) with one axial, three equatorial. Co(4)-C distances range from 1.82(3)Å to 1.71(3)Å with the C-O distances ranging from 1.23(3)Å to 1.12(3)Å. Nine carbonyl ligands are distributed three to each cobalt atom in the oxymethylidine group. Six carbonyls lie approximately in the plane of the cobalt triangle with the other three pointing away from the bridging carbon atom. This arrangement of the nine carbonyls around the cobalt triangle is also seen for $(CO)_4CoSiCo_3(CO)_9$ and $[Et_4N][(CO)_{11}Co_4Cl_2SiOCCo_3(CO)_9]$ which both contain the $Co_3(CO)_9$ group. The average Co-C and C-O distances to the cobalt triangle are 1.79Å and 1.15Å respectively.

6.4 REACTION OF $(CO)_4CoCl_2SiOCCo_3(CO)_9$ WITH $K[Co(CO)_4]$

6.4.1 INTRODUCTION

The red product formed from the reaction of $SiCl_4$ with $K[Co(CO)_4]$ has two chlorine atoms available for further substitution. The following reaction was investigated to see if these could be replaced to form a larger silicon-cobalt complex with the possible formation of $(CO)_9Co_3SiOCCo_3(CO)_9$.

6.4.2 EXPERIMENTAL

$(CO)_4CoCl_2SiOCCo_3(CO)_9$ (0.26g, 0.358mmol) was added to a 5ml diethylether solution of $K[Co(CO)_4]$ (0.23g, 1.1mmol). The reaction was heated to 55°C for 3 days which resulted in a red/brown solution with a black precipitate. Incondensable CO gas was measured giving a total of 1.37mmol. This possibly indicates that compounds with a greater amount of metal-metal bonds may have formed. This loss would give an overall cobalt to carbonyl ratio of less than 1 to 3. The diethylether solvent was evaporated and 5ml of hexane was added to extract neutral compounds. Infrared spectra showed that $Co_4(CO)_{12}$ was the major hexane-soluble species.

A solution of Et_4NBr in dichloromethane was added to give a black coloured solution which was filtered from the KBr precipitate. This solution was slowly cooled to -30°C with the formation of black crystals.

The black anionic cluster can also be prepared directly from the reaction of $SiCl_4$ with $K[Co(CO)_4]$. $SiCl_4$ (0.171g, 1.01mmol) was reacted with $K[Co(CO)_4]$ (1.1g, 5.2mmol) in 5ml of diethylether for 5 days at 55°C. The neutral fraction contained $Co_4(CO)_{12}$ as the major product. The ionic fraction was extracted using a solution of Et_4NBr in CH_2Cl_2. This contained a small amount of $[Co(CO)_4]^-$ and the black cluster in 30-40% yield. The remaining grey residue was insoluble and would probable have contained silicon and cobalt oxides, etc.

6.4.3 INFRARED SPECTRUM OF $[Et_4N]_2[Co_6C(CO)_{15}]$

The infrared spectrum of $[Et_4N]_2[Co_6C(CO)_{15}]$ in THF is shown in Figure 6.6. Two carbonyl peaks (υCO, 2008 vw sh, 1981 vs, cm^{-1}) are assigned to the six terminal carbonyl ligands. Peaks at (υCO, 1859 w, 1826 s, 1814 s, 1774 mw sh, 1750 w sh, cm^{-1}) are assigned to the nine bridging carbonyls.

Figure 6.6

INFRARED SPECTRUM OF $[Et_4N]_2[Co_6C(CO)_{15}]$

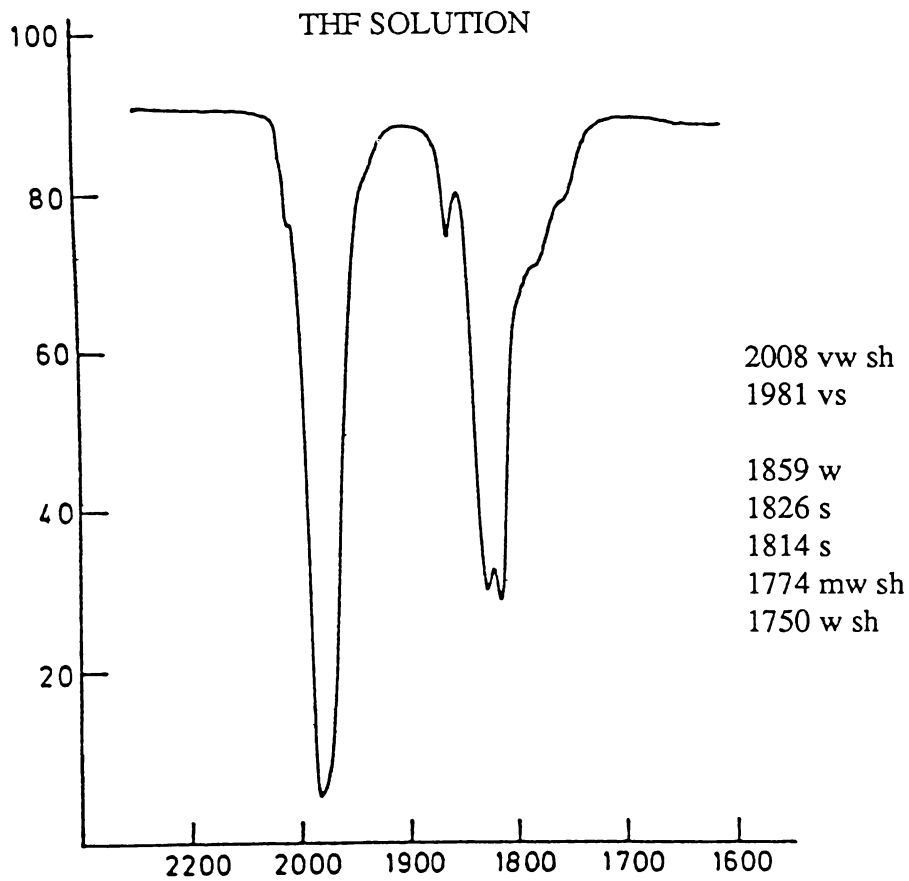

The anion possesses D_{3h} symmetry with an overall representation for the carbonyl stretches of $3A_1' + 3E' + 2A_2'' + 2E''$. The infrared active modes are $3E' + 2A_2''$ therefore five infrared peaks are expected. The terminal carbonyl stretches occur at 1981 cm^{-1} with the bridging carbonyls between 1859 cm^{-1} and 1750 cm^{-1}. The shift to lower frequency is consistent with the cluster having a negative charge.

6.4.4 X-RAY CRYSTALLOGRAPHIC STUDY OF $[Et_4N]_2[Co_6C(CO)_{15}]$

Black rectangular crystals of $[Et_4N]_2[Co_6C(CO)_{15}]$ were obtained from a cooled CH_2Cl_2 solution. A suitable crystal was mounted on a glass fibre using grease (apiezon N). Preliminary precession photographs using Cu-Kα radiation indicated that the crystal had monoclinic symmetry and belonged to the space group $P2_1/c$.

Intensity data were collected on a suitable crystal of dimensions 0.58 x 0.50 x 0.16 mm for 5255 unique reflections, in the range $4°<2\theta<45°$, at the University of Canterbury on a Nicolet P3 diffractometer. Mo-Kα radiation and a θ-2θ scan technique were used. Standard reflections were measured at regular intervals, with no significant decay observed. For structure solution and refinement, 2459 reflections were used with $I>3\sigma(I)$. Data were corrected for absorption effects using an empirical ϕ-scan technique with transmission factors, 0.856 maximum and 0.427 minimum. Crystal data for $[Et_4N]_2[Co_6C(CO)_{15}]$ are given in Table 6.6.

For all computations the SHELX-76 and SHELXS-86 [98] package of crystallographic programs were used. The positions of the heavy atoms were obtained using TREF and showed the overall geometry of the metal cluster to be that of a trigonal prism. The remaining atoms were located after preliminary refinement of the structure by least squares. Anisotropic temperature factors were assigned to the six cobalt atoms while other atoms were treated isotropically with an overall 9.8 reflections per parameter. The hydrogen atoms were not located on either of the two $[Et_4N]^+$ cations. The final refinement converged to $R = 0.0643$, $R_w = 0.0702$ with $w = 1.595[\sigma^2(F) + 0.00197F^2]^{-1}$. The largest shift/e.s.d in the final refinement cycle was 0.006 with no electron

density greater than 0.7 e $Å^{-3}$being found in the final difference map.

Positional and thermal parameters along with full bond lengths and angles are given in Appendix Eight. Tables of calculated and observed structure factors have been retained at the University of Waikato.

Table 6.6

CRYSTAL DATA FOR $[Et_4N]_2[Co_6C(CO)_{15}]$	
Formula: $C_{32}H_{40}Co_6N_2O_{15}$	Mr = 1046.27
Monoclinic	Space Group = $P2_1/c$
Cryst. Colour: Black	
Cryst. Dimensions: 0.58 x 0.50 x 0.16 mm	
a = 8.785(5) Å	$\alpha = 90.00°$
b = 22.495(8) Å	$\beta = 96.37(4)°$
c = 20.492(7) Å	$\gamma = 90.00°$
U = 4025(3) $Å^3$	Dcalc = 1.73 g cm^{-3}
Z = 4	
F(000) = 2112	Temp = 163 K
μ(Mo-Kα) = 24 cm^{-1}	
Unique Data = 5255	Range = $4°<2\theta<45°$
Refinement Data = 2459	Final R = 0.0643

6.4.5 STRUCTURE OF $[Et_4N]_2[Co_6C(CO)_{15}]$

The structure of the dianion $[Co_6C(CO)_{15}]^{2-}$ has been previously reported as the $[NMe_3(CH_2Ph)]^+$ salt [117]. This enables us to compare changes in these two structures with respect to the crystal packing forces.

Top view and stereo view of the dianion $[Co_6C(CO)_{15}]^{2-}$ are shown in Figures 6.7 and 6.8. A labelled perspective view of the dianion is shown in Figure 6.9. Selected bond lengths and angles are presented in Tables 6.7 and 6.8.

Figure 6.7 Top View of $[Co_6C(CO)_{15}]^{2-}$

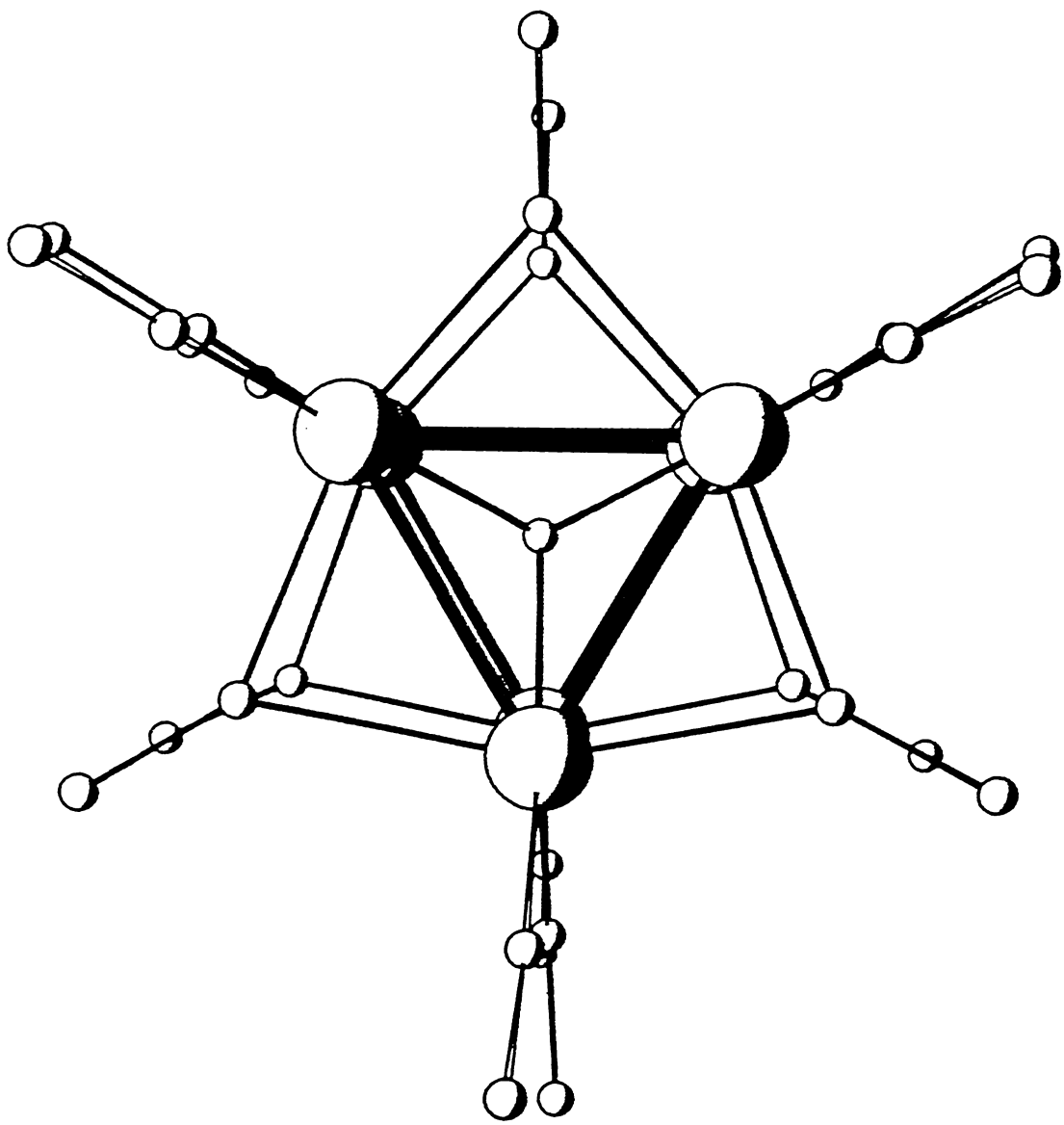

Figure 6.8 Stereo View of $[Co_6C(CO)_{15}]^{2-}$

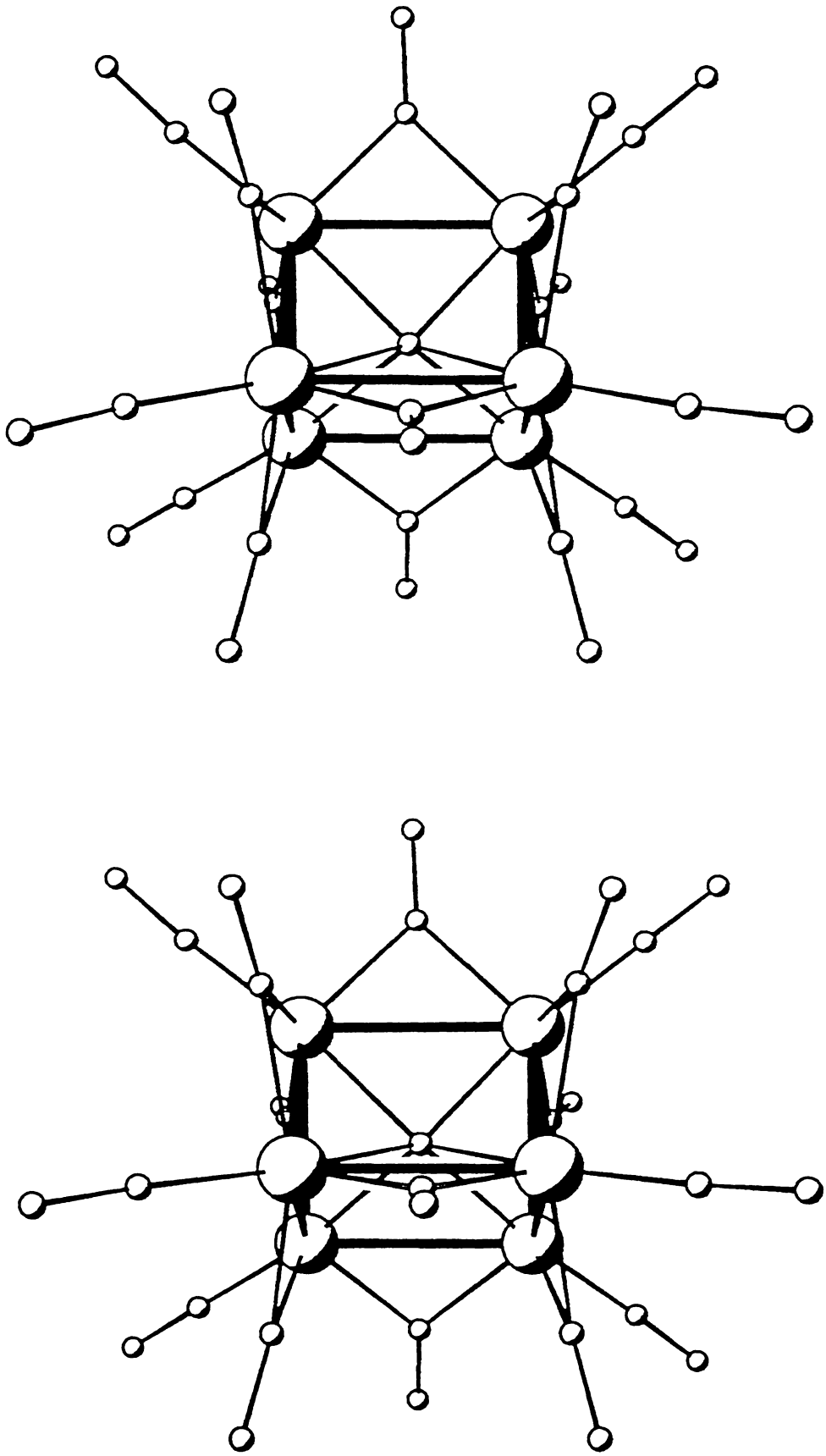

Figure 6.9 Labelled Perspective View of $[Co_6C(CO)_{15}]^{2-}$

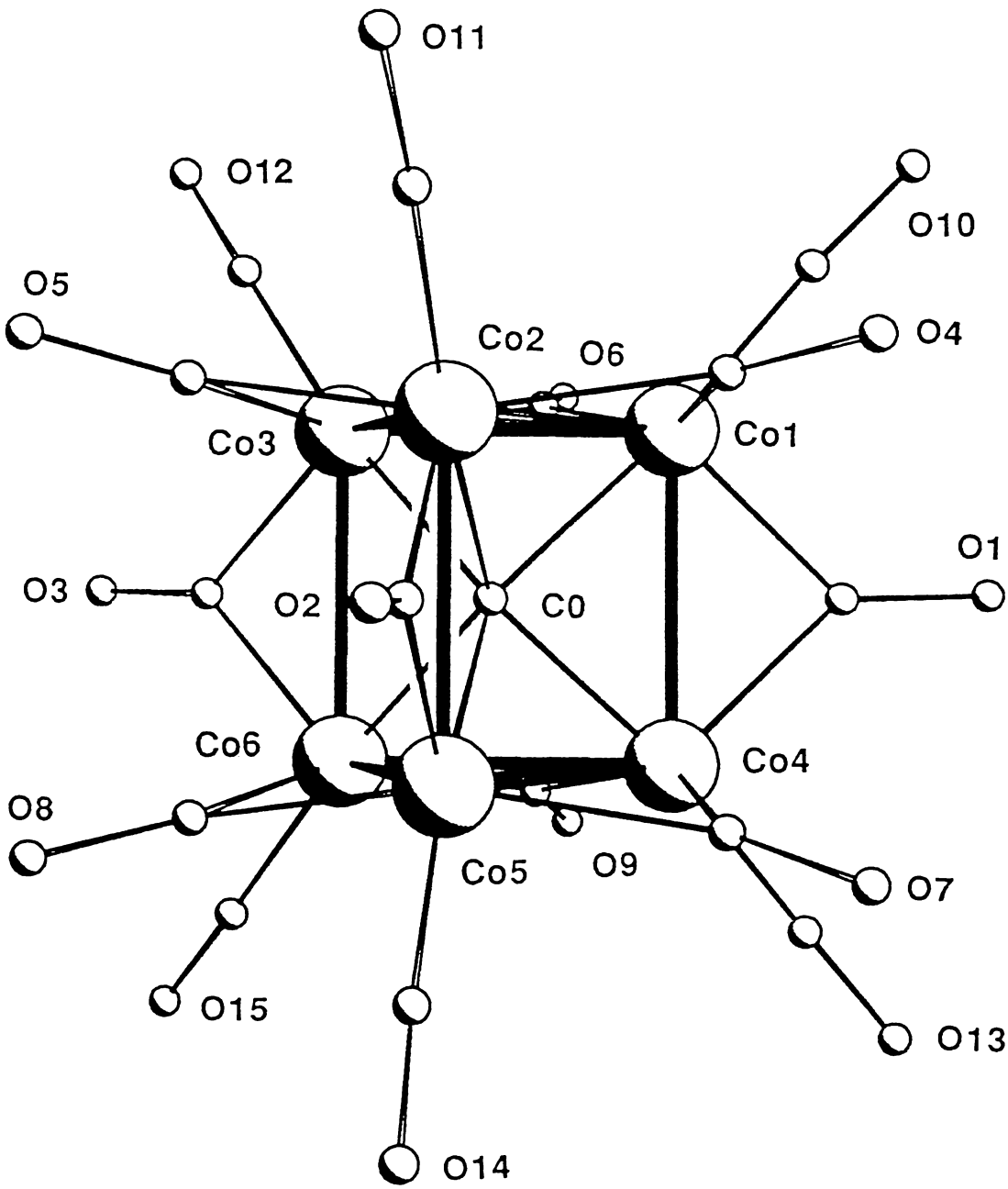

Table 6.7

SELECTED BOND LENGTHS FOR $[Et_4N]_2[Co_6C(CO)_{15}]$ (Å)			
Co(1) ---Co(2)	2.526(3)	Co(1) ---Co(3)	2.532(3)
Co(1) ---Co(4)	2.559(3)	Co(1) ---C(0)	1.93(2)
Co(2) ---Co(3)	2.519(3)	Co(2) ---Co(5)	2.579(3)
Co(2) ---C(0)	1.94(1)	Co(3) ---Co(6)	2.564(3)
Co(3) ---C(0)	1.98(2)	Co(4) ---Co(5)	2.521(3)
Co(4) ---Co(6)	2.551(3)	Co(4) ---C(0)	1.92(2)
Co(5) ---Co(6)	2.540(3)	Co(5) ---C(0)	1.93(1)
Co(6) ---C(0)	1.97(2)		

$[Co_6C(CO)_{15}]^{2-}$ consists of a hexanuclear metal atom cluster having a trigonal prismatic geometry. The fifteen carbonyls adopt a very symmetrical arrangement around this metal framework with six terminally bonded, one to each cobalt atom, with the remaining nine symmetrically bridging all the edges of the prism. The carbide atom is located at the centre of this prism.

Table 6.9 shows the average bond parameters of both salts of the prismatic dianion $[Co_6C(CO)_{15}]^{2-}$. The $[Et_4N]^+$ (R = 0.064) salt shows slightly more deviation in its bond lengths when compared to the $[NMe_3(CH_2Ph)]^+$ (R = 0.074) salt. This may be due to the higher symmetry found in the crystal of the latter salt. The $[NMe_3(CH_2Ph)]^+$ salt crystallises in the monoclinic space group C2/c whereas the $[Et_4N]^+$ salt belongs to the monoclinic space group $P2_1/c$. This gives the $[NMe_3(CH_2Ph)]^+$ salt a two-fold symmetry with the axis passing through an inter-basal (rectangular face) bridging carbonyl and the centre of the opposite rectangular face.

The Co-Co bond lengths in the triangular face (basal) for $[NMe_3(CH_2Ph)]^+$ range from 2.533(2)Å to 2.541(1)Å compared with 2.519(3)Å to 2.551(3)Å for the $[Et_4N]^+$ salt. The shortest inter-basal (rectangular face) Co-Co distance for the $[NMe_3(CH_2Ph)]^+$ salt is 2.574(2)Å compared to 2.559(3)Å for the $[Et_4N]^+$ salt (Table 6.9).

Table 6.8

SELECTED BOND ANGLES FOR $[Et_4N]_2[Co_6C(CO)_{15}]$ (°)			
Co(2) -Co(1) -Co(3)	59.7(1)	Co(2) -Co(5) -C(0)	48.3(4)
Co(2) -Co(1) -Co(4)	90.0(1)	Co(4) -Co(5) -Co(6)	60.6(1)
Co(2) -Co(1) -C(0)	49.4(4)	Co(4) -Co(5) -C(0)	48.9(5)
Co(3) -Co(1) -Co(4)	90.4(1)	Co(6) -Co(5) -C(0)	50.2(4)
Co(3) -Co(1) -C(0)	50.5(5)	Co(3) -Co(6) -Co(4)	89.9(1)
Co(4) -Co(1) -C(0)	48.2(5)	Co(3) -Co(6) -Co(5)	89.9(1)
Co(1) -Co(2) -Co(3)	60.3(1)	Co(3) -Co(6) -C(0)	49.7(4)
Co(1) -Co(2) -Co(5)	89.8(1)	Co(4) -Co(6) -Co(5)	59.4(1)
Co(1) -Co(2) -C(0)	49.1(4)	Co(4) -Co(6) -C(0)	48.2(5)
Co(3) -Co(2) -Co(5)	90.0(1)	Co(5) -Co(6) -C(0)	48.7(4)
Co(3) -Co(2) -C(0)	50.7(5)	Co(1) -C(0) -Co(2)	81.5(6)
Co(5) -Co(2) -C(0)	48.0(4)	Co(1) -C(0) -Co(3)	80.7(6)
Co(1) -Co(3) -Co(2)	60.0(1)	Co(1) -C(0) -Co(4)	83.3(6)
Co(1) -Co(3) -Co(6)	90.0(1)	Co(1) -C(0) -Co(5)	138.1(9)
Co(1) -Co(3) -C(0)	48.8(4)	Co(1) -C(0) -Co(6)	134.8(8)
Co(2) -Co(3) -Co(6)	90.4(1)	Co(2) -C(0) -Co(3)	80.0(6)
Co(2) -Co(3) -C(0)	49.3(4)	Co(2) -C(0) -Co(4)	137.6(9)
Co(6) -Co(3) -C(0)	49.5(4)	Co(2) -C(0) -Co(5)	83.6(6)
Co(1) -Co(4) -Co(5)	90.4(1)	Co(2) -C(0) -Co(6)	134.5(9)
Co(1) -Co(4) -Co(6)	89.7(1)	Co(3) -C(0) -Co(4)	135.7(8)
Co(1) -Co(4) -C(0)	48.5(4)	Co(3) -C(0) -Co(5)	134.5(9)
Co(5) -Co(4) -Co(6)	60.1(1)	Co(3) -C(0) -Co(6)	80.8(6)
Co(5) -Co(4) -C(0)	49.3(4)	Co(4) -C(0) -Co(5)	81.8(6)
Co(6) -Co(4) -C(0)	50.0(4)	Co(4) -C(0) -Co(6)	81.9(6)
Co(2) -Co(5) -Co(4)	89.7(1)	Co(5) -C(0) -Co(6)	81.2(6)
Co(2) -Co(5) -Co(6)	89.6(1)		

The Co-Co bond lengths are shorter overall for the $[Et_4N]^+$ salt due to a more densely packed structure.

Table 6.9

BOND LENGTHS (Å) FOR THE DIANION $[Co_6C(CO)_{15}]^{2-}$		
BOND	**CATION --- $[NMe_3(CH_2Ph)]^+$**	**$[Et_4N]^+$**
BASAL		
Co-Co (average)	2.537	2.532
Co-Co (longest)	2.541(1)	2.551(3)
Co-Co (shortest)	2.533(2)	2.519(3)
INTER-BASAL		
Co-Co (average)	2.575	2.567
Co-Co (longest)	2.578(2)	2.579(3)
Co-Co (shortest)	2.574(2)	2.559(3)
CARBIDE		
Co-C (average)	1.95	1.95
Co-C (longest)	1.95(1)	1.98(1)
Co-C (shortest)	1.95(1)	1.92(1)
CARBONYLS		
Co-C (terminal)	1.75	1.73
C-O (terminal)	1.14	1.16
Co-C (basal, bridging)	1.97	1.94
C-O (basal, bridging)	1.16	1.18
Co-C (inter-basal, bridging)	1.90	1.87
C-O (inter-basal, bridging)	1.18	1.20

The Co-Co bond lengths in $[Co_6C(CO)_{15}]^{2-}$ range from 2.519(3) to 2.579(3)Å, average 2.544(3)Å, which can be compared with those found for other di-anionic carbido clusters. In $[Co_6C(CO)_{13}]^{2-}$ [152] the bridged edges range from 2.465(1)Å to 2.505(1)Å, average 2.483(1)Å and in $[Co_8C(CO)_{18}]^{2-}$ [112] the six symmetrically bridged Co-Co bond lengths average 2.484(4)Å.

This shows that there is a significant lengthening in the Co-Co distance in the $[Co_6C(CO)_{15}]^{2-}$ cluster due to the number of carbonyls that have to be accommodated. This has resulted in an expanded central cavity.

The larger central cavity can also be seen in the longer Co-C (carbide) distances compared to other cobalt-carbido clusters containing a six metal framework. The Co-C (carbide) distances range from 1.920(15)Å to 1.981(14)Å, average 1.946(15)Å. This can be compared to $[Co_6C(CO)_{13}]^{2-}$ [152] with Co-C (carbide) distances ranging from 1.86 to 1.88Å, average 1.87Å and in $[Co_6C(CO)_{14}]^{-}$ [40] range from 1.84 to 1.94Å, average 1.88Å. Also the carbido atom is located closer to one square face, average 1.93Å as compared to 1.98Å for the opposite edge. This deviation is also seen in the cluster $[Co_6C(CO)_{14}]^{-}$ [40] with average values of 1.85Å and 1.93Å respectively.

The structure adopted by Co_6-carbido clusters depends on the number of carbonyl ligands that the structure contains. The $[Co_6C(CO)_{13}]^{2-}$ (Figure 6.10) anion possesses idealised C_2 symmetry and contains a distorted octahedron of cobalt atoms, whose cavity is occupied by the carbide atom. Five carbonyl ligands are bridging on opposite edges of the three octahedron equators, and eight are terminal. The structure of anion $[Co_6C(CO)_{14}]^{-}$ (Figure 6.11) consists of distorted octahedron of C_{2V} idealised symmetry. Of the 14 carbonyl ligands, six unsymmetrically bridge Co-Co edges with the remaining eight terminally bonded and conform to the overall cluster symmetry. This shows the difference when compared to the trigonal prismatic geometry of $[Co_6C(CO)_{15}]^{2-}$ which has nine bridging carbonyls and one terminal on each cobalt atom.

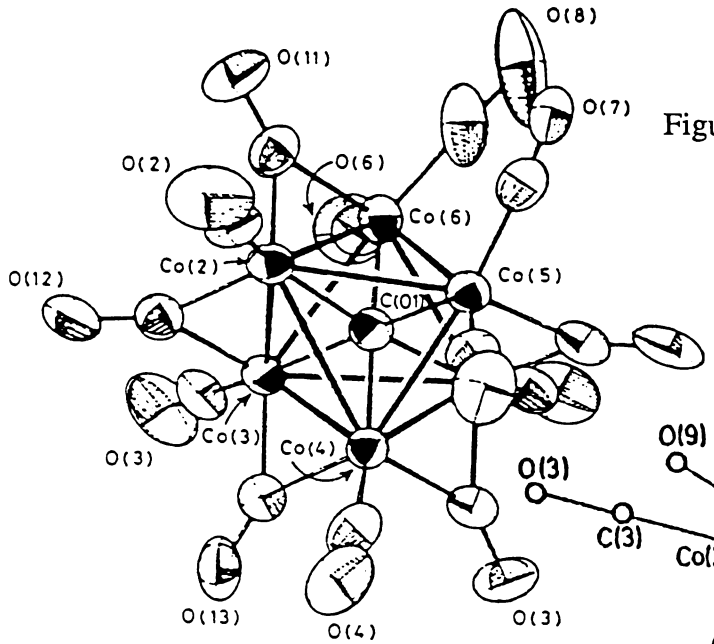

Figure 6.10 $[Co_6C(CO)_{13}]^{2-}$

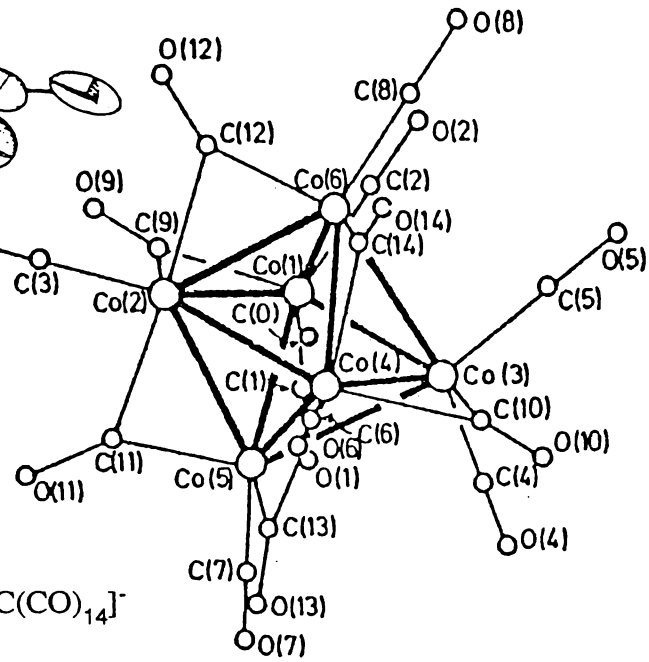

Figure 6.11 $[Co_6C(CO)_{14}]^-$

6.4.6 DISCUSSION

The reaction pathway of $SiCl_4$ with $[Co(CO)_4]^-$ in diethylether solvent has lead to the isolation of two intermediate products, $Cl_3SiOCCo_3(CO)_9$ **{1}** and $(CO)_4CoCl_2SiOCCo_3(CO)_9$ **{1}** which react further with $[Co(CO)_4]^-$ to ultimately lead to the formation of the cluster $[Co_6C(CO)_{15}]^{2-}$.

The cluster $[Co_6C(CO)_{15}]^{2-}$ can be prepared directly from the reaction of $SiCl_4$ with $[Co(CO)_4]^-$ in 30-40% yield (see section 6.3.2). This reaction is analogous to the preparation of the cluster directly from CCl_4 with $[Co(CO)_4]^-$ [117] according to equation (1).

$$\mathbf{CCl_4 + 6[Co(CO)_4]^- \rightarrow [Co_6C(CO)_{15}]^{2-} + 4Cl^- + 9CO \ (1)}$$

Better yields (40-50%) are obtained by the reaction of $ClCCo_3(CO)_9$ with $Na[Co(CO)_4]$ in di-isopropyl ether solvent [117] (equation (2)).

$$\mathbf{ClCCo_3(CO)_9 + 3Na[Co(CO)_4] \rightarrow Na_2[Co_6C(CO)_{15}] + NaCl + 6CO \ (2)}$$

The silicon tetrachloride reaction initially forms the siloxy cluster $Cl_3SiOCCo_3(CO)_9$ **{1}** which is similar to the starting material in equation (2). This then undergoes salt-elimination to replace one chlorine atom with a $Co(CO)_4$ group (equation (3)).

$$Cl_3SiOCCo_3(CO)_9 + [Co(CO)_4]^- \rightarrow (CO)_4CoCl_2SiOCCo_3(CO)_9 + Cl^- \quad (3)$$

Further reaction with $[Co(CO)_4]^-$ forms the carbido cluster by using the $(CO)_4CoCl_2SiO$ as a leaving group. This is analogous to $ClCCo_3(CO)_9$ (equation (2)) in which the chlorine atom is removed.

6.5 REACTION OF Si_2Cl_6 WITH $[Co(CO)_4]^-$

6.5.1 EXPERIMENTAL

Si_2Cl_6 (0.183g, 0.680mmol) was added to a 10ml CH_2Cl_2 solution of $[Et_4N][Co(CO)_4]$ (1.20g, 3.98mmol) in a high pressure ampoule giving a reaction ratio of 1 to 6. This was allowed to react for 2 months in the dark at room temperature. Initially the solution was a very light yellow colour which on completion had changed to a brown solution with large blue crystals.

The contents were transferred to a Schlenk flask leaving the large blue crystals in the ampoule. These blue crystals were soluble in water and showed to contain chlorine by precipitation with silver nitrate solution, tentatively identified as $[Et_4N]_2CoCl_4$. The solvent was removed and hexane (10ml) was added giving a red solution. Infrared spectrum showed four peaks at (υCO, (hexane) 2061 w, 2051 s, 2037 s, 2028 m, cm^{-1}).

CH_2Cl_2 (20ml) was added to the remaining solid giving a brown solution which contained mainly unreacted $[Co(CO)_4]^-$ and an uncharacterised product.

6.5.2 INFRARED SPECTRUM OF Si_2Cl_6 WITH $[Co(CO)_4]^-$

The infrared spectrum of the red hexane-soluble product is shown in Figure 6.12. This spectrum shows four peaks at (υCO, (hexane) 2061 w, 2051 s, 2037 s, 2028 m, cm^{-1}) which corresponds partially to the O-C-$Co_3(CO)_9$ group

and overall is very similar to the prominent peaks in $(CO)_4CoCl_2SiOCCo_3(CO)_9$. Therefore the product is tentatively characterised as $(CO)_4CoCl_4Si_2OCCo_3(CO)_9$.

Table 6.10

INFRARED SPECTRUM OF $(CO)_4CoCl_4Si_2OCCo_3(CO)_9$ COMPARED TO SIMILAR SPECIES			
	Y = $-OCCo_3(CO)_9$		
$(CO)_4CoCl_4Si_2$-Y	$(CO)_4CoCl_2Si$-Y	Cl_3Si-Y	$Cl_3SiCo(CO)_4$
	2120 w		2118 s
	2105 w	2104 w	
2061 w	2064 w		2066 s
2051 s	2057 vs	2056 vs	
2037 s	2042 m	2040 s	
2028 m	2037 m		2039 vs
		2020 sh w	
			1999 w

Figure 6.12

INFRARED SPECTRUM OF Si_2Cl_6 WITH $[Co(CO)_4]^-$

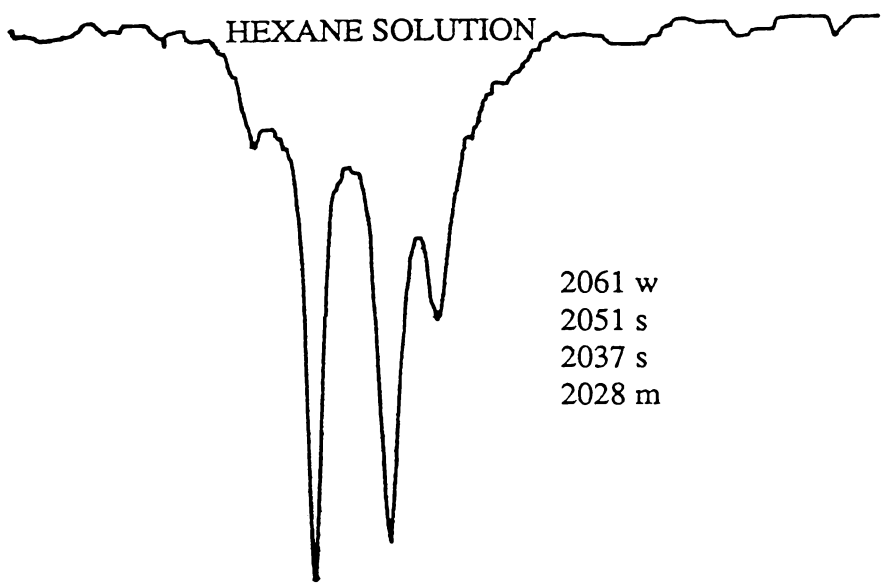

6.5.3 MASS SPECTRUM OF $(CO)_4CoCl_4Si_2OCCo_3(CO)_9$

The mass spectrum assigned to $(CO)_4CoCl_4Si_2OCCo_3(CO)_9$ was obtained (Table 6.11). The parent ion $[Cl_4Si_2Co_4(CO)_{14}]^+$ at m/e = 824 was seen and a series due to the loss of all 14 carbonyl groups is observed. The final ion $[Cl_4Si_2Co_4]^+$ m/e = 432 could also be due to the loss of Si but both possibilities require substantial rearrangement. The Cl_4 isotope pattern is observed for the above series. With the loss of $SiCl_2$ a series is seen for $[Cl_2SiCo_4(CO)_n]^+$ (n = 0 - 14) m/e = 334-726. These two series dominate the mass spectrum.

The $Co(CO)_4$ group is most likely bonded to the same silicon atom as the oxymethylidine cluster moiety due to the second series in the mass spectrum losing $SiCl_2$ instead of $ClSiCo(CO)_4$. If the $Co(CO)_4$ moiety was bonded in a Co-Si-Si-O-C-Co_3 fashion we would expect to see a fragment series due to the ion $[Cl_3SiCo_3(CO)_n]^+$ (n = 0-9).

Table 6.11

MASS SPECTRUM OF $(CO)_4CoCl_4Si_2OCCo_3(CO)_9$			
m/e	**Int**	**Assignment**	
824	w	$[Cl_4Si_2Co_4(CO)_n]^+$	n = 14
796	w		n = 13
768	w		n = 12
740	w		n = 11
712	w		n = 10
684	w		n = 9
656	m		n = 8
628	m		n = 7
600	s		n = 6
572	s		n = 5
544	m		n = 4
516	m		n = 3

Table 6.11 (continued)

m/e	Int	Assignment	
488	m		n = 2
460	m		n = 1
432	m		n = 0
726	w	$[Cl_2SiCo_4(CO)_n]^+$	n = 14
698	w		n = 13
670	w		n = 12
642	w		n = 11
614	m		n = 10
586	m		n = 9
558	s		n = 8
530	s		n = 7
502	m		n = 6
474	m		n = 5
446	m		n = 4
418	s		n = 3
390	m		n = 2
362	m		n = 1
334	s		n = 0
304	m	$[Cl_3Si_2Co(CO)_n]^+$	n = 3
276	m		n = 2
248	m		n = 1
220	s		n = 0
205	s	$[SiCo_3]^+$ or $[OCCo_3]^+$	

6.6 REACTION OF $Cl_3SiOSiCl_3$ WITH $[Co(CO)_4]^-$

6.6.1 EXPERIMENTAL

$Cl_3SiOSiCl_3$ (0.183g, 0.642mmol) was condensed into a 50ml ampoule containing a CH_2Cl_2 (10ml) solution of $[Et_4N][Co(CO)_4]$ (1.13g, 3.75mmol). The reaction was allowed to proceed at room temperature for one month in which time the solution had changed from light green to a green/black colour.

The contents were transferred to a Schlenk flask and the solvent removed. Hexane (15ml) was added which extracted a red compound (see infrared spectrum in section 6.6.2).

The remaining green/black CH_2Cl_2 solution contained unreacted $[Et_4N][Co(CO)_4]$ and several other uncharacterised products (υCO, (CH_2Cl_2) 2114 w, 2099 w, 2068 m, 2049 s, 2025 s, cm^{-1}).

6.6.2 INFRARED SPECTRUM OF $Cl_3SiOSiCl_3$ WITH $[Co(CO)_4]^-$

The infrared spectrum (Figure 6.13) of the red hexane-soluble product showed peaks at (υCO, 2099 w, 2051 vs, 2037 m, 2019 w, cm^{-1}). These peaks show good correlation to the $OCCo_3(CO)_9$ group and therefore this red compound is tentatively characterised as $Cl_3SiOSi(Cl)_2OCCo_3(CO)_9$.

Table 6.12

INFRARED SPECTRUM OF $Cl_3SiOSi(Cl)_2OCCo_3(CO)_9$ COMPARED TO SIMILAR SPECIES		
	Y = $OCCo_3(CO)_9$	
Cl_5OSi_2-Y	Cl_3Si-Y	$MeCl_2Si$-Y
2099 w	2104 w	2104 w
2051 vs	2056 vs	2053 s
2037 m	2040 s	2039 s
2019 w	2020 sh w	2020 w

Figure 6.13

INFRARED SPECTRUM OF $Cl_3SiOSiCl_3$ WITH $[Et_4N][Co(CO)_4]$

HEXANE SOLUTION

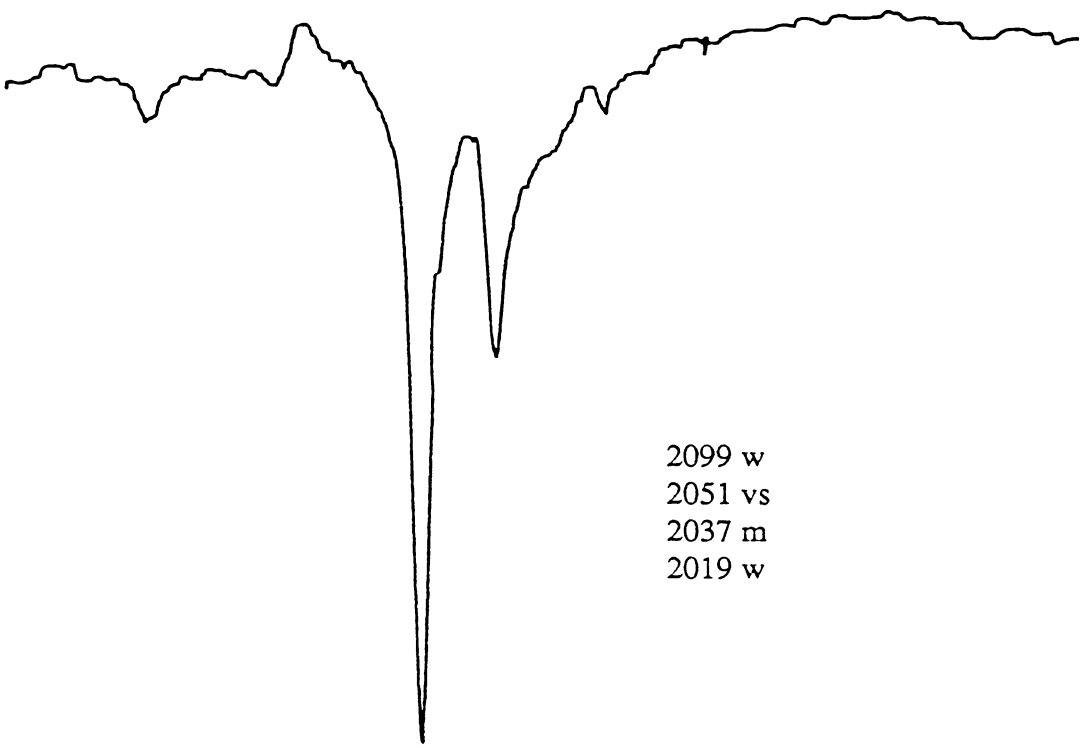

6.6.3 EXPERIMENTAL

$Cl_3SiOSiCl_3$ (0.262g, 0.921mmol) was condensed into a 50ml ampoule with $K[Co(CO)_4]$ (1.18g, 5.62mmol) in 20ml of diethylether. This was left to react in the dark for 3 years at room temperature after which a red/black solution with a large amount of black precipitate had formed. The contents of the ampoule were transferred to a Schlenk flask and the solvent removed. Hexane (30ml) was added to the flask to extract the neutral compounds giving a red/brown solution. An infrared spectrum showed this to contain $Co_2(CO)_8$, $Co_4(CO)_{12}$ and a new compound. $Co_2(CO)_8$ was sublimed onto a cold finger and removed with the remaining residue extracted with hexane. This was cooled to crystallise out the $Co_4(CO)_{12}$ leaving the new product reasonably pure in a yield of 5-10%.

To the hexane insoluble fraction a solution of Et_4NBr in 30ml of CH_2Cl_2 was added giving a brown/black solution with most of the brown precipitate being insoluble in acetone or water. This insoluble component was due to the long reaction time which resulted in the formation of cobalt oxides. The infrared spectrum of the CH_2Cl_2 fraction showed a large peak at 1886 cm^{-1} due to $[Co(CO)_4]^-$ and smaller peaks between 2050 cm^{-1} and 2020 cm^{-1} which remain uncharacterised.

6.6.4 INFRARED CHARACTERISATION

The infrared spectrum of the red/brown hexane-soluble product is shown in Figure 6.14. This spectrum can be compared to those of $Cl_3SiOSi(Cl)_2OCCo_3(CO)_9$ and $Cl_3SiOCCo_3(CO)_9$, showing a very good correlation with products containing an $-OCCo_3(CO)_9$ group (see Table 6.13).

Table 6.13

INFRARED CHARACTERISATION OF $Cl_3SiOSiCl_3$ WITH $K[Co(CO)_4]$		
	Y = $-OCCo_3(CO)_9$	
PRODUCT	Cl_5OSi_2-Y	Cl_3Si-Y
2101 w	2099 w	2104 w
2081 m		
2065 s		
2052 vs	2051 vs	2056 vs
2038 s	2037 m	2040 s
2029 w		
2018 w	2019 w	2020 sh w

Figure 6.14

INFRARED SPECTRUM OF $Cl_3SiOSiCl_3$ WITH $K[Co(CO)_4]$

HEXANE SOLUTION

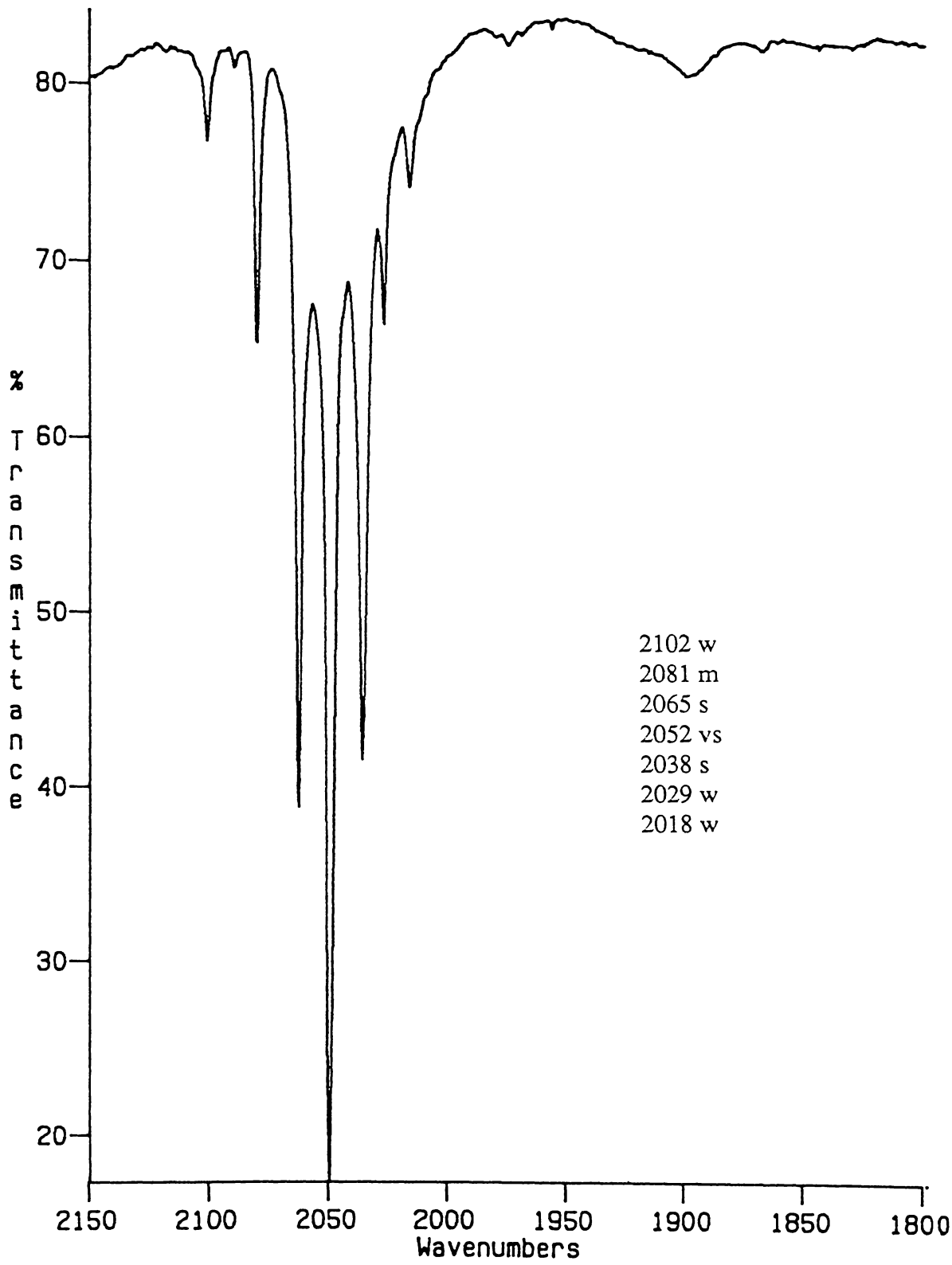

6.6.5 DISCUSSION

This work shows that various silicon chlorides ($SiCl_4$, Si_2Cl_6 and $Cl_3SiOSiCl_3$) all initially form the siloxymethylidine cluster group ($Si\text{-}OCCo_3(CO)_9$) and then proceed with a salt-elimination step to substitute a chlorine atom for a $Co(CO)_4$ group. This substitution occurs to a very limited extent, generally only once which is possibly due to steric constraints limiting access of the bulky $Co(CO)_4$ group. $SiCl_4$ with $[Co(CO)_4]^-$ forms $(CO)_4CoCl_2SiOCCo_3(CO)_9$ as the highest substituted product. Si_2Cl_6 with $[Co(CO)_4]^-$ forms $(CO)_4Co(Cl_3Si)ClSiOCCo_3(CO)_9$ as the highest substituted product. It is interesting to note that the $Co(CO)_4$ group is located on the same silicon atom as the oxymethylidine cluster (from mass spectral data) which due to steric effects may best be located on the other silicon atom. The last silicon chloride to be investigated $Cl_3SiOSiCl_3$ showed one product consistent with the possible formation of $Cl_3SiOSi(Cl)_2OCCo_3(CO)_9$ and an uncharacterised product in which further substitution had occurred. This further substitution may have taken place on the silicon further away from the oxymethylidine group due to the long Si-O-Si distance minimising steric effects. Comparison with $(CO)_4CoCl_2SiOCCo_3(CO)_9$ shows that this further substituted product is unlikely to contain a terminal moiety $Co(CO)_4$, or a $Co_2(CO)_7$ group as no bridging carbonyls are observed in the infrared spectrum. Possible products include $O[SiCl_2OCCo_3(CO)_9]_2$ or a similar product with the second $-OCCo_3(CO)_9$ group attached to the same silicon.

Further reaction at higher temperatures or longer reaction times results in the formation of the carbido cluster $[Co_6C(CO)_{15}]^{2-}$. This is plausible since the $Cl_3Si\text{-}O\text{-}$ or $(CO)_4CoCl_2Si\text{-}O\text{-}$ group can be considered a leaving group for the formation of carbido clusters. Carbido clusters (e.g. $[Co_6C(CO)_{15}]^{2-}$) can be synthesised from the reaction of $ClCCo_3(CO)_9$ with $[Co(CO)_4]^-$ [117] in which the chlorine atom is the leaving group.

The reaction of SiI_4 with $[Co(CO)_4]^-$ has formed the cluster $(CO)_4CoSiCo_3(CO)_9$ [46] in which all the iodine atoms have been substituted without the formation of the oxymethylidine group. The formation of the oxymethylidine group is probably due to the acidity of the silicon centre which

initially forms $(CO)_3Co\text{-}C\text{-}O/SiCl_4$ adducts which presumably react further to form the oxymethylidine cluster. As the halogen gets heavier (Br, I), this acidity reduces. Therefore other silicon halides such as SiX_4, Si_2X_6 and $X_3SiOSiX_3$ (X = Br or I) may substitute more fully. Also weaker Si-X bond strengths are involved.

APPENDIX

APPENDIX ONE

FINAL POSITIONAL AND EQUIVALENT THERMAL PARAMETERS FOR $H_2Si_3Co_6(CO)_{20}$

MOLECULE ONE

ATOM	X/A	Y/B	Z/C	Ueq/U11
Co(11)	0.4733(1)	0.9761(1)	0.2623(1)	0.016
Co(12)	0.5650(1)	0.8291(1)	0.3336(1)	0.017
Co(13)	0.8993(1)	0.9698(1)	0.1978(1)	0.018
Co(14)	0.8485(1)	0.0422(1)	0.2891(1)	0.016
Co(15)	0.2698(2)	0.9051(1)	0.4649(1)	0.026
Co(16)	0.9617(1)	1.2399(1)	0.0955(1)	0.024
Si(11)	0.6955(3)	0.9568(2)	0.2703(1)	0.015
Si(12)	0.4634(3)	0.9280(2)	0.3770(1)	0.018
Si(13)	0.8425(3)	1.1110(2)	0.1756(1)	0.018
C(11)	0.522(1)	0.9954(6)	0.1742(5)	0.024(2)
O(11)	0.5503(7)	1.0093(5)	0.1174(4)	0.033(2)
C(12)	0.451(1)	1.0827(6)	0.2626(5)	0.022(2)
O(12)	0.4335(8)	1.1537(5)	0.2595(4)	0.033(2)
C(13)	0.312(1)	0.9264(6)	0.2713(5)	0.023(2)
O(13)	0.2104(8)	0.8930(5)	0.2743(4)	0.037(2)
C(14)	0.668(1)	0.7845(7)	0.3934(5)	0.027(2)
O(14)	0.7327(9)	0.7504(6)	0.4337(4)	0.050(2)
C(15)	0.626(1)	0.7908(6)	0.2654(5)	0.025(2)
O(15)	0.6613(8)	0.7667(5)	0.2216(4)	0.042(2)
C(16)	0.420(1)	0.7545(6)	0.3713(5)	0.024(2)
O(16)	0.3326(8)	0.7024(5)	0.3968(4)	0.039(2)
C(17)	0.928(1)	0.8627(7)	0.2552(6)	0.031(3)
O(17)	0.9446(9)	0.7955(5)	0.2931(4)	0.046(2)
C(18)	1.075(1)	1.0058(6)	0.1608(5)	0.021(2)
O(18)	1.1845(8)	1.0269(5)	0.1379(4)	0.036(2)
C(19)	0.846(1)	0.9498(7)	0.1319(6)	0.034(3)
O(19)	0.8176(9)	0.9346(6)	0.0880(5)	0.057(3)
C(110)	0.741(1)	1.1219(6)	0.3052(5)	0.021(2)
O(110)	0.6731(8)	1.1704(5)	0.3204(4)	0.035(2)
C(111)	0.839(1)	0.9633(6)	0.3726(5)	0.025(2)
O(111)	0.8320(8)	0.9204(5)	0.4283(4)	0.038(2)
C(112)	1.023(1)	1.0765(6)	0.2808(5)	0.024(2)
O(112)	1.1327(8)	1.0911(5)	0.2803(4)	0.031(2)
C(113)	0.169(1)	0.8509(7)	0.4289(6)	0.031(3)
O(113)	0.0940(9)	0.8165(5)	0.4114(4)	0.049(2)
C(114)	0.137(1)	0.8942(7)	0.5353(6)	0.037(3)
O(114)	0.0473(9)	0.8886(5)	0.5791(4)	0.052(2)
C(115)	0.285(1)	1.0202(8)	0.4334(6)	0.037(3)
O(115)	0.2933(9)	1.0962(6)	0.4137(5)	0.055(2)

C(116)	0.387(1)	0.8426(8)	0.5115(6)	0.040(3)
O(116)	0.466(1)	0.8022(6)	0.5406(5)	0.063(3)
C(117)	1.126(1)	1.2156(6)	0.1199(5)	0.025(2)
O(117)	1.2298(9)	1.2057(5)	0.1307(4)	0.045(2)
C(118)	0.845(1)	1.2870(7)	0.1449(6)	0.031(3)
O(118)	0.7690(8)	1.3192(5)	0.1742(4)	0.043(2)
C(119)	0.911(1)	1.1923(7)	0.0414(6)	0.034(3)
O(119)	0.880(1)	1.1630(6)	0.0054(5)	0.058(3)
C(120)	1.019(1)	1.3436(7)	0.0294(6)	0.034(3)
O(120)	1.0511(9)	1.4096(6)	-0.0123(5)	0.053(2)

MOLECULE TWO

ATOM	X/A	Y/B	Z/C	Ueq/U11
Co(21)	0.5034(1)	0.4800(1)	0.8606(1)	0.020
Co(22)	0.7447(1)	0.4219(1)	0.8731(1)	0.019
Co(23)	0.7606(1)	0.6312(1)	0.6830(1)	0.019
Co(24)	0.7282(1)	0.4828(1)	0.6689(1)	0.016
Co(25)	0.4698(1)	0.2059(1)	0.9458(1)	0.021
Co(26)	1.1411(1)	0.5705(1)	0.5978(1)	0.024
Si(21)	0.6855(3)	0.5031(2)	0.7714(1)	0.017
Si(22)	0.5630(3)	0.3425(2)	0.8681(1)	0.018
Si(23)	0.9310(3)	0.5395(2)	0.6744(1)	0.018
C(21)	0.535(1)	0.5907(7)	0.8542(5)	0.028(3)
O(21)	0.5561(8)	0.6607(5)	0.8503(4)	0.036(2)
C(22)	0.370(1)	0.4856(6)	0.8160(5)	0.026(2)
O(22)	0.2788(9)	0.4907(5)	0.7901(4)	0.048(2)
C(23)	0.415(1)	0.4371(7)	0.9478(5)	0.026(2)
O(23)	0.3604(8)	0.4092(5)	1.0032(4)	0.037(2)
C(24)	0.844(1)	0.3409(7)	0.8551(5)	0.028(3)
O(24)	0.9158(9)	0.2893(5)	0.8452(4)	0.045(2)
C(25)	0.869(1)	0.5062(6)	0.8579(5)	0.025(2)
O(25)	0.9507(9)	0.5553(5)	0.8539(4)	0.049(2)
C(26)	0.708(1)	0.3989(6)	0.9631(5)	0.023(2)
O(26)	0.6919(8)	0.3907(5)	1.0192(4)	0.034(2)
C(27)	0.586(1)	0.6584(6)	0.6844(5)	0.026(2)
O(27)	0.4739(9)	0.6703(5)	0.6852(4)	0.050(2)
C(28)	0.830(1)	0.7047(6)	0.5978(5)	0.023(2)
O(28)	0.8768(8)	0.7518(5)	0.5452(4)	0.036(2)
C(29)	0.827(1)	0.6807(7)	0.7309(6)	0.033(3)
O(29)	0.8730(9)	0.7167(5)	0.7596(4)	0.046(2)
C(210)	0.798(1)	0.3791(7)	0.6935(5)	0.027(2)
O(210)	0.8360(8)	0.3102(5)	0.7094(4)	0.040(2)
C(211)	0.553(1)	0.4559(6)	0.6807(5)	0.025(2)
O(211)	0.4432(8)	0.4355(5)	0.6845(4)	0.041(2)
C(212)	0.749(1)	0.5272(6)	0.5782(5)	0.025(2)
O(212)	0.7498(8)	0.5519(5)	0.5210(4)	0.035(2)
C(213)	0.519(1)	0.2195(6)	1.0178(5)	0.024(2)
O(213)	0.5489(8)	0.2216(5)	1.0653(4)	0.043(2)

C(214)	0.397(1)	0.0959(6)	0.9913(5)	0.023(2)
O(214)	0.3515(8)	0.0261(5)	1.0174(4)	0.035(2)
C(215)	0.316(1)	0.2539(6)	0.9230(5)	0.025(2)
O(215)	0.2164(9)	0.2827(5)	0.9103(4)	0.043(2)
C(216)	0.596(1)	0.1716(7)	0.8920(6)	0.032(3)
O(216)	0.6757(9)	0.1506(5)	0.8553(4)	0.047(2)
C(217)	1.150(1)	0.6454(8)	0.6381(6)	0.040(3)
O(217)	1.155(1)	0.6956(6)	0.6642(5)	0.059(3)
C(218)	1.315(1)	0.5878(8)	0.5560(6)	0.039(3)
O(218)	1.427(1)	0.5968(6)	0.5314(5)	0.059(3)
C(219)	1.070(1)	0.5994(7)	0.5222(5)	0.029(3)
O(219)	1.0306(8)	0.6156(5)	0.4733(4)	0.043(2)
C(220)	1.154(1)	0.4565(8)	0.6394(6)	0.036(3)
O(220)	1.1641(9)	0.3827(6)	0.6640(4)	0.049(2)

THERMAL PARAMETERS FOR $H_2Si_3Co_6(CO)_{20}$

MOLECULE ONE

ATOM	U11	U22	U33	U23	U13	U12
Co(11)	0.0149(7)	0.0150(6)	0.0150(7)	-0.0026(5)	-0.0037(6)	-0.0018(5)
Co(12)	0.0212(8)	0.0112(6)	0.0166(7)	-0.0022(5)	-0.0060(6)	-0.0011(5)
Co(13)	0.0182(8)	0.0170(7)	0.0206(7)	-0.0080(6)	-0.0027(6)	-0.0007(6)
Co(14)	0.0176(7)	0.0135(6)	0.0161(7)	-0.0049(5)	-0.0040(6)	-0.0020(5)
Co(15)	0.0286(9)	0.0263(8)	0.0186(7)	-0.0083(6)	0.0036(6)	-0.0054(6)
Co(16)	0.0267(9)	0.0200(7)	0.0192(7)	-0.0023(6)	-0.0008(6)	-0.0052(6)
Si(11)	0.018(2)	0.011(1)	0.015(1)	-0.004(1)	-0.005(1)	0.001(1)
Si(12)	0.022(2)	0.015(1)	0.015(1)	-0.004(1)	-0.002(1)	-0.002(1)
Si(13)	0.021(2)	0.014(1)	0.015(1)	-0.002(1)	-0.001(1)	-0.003(1)

MOLECULE TWO

Co(21)	0.0261(8)	0.0138(7)	0.0159(7)	-0.0032(5)	-0.0012(6)	0.0011(6)
Co(22)	0.0250(8)	0.0144(7)	0.0140(7)	-0.0010(5)	-0.0036(6)	-0.0028(6)
Co(23)	0.0279(8)	0.0099(6)	0.0150(7)	-0.0016(5)	-0.0011(6)	-0.0007(6)
Co(24)	0.0214(8)	0.0117(6)	0.0143(7)	-0.0034(5)	-0.0024(6)	-0.0013(5)
Co(25)	0.0292(8)	0.0134(7)	0.0148(7)	-0.0018(5)	-0.0003(6)	-0.0037(6)
Co(26)	0.0217(8)	0.0205(7)	0.0258(8)	-0.0047(6)	0.0000(7)	-0.0043(6)
Si(21)	0.023(2)	0.010(1)	0.015(1)	-0.001(1)	-0.003(1)	-0.002(1)
Si(22)	0.021(2)	0.014(1)	0.017(1)	-0.002(1)	-0.004(1)	0.000(1)
Si(23)	0.023(2)	0.015(1)	0.015(1)	-0.003(1)	-0.003(1)	-0.002(1)

SELECTED BOND LENGTHS AND ANGLES FOR $H_2Si_3Co_6(CO)_{20}$

BOND LENGTHS (Å) FOR MOLECULE ONE

Co(11)---Co(12)	2.618(2)	Co(15)---C(116)	1.77(1)
Co(11)---Si(11)	2.281(3)	Co(16)---Si(13)	2.371(3)
Co(11)---Si(12)	2.298(3)	Co(16)---C(117)	1.82(1)
Co(11)---C(11)	1.78(1)	Co(16)---C(118)	1.79(1)
Co(11)---C(12)	1.76(1)	Co(16)---C(119)	1.77(2)
Co(11)---C(13)	1.78(1)	Co(16)---C(120)	1.81(1)
Co(12)---Si(11)	2.322(3)	C(11) ---O(11)	1.14(1)
Co(12)---Si(12)	2.287(3)	C(12) ---O(12)	1.16(1)
Co(12)---C(14)	1.75(1)	C(13) ---O(13)	1.15(1)
Co(12)---C(15)	1.80(1)	C(14) ---O(14)	1.16(2)
Co(12)---C(16)	1.79(1)	C(15) ---O(15)	1.15(2)
Co(13)---Co(14)	2.614(2)	C(16) ---O(16)	1.15(1)
Co(13)---Si(11)	2.291(3)	C(17) ---O(17)	1.15(1)
Co(13)---Si(13)	2.281(3)	C(18) ---O(18)	1.13(1)
Co(13)---C(17)	1.81(1)	C(19) ---O(19)	1.15(2)
Co(13)---C(18)	1.81(1)	C(110)---O(110)	1.13(1)
Co(13)---C(19)	1.75(1)	C(111)---O(111)	1.15(1)
Co(14)---Si(11)	2.292(3)	C(112)---O(112)	1.13(1)
Co(14)---Si(13)	2.314(3)	C(113)---O(113)	1.15(2)
Co(14)---C(110)	1.77(1)	C(114)---O(114)	1.15(2)
Co(14)---C(111)	1.791(9)	C(115)---O(115)	1.17(2)
Co(14)---C(112)	1.81(1)	C(116)---O(116)	1.16(2)
Co(15)---Si(12)	2.375(3)	C(117)---O(117)	1.11(2)
Co(15)---C(113)	1.81(1)	C(118)---O(118)	1.14(2)
Co(15)---C(114)	1.78(1)	C(119)---O(119)	1.14(2)
Co(15)---C(115)	1.77(1)	C(120)---O(120)	1.14(1)

BOND ANGLES (°) FOR MOLECULE ONE

Co(12)-Co(11)-Si(11)	56.1(1)	Si(13)-Co(14)-C(112)	95.1(3)
Co(12)-Co(11)-Si(12)	55.0(1)	C(110)-Co(14)-C(111)	101.5(5)
Co(12)-Co(11)-C(11)	110.5(3)	C(110)-Co(14)-C(112)	108.9(5)
Co(12)-Co(11)-C(12)	139.1(4)	C(111)-Co(14)-C(112)	94.1(5)
Co(12)-Co(11)-C(13)	92.6(3)	Si(12)-Co(15)-C(113)	94.2(4)
Si(11)-Co(11)-Si(12)	77.4(1)	Si(12)-Co(15)-C(114)	173.0(5)
Si(11)-Co(11)-C(11)	88.3(4)	Si(12)-Co(15)-C(115)	80.5(4)
Si(11)-Co(11)-C(12)	102.3(4)	Si(12)-Co(15)-C(116)	79.8(4)
Si(11)-Co(11)-C(13)	147.1(3)	C(113)-Co(15)-C(114)	92.8(6)
Si(12)-Co(11)-C(11)	163.8(3)	C(113)-Co(15)-C(115)	119.3(6)
Si(12)-Co(11)-C(12)	88.6(3)	C(113)-Co(15)-C(116)	117.4(6)
Si(12)-Co(11)-C(13)	93.3(3)	C(114)-Co(15)-C(115)	96.2(5)
C(11) -Co(11)-C(12)	102.1(5)	C(114)-Co(15)-C(116)	96.9(6)
C(11) -Co(11)-C(13)	94.7(5)	C(115)-Co(15)-C(116)	120.8(6)

C(12) -Co(11)-C(13)	109.0(5)	Si(13)-Co(16)-C(117)	96.8(3)
Co(11)-Co(12)-Si(11)	54.6(1)	Si(13)-Co(16)-C(118)	80.8(3)
Co(11)-Co(12)-Si(12)	55.4(1)	Si(13)-Co(16)-C(119)	78.9(3)
Co(11)-Co(12)-C(14)	142.8(4)	Si(13)-Co(16)-C(120)	168.2(4)
Co(11)-Co(12)-C(15)	97.5(3)	C(117)-Co(16)-C(118)	116.3(6)
Co(11)-Co(12)-C(16)	105.6(3)	C(117)-Co(16)-C(119)	119.2(6)
Si(11)-Co(12)-Si(12)	76.8(1)	C(117)-Co(16)-C(120)	95.0(5)
Si(11)-Co(12)-C(14)	97.6(3)	C(118)-Co(16)-C(119)	122.5(6)
Si(11)-Co(12)-C(15)	87.6(3)	C(118)-Co(16)-C(120)	94.0(5)
Si(11)-Co(12)-C(16)	160.2(3)	C(119)-Co(16)-C(120)	95.3(6)
Si(12)-Co(12)-C(14)	97.8(4)	Co(11)-Si(11)-Co(12)	69.3(1)
Si(12)-Co(12)-C(15)	152.9(3)	Co(11)-Si(11)-Co(13)	137.2(1)
Si(12)-Co(12)-C(16)	91.7(4)	Co(11)-Si(11)-Co(14)	130.4(1)
C(14) -Co(12)-C(15)	106.2(5)	Co(12)-Si(11)-Co(13)	126.6(1)
C(14) -Co(12)-C(16)	99.9(5)	Co(12)-Si(11)-Co(14)	136.4(1)
C(15) -Co(12)-C(16)	96.1(5)	Co(13)-Si(11)-Co(14)	69.5(1)
Co(14)-Co(13)-Si(11)	55.3(1)	Co(11)-Si(12)-Co(12)	69.6(1)
Co(14)-Co(13)-Si(13)	55.9(1)	Co(11)-Si(12)-Co(15)	128.5(1)
Co(14)-Co(13)-C(17)	96.1(4)	Co(12)-Si(12)-Co(15)	128.1(1)
Co(14)-Co(13)-C(18)	101.1(4)	Co(13)-Si(13)-Co(14)	69.3(1)
Co(14)-Co(13)-C(19)	147.2(4)	Co(13)-Si(13)-Co(16)	128.8(1)
Si(11)-Co(13)-Si(13)	77.0(1)	Co(14)-Si(13)-Co(16)	129.4(2)
Si(11)-Co(13)-C(17)	85.6(3)	Co(11)-C(11) -O(11)	178.0(9)
Si(11)-Co(13)-C(18)	156.3(4)	Co(11)-C(12) -O(12)	176(1)
Si(11)-Co(13)-C(19)	100.4(4)	Co(11)-C(13) -O(13)	176(1)
Si(13)-Co(13)-C(17)	152.0(4)	Co(12)-C(14) -O(14)	176(1)
Si(13)-Co(13)-C(18)	90.1(3)	Co(12)-C(15) -O(15)	178(1)
Si(13)-Co(13)-C(19)	100.5(4)	Co(12)-C(16) -O(16)	175.5(9)
C(17) -Co(13)-C(18)	97.9(5)	Co(13)-C(17) -O(17)	178(1)
C(17) -Co(13)-C(19)	104.1(6)	Co(13)-C(18) -O(18)	178.9(9)
C(18) -Co(13)-C(19)	101.4(5)	Co(13)-C(19) -O(19)	176(1)
Co(13)-Co(14)-Si(11)	55.2(1)	Co(14)-C(110)-O(110)	175.0(9)
Co(13)-Co(14)-Si(13)	54.7(1)	Co(14)-C(111)-O(111)	172(1)
Co(13)-Co(14)-C(110)	137.2(4)	Co(14)-C(112)-O(112)	173.7(8)
Co(13)-Co(14)-C(111)	111.4(4)	Co(15)-C(113)-O(113)	172(1)
Co(13)-Co(14)-C(112)	95.6(4)	Co(15)-C(114)-O(114)	177(1)
Si(11)-Co(14)-Si(13)	76.3(1)	Co(15)-C(115)-O(115)	178(1)
Si(11)-Co(14)-C(110)	100.2(4)	Co(15)-C(116)-O(116)	178(1)
Si(11)-Co(14)-C(111)	89.2(4)	Co(16)-C(117)-O(117)	174.9(8)
Si(11)-Co(14)-C(112)	149.3(4)	Co(16)-C(118)-O(118)	177(1)
Si(13)-Co(14)-C(110)	87.8(3)	Co(16)-C(119)-O(119)	178.4(9)
Si(13)-Co(14)-C(111)	164.1(4)	Co(16)-C(120)-O(120)	177(1)

BOND LENGTHS (Å) FOR MOLECULE TWO

Co(21)---Co(22)	2.616(2)	Co(25)---C(216)	1.77(1)
Co(21)---Si(21)	2.316(3)	Co(26)---Si(23)	2.360(3)
Co(21)---Si(22)	2.285(3)	Co(26)---C(217)	1.76(2)

Co(21)---C(21)	1.81(1)	Co(26)---C(218)	1.79(1)
Co(21)---C(22)	1.78(1)	Co(26)---C(219)	1.81(1)
Co(21)---C(23)	1.81(1)	Co(26)---C(220)	1.78(1)
Co(22)---Si(21)	2.307(3)	C(21) ---O(21)	1.14(1)
Co(22)---Si(22)	2.312(3)	C(22) ---O(22)	1.15(2)
Co(22)---C(24)	1.76(1)	C(23) ---O(23)	1.15(1)
Co(22)---C(25)	1.79(1)	C(24) ---O(24)	1.15(2)
Co(22)---C(26)	1.81(1)	C(25) ---O(25)	1.14(2)
Co(23)---Co(24)	2.602(2)	C(26) ---O(26)	1.15(1)
Co(23)---Si(21)	2.301(2)	C(27) ---O(27)	1.14(1)
Co(23)---Si(23)	2.283(3)	C(28) ---O(28)	1.14(1)
Co(23)---C(27)	1.80(1)	C(29) ---O(29)	1.15(2)
Co(23)---C(28)	1.813(9)	C(210)---O(210)	1.14(1)
Co(23)---C(29)	1.75(1)	C(211)---O(211)	1.14(1)
Co(24)---Si(21)	2.315(3)	C(212)---O(212)	1.15(1)
Co(24)---Si(23)	2.304(3)	C(213)---O(213)	1.14(2)
Co(24)---C(210)	1.77(1)	C(214)---O(214)	1.14(1)
Co(24)---C(211)	1.78(1)	C(215)---O(215)	1.13(1)
Co(24)---C(212)	1.80(1)	C(216)---O(216)	1.16(2)
Co(25)---Si(22)	2.354(3)	C(217)---O(217)	1.16(2)
Co(25)---C(213)	1.80(1)	C(218)---O(218)	1.14(2)
Co(25)---C(214)	1.815(9)	C(219)---O(219)	1.14(2)
Co(25)---C(215)	1.80(1)	C(220)---O(220)	1.15(1)

BOND ANGLES (°) FOR MOLECULE TWO

Co(22)-Co(21)-Si(21)	55.4(1)	Si(23)-Co(24)-C(212)	96.5(4)
Co(22)-Co(21)-Si(22)	55.8(1)	C(210)-Co(24)-C(211)	102.4(5)
Co(22)-Co(21)-C(21)	98.9(4)	C(210)-Co(24)-C(212)	109.2(5)
Co(22)-Co(21)-C(22)	143.8(4)	C(211)-Co(24)-C(212)	93.2(5)
Co(22)-Co(21)-C(23)	100.7(3)	Si(22)-Co(25)-C(213)	95.1(3)
Si(21)-Co(21)-Si(22)	76.3(1)	Si(22)-Co(25)-C(214)	168.9(4)
Si(21)-Co(21)-C(21)	87.5(3)	Si(22)-Co(25)-C(215)	81.5(3)
Si(21)-Co(21)-C(22)	98.6(3)	Si(22)-Co(25)-C(216)	80.2(3)
Si(21)-Co(21)-C(23)	156.0(4)	C(213)-Co(25)-C(214)	95.7(5)
Si(22)-Co(21)-C(21)	154.6(4)	C(213)-Co(25)-C(215)	116.7(5)
Si(22)-Co(21)-C(22)	96.6(4)	C(213)-Co(25)-C(216)	116.9(5)
Si(22)-Co(21)-C(23)	89.6(4)	C(214)-Co(25)-C(215)	96.1(5)
C(21) -Co(21)-C(22)	105.1(5)	C(214)-Co(25)-C(216)	92.5(5)
C(21) -Co(21)-C(23)	98.3(5)	C(215)-Co(25)-C(216)	124.4(6)
C(22) -Co(21)-C(23)	102.2(5)	Si(23)-Co(26)-C(217)	78.9(4)
Co(21)-Co(22)-Si(21)	55.7(1)	Si(23)-Co(26)-C(218)	167.6(4)
Co(21)-Co(22)-Si(22)	54.8(1)	Si(23)-Co(26)-C(219)	95.8(3)
Co(21)-Co(22)-C(24)	137.3(4)	Si(23)-Co(26)-C(220)	81.1(4)
Co(21)-Co(22)-C(25)	113.0(3)	C(217)-Co(26)-C(218)	94.6(6)
Co(21)-Co(22)-C(26)	91.9(3)	C(217)-Co(26)-C(219)	121.0(5)
Si(21)-Co(22)-Si(22)	75.9(1)	C(217)-Co(26)-C(220)	122.3(6)
Si(21)-Co(22)-C(24)	104.1(4)	C(218)-Co(26)-C(219)	96.5(5)

Si(21)-Co(22)-C(25)	88.4(3)	C(218)-Co(26)-C(220)	93.8(5)
Si(21)-Co(22)-C(26)	144.5(3)	C(219)-Co(26)-C(220)	114.4(6)
Si(22)-Co(22)-C(24)	85.3(4)	Co(21)-Si(21)-Co(22)	68.9(1)
Si(22)-Co(22)-C(25)	163.9(3)	Co(21)-Si(21)-Co(23)	128.2(1)
Si(22)-Co(22)-C(26)	97.9(4)	Co(21)-Si(21)-Co(24)	136.8(2)
C(24) -Co(22)-C(25)	102.3(5)	Co(22)-Si(21)-Co(23)	137.0(2)
C(24) -Co(22)-C(26)	110.2(5)	Co(22)-Si(21)-Co(24)	130.2(1)
C(25) -Co(22)-C(26)	92.7(5)	Co(23)-Si(21)-Co(24)	68.6(1)
Co(24)-Co(23)-Si(21)	55.9(1)	Co(21)-Si(22)-Co(22)	69.4(1)
Co(24)-Co(23)-Si(23)	55.8(1)	Co(21)-Si(22)-Co(25)	130.4(1)
Co(24)-Co(23)-C(27)	95.1(4)	Co(22)-Si(22)-Co(25)	127.7(1)
Co(24)-Co(23)-C(28)	103.7(4)	Co(23)-Si(23)-Co(24)	69.1(1)
Co(24)-Co(23)-C(29)	143.5(3)	Co(23)-Si(23)-Co(26)	128.5(1)
Si(21)-Co(23)-Si(23)	76.4(1)	Co(24)-Si(23)-Co(26)	130.5(2)
Si(21)-Co(23)-C(27)	87.9(3)	Co(21)-C(21) -O(21)	179.5(9)
Si(21)-Co(23)-C(28)	159.4(4)	Co(21)-C(22) -O(22)	175(1)
Si(21)-Co(23)-C(29)	96.0(3)	Co(21)-C(23) -O(23)	179.2(9)
Si(23)-Co(23)-C(27)	150.9(4)	Co(22)-C(24) -O(24)	175(1)
Si(23)-Co(23)-C(28)	89.7(3)	Co(22)-C(25) -O(25)	173.6(9)
Si(23)-Co(23)-C(29)	98.1(4)	Co(22)-C(26) -O(26)	173.8(9)
C(27) -Co(23)-C(28)	97.7(4)	Co(23)-C(27) -O(27)	175(1)
C(27) -Co(23)-C(29)	107.9(6)	Co(23)-C(28) -O(28)	177(1)
C(28) -Co(23)-C(29)	101.0(5)	Co(23)-C(29) -O(29)	176.7(8)
Co(23)-Co(24)-Si(21)	55.4(1)	Co(24)-C(210)-O(210)	175(1)
Co(23)-Co(24)-Si(23)	55.0(1)	Co(24)-C(211)-O(211)	174(1)
Co(23)-Co(24)-C(210)	137.5(4)	Co(24)-C(212)-O(212)	173(1)
Co(23)-Co(24)-C(211)	110.1(4)	Co(25)-C(213)-O(213)	174.9(9)
Co(23)-Co(24)-C(212)	95.8(4)	Co(25)-C(214)-O(214)	177(1)
Si(21)-Co(24)-Si(23)	75.7(1)	Co(25)-C(215)-O(215)	178.1(8)
Si(21)-Co(24)-C(210)	100.0(4)	Co(25)-C(216)-O(216)	177(1)
Si(21)-Co(24)-C(211)	88.9(4)	Co(26)-C(217)-O(217)	178(1)
Si(21)-Co(24)-C(212)	149.6(4)	Co(26)-C(218)-O(218)	177(1)
Si(23)-Co(24)-C(210)	87.6(4)	Co(26)-C(219)-O(219)	176(1)
Si(23)-Co(24)-C(211)	163.0(4)	Co(26)-C(220)-O(220)	177(1)

APPENDIX TWO

FINAL POSITIONAL AND EQUIVALENT THERMAL PARAMETERS FOR $[Fe(THF)_4(H_2O)_2][FeCo_3(CO)_{12}]_2.4THF$

ATOM	X/A	Y/B	Z/C	Ueq/U11
Co(1)	0.4291(2)	0.0000(0)	0.2583(3)	0.044
Co(2)	0.3654(1)	0.0928(3)	0.3886(2)	0.053
Fe(1)	0.3077(2)	0.0000(0)	0.2367(3)	0.074
Fe(2)	0.0000(0)	0.0000(0)	0.0000(0)	0.050
C(1)	0.513(1)	0.000(0)	0.282(2)	0.045(7)
O(1)	0.5706(9)	0.0000(0)	0.290(2)	0.055(5)
C(2)	0.424(1)	0.000(0)	0.120(2)	0.041(7)
O(2)	0.424(1)	0.000(0)	0.029(2)	0.070(6)
C(3)	0.293(1)	0.097(2)	0.146(2)	0.062(6)
O(3)	0.287(1)	0.163(2)	0.087(2)	0.097(6)
C(4)	0.231(2)	0.000(0)	0.286(4)	0.11(2)
O(4)	0.179(2)	0.000(0)	0.313(3)	0.12(1)
C(5)	0.319(2)	0.000(0)	0.473(3)	0.07(1)
O(5)	0.277(1)	0.000(0)	0.535(2)	0.089(8)
C(6)	0.408(1)	0.154(2)	0.493(2)	0.057(6)
O(6)	0.4340(8)	0.196(1)	0.559(1)	0.083(5)
C(7)	0.300(2)	0.165(2)	0.372(2)	0.095(9)
O(7)	0.261(1)	0.235(2)	0.366(2)	0.097(6)
C(8)	0.410(1)	0.148(2)	0.270(2)	0.066(7)
O(8)	0.4255(8)	0.218(1)	0.225(1)	0.075(5)
O(11)	0.062(1)	0.000(0)	-0.126(2)	0.058(6)
C(31)	0.069(1)	0.085(2)	0.617(2)	0.063(6)
O(33)	0.0451(9)	0.0000(0)	0.663(2)	0.014(5)
C(33)	0.108(1)	0.054(2)	-0.478(2)	0.078(7)
O(21)	0.0567(6)	0.110(1)	0.078(1)	0.052(4)
C(21)	0.057(2)	0.130(3)	0.184(3)	0.11(1)
C(22)	0.108(2)	0.217(3)	0.203(3)	0.13(1)
C(23)	0.109(2)	0.259(3)	0.108(3)	0.14(1)
C(24)	0.097(2)	0.182(4)	0.023(4)	0.15(1)
O(41)	0.191(1)	0.000(0)	0.874(2)	0.091(8)
C(41)	0.287(2)	0.000(0)	0.806(3)	0.08(1)
C(42)	0.218(1)	0.087(2)	0.837(2)	0.084(8)
C(43)	0.271(2)	0.084(3)	0.766(3)	0.14(1)

THERMAL PARAMETERS FOR $[Fe(THF)_4(H_2O)_2][FeCo_3(CO)_{12}]_2.4THF$

ATOM	U11	U22	U33	U23	U13	U12
Co(1)	0.035(2)	0.053(3)	0.043(2)	0.000(0)	0.012(2)	0.000(0)
Co(2)	0.036(2)	0.088(3)	0.036(2)	-0.004(2)	0.004(1)	0.020(2)
Fe(1)	0.038(2)	0.144(5)	0.042(3)	0.000(0)	0.006(2)	0.000(0)
Fe(2)	0.016(3)	0.109(6)	0.026(3)	0.000(0)	0.005(2)	0.000(0)

SELECTED BOND LENGTHS AND ANGLES FOR $[FE(THF)_4(H_2O)_2][FECO_3(CO)_{12}]_2.4THF$

BOND LENGTHS (Å) FOR $[Fe(THF)_4(H_2O)_2][FeCo_3(CO)_{12}]_2.4THF$

Co(1)	---Co(2)	2.502(4)	C(3)	---O(3)	1.17(3)
Co(1)	---Fe(1)	2.533(5)	C(4)	---O(4)	1.15(5)
Co(1)	---C(1)	1.76(3)	C(5)	---O(5)	1.22(4)
Co(1)	---C(2)	1.74(3)	C(6)	---O(6)	1.13(2)
Co(1)	---C(8)	2.05(3)	C(7)	---O(7)	1.24(3)
Co(2)	---Co(2)	2.515(7)	C(8)	---O(8)	1.17(3)
Co(2)	---Fe(1)	2.551(5)	C(31)	---O(33)	1.39(3)
Co(2)	---C(5)	1.93(3)	C(31)	---C(33)	1.54(3)
Co(2)	---C(6)	1.76(2)	C(33)	---C(33)	1.47(5)
Co(2)	---C(7)	1.69(3)	O(21)	---C(21)	1.37(3)
Co(2)	---C(8)	1.95(3)	O(21)	---C(24)	1.49(5)
Fe(1)	---C(3)	1.76(3)	C(21)	---C(22)	1.60(5)
Fe(1)	---C(4)	1.75(5)	C(22)	---C(23)	1.34(5)
Fe(2)	---O(11)	2.10(2)	C(23)	---C(24)	1.52(5)
Fe(2)	---O(21)	2.12(1)	O(41)	---C(42)	1.40(3)
C(1)	---O(1)	1.20(3)	C(41)	---C(42)	1.92(4)
C(2)	---O(2)	1.16(3)	C(41)	---C(43)	1.28(4)
C(42)	---C(43)	1.45(5)			

BOND ANGLES (°) FOR $[Fe(THF)_4(H_2O)_2][FeCo_3(CO)_{12}]_2.4THF$

Co(2)	-Co(1)	-Fe(1)	60.9(1)	Co(2)	-Fe(1)	-Co(2)	59.1(1)
Co(2)	-Co(1)	-C(1)	116.1(8)	Co(2)	-Fe(1)	-C(3)	100.6(8)
Co(2)	-Co(1)	-C(2)	130.3(7)	Co(2)	-Fe(1)	-C(4)	98(1)
Co(2)	-Co(1)	-C(8)	49.5(7)	C(3)	-Fe(1)	-C(4)	95(1)
Co(2)	-Co(1)	-Co(2)	60.4(2)	O(11)	-Fe(2)	-O(21)	90.4(5)
Fe(1)	-Co(1)	-C(1)	176.3(9)	Co(1)	-C(1)	-O(1)	174(2)
Fe(1)	-Co(1)	-C(2)	82.7(9)	Co(1)	-C(2)	-O(2)	176(3)
Fe(1)	-Co(1)	-C(8)	79.3(7)	Fe(1)	-C(3)	-O(3)	176(2)
C(1)	-Co(1)	-C(2)	101(1)	Fe(1)	-C(4)	-O(4)	176(5)

C(1)	-Co(1) -C(8)	100.3(7)	
C(2)	-Co(1) -C(8)	94.0(7)	
Co(1)	-Co(2) -Fe(1)	60.2(1)	
Co(1)	-Co(2) -C(5)	109.2(7)	
Co(1)	-Co(2) -C(6)	117.6(7)	
Co(1)	-Co(2) -C(7)	131(1)	
Co(1)	-Co(2) -C(8)	53.0(8)	
Fe(1)	-Co(2) -C(5)	82.3(9)	
Fe(1)	-Co(2) -C(6)	177.7(7)	
Fe(1)	-Co(2) -C(7)	80(1)	
Fe(1)	-Co(2) -C(8)	80.6(7)	
C(5)	-Co(2) -C(6)	98(1)	
C(5)	-Co(2) -C(7)	91(1)	
C(5)	-Co(2) -C(8)	160(1)	
C(6)	-Co(2) -C(7)	101(1)	
C(6)	-Co(2) -C(8)	98(1)	
C(7)	-Co(2) -C(8)	95(1)	
Co(1)	-Fe(1) -Co(2)	59.0(1)	
Co(1)	-Fe(1) -C(3)	102.1(8)	
Co(1)	-Fe(1) -C(4)	153(2)	
Co(2)	-C(5) -Co(2)	81(1)	
Co(2)	-C(5) -O(5)	139.0(8)	
Co(2)	-C(6) -O(6)	177(2)	
Co(2)	-C(7) -O(7)	165(3)	
Co(1)	-C(8) -Co(2)	77(1)	
Co(1)	-C(8) -O(8)	135(2)	
Co(2)	-C(8) -O(8)	147(2)	
O(33)	-C(31) -C(33)	108(2)	
Fe(2)	-O(21) -C(21)	124(2)	
Fe(2)	-O(21) -C(24)	123(2)	
C(21)	-O(21) -C(24)	111(3)	
O(21)	-C(21) -C(22)	105(3)	
C(21)	-C(22) -C(23)	102(3)	
C(22)	-C(23) -C(24)	109(4)	
O(21)	-C(24) -C(23)	101(3)	
C(42)	-C(41) -C(43)	49(2)	
O(41)	-C(42) -C(41)	82(2)	
O(41)	-C(42) -C(43)	120(3)	
C(41)	-C(42) -C(43)	41(2)	
C(41)	-C(43) -C(42)	88(4)	

APPENDIX THREE

FINAL POSITIONAL AND EQUIVALENT THERMAL PARAMETERS FOR $[Cp(CO)_2FeGe]_2Fe_3(CO)_9$

ATOM	X/A	Y/B	Z/C	Ueq
Ge(1)	0.9903(1)	0.6159(1)	0.1477(1)	0.021
Ge(2)	1.2135(1)	0.8540(1)	0.1024(1)	0.022
Fe(1)	0.9816(1)	0.8254(2)	0.1091(1)	0.023
Fe(2)	1.1575(1)	0.6250(2)	0.0920(1)	0.022
Fe(3)	1.1682(1)	0.7548(2)	0.1764(1)	0.020
Fe(4)	0.8492(2)	0.4544(2)	0.1752(1)	0.027
Fe(5)	1.3633(2)	1.0038(2)	0.0726(1)	0.027
C(11)	0.994(1)	1.000(1)	0.0974(5)	0.045
O(11)	0.9873(9)	1.113(1)	0.0911(5)	0.074
C(12)	0.838(1)	0.844(1)	0.1440(5)	0.041
O(12)	0.7477(8)	0.859(1)	0.1653(4)	0.061
C(13)	0.904(1)	0.772(1)	0.0551(4)	0.030
O(13)	0.8470(8)	0.7361(9)	0.0216(3)	0.044
C(21)	1.250(1)	0.653(1)	0.0411(4)	0.028
O(21)	1.3072(8)	0.6591(9)	0.0063(3)	0.048
C(22)	1.054(1)	0.498(1)	0.0648(4)	0.024
O(22)	0.9930(8)	0.4156(8)	0.0460(3)	0.033
C(23)	1.276(1)	0.526(1)	0.1248(5)	0.034
O(23)	1.3502(9)	0.4581(9)	0.1452(3)	0.050
C(31)	1.339(1)	0.788(1)	0.1858(4)	0.028
O(31)	1.4514(8)	0.8023(9)	0.1941(3)	0.040
C(32)	1.096(1)	0.894(1)	0.2057(4)	0.028
O(32)	1.0535(8)	0.9812(9)	0.2266(3)	0.042
C(33)	1.1583(9)	0.640(1)	0.2239(4)	0.023
O(33)	1.1565(8)	0.5691(8)	0.2558(3)	0.036
C(41)	0.853(1)	0.534(1)	0.2304(5)	0.032
O(41)	0.8524(8)	0.585(1)	0.2668(3)	0.049
C(42)	0.991(1)	0.353(1)	0.1865(4)	0.034
O(42)	1.0819(9)	0.2859(9)	0.1938(3)	0.047
C(1)	0.6560(8)	0.385(1)	0.1818(3)	0.051
C(2)	0.7278(8)	0.290(1)	0.1560(3)	0.039
C(3)	0.7702(8)	0.353(1)	0.1144(3)	0.039
C(4)	0.7247(8)	0.487(1)	0.1145(3)	0.041
C(5)	0.6540(8)	0.507(1)	0.1561(3)	0.060
C(51)	1.289(1)	0.976(1)	0.0153(4)	0.033
O(51)	1.2449(8)	0.9588(9)	-0.0223(3)	0.041
C(52)	1.479(1)	0.872(1)	0.0713(4)	0.038
O(52)	1.5565(8)	0.787(1)	0.0698(3)	0.046
C(6)	1.2851(8)	1.1951(9)	0.0831(3)	0.042
C(7)	1.3127(8)	1.1338(9)	0.1277(3)	0.036
C(8)	1.4501(8)	1.1055(9)	0.1316(3)	0.044

C(9)	1.5075(8)	1.1492(9)	0.0894(3)	0.055
C(10)	1.4055(8)	1.2046(9)	0.0594(3)	0.050

FINAL POSITIONAL AND THERMAL PARAMETERS OF CALCULATED HYDROGEN ATOMS FOR $[Cp(CO)_2FeGe]_2Fe_3(CO)_9$

ATOM	X/A	Y/B	Z/C	U11
H(1)	0.6107(8)	0.368(1)	0.2151(3)	0.080
H(2)	0.7468(8)	0.188(1)	0.1662(3)	0.080
H(3)	0.8272(8)	0.307(1)	0.0874(3)	0.080
H(4)	0.7409(8)	0.561(1)	0.0876(3)	0.080
H(5)	0.6071(8)	0.599(1)	0.1665(3)	0.080
H(6)	1.1893(8)	1.2285(9)	0.0696(3)	0.080
H(7)	1.2416(8)	1.1125(9)	0.1540(3)	0.080
H(8)	1.5020(8)	1.0589(9)	0.1614(3)	0.080
H(9)	1.6106(8)	1.1417(9)	0.0815(3)	0.080
H(10)	1.4174(8)	1.2466(9)	0.0247(3)	0.080

THERMAL PARAMETERS FOR $[Cp(CO)_2FeGe]_2Fe_3(CO)_9$

ATOM	U11	U22	U33	U23	U13	U12
Ge(1)	0.0160(6)	0.0263(7)	0.0214(6)	-0.0025(5)	0.0008(5)	-0.0029(5)
Ge(2)	0.0187(6)	0.0235(7)	0.0224(7)	-0.0001(5)	0.0009(5)	-0.0027(5)
Fe(1)	0.0169(8)	0.0235(9)	0.0291(9)	-0.0018(7)	-0.0003(7)	0.0021(7)
Fe(2)	0.0179(8)	0.0221(9)	0.0247(9)	-0.0040(7)	0.0017(7)	-0.0018(7)
Fe(3)	0.0162(8)	0.0232(9)	0.0208(9)	0.0003(7)	-0.0020(6)	-0.0012(7)
Fe(4)	0.0205(9)	0.032(1)	0.028(1)	-0.0040(8)	0.0026(7)	-0.0087(7)
Fe(5)	0.0291(9)	0.0294(9)	0.0210(9)	-0.0006(8)	-0.0001(7)	-0.0100(8)
C(11)	0.029(7)	0.038(8)	0.07(1)	-0.005(7)	-0.026(7)	0.002(6)
O(11)	0.051(6)	0.025(6)	0.14(1)	0.007(7)	-0.037(7)	-0.001(5)
C(12)	0.048(8)	0.043(8)	0.032(8)	0.006(6)	-0.007(7)	0.013(7)
O(12)	0.025(5)	0.083(8)	0.077(8)	-0.028(6)	0.025(5)	0.007(5)
C(13)	0.014(6)	0.040(8)	0.037(8)	0.000(6)	-0.002(5)	0.013(5)
O(13)	0.046(6)	0.050(6)	0.036(6)	-0.004(5)	-0.019(5)	0.026(5)
C(21)	0.028(6)	0.027(7)	0.028(7)	-0.012(5)	0.005(6)	-0.014(5)
O(21)	0.045(5)	0.055(7)	0.045(6)	-0.006(5)	0.024(5)	-0.011(5)
C(22)	0.019(6)	0.032(7)	0.020(6)	0.005(6)	0.002(5)	0.009(5)
O(22)	0.036(5)	0.030(5)	0.034(5)	-0.011(4)	0.000(4)	-0.013(4)
C(23)	0.030(7)	0.029(7)	0.040(8)	-0.003(6)	-0.008(6)	0.014(6)
O(23)	0.044(6)	0.046(6)	0.059(7)	-0.015(5)	-0.024(5)	0.006(5)
C(31)	0.038(7)	0.017(6)	0.028(7)	0.000(5)	0.006(6)	0.004(5)
O(31)	0.018(5)	0.059(6)	0.042(5)	0.002(5)	-0.007(4)	-0.006(4)
C(32)	0.019(6)	0.033(7)	0.033(7)	-0.002(6)	0.000(5)	-0.010(5)
O(32)	0.045(5)	0.042(6)	0.040(6)	-0.017(5)	0.003(4)	0.004(5)

C(33)	0.012(5)	0.030(7)	0.026(7)	0.000(6)	-0.005(5)	-0.005(5)
O(33)	0.038(5)	0.041(5)	0.030(5)	0.010(4)	-0.005(4)	-0.007(4)
C(41)	0.014(6)	0.036(7)	0.047(8)	0.001(7)	0.002(6)	-0.010(5)
O(41)	0.032(5)	0.069(7)	0.047(6)	-0.023(5)	0.008(5)	0.002(5)
C(42)	0.027(7)	0.034(8)	0.041(8)	-0.007(6)	0.004(6)	-0.006(6)
O(42)	0.047(6)	0.039(6)	0.055(6)	0.002(5)	0.008(5)	0.014(5)
C(1)	0.030(7)	0.08(1)	0.044(9)	-0.016(9)	0.010(7)	-0.030(8)
C(2)	0.046(7)	0.040(8)	0.030(7)	-0.009(6)	-0.004(6)	-0.028(6)
C(3)	0.020(6)	0.06(1)	0.040(8)	-0.001(7)	-0.010(6)	-0.015(6)
C(4)	0.012(6)	0.06(1)	0.048(9)	0.008(7)	-0.010(6)	-0.016(6)
C(5)	0.039(9)	0.07(1)	0.07(1)	-0.010(9)	-0.003(8)	-0.004(8)
C(51)	0.036(7)	0.038(8)	0.026(7)	-0.003(6)	0.006(6)	-0.007(6)
O(51)	0.041(5)	0.051(6)	0.030(5)	-0.006(5)	-0.002(4)	0.004(5)
C(52)	0.040(8)	0.057(9)	0.019(7)	-0.004(7)	0.010(6)	-0.037(7)
O(52)	0.021(5)	0.062(7)	0.054(6)	0.000(5)	0.000(4)	0.009(5)
C(6)	0.057(9)	0.033(7)	0.036(8)	-0.002(6)	-0.004(7)	-0.008(7)
C(7)	0.055(8)	0.016(7)	0.037(8)	-0.004(6)	-0.006(6)	-0.010(6)
C(8)	0.065(9)	0.034(8)	0.033(8)	-0.010(6)	-0.008(7)	-0.021(7)
C(9)	0.049(9)	0.06(1)	0.06(1)	-0.034(8)	0.020(8)	-0.050(8)
C(10)	0.08(1)	0.030(8)	0.038(9)	0.000(7)	0.010(8)	-0.024(8)

SELECTED BOND LENGTHS AND ANGLES FOR $[Cp(CO)_2FeGe]_2Fe_3(CO)_9$

BOND LENGTHS (Å) FOR $[Cp(CO)_2FeGe]_2Fe_3(CO)_9$

Ge(1)	---Fe(1)	2.367(2)	Fe(5)	---C(52)	1.77(2)
Ge(1)	---Fe(2)	2.365(2)	Fe(5)	---C(6)	2.101(8)
Ge(1)	---Fe(3)	2.391(2)	Fe(5)	---C(7)	2.113(9)
Ge(1)	---Fe(4)	2.316(2)	Fe(5)	---C(8)	2.115(9)
Ge(2)	---Fe(1)	2.382(2)	Fe(5)	---C(9)	2.103(9)
Ge(2)	---Fe(2)	2.380(2)	Fe(5)	---C(10)	2.094(9)
Ge(2)	---Fe(3)	2.383(2)	C(11)	---O(11)	1.15(2)
Ge(2)	---Fe(5)	2.319(2)	C(12)	---O(12)	1.13(1)
Fe(1)	---Fe(2)	2.742(2)	C(13)	---O(13)	1.15(1)
Fe(1)	---Fe(3)	2.717(2)	C(21)	---O(21)	1.17(1)
Fe(1)	---C(11)	1.79(1)	C(22)	---O(22)	1.15(1)
Fe(1)	---C(12)	1.80(1)	C(23)	---O(23)	1.15(1)
Fe(1)	---C(13)	1.77(1)	C(31)	---O(31)	1.16(1)
Fe(2)	---Fe(3)	2.719(2)	C(32)	---O(32)	1.14(1)
Fe(2)	---C(21)	1.78(1)	C(33)	---O(33)	1.15(1)
Fe(2)	---C(22)	1.80(1)	C(41)	---O(41)	1.15(1)
Fe(2)	---C(23)	1.78(1)	C(42)	---O(42)	1.15(1)
Fe(3)	---C(31)	1.77(1)	C(1)	---C(2)	1.42(0)
Fe(3)	---C(32)	1.80(1)	C(1)	---C(5)	1.42(0)
Fe(3)	---C(33)	1.78(1)	C(2)	---C(3)	1.42(0)
Fe(4)	---C(41)	1.75(1)	C(3)	---C(4)	1.42(0)
Fe(4)	---C(42)	1.78(1)	C(4)	---C(5)	1.42(0)

Fe(4)	---C(1)	2.092(8)	C(51)	---O(51)	1.15(1)
Fe(4)	---C(2)	2.111(9)	C(52)	---O(52)	1.16(2)
Fe(4)	---C(3)	2.124(9)	C(6)	---C(7)	1.42(0)
Fe(4)	---C(4)	2.112(9)	C(6)	---C(10)	1.42(0)
Fe(4)	---C(5)	2.092(9)	C(7)	---C(8)	1.42(0)
Fe(5)	---C(51)	1.78(1)	C(8)	---C(9)	1.42(0)
C(9)	---C(10)	1.42(0)			

BOND ANGLES (°) FOR $[Cp(CO)_2FeGe]_2Fe_3(CO)_9$

Fe(1)	-Ge(1)	-Fe(2)	70.8(1)	C(41)	-Fe(4)	-C(5)	95.8(4)
Fe(1)	-Ge(1)	-Fe(3)	69.6(1)	C(42)	-Fe(4)	-C(1)	123.1(5)
Fe(1)	-Ge(1)	-Fe(4)	139.8(1)	C(42)	-Fe(4)	-C(2)	93.2(5)
Fe(2)	-Ge(1)	-Fe(3)	69.7(1)	C(42)	-Fe(4)	-C(3)	98.3(5)
Fe(2)	-Ge(1)	-Fe(4)	136.2(1)	C(42)	-Fe(4)	-C(4)	133.1(5)
Fe(3)	-Ge(1)	-Fe(4)	139.4(1)	C(42)	-Fe(4)	-C(5)	159.5(5)
Fe(1)	-Ge(2)	-Fe(2)	70.3(1)	C(1)	-Fe(4)	-C(2)	39.5(2)
Fe(1)	-Ge(2)	-Fe(3)	69.5(1)	C(1)	-Fe(4)	-C(3)	66.0(3)
Fe(1)	-Ge(2)	-Fe(5)	140.3(1)	C(1)	-Fe(4)	-C(4)	66.3(3)
Fe(2)	-Ge(2)	-Fe(3)	69.6(1)	C(1)	-Fe(4)	-C(5)	39.7(2)
Fe(2)	-Ge(2)	-Fe(5)	137.4(1)	C(2)	-Fe(4)	-C(3)	39.2(2)
Fe(3)	-Ge(2)	-Fe(5)	138.1(1)	C(2)	-Fe(4)	-C(4)	65.9(3)
Ge(1)	-Fe(1)	-Ge(2)	97.3(1)	C(2)	-Fe(4)	-C(5)	66.3(3)
Ge(1)	-Fe(1)	-Fe(2)	54.6(1)	C(3)	-Fe(4)	-C(4)	39.2(2)
Ge(1)	-Fe(1)	-Fe(3)	55.6(1)	C(3)	-Fe(4)	-C(5)	66.0(3)
Ge(1)	-Fe(1)	-C(11)	162.4(5)	C(4)	-Fe(4)	-C(5)	39.5(2)
Ge(1)	-Fe(1)	-C(12)	81.7(4)	Ge(2)	-Fe(5)	-C(51)	88.6(4)
Ge(1)	-Fe(1)	-C(13)	97.8(4)	Ge(2)	-Fe(5)	-C(52)	87.9(3)
Ge(2)	-Fe(1)	-Fe(2)	54.8(1)	Ge(2)	-Fe(5)	-C(6)	106.4(3)
Ge(2)	-Fe(1)	-Fe(3)	55.3(1)	Ge(2)	-Fe(5)	-C(7)	87.0(3)
Ge(2)	-Fe(1)	-C(11)	77.8(4)	Ge(2)	-Fe(5)	-C(8)	106.3(3)
Ge(2)	-Fe(1)	-C(12)	148.5(4)	Ge(2)	-Fe(5)	-C(9)	145.6(3)
Ge(2)	-Fe(1)	-C(13)	111.7(4)	Ge(2)	-Fe(5)	-C(10)	146.0(3)
Fe(2)	-Fe(1)	-Fe(3)	59.7(1)	C(51)	-Fe(5)	-C(52)	96.8(6)
Fe(2)	-Fe(1)	-C(11)	129.3(4)	C(51)	-Fe(5)	-C(6)	97.2(5)
Fe(2)	-Fe(1)	-C(12)	136.0(4)	C(51)	-Fe(5)	-C(7)	131.5(5)
Fe(2)	-Fe(1)	-C(13)	83.9(3)	C(51)	-Fe(5)	-C(8)	159.9(5)
Fe(3)	-Fe(1)	-C(11)	109.4(4)	C(51)	-Fe(5)	-C(9)	125.1(5)
Fe(3)	-Fe(1)	-C(12)	101.3(4)	C(51)	-Fe(5)	-C(10)	93.9(5)
Fe(3)	-Fe(1)	-C(13)	142.7(4)	C(52)	-Fe(5)	-C(6)	160.2(4)
C(11)	-Fe(1)	-C(12)	93.7(6)	C(52)	-Fe(5)	-C(7)	131.2(4)
C(11)	-Fe(1)	-C(13)	99.7(6)	C(52)	-Fe(5)	-C(8)	97.2(4)
C(12)	-Fe(1)	-C(13)	99.5(5)	C(52)	-Fe(5)	-C(9)	94.2(4)
Ge(1)	-Fe(2)	-Ge(2)	97.4(1)	C(52)	-Fe(5)	-C(10)	125.3(4)
Ge(1)	-Fe(2)	-Fe(1)	54.6(1)	C(6)	-Fe(5)	-C(7)	39.4(2)
Ge(1)	-Fe(2)	-Fe(3)	55.6(1)	C(6)	-Fe(5)	-C(8)	66.1(3)
Ge(1)	-Fe(2)	-C(21)	165.0(4)	C(6)	-Fe(5)	-C(9)	66.3(3)
Ge(1)	-Fe(2)	-C(22)	80.6(3)	C(6)	-Fe(5)	-C(10)	39.6(2)

Ge(1)	-Fe(2)	-C(23)	96.7(4)
Ge(2)	-Fe(2)	-Fe(1)	54.9(1)
Ge(2)	-Fe(2)	-Fe(3)	55.2(1)
Ge(2)	-Fe(2)	-C(21)	79.6(3)
Ge(2)	-Fe(2)	-C(22)	150.0(4)
Ge(2)	-Fe(2)	-C(23)	108.6(4)
Fe(1)	-Fe(2)	-Fe(3)	59.7(1)
Fe(1)	-Fe(2)	-C(21)	113.5(4)
Fe(1)	-Fe(2)	-C(22)	102.9(3)
Fe(1)	-Fe(2)	-C(23)	137.9(4)
Fe(3)	-Fe(2)	-C(21)	129.6(3)
Fe(3)	-Fe(2)	-C(22)	135.6(3)
Fe(3)	-Fe(2)	-C(23)	79.0(4)
C(21)	-Fe(2)	-C(22)	94.6(5)
C(21)	-Fe(2)	-C(23)	98.2(6)
C(22)	-Fe(2)	-C(23)	101.3(5)
Ge(1)	-Fe(3)	-Ge(2)	96.6(1)
Ge(1)	-Fe(3)	-Fe(1)	54.8(1)
Ge(1)	-Fe(3)	-Fe(2)	54.7(1)
Ge(1)	-Fe(3)	-C(31)	151.4(4)
Ge(1)	-Fe(3)	-C(32)	107.0(3)
Ge(1)	-Fe(3)	-C(33)	79.2(3)
Ge(2)	-Fe(3)	-Fe(1)	55.2(1)
Ge(2)	-Fe(3)	-Fe(2)	55.1(1)
Ge(2)	-Fe(3)	-C(31)	80.1(4)
Ge(2)	-Fe(3)	-C(32)	100.4(4)
Ge(2)	-Fe(3)	-C(33)	162.8(4)
Fe(1)	-Fe(3)	-Fe(2)	60.6(1)
Fe(1)	-Fe(3)	-C(31)	134.4(4)
Fe(1)	-Fe(3)	-C(32)	80.5(4)
Fe(1)	-Fe(3)	-C(33)	129.7(3)
Fe(2)	-Fe(3)	-C(31)	102.9(4)
Fe(2)	-Fe(3)	-C(32)	140.9(4)
Fe(2)	-Fe(3)	-C(33)	110.6(4)
C(31)	-Fe(3)	-C(32)	101.5(5)
C(31)	-Fe(3)	-C(33)	95.6(5)
C(32)	-Fe(3)	-C(33)	96.8(5)
Ge(1)	-Fe(4)	-C(41)	89.5(4)
Ge(1)	-Fe(4)	-C(42)	87.4(4)
Ge(1)	-Fe(4)	-C(1)	148.7(3)
Ge(1)	-Fe(4)	-C(2)	145.0(2)
Ge(1)	-Fe(4)	-C(3)	106.1(2)
Ge(1)	-Fe(4)	-C(4)	88.4(2)
Ge(1)	-Fe(4)	-C(5)	109.1(3)
C(41)	-Fe(4)	-C(42)	96.4(6)
C(41)	-Fe(4)	-C(1)	93.3(4)
C(41)	-Fe(4)	-C(2)	125.1(4)
C(41)	-Fe(4)	-C(3)	159.0(4)
C(41)	-Fe(4)	-C(4)	130.2(5)
C(7)	-Fe(5)	-C(8)	39.3(2)
C(7)	-Fe(5)	-C(9)	66.0(3)
C(7)	-Fe(5)	-C(10)	66.2(3)
C(8)	-Fe(5)	-C(9)	39.3(2)
C(8)	-Fe(5)	-C(10)	66.2(3)
C(9)	-Fe(5)	-C(10)	39.5(2)
Fe(1)	-C(11)	-O(11)	172(1)
Fe(1)	-C(12)	-O(12)	178(1)
Fe(1)	-C(13)	-O(13)	176(1)
Fe(2)	-C(21)	-O(21)	173(1)
Fe(2)	-C(22)	-O(22)	176.5(9)
Fe(2)	-C(23)	-O(23)	177(1)
Fe(3)	-C(31)	-O(31)	175(1)
Fe(3)	-C(32)	-O(32)	176(1)
Fe(3)	-C(33)	-O(33)	176.6(9)
Fe(4)	-C(41)	-O(41)	178(1)
Fe(4)	-C(42)	-O(42)	179(1)
Fe(4)	-C(1)	-C(2)	71.0(3)
Fe(4)	-C(1)	-C(5)	70.2(3)
C(2)	-C(1)	-C(5)	108.00(0
Fe(4)	-C(2)	-C(1)	69.5(2)
Fe(4)	-C(2)	-C(3)	70.9(2)
C(1)	-C(2)	-C(3)	108.00(0
Fe(4)	-C(3)	-C(2)	69.9(2)
Fe(4)	-C(3)	-C(4)	70.0(3)
C(2)	-C(3)	-C(4)	108.00(0
Fe(4)	-C(4)	-C(3)	70.9(3)
Fe(4)	-C(4)	-C(5)	69.5(2)
C(3)	-C(4)	-C(5)	108.00(0
Fe(4)	-C(5)	-C(1)	70.1(3)
Fe(4)	-C(5)	-C(4)	71.0(2)
C(1)	-C(5)	-C(4)	108.00(0
Fe(5)	-C(51)	-O(51)	178(1)
Fe(5)	-C(52)	-O(52)	178(1)
Fe(5)	-C(6)	-C(7)	70.8(2)
Fe(5)	-C(6)	-C(10)	70.0(3)
C(7)	-C(6)	-C(10)	108.00(0
Fe(5)	-C(7)	-C(6)	69.8(2)
Fe(5)	-C(7)	-C(8)	70.4(2)
C(6)	-C(7)	-C(8)	108.00(0
Fe(5)	-C(8)	-C(7)	70.3(2)
Fe(5)	-C(8)	-C(9)	69.9(3)
C(7)	-C(8)	-C(9)	108.00(0
Fe(5)	-C(9)	-C(8)	70.8(3)
Fe(5)	-C(9)	-C(10)	69.9(2)
C(8)	-C(9)	-C(10)	108.00(0
Fe(5)	-C(10)	-C(6)	70.5(2)
Fe(5)	-C(10)	-C(9)	70.6(2)
C(6)	-C(10)	-C(9)	108.00(0

APPENDIX FOUR

FINAL POSITIONAL AND EQUIVALENT THERMAL PARAMETERS $(PhSi)_2Co_4(CO)_{11}$

ATOM	X/A	Y/B	Z/C	Ueq
Co(1)	0.1508(1)	0.2360(1)	0.3644(1)	0.015
Co(2)	-0.0611(1)	0.2752(1)	0.4556(1)	0.016
Co(3)	-0.2325(1)	0.2648(1)	0.3154(1)	0.016
Co(4)	-0.0101(1)	0.2222(1)	0.2167(1)	0.015
Si(1)	-0.0709(1)	0.1906(0)	0.3603(1)	0.015
Si(2)	-0.0091(1)	0.3081(0)	0.3101(1)	0.014
C(1)	0.1372(4)	0.2613(2)	0.4865(2)	0.020
O(1)	0.2058(3)	0.2661(1)	0.5510(2)	0.035
C(2)	0.2361(4)	0.1633(2)	0.3928(2)	0.021
O(2)	0.2955(3)	0.1198(1)	0.4135(2)	0.031
C(3)	0.2967(4)	0.2862(2)	0.3349(2)	0.019
O(3)	0.3914(3)	0.3165(1)	0.3172(2)	0.033
C(4)	-0.1205(4)	0.2286(2)	0.5490(2)	0.021
O(4)	-0.1527(3)	0.2005(1)	0.6104(2)	0.035
C(5)	-0.0531(4)	0.3542(2)	0.5008(2)	0.024
O(5)	-0.0413(3)	0.4013(1)	0.5325(2)	0.041
C(6)	-0.3604(4)	0.2038(2)	0.2941(3)	0.026
O(6)	-0.4447(3)	0.1685(1)	0.2771(2)	0.048
C(7)	-0.2925(4)	0.3220(2)	0.2348(3)	0.023
O(7)	-0.3338(3)	0.3550(1)	0.1811(2)	0.038
C(8)	-0.3031(4)	0.2957(2)	0.4184(3)	0.028
O(8)	-0.3799(3)	0.3155(1)	0.4705(2)	0.037
C(9)	-0.1157(4)	0.1586(2)	0.1730(2)	0.025
O(9)	-0.1837(3)	0.1195(1)	0.1461(2)	0.044
C(10)	0.1604(4)	0.1876(2)	0.2024(2)	0.025
O(10)	0.2597(3)	0.1621(2)	0.1807(2)	0.037
C(11)	-0.0111(4)	0.2770(2)	0.1237(2)	0.022
O(11)	-0.0123(3)	0.3099(1)	0.0644(2)	0.032
C(12)	-0.1196(3)	0.1087(1)	0.3897(2)	0.021
C(13)	-0.0390(3)	0.0596(1)	0.3568(2)	0.029
C(14)	-0.0797(3)	-0.0013(1)	0.3743(2)	0.039
C(15)	-0.2011(3)	-0.0132(1)	0.4246(2)	0.040
C(16)	-0.2817(3)	0.0360(1)	0.4575(2)	0.041
C(17)	-0.2410(3)	0.0969(1)	0.4401(2)	0.029
Hdum	-0.0881(3)	0.1559(1)	0.3762(2)	0.043(4)
C(18)	0.0205(2)	0.3911(1)	0.2762(2)	0.017
C(19)	0.1326(2)	0.4089(1)	0.2210(2)	0.022
C(20)	0.1503(2)	0.4711(1)	0.1981(2)	0.028
C(21)	0.0560(2)	0.5155(1)	0.2305(2)	0.032
C(22)	-0.0560(2)	0.4977(1)	0.2857(2)	0.032
C(23)	-0.0738(2)	0.4355(1)	0.3085(2)	0.026

Hdum	0.0068(2)	0.3429(1)	0.2938(2)	0.043(4)
C(24)	1.074(1)	0.0155(5)	0.932(1)	0.189
C(25)	0.819(1)	0.0259(5)	0.9237(7)	0.133
C(26)	0.937(1)	0.0267(5)	0.8724(8)	0.059
C(27)	1.175(2)	0.0024(8)	0.984(1)	0.116
C(28)	0.963(4)	0.0095(5)	0.977(1)	0.155

FINAL POSITIONAL AND THERMAL PARAMETERS OF CALCULATED HYDROGEN ATOMS $(PhSi)_2Co_4(CO)_{11}$

ATOM	X/A	Y/B	Z/C	U11
H(13)	0.0550(3)	0.0688(1)	0.3178(2)	0.043
H(14)	-0.0172(3)	-0.0394(1)	0.3488(2)	0.043
H(15)	-0.2326(3)	-0.0603(1)	0.4381(2)	0.043
H(16)	-0.3757(3)	0.0268(1)	0.4965(2)	0.043
H(17)	-0.3035(3)	0.1349(1)	0.4656(2)	0.043
H(23)	0.2056(2)	0.3746(1)	0.1959(2)	0.043
H(24)	0.2371(2)	0.4850(1)	0.1554(2)	0.043
H(25)	0.0697(2)	0.5637(1)	0.2128(2)	0.043
H(26)	-0.1290(2)	0.5321(1)	0.3108(2)	0.043
H(27)	-0.1605(2)	0.4217(1)	0.3513(2)	0.043

THERMAL PARAMETERS $(PhSi)_2Co_4(CO)_{11}$

ATOM	U11	U22	U33	U23	U13	U12
Co(1)	0.0121(2)	0.0145(2)	0.0182(2)	0.0012(2)	-0.0008(2)	0.0004(2)
Co(2)	0.0174(3)	0.0158(3)	0.0150(2)	0.0002(2)	0.0020(2)	0.0001(2)
Co(3)	0.0116(2)	0.0161(3)	0.0190(2)	0.0026(2)	-0.0004(2)	-0.0011(2)
Co(4)	0.0159(3)	0.0143(2)	0.0148(2)	0.0006(2)	-0.0005(2)	-0.0018(2)
Si(1)	0.0151(5)	0.0132(5)	0.0167(5)	0.0020(4)	0.0004(4)	-0.0010(4)
Si(2)	0.0124(5)	0.0116(5)	0.0178(5)	0.0014(4)	0.0009(4)	-0.0007(4)
C(1)	0.020(2)	0.022(2)	0.019(2)	0.000(2)	-0.001(2)	-0.002(2)
O(1)	0.029(2)	0.053(2)	0.024(1)	-0.007(1)	-0.011(1)	0.006(1)
C(2)	0.021(2)	0.022(2)	0.020(2)	0.000(2)	-0.002(2)	-0.001(2)
O(2)	0.034(2)	0.023(2)	0.038(2)	0.005(1)	-0.001(1)	0.010(1)
C(3)	0.013(2)	0.024(2)	0.020(2)	-0.002(2)	-0.003(1)	0.006(2)
O(3)	0.019(2)	0.037(2)	0.041(2)	0.006(1)	-0.004(1)	-0.010(1)
C(4)	0.020(2)	0.025(2)	0.019(2)	0.002(2)	0.004(2)	-0.001(2)
O(4)	0.044(2)	0.038(2)	0.023(2)	0.008(1)	0.006(1)	-0.008(1)
C(5)	0.026(2)	0.023(2)	0.024(2)	0.000(2)	0.000(2)	0.001(2)
O(5)	0.061(2)	0.023(2)	0.037(2)	-0.011(1)	-0.001(2)	-0.004(2)
C(6)	0.018(2)	0.024(2)	0.038(2)	0.005(2)	-0.005(2)	-0.001(2)
O(6)	0.028(2)	0.029(2)	0.086(3)	0.001(2)	-0.015(2)	-0.011(1)
C(7)	0.017(2)	0.023(2)	0.028(2)	0.002(2)	-0.002(2)	-0.002(2)

O(7)	0.036(2)	0.035(2)	0.044(2)	0.016(2)	-0.012(1)	0.003(1)
C(8)	0.024(2)	0.031(2)	0.027(2)	0.006(2)	0.000(2)	-0.002(2)
O(8)	0.026(2)	0.056(2)	0.029(2)	-0.001(1)	0.005(1)	0.009(2)
C(9)	0.029(2)	0.024(2)	0.021(2)	0.003(2)	-0.005(2)	0.001(2)
O(9)	0.056(2)	0.028(2)	0.047(2)	-0.004(1)	-0.018(2)	-0.016(2)
C(10)	0.025(2)	0.030(2)	0.020(2)	0.004(2)	0.001(2)	0.001(2)
O(10)	0.027(2)	0.056(2)	0.028(2)	-0.001(1)	0.003(1)	0.014(2)
C(11)	0.020(2)	0.026(2)	0.018(2)	0.001(2)	-0.001(1)	-0.002(2)
O(11)	0.039(2)	0.034(2)	0.024(1)	0.011(1)	-0.005(1)	-0.005(1)
C(12)	0.026(2)	0.017(2)	0.020(2)	0.004(1)	-0.001(2)	-0.003(2)
C(13)	0.036(2)	0.018(2)	0.034(2)	-0.001(2)	-0.003(2)	-0.001(2)
C(14)	0.056(3)	0.018(2)	0.042(3)	-0.001(2)	-0.005(2)	0.000(2)
C(15)	0.068(3)	0.022(2)	0.032(2)	-0.001(2)	0.000(2)	-0.018(2)
C(16)	0.055(3)	0.040(3)	0.029(2)	0.000(2)	0.009(2)	-0.025(2)
C(17)	0.037(2)	0.026(2)	0.024(2)	0.003(2)	0.004(2)	-0.009(2)
Hdum	0.043(4)					
C(18)	0.018(2)	0.012(2)	0.021(2)	0.001(1)	-0.001(1)	0.000(1)
C(19)	0.025(2)	0.018(2)	0.024(2)	0.001(2)	0.000(2)	-0.001(2)
C(20)	0.032(2)	0.021(2)	0.030(2)	0.003(2)	0.007(2)	-0.006(2)
C(21)	0.040(3)	0.019(2)	0.038(2)	0.007(2)	0.001(2)	-0.003(2)
C(22)	0.038(3)	0.017(2)	0.041(3)	0.001(2)	0.007(2)	0.007(2)
C(23)	0.027(2)	0.022(2)	0.028(2)	0.003(2)	0.003(2)	0.003(2)
Hdum	0.043(4)					
C(24)	0.059(6)	0.078(7)	0.43(3)	-0.06(1)	0.07(1)	-0.027(6)
C(25)	0.108(8)	0.141(9)	0.15(1)	0.029(7)	-0.043(7)	-0.011(7)
C(26)	0.066(8)	0.054(7)	0.058(7)	0.015(6)	0.021(6)	0.007(6)
C(27)	0.17(2)	0.07(1)	0.11(1)	-0.05(1)	0.09(1)	-0.08(1)
C(28)	0.34(3)	0.014(6)	0.11(1)	0.025(8)	-0.14(2)	-0.05(1)

SELECTED BOND LENGTHS AND ANGLES FOR $(PhSi)_2Co_4(CO)_{11}$

BOND LENGTHS (A) FOR $(PhSi)_2Co_4(CO)_{11}$

Co(1)	---Co(2)	2.565(1)	C(2)	---O(2)	1.137(5)
Co(1)	---Co(4)	2.685(1)	C(3)	---O(3)	1.140(4)
Co(1)	---Si(1)	2.315(1)	C(4)	---O(4)	1.136(5)
Co(1)	---Si(2)	2.312(1)	C(5)	---O(5)	1.124(5)
Co(1)	---C(1)	1.899(3)	C(6)	---O(6)	1.131(5)
Co(1)	---C(2)	1.814(4)	C(7)	---O(7)	1.137(5)
Co(1)	---C(3)	1.808(4)	C(8)	---O(8)	1.145(5)
Co(2)	---Co(3)	2.647(1)	C(9)	---O(9)	1.133(5)
Co(2)	---Si(1)	2.312(1)	C(10)	---O(10)	1.137(5)
Co(2)	---Si(2)	2.327(1)	C(11)	---O(11)	1.129(4)
Co(2)	---C(1)	1.954(4)	C(12)	---C(13)	1.395(3)
Co(2)	---C(4)	1.804(4)	C(12)	---C(17)	1.395(3)
Co(2)	---C(5)	1.834(4)	C(13)	---C(14)	1.395(3)
Co(2)	---C(8)	2.395(4)	C(14)	---C(15)	1.395(3)

Co(3)	---Co(4)	2.726(1)	C(15)	---C(16)	1.395(3)
Co(3)	---Si(1)	2.310(1)	C(16)	---C(17)	1.395(3)
Co(3)	---Si(2)	2.312(1)	C(18)	---C(19)	1.395(3)
Co(3)	---C(6)	1.815(4)	C(18)	---C(23)	1.395(3)
Co(3)	---C(7)	1.811(4)	C(19)	---C(20)	1.395(2)
Co(3)	---C(8)	1.798(4)	C(20)	---C(21)	1.395(3)
Co(4)	---Si(1)	2.312(1)	C(21)	---C(22)	1.395(3)
Co(4)	---Si(2)	2.316(1)	C(22)	---C(23)	1.395(2)
Co(4)	---C(9)	1.816(4)	C(24)	---C(26)	1.58(2)
Co(4)	---C(10)	1.790(4)	C(24)	---C(27)	1.26(3)
Co(4)	---C(11)	1.819(4)	C(24)	---C(28)	1.25(4)
Si(1)	---C(12)	1.878(2)	C(25)	---C(26)	1.35(2)
Si(2)	---C(18)	1.883(2)	C(25)	---C(28)	1.61(3)
C(1)	---O(1)	1.161(4)	C(26)	---C(28)	1.61(2)
C(28)	---C(28)	1.07(5)			

BOND ANGLES (°) FOR $(PhSi)_2Co_4(CO)_{11}$

Co(2)	-Co(1)	-Co(4)	91.50(0)	Co(3)	-Co(4)	-Si(1)	53.80(0
Co(2)	-Co(1)	-Si(1)	56.30(0)	Co(3)	-Co(4)	-Si(2)	53.80(0
Co(2)	-Co(1)	-Si(2)	56.70(0)	Co(3)	-Co(4)	-C(9)	91.3(1)
Co(2)	-Co(1)	-C(1)	49.2(1)	Co(3)	-Co(4)	-C(10)	154.2(1)
Co(2)	-Co(1)	-C(2)	120.7(1)	Co(3)	-Co(4)	-C(11)	100.7(1)
Co(2)	-Co(1)	-C(3)	121.9(1)	Si(1)	-Co(4)	-Si(2)	71.50(0
Co(4)	-Co(1)	-Si(1)	54.50(0)	Si(1)	-Co(4)	-C(9)	88.3(1)
Co(4)	-Co(1)	-Si(2)	54.60(0)	Si(1)	-Co(4)	-C(10)	102.3(1)
Co(4)	-Co(1)	-C(1)	140.7(1)	Si(1)	-Co(4)	-C(11)	153.0(1)
Co(4)	-Co(1)	-C(2)	110.2(1)	Si(2)	-Co(4)	-C(9)	145.1(1)
Co(4)	-Co(1)	-C(3)	107.5(1)	Si(2)	-Co(4)	-C(10)	113.7(1)
Si(1)	-Co(1)	-Si(2)	71.50(0)	Si(2)	-Co(4)	-C(11)	86.2(1)
Si(1)	-Co(1)	-C(1)	94.8(1)	C(9)	-Co(4)	-C(10)	97.9(2)
Si(1)	-Co(1)	-C(2)	92.4(1)	C(9)	-Co(4)	-C(11)	102.6(2)
Si(1)	-Co(1)	-C(3)	159.8(1)	C(10)	-Co(4)	-C(11)	100.6(2)
Si(2)	-Co(1)	-C(1)	95.4(1)	Co(1)	-Si(1)	-Co(2)	67.30(0
Si(2)	-Co(1)	-C(2)	162.3(1)	Co(1)	-Si(1)	-Co(3)	108.30(0
Si(2)	-Co(1)	-C(3)	90.7(1)	Co(1)	-Si(1)	-Co(4)	70.90(0
C(1)	-Co(1)	-C(2)	93.3(2)	Co(1)	-Si(1)	-C(12)	127.9(1)
C(1)	-Co(1)	-C(3)	96.5(2)	Co(2)	-Si(1)	-Co(3)	69.90(0
C(2)	-Co(1)	-C(3)	103.5(2)	Co(2)	-Si(1)	-Co(4)	108.80(0
Co(1)	-Co(2)	-Co(3)	92.00(0)	Co(2)	-Si(1)	-C(12)	127.6(1)
Co(1)	-Co(2)	-Si(1)	56.40(0)	Co(3)	-Si(1)	-Co(4)	72.30(0
Co(1)	-Co(2)	-Si(2)	56.20(0)	Co(3)	-Si(1)	-C(12)	123.8(1)
Co(1)	-Co(2)	-C(1)	47.3(1)	Co(4)	-Si(1)	-C(12)	123.5(1)
Co(1)	-Co(2)	-C(4)	117.8(1)	Co(1)	-Si(2)	-Co(2)	67.10(0
Co(1)	-Co(2)	-C(5)	117.9(1)	Co(1)	-Si(2)	-Co(3)	108.30(0
Co(1)	-Co(2)	-C(8)	133.3(1)	Co(1)	-Si(2)	-Co(4)	70.90(0
Co(3)	-Co(2)	-Si(1)	55.00(0)	Co(1)	-Si(2)	-C(18)	129.4(1)
Co(3)	-Co(2)	-Si(2)	54.90(0)	Co(2)	-Si(2)	-Co(3)	69.60(0

Co(3)	-Co(2)	-C(1)	139.3(1)	Co(2)	-Si(2)	-Co(4)	108.20(0
Co(3)	-Co(2)	-C(4)	111.5(1)	Co(2)	-Si(2)	-C(18)	124.8(1)
Co(3)	-Co(2)	-C(5)	113.1(1)	Co(3)	-Si(2)	-Co(4)	72.20(0
Co(3)	-Co(2)	-C(8)	41.4(1)	Co(3)	-Si(2)	-C(18)	122.0(1)
Si(1)	-Co(2)	-Si(2)	71.30(0)	Co(4)	-Si(2)	-C(18)	127.0(1)
Si(1)	-Co(2)	-C(1)	93.4(1)	Co(1)	-C(1)	-Co(2)	83.5(1)
Si(1)	-Co(2)	-C(4)	91.0(1)	Co(1)	-C(1)	-O(1)	140.9(3)
Si(1)	-Co(2)	-C(5)	163.7(1)	Co(2)	-C(1)	-O(1)	135.7(3)
Si(1)	-Co(2)	-C(8)	88.1(1)	Co(1)	-C(2)	-O(2)	175.8(3)
Si(2)	-Co(2)	-C(1)	93.5(1)	Co(1)	-C(3)	-O(3)	178.0(3)
Si(2)	-Co(2)	-C(4)	161.8(1)	Co(2)	-C(4)	-O(4)	176.6(3)
Si(2)	-Co(2)	-C(5)	92.8(1)	Co(2)	-C(5)	-O(5)	175.3(3)
Si(2)	-Co(2)	-C(8)	86.2(1)	Co(3)	-C(6)	-O(6)	175.4(4)
C(1)	-Co(2)	-C(4)	91.9(2)	Co(3)	-C(7)	-O(7)	175.7(3)
C(1)	-Co(2)	-C(5)	91.1(2)	Co(2)	-C(8)	-Co(3)	76.8(1)
C(1)	-Co(2)	-C(8)	178.3(1)	Co(2)	-C(8)	-O(8)	121.4(3)
C(4)	-Co(2)	-C(5)	104.5(2)	Co(3)	-C(8)	-O(8)	161.8(3)
C(4)	-Co(2)	-C(8)	89.0(1)	Co(4)	-C(9)	-O(9)	178.8(4)
C(5)	-Co(2)	-C(8)	87.3(2)	Co(4)	-C(10)	-O(10)	168.9(3)
Co(2)	-Co(3)	-Co(4)	88.80(0)	Co(4)	-C(11)	-O(11)	178.2(3)
Co(2)	-Co(3)	-Si(1)	55.10(0)	Si(1)	-C(12)	-C(13)	119.9(2)
Co(2)	-Co(3)	-Si(2)	55.50(0)	Si(1)	-C(12)	-C(17)	120.0(1)
Co(2)	-Co(3)	-C(6)	127.3(1)	C(13)	-C(12)	-C(17)	120.0(2)
Co(2)	-Co(3)	-C(7)	130.8(1)	C(12)	-C(13)	-C(14)	120.0(2)
Co(2)	-Co(3)	-C(8)	61.8(1)	C(13)	-C(14)	-C(15)	120.0(2)
Co(4)	-Co(3)	-Si(1)	53.90(0)	C(14)	-C(15)	-C(16)	120.0(2)
Co(4)	-Co(3)	-Si(2)	54.00(0)	C(15)	-C(16)	-C(17)	120.0(2)
Co(4)	-Co(3)	-C(6)	100.1(1)	C(12)	-C(17)	-C(16)	120.0(2)
Co(4)	-Co(3)	-C(7)	96.7(1)	Si(2)	-C(18)	-C(19)	122.2(1)
Co(4)	-Co(3)	-C(8)	150.5(1)	Si(2)	-C(18)	-C(23)	117.8(2)
Si(1)	-Co(3)	-Si(2)	71.60(0)	C(19)	-C(18)	-C(23)	120.0(2)
Si(1)	-Co(3)	-C(6)	89.4(1)	C(18)	-C(19)	-C(20)	120.0(2)
Si(1)	-Co(3)	-C(7)	150.4(1)	C(19)	-C(20)	-C(21)	120.0(2)
Si(1)	-Co(3)	-C(8)	104.9(1)	C(20)	-C(21)	-C(22)	120.0(2)
Si(2)	-Co(3)	-C(6)	153.6(1)	C(21)	-C(22)	-C(23)	120.0(2)
Si(2)	-Co(3)	-C(7)	89.3(1)	C(18)	-C(23)	-C(22)	120.0(2)
Si(2)	-Co(3)	-C(8)	102.7(1)	C(26)	-C(24)	-C(27)	173(2)
C(6)	-Co(3)	-C(7)	99.8(2)	C(26)	-C(24)	-C(28)	68(1)
C(6)	-Co(3)	-C(8)	99.7(2)	C(27)	-C(24)	-C(28)	106(2)
C(7)	-Co(3)	-C(8)	101.1(2)	C(26)	-C(25)	-C(28)	65(1)
Co(1)	-Co(4)	-Co(3)	87.70(0)	C(24)	-C(26)	-C(25)	111(1)
Co(1)	-Co(4)	-Si(1)	54.60(0)	C(24)	-C(26)	-C(28)	46(1)
Co(1)	-Co(4)	-Si(2)	54.50(0)	C(25)	-C(26)	-C(28)	65(1)
Co(1)	-Co(4)	-C(9)	133.4(1)	C(24)	-C(28)	-C(25)	114(2)
Co(1)	-Co(4)	-C(10)	68.5(1)	C(24)	-C(28)	-C(26)	65(1)
Co(1)	-Co(4)	-C(11)	123.3(1)	C(25)	-C(28)	-C(26)	49(1)

APPENDIX FIVE

FINAL POSITIONAL AND EQUIVALENT THERMAL PARAMETERS $SSi_2Co_4(CO)_{14}$

ATOM	X/A	Y/B	Z/C	Ueq
Co(1)	0.3490(1)	0.1869(1)	0.2164(1)	0.020
Co(2)	0.4810(1)	0.2516(1)	0.5667(1)	0.019
Co(3)	0.3186(1)	0.1669(1)	0.4468(1)	0.016
Co(4)	0.3459(1)	0.3672(1)	0.4101(1)	0.018
Si(1)	0.3687(1)	0.2188(1)	0.3390(1)	0.016
Si(2)	0.4170(1)	0.2472(1)	0.4636(1)	0.016
S(1)	0.4685(1)	0.1905(1)	0.3668(1)	0.020
C(11)	0.3920(3)	0.0608(5)	0.2296(3)	0.028
O(11)	0.4191(2)	-0.0170(3)	0.2366(2)	0.042
C(12)	0.3925(3)	0.3118(4)	0.2092(3)	0.026
O(12)	0.4187(2)	0.3921(3)	0.2038(2)	0.042
C(13)	0.2645(3)	0.1843(5)	0.2380(3)	0.032
O(13)	0.2115(2)	0.1810(4)	0.2495(2)	0.049
C(14)	0.3392(3)	0.1725(5)	0.1177(3)	0.029
O(14)	0.3337(2)	0.1650(4)	0.0555(2)	0.047
C(21)	0.5368(3)	0.3205(5)	0.5078(3)	0.026
O(21)	0.5722(2)	0.3685(4)	0.4725(2)	0.044
C(22)	0.4648(3)	0.1096(5)	0.5643(3)	0.027
O(22)	0.4521(2)	0.0195(3)	0.5636(2)	0.036
C(23)	0.4230(3)	0.3369(4)	0.6136(3)	0.026
O(23)	0.3887(2)	0.3893(3)	0.6446(2)	0.040
C(24)	0.5347(3)	0.2444(5)	0.6461(3)	0.027
O(24)	0.5672(2)	0.2418(3)	0.6962(2)	0.037
C(31)	0.3065(2)	0.1672(4)	0.5439(3)	0.028
O(31)	0.2998(2)	0.1650(4)	0.6070(2)	0.040
C(32)	0.2343(2)	0.1791(4)	0.4206(3)	0.024
O(32)	0.1815(2)	0.1870(3)	0.4089(2)	0.034
C(33)	0.3472(2)	0.0352(4)	0.4267(3)	0.023
O(33)	0.3666(2)	-0.0500(3)	0.4146(2)	0.032
C(41)	0.3132(3)	0.4266(4)	0.4925(3)	0.026
O(41)	0.2912(2)	0.4661(4)	0.5442(2)	0.044
C(42)	0.2845(3)	0.4040(4)	0.3457(3)	0.027
O(42)	0.2478(2)	0.4291(4)	0.3024(2)	0.043
C(43)	0.4123(3)	0.4456(4)	0.3822(3)	0.029
O(43)	0.4544(2)	0.4982(3)	0.3631(3)	0.042

THERMAL PARAMETERS FOR $SSi_2Co_4(CO)_{14}$

ATOM	U11	U22	U33	U23	U13	U12
Co(1)	0.0222(4)	0.0226(4)	0.0151(3)	0.0009(3)	-0.0001(3)	0.0008(3)
Co(2)	0.0198(3)	0.0211(3)	0.0164(3)	-0.0007(3)	-0.0010(3)	-0.0012(3)
Co(3)	0.0172(3)	0.0165(3)	0.0157(3)	0.0002(3)	0.0015(3)	-0.0015(3)
Co(4)	0.0203(3)	0.0146(3)	0.0201(4)	0.0001(3)	0.0009(3)	0.0024(3)
Si(1)	0.0177(6)	0.0162(6)	0.0144(7)	0.0009(5)	-0.0002(5)	0.0002(5)
Si(2)	0.0177(6)	0.0153(6)	0.0161(7)	0.0008(6)	0.0001(5)	-0.0002(5)
S(1)	0.0176(6)	0.0223(6)	0.0188(6)	-0.0006(5)	0.0002(5)	0.0028(5)
C(11)	0.040(3)	0.027(3)	0.016(3)	-0.001(2)	0.000(2)	0.001(3)
O(11)	0.062(3)	0.026(2)	0.039(3)	0.000(2)	-0.006(2)	0.011(2)
C(12)	0.031(3)	0.027(3)	0.019(3)	0.004(2)	0.003(2)	0.002(3)
O(12)	0.060(3)	0.032(2)	0.034(3)	0.004(2)	0.010(2)	-0.009(2)
C(13)	0.027(3)	0.046(4)	0.022(3)	-0.004(3)	-0.004(2)	-0.003(3)
O(13)	0.025(2)	0.086(4)	0.037(3)	0.001(3)	-0.001(2)	-0.006(2)
C(14)	0.033(3)	0.033(3)	0.022(3)	-0.004(3)	-0.004(2)	0.004(3)
O(14)	0.060(3)	0.064(3)	0.016(2)	-0.006(2)	-0.003(2)	0.006(3)
C(21)	0.024(3)	0.037(3)	0.018(3)	-0.009(2)	-0.007(2)	-0.005(2)
O(21)	0.037(2)	0.066(3)	0.030(2)	0.000(2)	0.005(2)	-0.023(2)
C(22)	0.025(3)	0.031(3)	0.024(3)	-0.002(2)	-0.005(2)	0.006(2)
O(22)	0.051(3)	0.023(2)	0.034(2)	0.004(2)	-0.009(2)	0.002(2)
C(23)	0.032(3)	0.023(3)	0.023(3)	-0.006(2)	-0.005(2)	-0.005(2)
O(23)	0.037(2)	0.039(2)	0.045(3)	-0.014(2)	0.001(2)	0.008(2)
C(24)	0.026(3)	0.035(3)	0.020(3)	0.003(2)	0.005(2)	-0.007(2)
O(24)	0.038(2)	0.046(3)	0.026(2)	0.002(2)	-0.013(2)	-0.004(2)
C(31)	0.025(3)	0.029(3)	0.029(3)	0.001(3)	0.002(2)	-0.004(2)
O(31)	0.043(3)	0.055(3)	0.021(2)	-0.005(2)	0.005(2)	-0.016(2)
C(32)	0.022(3)	0.024(3)	0.025(3)	0.002(2)	0.003(2)	-0.004(2)
O(32)	0.020(2)	0.050(3)	0.033(2)	0.001(2)	-0.002(2)	0.000(2)
C(33)	0.025(3)	0.025(3)	0.019(3)	0.003(2)	-0.001(2)	-0.006(2)
O(33)	0.043(2)	0.015(2)	0.040(2)	-0.003(2)	-0.001(2)	0.001(2)
C(41)	0.032(3)	0.021(3)	0.025(3)	0.003(2)	0.001(2)	0.011(2)
O(41)	0.049(3)	0.052(3)	0.033(2)	-0.005(2)	0.006(2)	0.023(2)
C(42)	0.033(3)	0.027(3)	0.022(3)	0.003(2)	0.004(2)	0.007(2)
O(42)	0.051(3)	0.041(3)	0.037(2)	-0.001(2)	-0.008(2)	0.021(2)
C(43)	0.034(3)	0.018(3)	0.036(3)	-0.006(2)	0.008(3)	0.001(3)
O(43)	0.048(3)	0.027(2)	0.052(3)	-0.008(2)	0.013(2)	-0.015(2)

SELECTED BOND LENGTHS AND ANGLES FOR $SSi_2Co_4(CO)_{14}$

BOND LENGTHS (Å) FOR $SSi_2Co_4(CO)_{14}$

Co(1) ---Si(1)	2.295(1)	Co(4) ---C(42)	1.792(6)
Co(1) ---C(11)	1.811(6)	Co(4) ---C(43)	1.762(6)
Co(1) ---C(12)	1.793(6)	Si(1) ---Si(2)	2.499(2)

Co(1)	---C(13)	1.803(6)	
Co(1)	---C(14)	1.812(6)	
Co(2)	---Si(2)	2.299(1)	
Co(2)	---C(21)	1.794(6)	
Co(2)	---C(22)	1.786(6)	
Co(2)	---C(23)	1.814(6)	
Co(2)	---C(24)	1.826(6)	
Co(3)	---Co(4)	2.623(1)	
Co(3)	---Si(1)	2.309(1)	
Co(3)	---Si(2)	2.297(1)	
Co(3)	---C(31)	1.780(6)	
Co(3)	---C(32)	1.825(5)	
Co(3)	---C(33)	1.770(5)	
Co(4)	---Si(1)	2.291(1)	
Co(4)	---Si(2)	2.309(1)	
Co(4)	---C(41)	1.799(5)	
Si(1)	---S(1)	2.169(2)	
Si(2)	---S(1)	2.174(2)	
C(11)	---O(11)	1.121(7)	
C(12)	---O(12)	1.136(6)	
C(13)	---O(13)	1.126(7)	
C(14)	---O(14)	1.139(7)	
C(21)	---O(21)	1.144(7)	
C(22)	---O(22)	1.143(7)	
C(23)	---O(23)	1.116(6)	
C(24)	---O(24)	1.134(7)	
C(31)	---O(31)	1.154(6)	
C(32)	---O(32)	1.125(6)	
C(33)	---O(33)	1.148(6)	
C(41)	---O(41)	1.152(6)	
C(42)	---O(42)	1.139(7)	
C(43)	---O(43)	1.146(6)	

BOND ANGLES (°) FOR $SSi_2Co_4(CO)_{14}$

Si(1)	-Co(1)	-C(11)	86.0(2)	Si(1)	-Co(4)	-C(42)	89.0(2)
Si(1)	-Co(1)	-C(12)	80.4(2)	Si(1)	-Co(4)	-C(43)	96.5(2)
Si(1)	-Co(1)	-C(13)	88.1(2)	Si(2)	-Co(4)	-C(41)	98.9(2)
Si(1)	-Co(1)	-C(14)	174.2(2)	Si(2)	-Co(4)	-C(42)	153.5(2)
C(11)	-Co(1)	-C(12)	120.0(2)	Si(2)	-Co(4)	-C(43)	88.3(2)
C(11)	-Co(1)	-C(13)	116.0(3)	C(41)	-Co(4)	-C(42)	99.7(2)
C(11)	-Co(1)	-C(14)	95.9(2)	C(41)	-Co(4)	-C(43)	108.2(3)
C(12)	-Co(1)	-C(13)	121.6(3)	C(42)	-Co(4)	-C(43)	103.5(3)
C(12)	-Co(1)	-C(14)	93.9(3)	Co(1)	-Si(1)	-Co(3)	133.8(1)
C(13)	-Co(1)	-C(14)	95.9(2)	Co(1)	-Si(1)	-Co(4)	130.2(1)
Si(2)	-Co(2)	-C(21)	84.4(2)	Co(1)	-Si(1)	-Si(2)	166.5(1)
Si(2)	-Co(2)	-C(22)	81.2(2)	Co(1)	-Si(1)	-S(1)	111.7(1)
Si(2)	-Co(2)	-C(23)	90.5(2)	Co(3)	-Si(1)	-Co(4)	69.5(1)
Si(2)	-Co(2)	-C(24)	175.2(2)	Co(3)	-Si(1)	-Si(2)	56.9(1)
C(21)	-Co(2)	-C(22)	125.0(2)	Co(3)	-Si(1)	-S(1)	101.1(1)
C(21)	-Co(2)	-C(23)	115.8(2)	Co(4)	-Si(1)	-Si(2)	57.4(1)
C(21)	-Co(2)	-C(24)	95.5(2)	Co(4)	-Si(1)	-S(1)	101.3(1)
C(22)	-Co(2)	-C(23)	117.1(2)	Si(2)	-Si(1)	-S(1)	55.0(1)
C(22)	-Co(2)	-C(24)	95.0(2)	Co(2)	-Si(2)	-Co(3)	129.5(1)
C(23)	-Co(2)	-C(24)	93.8(2)	Co(2)	-Si(2)	-Co(4)	134.3(1)
Co(4)	-Co(3)	-Si(1)	54.9(1)	Co(2)	-Si(2)	-Si(1)	166.7(1)
Co(4)	-Co(3)	-Si(2)	55.5(1)	Co(2)	-Si(2)	-S(1)	112.2(1)
Co(4)	-Co(3)	-C(31)	106.2(2)	Co(3)	-Si(2)	-Co(4)	69.4(1)
Co(4)	-Co(3)	-C(32)	93.7(2)	Co(3)	-Si(2)	-Si(1)	57.4(1)
Co(4)	-Co(3)	-C(33)	137.8(2)	Co(3)	-Si(2)	-S(1)	101.3(1)
Si(1)	-Co(3)	-Si(2)	65.7(1)	Co(4)	-Si(2)	-Si(1)	56.8(1)
Si(1)	-Co(3)	-C(31)	154.5(2)	Co(4)	-Si(2)	-S(1)	100.6(1)
Si(1)	-Co(3)	-C(32)	101.1(2)	Si(1)	-Si(2)	-S(1)	54.8(1)
Si(1)	-Co(3)	-C(33)	85.9(2)	Si(1)	-S(1)	-Si(2)	70.3(1)

Si(2)	-Co(3)	-C(31)	89.7(2)	Co(1)	-C(11)	-O(11)	178.8(5)
Si(2)	-Co(3)	-C(32)	149.0(2)	Co(1)	-C(12)	-O(12)	178.3(5)
Si(2)	-Co(3)	-C(33)	97.1(2)	Co(1)	-C(13)	-O(13)	177.9(5)
C(31)	-Co(3)	-C(32)	97.0(2)	Co(1)	-C(14)	-O(14)	178.8(6)
C(31)	-Co(3)	-C(33)	104.7(2)	Co(2)	-C(21)	-O(21)	176.8(5)
C(32)	-Co(3)	-C(33)	110.2(2)	Co(2)	-C(22)	-O(22)	177.4(5)
Co(3)	-Co(4)	-Si(1)	55.5(1)	Co(2)	-C(23)	-O(23)	177.5(5)
Co(3)	-Co(4)	-Si(2)	55.1(1)	Co(2)	-C(24)	-O(24)	178.3(5)
Co(3)	-Co(4)	-C(41)	95.2(2)	Co(3)	-C(31)	-O(31)	178.1(5)
Co(3)	-Co(4)	-C(42)	104.5(2)	Co(3)	-C(32)	-O(32)	175.8(5)
Co(3)	-Co(4)	-C(43)	139.5(2)	Co(3)	-C(33)	-O(33)	178.7(5)
Si(1)	-Co(4)	-Si(2)	65.8(1)	Co(4)	-C(41)	-O(41)	178.3(5)
Si(1)	-Co(4)	-C(41)	150.8(2)	Co(4)	-C(42)	-O(42)	176.6(5)
Co(4)	-C(43)	-O(43)	178.3(5)				

APPENDIX SIX

FINAL POSITIONAL AND EQUIVALENT THERMAL PARAMETERS $S_2Co_4(CO)_{10}$

ATOM	X/A	Y/B	Z/C	Ueq
Co(1)	0.5150(1)	0.4574(1)	0.3580(1)	0.013
Co(2)	0.3249(1)	0.4290(1)	0.4709(1)	0.013
S(1)	0.4647(1)	0.6972(1)	0.4765(1)	0.017
C(1)	0.3276(3)	0.3774(4)	0.3159(2)	0.019
O(1)	0.2564(2)	0.3306(4)	0.2396(2)	0.028
C(2)	0.5225(3)	0.6370(5)	0.2493(2)	0.019
O(2)	0.5280(2)	0.7456(3)	0.1791(2)	0.029
C(3)	0.6012(3)	0.2550(5)	0.2974(2)	0.019
O(3)	0.6577(2)	0.1339(4)	0.2585(2)	0.031
C(4)	0.1735(3)	0.5826(4)	0.4549(2)	0.016
O(4)	0.0763(2)	0.6722(3)	0.4439(2)	0.024
C(5)	0.2454(3)	0.2006(5)	0.5093(2)	0.019
O(5)	0.1934(2)	0.0621(3)	0.5362(2)	0.033

THERMAL PARAMETERS FOR $S_2Co_4(CO)_{10}$

ATOM	U11	U22	U33	U23	U13	U12
Co(1)	0.0115(2)	0.0159(2)	0.0126(2)	0.0000(2)	0.0020(1)	-0.0004(2)
Co(2)	0.0104(2)	0.0148(2)	0.0142(2)	0.0003(2)	0.0015(1)	-0.0008(2)
S(1)	0.0155(4)	0.0166(3)	0.0176(4)	0.0012(3)	0.0009(3)	0.0007(3)
C(1)	0.016(2)	0.021(2)	0.019(2)	-0.002(1)	0.006(1)	-0.001(1)
O(1)	0.020(1)	0.044(1)	0.021(1)	-0.013(1)	0.0036(9)	-0.010(1)
C(2)	0.012(1)	0.026(2)	0.018(2)	-0.003(1)	0.001(1)	0.001(1)
O(2)	0.029(1)	0.036(1)	0.024(1)	0.011(1)	0.006(1)	0.003(1)
C(3)	0.015(1)	0.026(2)	0.016(1)	0.003(1)	0.002(1)	0.000(1)
O(3)	0.026(1)	0.036(1)	0.032(1)	-0.006(1)	0.005(1)	0.009(1)
C(4)	0.017(2)	0.018(2)	0.014(1)	-0.002(1)	0.002(1)	-0.006(1)
O(4)	0.017(1)	0.026(1)	0.028(1)	0.000(1)	0.0039(9)	0.005(1)
C(5)	0.015(1)	0.022(2)	0.021(2)	0.000(1)	0.000(1)	-0.001(1)
O(5)	0.031(1)	0.023(1)	0.046(2)	0.008(1)	0.006(1)	-0.008(1)

SELECTED BOND LENGTHS AND ANGLES FOR $S_2Co_4(CO)_{10}$

BOND LENGTHS (Å) FOR $S_2Co_4(CO)_{10}$

Co(1)	---Co(2)	2.488(1)	Co(2)	---C(4)	1.818(3)
Co(1)	---S(1)	2.270(1)	Co(2)	---C(5)	1.814(3)
Co(1)	---C(1)	1.953(3)	C(1)	---O(1)	1.154(4)
Co(1)	---C(2)	1.811(3)	C(2)	---O(2)	1.137(4)
Co(1)	---C(3)	1.814(3)	C(3)	---O(3)	1.128(4)
Co(2)	---S(1)	2.271(1)	C(4)	---O(4)	1.134(3)
Co(2)	---C(1)	1.947(3)	C(5)	---O(5)	1.133(4)

BOND ANGLES (°) FOR $S_2Co_4(CO)_{10}$

Co(2)	-Co(1)	-S(1)	56.8(1)	S(1)	-Co(2)	-C(1)	95.2(1)
Co(2)	-Co(1)	-C(1)	50.3(1)	S(1)	-Co(2)	-C(4)	93.0(1)
Co(2)	-Co(1)	-C(2)	124.5(1)	S(1)	-Co(2)	-C(5)	161.2(1)
Co(2)	-Co(1)	-C(3)	127.0(1)	C(1)	-Co(2)	-C(4)	95.8(1)
S(1)	-Co(1)	-C(1)	95.1(1)	C(1)	-Co(2)	-C(5)	99.4(1)
S(1)	-Co(1)	-C(2)	92.1(1)	C(4)	-Co(2)	-C(5)	97.2(1)
S(1)	-Co(1)	-C(3)	161.3(1)	Co(1)	-S(1)	-Co(2)	66.4(1)
C(1)	-Co(1)	-C(2)	96.2(1)	Co(1)	-C(1)	-Co(2)	79.3(1)
C(1)	-Co(1)	-C(3)	99.7(1)	Co(1)	-C(1)	-O(1)	140.2(2)
C(2)	-Co(1)	-C(3)	97.5(1)	Co(2)	-C(1)	-O(1)	140.5(2)
Co(1)	-Co(2)	-S(1)	56.8(1)	Co(1)	-C(2)	-O(2)	178.1(3)
Co(1)	-Co(2)	-C(1)	50.5(1)	Co(1)	-C(3)	-O(3)	177.6(3)
Co(1)	-Co(2)	-C(4)	124.9(1)	Co(2)	-C(4)	-O(4)	177.4(3)
Co(1)	-Co(2)	-C(5)	126.6(1)	Co(2)	-C(5)	-O(5)	177.3(3)

APPENDIX SEVEN

FINAL POSITIONAL AND EQUIVALENT THERMAL PARAMETERS $(CO)_4CoCl_2SiOCCo(CO)_9$

ATOM	X/A	Y/B	Z/C	Ueq/U11
Co(1)	0.0346(5)	0.1406(4)	0.1165(2)	0.028
Co(2)	0.3360(5)	0.0182(4)	0.1566(2)	0.026
Co(3)	0.1098(5)	0.2941(4)	0.1767(2)	0.030
Co(4)	-0.2636(5)	-0.2059(4)	0.4260(2)	0.038
Si(1)	0.000(1)	-0.1190(9)	0.3571(4)	0.035
Cl(1)	0.250(1)	-0.3164(9)	0.3496(5)	0.060
Cl(2)	0.056(1)	0.040(1)	0.3935(4)	0.062
C(1)	0.076(3)	0.075(3)	0.211(1)	0.028(6)
O(1)	-0.026(2)	-0.014(2)	0.2726(9)	0.027(4)
C(2)	0.138(4)	0.241(3)	0.021(2)	0.047(7)
O(2)	0.200(3)	0.304(2)	-0.039(1)	0.054(5)
C(3)	-0.209(4)	0.260(3)	0.128(1)	0.032(6)
O(3)	-0.374(3)	0.333(2)	0.135(1)	0.051(5)
C(4)	-0.003(4)	-0.054(4)	0.120(2)	0.049(7)
O(4)	0.029(3)	0.173(3)	0.878(1)	0.066(6)
C(5)	0.500(3)	0.094(3)	0.071(1)	0.026(5)
O(5)	0.606(3)	0.134(2)	0.019(1)	0.044(5)
C(6)	0.480(3)	-0.028(3)	0.217(1)	0.025(5)
O(6)	0.562(3)	-0.055(2)	0.258(1)	0.058(6)
C(7)	0.370(4)	-0.190(3)	0.160(2)	0.037(6)
O(7)	0.381(3)	-0.332(3)	0.164(1)	0.062(6)
C(8)	0.214(4)	0.441(3)	0.095(2)	0.034(6)
O(8)	0.273(3)	0.535(2)	0.041(1)	0.053(5)
C(9)	0.213(4)	0.313(3)	0.238(1)	0.031(6)
O(9)	0.287(3)	0.326(2)	0.274(1)	0.048(5)
C(10)	-0.129(4)	0.412(3)	0.212(2)	0.046(7)
O(10)	-0.283(4)	0.491(3)	0.234(1)	0.072(6)
C(11)	-0.481(6)	0.727(5)	0.479(2)	0.08(1)
O(11)	-0.379(4)	0.315(3)	0.482(2)	0.081(7)
C(12)	-0.160(4)	0.723(4)	0.497(2)	0.049(7)
O(12)	0.075(3)	0.329(2)	0.455(1)	0.050(5)
C(13)	-0.189(4)	0.665(3)	0.368(2)	0.045(7)
O(13)	-0.149(3)	0.589(3)	0.328(1)	0.071(6)
C(14)	-0.384(4)	1.017(4)	0.396(2)	0.047(7)
O(14)	-0.456(3)	1.156(3)	0.375(1)	0.066(6)

THERMAL PARAMETERS FOR $(CO)_4CoCl_2SiOCCo(CO)_9$

ATOM	U11	U22	U33	U23	U13	U12
Co(1)	0.029(2)	0.031(2)	0.021(2)	-0.005(1)	-0.007(2)	-0.006(1)
Co(2)	0.028(2)	0.024(2)	0.020(2)	-0.003(1)	-0.005(2)	-0.002(1)
Co(3)	0.038(2)	0.023(2)	0.023(2)	-0.006(1)	-0.005(2)	-0.004(1)
Co(4)	0.043(2)	0.042(2)	0.023(2)	-0.008(2)	-0.001(2)	-0.014(2)
Si(1)	0.036(4)	0.040(4)	0.024(4)	-0.003(3)	-0.005(4)	-0.015(3)
Cl(1)	0.049(5)	0.051(4)	0.048(5)	0.009(4)	-0.006(4)	-0.009(4)
Cl(2)	0.091(6)	0.071(5)	0.030(4)	-0.008(4)	-0.010(4)	-0.044(5)

SELECTED BOND LENGTHS AND ANGLES FOR $(CO)_4CoCl_2SiOCCo(CO)_9$

BOND LENGTHS (Å) FOR $(CO)_4CoCl_2SiOCCo(CO)_9$

Co(1) ---Co(2)	2.478(5)	Co(4) ---C(12)	1.71(3)
Co(1) ---Co(3)	2.472(5)	Co(4) ---C(13)	1.76(3)
Co(1) ---C(1)	1.90(3)	Co(4) ---C(14)	1.79(3)
Co(1) ---C(2)	1.83(3)	Si(1) ---Cl(1)	2.07(1)
Co(1) ---C(3)	1.77(3)	Si(1) ---Cl(2)	2.05(1)
Co(1) ---C(4)	1.81(3)	Si(1) ---O(1)	1.67(2)
Co(2) ---Co(3)	2.486(4)	C(1) ---O(1)	1.36(3)
Co(2) ---C(1)	1.90(2)	C(2) ---O(2)	1.14(3)
Co(2) ---C(5)	1.81(3)	C(3) ---O(3)	1.18(3)
Co(2) ---C(6)	1.79(2)	C(5) ---O(5)	1.12(3)
Co(2) ---C(7)	1.72(3)	C(6) ---O(6)	1.14(3)
Co(3) ---C(1)	1.87(2)	C(7) ---O(7)	1.20(3)
Co(3) ---C(8)	1.81(3)	C(8) ---O(8)	1.15(3)
Co(3) ---C(9)	1.79(3)	C(9) ---O(9)	1.16(3)
Co(3) ---C(10)	1.79(3)	C(10) ---O(10)	1.16(3)
Co(4) ---Si(1)	2.249(8)	C(13) ---O(13)	1.14(3)
Co(4) ---C(11)	1.82(4)	C(14) ---O(14)	1.12(3)

BOND ANGLES (°) FOR $(CO)_4CoCl_2SiOCCo(CO)_9$

Co(2) -Co(1) -Co(3)	60.3(1)	C(1) -Co(3) -C(8)	140(1)
Co(2) -Co(1) -C(1)	49.4(7)	C(1) -Co(3) -C(9)	108(1)
Co(2) -Co(1) -C(2)	96.9(9)	C(1) -Co(3) -C(10)	99(1)
Co(2) -Co(1) -C(3)	150.7(8)	C(8) -Co(3) -C(9)	97(1)
Co(2) -Co(1) -C(4)	100.2(9)	C(8) -Co(3) -C(10)	107(1)
Co(3) -Co(1) -C(1)	48.5(6)	C(9) -Co(3) -C(10)	95(1)
Co(3) -Co(1) -C(2)	100.4(9)	Si(1) -Co(4) -C(11)	177(1)
Co(3) -Co(1) -C(3)	94.2(8)	Si(1) -Co(4) -C(12)	85(1)
Co(3) -Co(1) -C(4)	148(1)	Si(1) -Co(4) -C(13)	84(1)

C(1)	-Co(1) -C(2)	140(1)	
C(1)	-Co(1) -C(3)	103(1)	
C(1)	-Co(1) -C(4)	100(1)	
C(2)	-Co(1) -C(3)	102(1)	
C(2)	-Co(1) -C(4)	106(1)	
C(3)	-Co(1) -C(4)	95(1)	
Co(1)	-Co(2) -Co(3)	59.7(1)	
Co(1)	-Co(2) -C(1)	49.3(8)	
Co(1)	-Co(2) -C(5)	99.4(8)	
Co(1)	-Co(2) -C(6)	154.3(8)	
Co(1)	-Co(2) -C(7)	95.8(9)	
Co(3)	-Co(2) -C(1)	48.2(6)	
Co(3)	-Co(2) -C(5)	101.1(7)	
Co(3)	-Co(2) -C(6)	98.7(7)	
Co(3)	-Co(2) -C(7)	148.4(9)	
C(1)	-Co(2) -C(5)	142(1)	
C(1)	-Co(2) -C(6)	106(1)	
C(1)	-Co(2) -C(7)	101(1)	
C(5)	-Co(2) -C(6)	98(1)	
C(5)	-Co(2) -C(7)	102(1)	
C(6)	-Co(2) -C(7)	98(1)	
Co(1)	-Co(3) -Co(2)	60.0(1)	
Co(1)	-Co(3) -C(1)	49.6(8)	
Co(1)	-Co(3) -C(8)	97.3(8)	
Co(1)	-Co(3) -C(9)	155.6(7)	
Co(1)	-Co(3) -C(10)	98.7(9)	
Co(2)	-Co(3) -C(1)	49.3(7)	
Co(2)	-Co(3) -C(8)	99.0(8)	
Co(2)	-Co(3) -C(9)	98.5(7)	
Co(2)	-Co(3) -C(10)	148.5(9)	
Si(1)	-Co(4) -C(14)	83(1)	
C(11)	-Co(4) -C(12)	96(2)	
C(11)	-Co(4) -C(13)	94(2)	
C(11)	-Co(4) -C(14)	95(1)	
C(12)	-Co(4) -C(13)	118(1)	
C(12)	-Co(4) -C(14)	119(1)	
C(13)	-Co(4) -C(14)	119(1)	
Co(4)	-Si(1) -Cl(1)	114.2(4)	
Co(4)	-Si(1) -Cl(2)	114.3(4)	
Co(4)	-Si(1) -O(1)	108.9(6)	
Cl(1)	-Si(1) -Cl(2)	104.2(5)	
Cl(1)	-Si(1) -O(1)	107.0(7)	
Cl(2)	-Si(1) -O(1)	107.8(6)	
Co(1)	-C(1) -Co(2)	81(1)	
Co(1)	-C(1) -Co(3)	81.9(9)	
Co(1)	-C(1) -O(1)	124(2)	
Co(2)	-C(1) -Co(3)	82(1)	
Co(2)	-C(1) -O(1)	132(2)	
Co(3)	-C(1) -O(1)	134(2)	
Si(1)	-O(1) -C(1)	135(2)	
Co(1)	-C(2) -O(2)	178(3)	
Co(1)	-C(3) -O(3)	176(2)	
Co(2)	-C(5) -O(5)	177(2)	
Co(2)	-C(6) -O(6)	176(2)	
Co(2)	-C(7) -O(7)	175(2)	
Co(3)	-C(8) -O(8)	176(2)	
Co(3)	-C(9) -O(9)	176(2)	
Co(3)	-C(10) -O(10)	178(3)	
Co(4)	-C(13) -O(13)	175(3)	
Co(4)	-C(14) -O(14)	178(3)	

APPENDIX EIGHT

FINAL POSITIONAL AND EQUIVALENT THERMAL PARAMETERS $[Et_4N]_2[Co_6C(CO)_{15}]$

ATOM	X/A	Y/B	Z/C	Ueq/U11
Co(1)	0.1673(2)	0.9043(1)	0.3020(1)	0.028
Co(2)	0.2130(2)	0.8075(1)	0.2449(1)	0.032
Co(3)	0.2384(2)	0.9045(1)	0.1856(1)	0.031
Co(4)	0.4507(2)	0.9086(1)	0.3470(1)	0.031
Co(5)	0.4989(2)	0.8123(1)	0.2898(1)	0.035
Co(6)	0.5228(2)	0.9101(1)	0.2298(1)	0.033
C(0)	0.349(2)	0.8739(6)	0.2684(8)	0.028(3)
C(1)	0.273(2)	0.9339(7)	0.3797(8)	0.030(4)
O(1)	0.237(1)	0.9588(5)	0.4279(6)	0.045(3)
C(2)	0.362(2)	0.7497(7)	0.2693(8)	0.031(4)
O(2)	0.366(1)	0.6967(5)	0.2736(6)	0.045(3)
C(3)	0.411(2)	0.9359(8)	0.1508(9)	0.039(5)
O(3)	0.436(1)	0.9598(5)	0.1017(6)	0.047(3)
C(4)	0.127(2)	0.8225(7)	0.3260(8)	0.028(4)
O(4)	0.077(1)	0.7971(5)	0.3699(6)	0.054(3)
C(5)	0.234(2)	0.8226(8)	0.1533(9)	0.047(5)
O(5)	0.233(1)	0.7968(6)	0.1031(6)	0.056(4)
C(6)	0.164(2)	0.9691(7)	0.2397(9)	0.036(4)
O(6)	0.142(1)	1.0202(5)	0.2351(6)	0.043(3)
C(7)	0.479(2)	0.8297(7)	0.3818(8)	0.034(4)
O(7)	0.485(1)	0.8031(6)	0.4326(6)	0.054(3)
C(8)	0.582(2)	0.8299(8)	0.2079(9)	0.044(5)
O(8)	0.641(2)	0.8046(6)	0.1665(7)	0.069(4)
C(9)	0.516(2)	0.9749(7)	0.2925(8)	0.036(4)
O(9)	0.546(1)	1.0232(5)	0.3017(6)	0.050(3)
C(10)	-0.007(2)	0.9269(7)	0.3243(8)	0.035(4)
O(10)	-0.119(1)	0.9422(5)	0.3433(6)	0.052(3)
C(11)	0.064(2)	0.7579(9)	0.2214(9)	0.056(5)
O(11)	-0.026(1)	0.7225(6)	0.2053(6)	0.058(4)
C(12)	0.115(2)	0.9291(7)	0.1197(9)	0.042(5)
O(12)	0.037(1)	0.9484(6)	0.0759(6)	0.059(4)
C(13)	0.567(2)	0.9377(8)	0.4126(9)	0.043(5)
O(13)	0.643(1)	0.9570(6)	0.4576(7)	0.064(4)
C(14)	0.653(2)	0.7670(8)	0.3146(9)	0.051(5)
O(14)	0.752(2)	0.7353(6)	0.3340(7)	0.074(4)
C(15)	0.691(2)	0.9373(7)	0.2050(8)	0.039(4)
O(15)	0.797(2)	0.9592(6)	0.1860(7)	0.070(4)
N(1)	-0.033(1)	0.1276(6)	0.4003(7)	0.041(4)
C(16)	-0.156(2)	0.0891(9)	0.427(1)	0.063(6)
C(17)	-0.306(2)	0.1245(9)	0.435(1)	0.060(5)
C(18)	-0.091(2)	0.1569(9)	0.333(1)	0.068(6)

C(19)	-0.148(2)	0.1104(8)	0.2801(9)	0.056(5)
C(20)	0.102(2)	0.0850(9)	0.393(1)	0.062(6)
C(21)	0.244(2)	0.1185(8)	0.3682(9)	0.056(5)
C(22)	0.015(2)	0.1819(9)	0.445(1)	0.070(6)
C(23)	0.092(3)	0.156(1)	0.516(1)	0.095(8)
N(2)	0.316(1)	0.1341(6)	0.0607(7)	0.042(4)
C(24)	0.194(2)	0.0851(7)	0.0637(8)	0.040(4)
C(25)	0.050(2)	0.1061(8)	0.0962(9)	0.058(5)
C(26)	0.250(2)	0.1931(8)	0.0332(9)	0.049(5)
C(27)	0.165(2)	0.186(1)	-0.038(1)	0.071(6)
C(28)	0.435(2)	0.1068(8)	0.0209(9)	0.058(5)
C(29)	0.577(2)	0.147(1)	0.015(1)	0.078(7)
C(30)	0.387(2)	0.1505(7)	0.1312(8)	0.039(4)
C(31)	0.466(2)	0.0992(9)	0.170(1)	0.066(6)

THERMAL PARAMETERS FOR $[Et_4N]_2[Co_6C(CO)_{15}]$

ATOM	U11	U22	U33	U23	U13	U12
Co(1)	0.023(1)	0.034(1)	0.028(2)	-0.001(1)	0.003(1)	0.000(1)
Co(2)	0.028(1)	0.035(1)	0.032(2)	-0.003(1)	0.005(1)	-0.002(1)
Co(3)	0.025(1)	0.037(2)	0.031(2)	0.000(1)	0.002(1)	-0.002(1)
Co(4)	0.023(1)	0.039(2)	0.030(2)	-0.001(1)	0.001(1)	-0.001(1)
Co(5)	0.027(1)	0.037(2)	0.041(2)	0.001(1)	0.005(1)	0.004(1)
Co(6)	0.025(1)	0.041(2)	0.033(2)	0.001(1)	0.006(1)	-0.002(1)

SELECTED BOND LENGTHS AND ANGLES FOR $[Et_4N]_2[Co_6C(CO)_{15}]$

BOND LENGTHS (Å) FOR $[Et_4N]_2[Co_6C(CO)_{15}]$

Co(1)	---Co(2)	2.526(3)	Co(6)	---C(3)	1.89(2)
Co(1)	---Co(3)	2.532(3)	Co(6)	---C(8)	1.94(2)
Co(1)	---Co(4)	2.559(3)	Co(6)	---C(9)	1.95(2)
Co(1)	---C(0)	1.93(2)	Co(6)	---C(15)	1.72(2)
Co(1)	---C(1)	1.87(2)	C(1)	---O(1)	1.21(2)
Co(1)	---C(4)	1.95(2)	C(2)	---O(2)	1.20(2)
Co(1)	---C(6)	1.94(2)	C(3)	---O(3)	1.18(2)
Co(1)	---C(10)	1.72(2)	C(4)	---O(4)	1.19(2)
Co(2)	---Co(3)	2.519(3)	C(5)	---O(5)	1.18(2)
Co(2)	---Co(5)	2.579(3)	C(6)	---O(6)	1.17(2)
Co(2)	---C(0)	1.94(1)	C(7)	---O(7)	1.20(2)
Co(2)	---C(2)	1.87(2)	C(8)	---O(8)	1.19(2)
Co(2)	---C(4)	1.93(2)	C(9)	---O(9)	1.13(2)
Co(2)	---C(5)	1.94(2)	C(10)	---O(10)	1.15(2)
Co(2)	---C(11)	1.75(2)	C(11)	---O(11)	1.14(2)

Co(3)	---Co(6)	2.564(3)	C(12)	---O(12)	1.15(2)
Co(3)	---C(0)	1.98(2)	C(13)	---O(13)	1.16(2)
Co(3)	---C(3)	1.88(2)	C(14)	---O(14)	1.16(2)
Co(3)	---C(5)	1.96(2)	C(15)	---O(15)	1.16(2)
Co(3)	---C(6)	1.98(2)	N(1)	---C(16)	1.53(2)
Co(3)	---C(12)	1.73(2)	N(1)	---C(18)	1.56(2)
Co(4)	---Co(5)	2.521(3)	N(1)	---C(20)	1.54(2)
Co(4)	---Co(6)	2.551(3)	N(1)	---C(22)	1.55(2)
Co(4)	---C(0)	1.92(2)	C(16)	---C(17)	1.57(3)
Co(4)	---C(1)	1.86(2)	C(18)	---C(19)	1.55(3)
Co(4)	---C(7)	1.92(2)	C(20)	---C(21)	1.59(3)
Co(4)	---C(9)	1.99(2)	C(22)	---C(23)	1.65(3)
Co(4)	---C(13)	1.73(2)	N(2)	---C(24)	1.54(2)
Co(5)	---Co(6)	2.540(3)	N(2)	---C(26)	1.53(2)
Co(5)	---C(0)	1.93(1)	N(2)	---C(28)	1.52(2)
Co(5)	---C(2)	1.87(2)	N(2)	---C(30)	1.55(2)
Co(5)	---C(7)	1.95(2)	C(24)	---C(25)	1.57(2)
Co(5)	---C(8)	1.94(2)	C(26)	---C(27)	1.56(3)
Co(5)	---C(14)	1.73(2)	C(28)	---C(29)	1.55(3)
Co(6)	---C(0)	1.97(2)	C(30)	---C(31)	1.53(2)

BOND ANGLES (°) FOR $[Et_4N]_2[Co_6C(CO)_{15}]$

Co(2)	-Co(1)	-Co(3)	59.7(1)	Co(2)	-Co(5)	-C(14)	141.5(6)
Co(2)	-Co(1)	-Co(4)	90.0(1)	Co(4)	-Co(5)	-Co(6)	60.6(1)
Co(2)	-Co(1)	-C(0)	49.4(4)	Co(4)	-Co(5)	-C(0)	48.9(5)
Co(2)	-Co(1)	-C(1)	127.7(5)	Co(4)	-Co(5)	-C(2)	127.8(5)
Co(2)	-Co(1)	-C(4)	49.1(5)	Co(4)	-Co(5)	-C(7)	48.8(5)
Co(2)	-Co(1)	-C(6)	109.6(5)	Co(4)	-Co(5)	-C(8)	108.9(5)
Co(2)	-Co(1)	-C(10)	124.6(5)	Co(4)	-Co(5)	-C(14)	122.4(6)
Co(3)	-Co(1)	-Co(4)	90.4(1)	Co(6)	-Co(5)	-C(0)	50.2(4)
Co(3)	-Co(1)	-C(0)	50.5(5)	Co(6)	-Co(5)	-C(2)	129.0(5)
Co(3)	-Co(1)	-C(1)	130.5(5)	Co(6)	-Co(5)	-C(7)	108.4(5)
Co(3)	-Co(1)	-C(4)	108.1(5)	Co(6)	-Co(5)	-C(8)	49.2(5)
Co(3)	-Co(1)	-C(6)	50.6(5)	Co(6)	-Co(5)	-C(14)	123.3(6)
Co(3)	-Co(1)	-C(10)	124.6(5)	C(0)	-Co(5)	-C(2)	94.7(6)
Co(4)	-Co(1)	-C(0)	48.2(5)	C(0)	-Co(5)	-C(7)	86.8(7)
Co(4)	-Co(1)	-C(1)	46.4(5)	C(0)	-Co(5)	-C(8)	88.3(7)
Co(4)	-Co(1)	-C(4)	98.2(4)	C(0)	-Co(5)	-C(14)	170.1(8)
Co(4)	-Co(1)	-C(6)	98.8(5)	C(2)	-Co(5)	-C(7)	104.1(7)
Co(4)	-Co(1)	-C(10)	138.8(5)	C(2)	-Co(5)	-C(8)	104.8(7)
C(0)	-Co(1)	-C(1)	94.5(6)	C(2)	-Co(5)	-C(14)	95.0(8)
C(0)	-Co(1)	-C(4)	86.3(6)	C(7)	-Co(5)	-C(8)	151.0(7)
C(0)	-Co(1)	-C(6)	89.2(7)	C(7)	-Co(5)	-C(14)	89.1(8)
C(0)	-Co(1)	-C(10)	173.0(7)	C(8)	-Co(5)	-C(14)	91.0(8)
C(1)	-Co(1)	-C(4)	102.0(7)	Co(3)	-Co(6)	-Co(4)	89.9(1)
C(1)	-Co(1)	-C(6)	105.3(7)	Co(3)	-Co(6)	-Co(5)	89.9(1)
C(1)	-Co(1)	-C(10)	92.4(7)	Co(3)	-Co(6)	-C(0)	49.7(4)

C(4)	-Co(1) -C(6)	152.6(7)	
C(4)	-Co(1) -C(10)	91.1(7)	
C(6)	-Co(1) -C(10)	90.1(7)	
Co(1)	-Co(2) -Co(3)	60.3(1)	
Co(1)	-Co(2) -Co(5)	89.8(1)	
Co(1)	-Co(2) -C(0)	49.1(4)	
Co(1)	-Co(2) -C(2)	128.1(5)	
Co(1)	-Co(2) -C(4)	49.7(4)	
Co(1)	-Co(2) -C(5)	109.6(6)	
Co(1)	-Co(2) -C(11)	121.8(6)	
Co(3)	-Co(2) -Co(5)	90.0(1)	
Co(3)	-Co(2) -C(0)	50.7(5)	
Co(3)	-Co(2) -C(2)	129.4(5)	
Co(3)	-Co(2) -C(4)	109.2(5)	
Co(3)	-Co(2) -C(5)	50.1(5)	
Co(3)	-Co(2) -C(11)	121.7(6)	
Co(5)	-Co(2) -C(0)	48.0(4)	
Co(5)	-Co(2) -C(2)	46.4(5)	
Co(5)	-Co(2) -C(4)	98.4(4)	
Co(5)	-Co(2) -C(5)	98.4(5)	
Co(5)	-Co(2) -C(11)	142.6(6)	
C(0)	-Co(2) -C(2)	94.4(6)	
C(0)	-Co(2) -C(4)	86.6(6)	
C(0)	-Co(2) -C(5)	89.1(7)	
C(0)	-Co(2) -C(11)	169.3(8)	
C(2)	-Co(2) -C(4)	102.7(7)	
C(2)	-Co(2) -C(5)	104.1(7)	
C(2)	-Co(2) -C(11)	96.2(8)	
C(4)	-Co(2) -C(5)	153.1(7)	
C(4)	-Co(2) -C(11)	89.7(8)	
C(5)	-Co(2) -C(11)	89.6(8)	
Co(1)	-Co(3) -Co(2)	60.0(1)	
Co(1)	-Co(3) -Co(6)	90.0(1)	
Co(1)	-Co(3) -C(0)	48.8(4)	
Co(1)	-Co(3) -C(3)	130.6(5)	
Co(1)	-Co(3) -C(5)	108.6(6)	
Co(1)	-Co(3) -C(6)	48.9(5)	
Co(1)	-Co(3) -C(12)	122.7(6)	
Co(2)	-Co(3) -Co(6)	90.4(1)	
Co(2)	-Co(3) -C(0)	49.3(4)	
Co(2)	-Co(3) -C(3)	128.8(5)	
Co(2)	-Co(3) -C(5)	49.3(5)	
Co(2)	-Co(3) -C(6)	108.2(5)	
Co(2)	-Co(3) -C(12)	125.0(6)	
Co(6)	-Co(3) -C(0)	49.5(4)	
Co(6)	-Co(3) -C(3)	47.3(5)	
Co(6)	-Co(3) -C(5)	98.6(5)	
Co(6)	-Co(3) -C(6)	97.9(5)	
Co(6)	-Co(3) -C(12)	139.7(6)	
C(0)	-Co(3) -C(3)	96.7(7)	
Co(3)	-Co(6) -C(3)	47.0(5)	
Co(3)	-Co(6) -C(8)	98.6(5)	
Co(3)	-Co(6) -C(9)	99.8(5)	
Co(3)	-Co(6) -C(15)	138.2(6)	
Co(4)	-Co(6) -Co(5)	59.4(1)	
Co(4)	-Co(6) -C(0)	48.2(5)	
Co(4)	-Co(6) -C(3)	130.5(5)	
Co(4)	-Co(6) -C(8)	107.8(5)	
Co(4)	-Co(6) -C(9)	50.2(5)	
Co(4)	-Co(6) -C(15)	126.3(6)	
Co(5)	-Co(6) -C(0)	48.7(4)	
Co(5)	-Co(6) -C(3)	128.1(5)	
Co(5)	-Co(6) -C(8)	49.2(5)	
Co(5)	-Co(6) -C(9)	108.6(5)	
Co(5)	-Co(6) -C(15)	124.7(6)	
C(0)	-Co(6) -C(3)	96.7(7)	
C(0)	-Co(6) -C(8)	87.1(7)	
C(0)	-Co(6) -C(9)	87.9(7)	
C(0)	-Co(6) -C(15)	172.1(7)	
C(3)	-Co(6) -C(8)	102.4(7)	
C(3)	-Co(6) -C(9)	106.5(7)	
C(3)	-Co(6) -C(15)	91.2(7)	
C(8)	-Co(6) -C(9)	151.1(7)	
C(8)	-Co(6) -C(15)	90.1(7)	
C(9)	-Co(6) -C(15)	91.0(7)	
Co(1)	-C(0) -Co(2)	81.5(6)	
Co(1)	-C(0) -Co(3)	80.7(6)	
Co(1)	-C(0) -Co(4)	83.3(6)	
Co(1)	-C(0) -Co(5)	138.1(9)	
Co(1)	-C(0) -Co(6)	134.8(8)	
Co(2)	-C(0) -Co(3)	80.0(6)	
Co(2)	-C(0) -Co(4)	137.6(9)	
Co(2)	-C(0) -Co(5)	83.6(6)	
Co(2)	-C(0) -Co(6)	134.5(9)	
Co(3)	-C(0) -Co(4)	135.7(8)	
Co(3)	-C(0) -Co(5)	134.5(9)	
Co(3)	-C(0) -Co(6)	80.8(6)	
Co(4)	-C(0) -Co(5)	81.8(6)	
Co(4)	-C(0) -Co(6)	81.9(6)	
Co(5)	-C(0) -Co(6)	81.2(6)	
Co(1)	-C(1) -Co(4)	86.7(7)	
Co(1)	-C(1) -O(1)	135(1)	
Co(4)	-C(1) -O(1)	138(1)	
Co(2)	-C(2) -Co(5)	87.1(6)	
Co(2)	-C(2) -O(2)	136(1)	
Co(5)	-C(2) -O(2)	135(1)	
Co(3)	-C(3) -Co(6)	85.7(7)	
Co(3)	-C(3) -O(3)	136(1)	
Co(6)	-C(3) -O(3)	137(1)	
Co(1)	-C(4) -Co(2)	81.2(6)	

C(0)	-Co(3)	-C(5)	87.3(7)
C(0)	-Co(3)	-C(6)	86.4(7)
C(0)	-Co(3)	-C(12)	170.5(7)
C(3)	-Co(3)	-C(5)	102.3(7)
C(3)	-Co(3)	-C(6)	105.5(7)
C(3)	-Co(3)	-C(12)	92.5(8)
C(5)	-Co(3)	-C(6)	152.0(7)
C(5)	-Co(3)	-C(12)	92.8(8)
C(6)	-Co(3)	-C(12)	89.2(7)
Co(1)	-Co(4)	-Co(5)	90.4(1)
Co(1)	-Co(4)	-Co(6)	89.7(1)
Co(1)	-Co(4)	-C(0)	48.5(4)
Co(1)	-Co(4)	-C(1)	46.9(5)
Co(1)	-Co(4)	-C(7)	100.4(4)
Co(1)	-Co(4)	-C(9)	99.0(4)
Co(1)	-Co(4)	-C(13)	139.8(6)
Co(5)	-Co(4)	-Co(6)	60.1(1)
Co(5)	-Co(4)	-C(0)	49.3(4)
Co(5)	-Co(4)	-C(1)	128.5(5)
Co(5)	-Co(4)	-C(7)	49.9(5)
Co(5)	-Co(4)	-C(9)	108.1(5)
Co(5)	-Co(4)	-C(13)	125.0(6)
Co(6)	-Co(4)	-C(0)	50.0(4)
Co(6)	-Co(4)	-C(1)	130.0(5)
Co(6)	-Co(4)	-C(7)	109.0(5)
Co(6)	-Co(4)	-C(9)	49.0(5)
Co(6)	-Co(4)	-C(13)	122.8(6)
C(0)	-Co(4)	-C(1)	95.4(6)
C(0)	-Co(4)	-C(7)	88.0(6)
C(0)	-Co(4)	-C(9)	88.3(7)
C(0)	-Co(4)	-C(13)	171.5(7)
C(1)	-Co(4)	-C(7)	103.3(7)
C(1)	-Co(4)	-C(9)	106.2(7)
C(1)	-Co(4)	-C(13)	93.0(7)
C(7)	-Co(4)	-C(9)	150.4(7)
C(7)	-Co(4)	-C(13)	91.2(7)
C(9)	-Co(4)	-C(13)	88.2(8)
Co(2)	-Co(5)	-Co(4)	89.7(1)
Co(2)	-Co(5)	-Co(6)	89.6(1)
Co(2)	-Co(5)	-C(0)	48.3(4)
Co(2)	-Co(5)	-C(2)	46.4(5)
Co(2)	-Co(5)	-C(7)	99.5(4)
Co(2)	-Co(5)	-C(8)	98.3(5)

Co(1)	-C(4)	-O(4)	137(1)
Co(2)	-C(4)	-O(4)	141(1)
Co(2)	-C(5)	-Co(3)	80.6(7)
Co(2)	-C(5)	-O(5)	140(2)
Co(3)	-C(5)	-O(5)	139(2)
Co(1)	-C(6)	-Co(3)	80.5(6)
Co(1)	-C(6)	-O(6)	141(2)
Co(3)	-C(6)	-O(6)	137(2)
Co(4)	-C(7)	-Co(5)	81.3(6)
Co(4)	-C(7)	-O(7)	141(1)
Co(5)	-C(7)	-O(7)	137(1)
Co(5)	-C(8)	-Co(6)	81.6(7)
Co(5)	-C(8)	-O(8)	139(2)
Co(6)	-C(8)	-O(8)	139(2)
Co(4)	-C(9)	-Co(6)	80.8(6)
Co(4)	-C(9)	-O(9)	135(2)
Co(6)	-C(9)	-O(9)	143(2)
Co(1)	-C(10)	-O(10)	175(2)
Co(2)	-C(11)	-O(11)	175(2)
Co(3)	-C(12)	-O(12)	176(2)
Co(4)	-C(13)	-O(13)	178(2)
Co(5)	-C(14)	-O(14)	175(2)
Co(6)	-C(15)	-O(15)	174(2)
C(16)	-N(1)	-C(18)	112(1)
C(16)	-N(1)	-C(20)	105(1)
C(16)	-N(1)	-C(22)	113(1)
C(18)	-N(1)	-C(20)	110(1)
C(18)	-N(1)	-C(22)	103(1)
C(20)	-N(1)	-C(22)	112(1)
N(1)	-C(16)	-C(17)	112(2)
N(1)	-C(18)	-C(19)	112(2)
N(1)	-C(20)	-C(21)	112(2)
N(1)	-C(22)	-C(23)	107(2)
C(24)	-N(2)	-C(26)	113(1)
C(24)	-N(2)	-C(28)	104(1)
C(24)	-N(2)	-C(30)	110(1)
C(26)	-N(2)	-C(28)	114(1)
C(26)	-N(2)	-C(30)	103(1)
C(28)	-N(2)	-C(30)	111(1)
N(2)	-C(24)	-C(25)	113(1)
N(2)	-C(26)	-C(27)	112(2)
N(2)	-C(28)	-C(29)	114(2)
N(2)	-C(30)	-C(31)	114(1)

STRUCTURES OF COMMONLY DISCUSSED COMPOUNDS

{1}

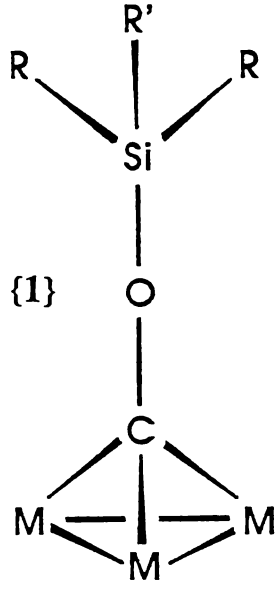

{2}

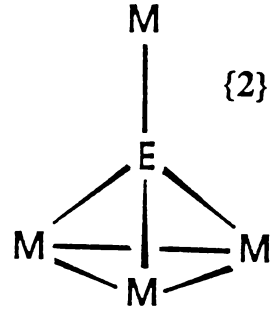

{3}

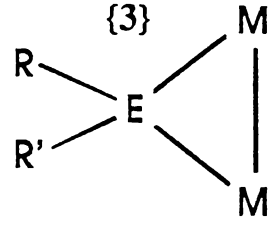

{4}

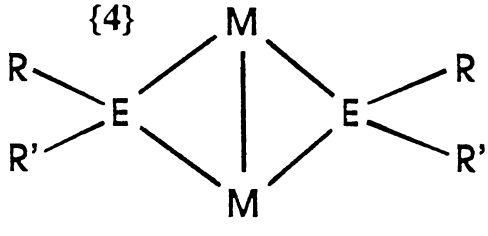

{5}

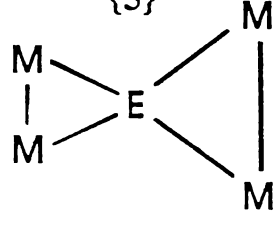

{6}

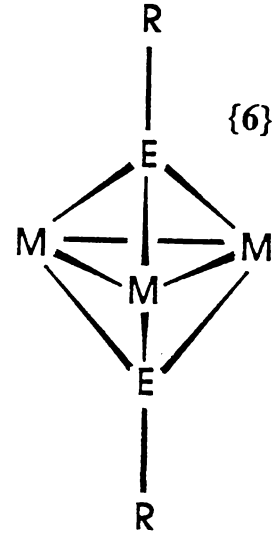

{7}

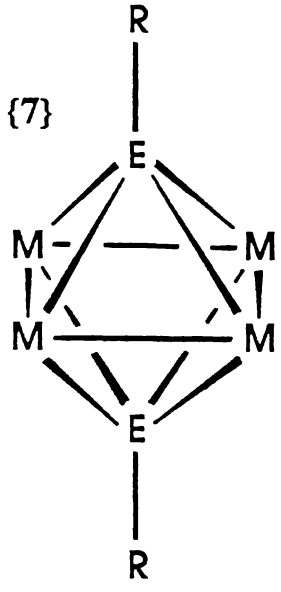

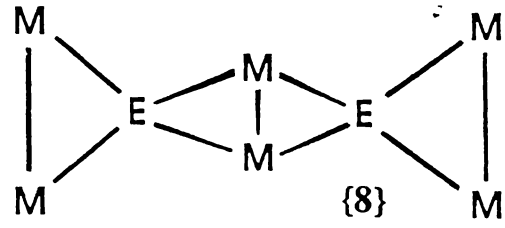

{8}

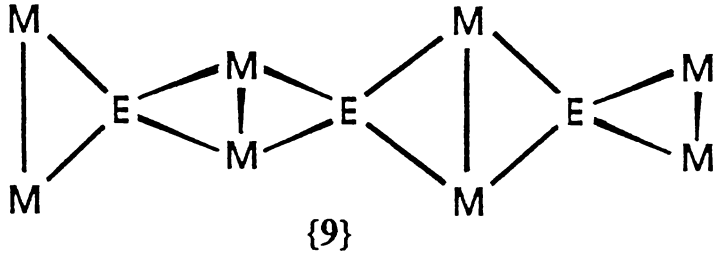

{9}

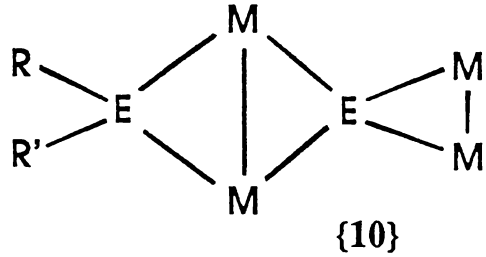

{10}

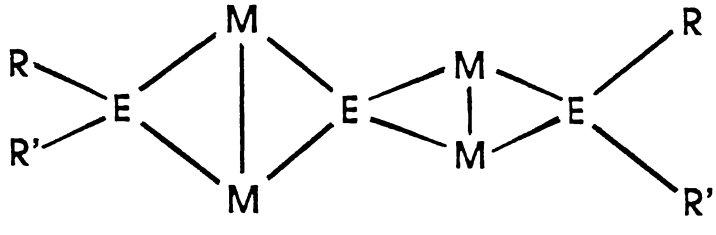

{11}

REFERENCES

REFERENCES

1 B.J Aylett,
Adv. Inorg. Chem. Radiochem. vol. 25 (1982)

2 B.K. Nicholson, K.M. Mackay and R.F. Gerlach,
Rev. of Silicon, Germanium and Tin Cpds. 5, 67 (1981)

3 K.H. Whitmire,
J. Coord. Chem. 17, 95 (1988)

4 J.N. Nicholls,
Pollhedron, 3 (1984), 1307

5 K.M. Mackay and B.K. Nicholson,
Comprehensive Organometallic Chemistry, 6, Ch 43, 1043

6 F. Glocking and S.R. Stobart,
"M.T.P" International Review of Science,
Inorganic Chemistry Series One,
Butterworths, London, (1972), Vol 6, p 64-119

7 K.M. Mackay and B.K. Nicholson,
"Comprehensive Organometallic Chemistry",
ed. G. Wilkinson, F.G.A Stone and E.W. Abel,
Permagon Press, (1982), Chapter 43

8 R.F. Gerlach, K.M. Mackay, B.K. Nicholson and
W.T. Robinson,
J. Chem. Soc. (Dalton). 80, (1981)

9 S.P. Foster, K.M. Mackay and B.K. Nicholson,
J. Chem. Soc., Chem. Comm. 1156 (1982)

10 A. Bonny,
Coordination Chem. Reviews. 25, 229 (1978)

11 M. Elder,
Inorg. Chem. 9, 762 (1970)

12 R. Ball, M.J. Bennett, E.H. Brooks, W.A.G. Graham,
J. Hoyano and S.M. Illingworth,
J. Chem. Soc., Chem. Comm. p.592 (1970)

13 K.M. Abraham, G. Urry,
Inorg. Chem. 12, 2850 (1973)

14 M.J. Bennett and K.A. Simpson,
J. Am. Chem. Soc. 93, 7156 (1971)

15 A.L. Bikovetz, O.V. Kuzmin, V.M. Vdovin and A.M. Krapivin,
J. Organomet. Chem. 194, C33 (1980)

16 A. Brookes, S.A.R. Knox and F.G.A. Stone,
J. Chem. Soc. A. p.3469 (1971)

17 M. Cowie and M.J. Bennett,
Inorg. Chem. 16, 2321 (1977)

18 M. Cowie and M.J. Bennett,
Inorg. Chem. 16, 2325 (1977)

19 M.M. Crozat and S.F. Watkins,
J. Chem. Soc., Dalton Trans. p.2512 (1972)

20 S.A. Fieldhouse, A.J. Cleland, B.H. Freeland,
C.D.M. Mann and R.J. O'Brien,
J. Chem. Soc. A. p.2536 (1971)

21 M. Ciriano, J.A.K. Howard, J.L. Spencer,
F.G.A. Stone and H. Wadepohl,
J. Chem. Soc., Dalton Trans. p.1749 (1979)

22 W. Malisch and W. Ries,
Angew. Chem., Int. Ed. Engl. 17, 120 (1978)

23 G. Schmid,
Angew. Chem., Int. Ed. Engl. 17, 392 (1978)

24 G.L. Simon and L.F. Dahl,
J. Am. Chem. Soc. 95, 783 (1973)

25 M.J. Bennett, W.A.G. Graham, J.K. Hoyano and
W.L. Hutcheon,
J. Am. Chem. Soc. 94, 6232 (1972)

26 A.J. Cleland, S.A. Fieldhouse, B.H. Freeland and
R.J. O'Brien,
J. Organomet. Chem. 32, C15 (1971)

27 R.C. Kerber and T. Pakkanen,
Inorg. Chim. Acta. 37, 61 (1979)

28 D. Kummer and J. Furrer,
Z. Naturforsch., B: Anorg. Chem., Org. Chem., Biochem., Biophys., Biol. 26B, 162 (1971)

29 G. Schmid and E. Welz,
Z. Naturforsch., B: Anorg. Chem., Org. Chem.
34B, 929 (1979)

30 G. Schmid and H.J. Balk,
J. Organomet. Chem. 80, 257 (1974)

31 G. Fritz and K. Hohenberger,
Z. Anorg. Allg. Chem. 464, 107 (1980)

32 O.V. Kuz'm, A.L. Bykoivets and V.M. Vdovin,
Izv. Akad Nauk. SSSR, Ser. Khim. 1448 (1980)

33 P. Gusbeth and H. Vahrenkamp,
Chem. Ber. 118, 1143 (1985)

34 K.M Mackay, B.K. Nicholson, W.T. Robinson and A.W. Sims,
J. Chem. Soc. Chem. Comm. 1276 (1984)

35 M.L. Van Tiel, K.M. Mackay and B.K. Nicholson,
J. Organomet. Chem. 326, C101 (1987)

36 S. Anema, PhD Thesis, University of Waikato (1989)

37 S.K. Lee, PhD Thesis, University of Waikato (1989)

38 S.G. Anema, K.M. Mackay, B.K. Nicholson and M.L. Van Tiel
Organometallics vol 9, 2436 (1990)

39 J.L. Vidal, W.E. Walker, R.L. Pruett and R.C. Schoening.
Inorg. Chem. 18, 129 (1979)

40 V.G. Albano, P. Chini, G. Ciani, M. Sansoni, D. Strumolo,
B.T. Heaton and S. Martinengo,
J. Amer. Chem. Soc. 98, 5027 (1976)

41 V.G. Albano, D. Braga, P. Chini, G. Ciani and
S. Martinengo,
J. Chem. Soc. Dalton Trans. 645 (1982)

42 J.T. McNeese, S. Wreford, L.D. Tipton and R. Bau
J. Chem. Soc., Chem. Comm. (1977) 390

43 K.M. Mackay and Tan Cham Chee,
J. Chem. Res. (S). 229 (1982)

44 W. Malisch, H.U. Wekel, I. Grob, F.H. Kohler and M. Bundler.
Z. Naturforsch. B. 37 (1982), 601

45 M.L. Van Tiel, M.Sc Thesis, University of Waikato (1987)

46 G. Schmid, V. Batzel and G. Etzrodt.
J. Organometal. Chem. 112, 345 (1976)

47 K.M. Mackay, B.K. Nicholson, A.W. Sims and C.C. Tan,
Acta. Cryst. C43, 633 (1987)

48 Glen C. Barris, PhD Thesis, University of Waikato (1990)

49 J.D. Cotton, S.A.R. Knox, I. Paul and F.G.A. Stone,
J. Chem. Soc. A. 264 (1967)

50 P.F. Lindley and P. Woodward,
J. Chem. Soc. A. 382 (1967)

51 K.H. Whitmire, C.B. Lagrone, M.R. Churchill, J.C. Fettinger and B.H. Robinson,
Inorg. Chem. 26, 3491 (1987)

52 O.V. Kuz'm, A.L. Bykoivets and V.M. Vdovin,
Izv. Akad Nauk. SSSR, Ser. Khim. 1448 (1980)

53 A.S. Batsanov, L.V. Rybin, M.I. Rybinskaya, Yu.T. Struchkov, I.M. Salimgareeva and N.G. Bogatova,
J. Organomet. Chem. 249, 319 (1983)

54 D. Meltzer and E. Weiss,
J. Organomet. Chem. 255, 335 (1983)

55 J.D. Cotton and R.M. Peachey,
Inorg. Chem. Nucl. Lett. 6, 727 (1970)

56 B.K. Nicholson and J. Simpson.
J. Organomet. Chem. 155 (1978), 237

57 S.A.R Knox and F.G.A. Stone,
J. Chem. Soc. A, (1971), 2874

58 J. Howard, S.A.R. Knox, F.G.A. Stone and P. Woodward,
J. Chem. Soc., Chem. Comm., (1970), 1477

59 J. Howard and P. Woodward,
J. Chem. Soc. A, 22, (1971) 3648

60 L.F. Dahl and R.E. Rundle
Acta Crystallogr. 16, 419 (1963)

61 R. Bau, B. Fontal, H.D. Kaesz and M.R. Churchill,
J. Am. Chem. Soc. 89, 6374 (1967)

62 M.R. Churchill, P.H. Bird, H.D. Kaesz, R. Bau and
B. Fontal,
J. Am. Chem. Soc. 90, 7135 (1968)

63 H. Tobita, Y. Kawano, M. Shimoi and H. Ogino,
Chem. Lett. 2247, (1987)

64 Wei-Dong Wang, S.I. Hommeltoft and R. Eisenberg,
Organometallics, 7, 2417 (1988)

65 W. Kruppa and G. Schmid,
J. Organomet. Chem. 202, (1980) 379

66 D. Seyferth,
Advan. Organometal. Chem., 14, (1976) 98

67 J.D. Smith and J.D. Corbett,
J. Am. Chem. Soc. 108, 1927 (1986)

68 J.D. Smith and J.D. Corbett,
J. Am. Chem. Soc. 107, 5704 (1985)

69 R.F. Bryan, P.T. Greene, M.J. Newlands and D.S. Field,
J. Chem. Soc., A, (1970) 3068

70 R.D. Adams, M.D. Brice and F.A. Cotton,
Inorg. Chem. 13, (1974) 1080

71 S.P. Foster, K.M. Mackay and B.K. Nicholson,
Inorg. Chem. 24 (1985), 909

72 S.G. Anema, K.M. Mackay, L.C. McLeod, B.K. Nicholson and J.M. Whittaker,
Angew. Chem. Int. Ed. Engl. 24 (1986), 759

73 S.P. Foster,
D. Phil. Thesis. University of Waikato. (1982)

74 K.M. Mackay and B.K. Nicholson,
Chem. in N.Z. (1984), Dec., 160

75 S.P. Foster and K.M. Mackay,
J. Organometal. Chem. 238 (1982), C46

76 L.C. McLeod,
M. Phil. Thesis, University of Waikato, 1987

77 J.M. Wittaker,
M.Sc. Thesis, University of Waikato, 1986

78 M. Service,
D. Phil. Thesis, University of Waikato, 1988

79 P. Gusbeth and H. Vahrenkamp.
Chem. Ber. 118 (1985), 1143

80 F.H. Kohler
Z. Naturforsch. B. 37 (1982), 601

81 R.D. Adams and J.E. Babin,
Inorg. Chem. 25, 3418 (1986)

82 G. Etzrodt and G. Schmid,
J. Organomet. Chem. 169 (1979), 259

83 B.W. Graham,
D. Phil. Thesis. University of Waikato. (1973)

84 S.A. Fieldhouse, A.J. Cleland, B.H. Freeland, C.D.M. Mann and R.J. O'Brien,
J. Chem. Soc. (A), (1971), 2536

85 L.G.L. Ward,
Inorganic Syntheses, Vol 11 (1968), 159

86 J.E. Drake, R.T. Hemmings and H.E. Henderson,
Inorganic Syntheses, Vol 18 (1978), 161

87 M. Elder and D. Hall,
Inorg. Chem., 8, 1424 (1969)

88 E.H. Brooks, M. Elder, W.A.G. Graham and D. Hall,
J. Amer. Chem. Soc., 90, 3587 (1968)

89 K. Triplett and M.D. Curtis,
Inorg. Chem., 14, 2284 (1975)

90 R.H. Summerville and R. Hoffman,
J. Amer. Chem. Soc., 101, 3821 (1979)

91 P. Gusbeth and H. Vahrenkamp,
Chem. Ber. 118, 1746 (1985)

92 C.H. Wei and L.F. Dahl,
Cryst. Struct. Comm., 4, 583 (1975)

93 R.C. Ryan and L.F. Dahl.
J. Am. Chem. Soc. 97 (1975), 6904

94 F. Jiang, X. Lei, Z. Huang, M. Hong, B. Kang,
D. Wu and H. Liu,
J. Chem. Soc. Chem. Commun. 1655, (1990)

95 C.M. Bolinger, T.B. Rauchfuss and A.L. Rheingold,
J. Am. Chem. Soc., 105, (1983) 6321

96 R.C. Ryan, C.U. Pittman, J.P. Oconnor and L.F. Dahl,
J. Organomet. Chem., 193, 247 (1980)

97 T.D. Goldfarb and S. Sujishi,
J. Am. Chem. Soc., 86, (1964) 1679

98 G.M. Sheldrick, **SHELX-76**: Program for X-ray Crystal
Structure Determination; University of Cambridge:
Cambridge, England, (1976)
SHELXS-86: Program for Solving Crystal Structures;
University of Gottingen: Gottingen, West Germany, (1986)

99 R.C. Kerber and T. Pakkanen,
Inorganica Chimica Acta, 37, (1979) 61

100 G. Schmid and G. Etzrodt,
J. Organometal. Chem. 137, (1977) 367

101 G. Schmid, V. Batzel and B. Stutte,
J. Organomet. Chem. 113, (1976) 67

102 V. Batzel, U. Muller and R. Allmann,
J. Organomet. Chem. 102, (1975) 109

103 F. Klanberg, W.B. Askew and L.J. Guggenberger,
Inorg. Chem. 7 (1968) 2265

104 H. Vahrenkamp and E.J. Wacherer.
Angew. Chem. Int. Ed. Engl. 20 (1981), 680

105 R.D. Adams, J.E. Babin and M. Tasi.
Inorg. Chem. 25 (1986), 4514

106 P. Mather, J. Mavunkal, V. Rugmini and M.F. Mahon,
Inorg. Chem., 29, 4838 (1990)

107 P. Mather, B.H.S. Thimmappa and A.L. Rheingold,
Inorg. Chem., 29, 4658 (1990)

108 M.B. Hall and A.A. Low,
Polyhedron, Vol 8, 1885 (1989)

109 W.A. Herrmann,
Angew. Chem. Int. Ed. Engl, 25 (1986), 56

110 R. Boese and G. Schmid,
J. Chem. Soc. (Chem. Comm.), (1979), 349

111 M. Service, PhD Thesis, University of Waikato (1988)

112 V.G. Albano, P. Chini, G. Ciani, S. Martinengo
and M. Sansoni,
J. Chem. Soc. (Dalton Trans). (1978), 463

113 J. Vidal,
Inorg. Chem. 20, (1981) 243, and references therein.

114 H.J. Haupt, A. Gotze and U. Florke,
Z. Anorg. Allg. Chem. (1988) 557, 82

115 H.J. Haupt and U. Florke,
Acta. Crystallogr. (1988) C44, 472

116 A.D. Norman, J.R. Webster and W.L. Jolly,
Inorganic Syntheses, Vol 11 (1968) 170

117 S. Martinengo, D. Strumolo, P. Chini, V.G. Albano and
D. Braga,
J. Chem. Soc. Dalton. Trans. (1985) 35

118 P. Skinner, M.W. Howard, I.A. Oxton, S.F.A. Kettle,
D.B. Powell and N. Sheppard,
J. Chem. Soc. Faraday Trans. 2 77, (1981) 1203

119 S.G. Anema, S.K. Lee, K.M. Mackay, L.C. McLeod,
B.K. Nicholson and M. Service,
J. Chem. Soc. Dalton Trans. (1991)

120 S. Anema, M.Sc Thesis, University of Waikato (1986)

121 G. Bor,
J. Organomet. Chem. 94, (1975) 181

122 P. Gusbeth and H. Vahrenkamp,
J. Organometal. Chem. 247, (1983) C53

123 S. Cradock,
Inorganic Syntheses, Vol 15 (1974) 161

124 J.E. Drake, B.M. Glavincevski, R.T. Hemmings and
H.E. Henderson,
Inorganic Syntheses, Vol 19 (1979) 268

125 J.E. Drake, B.M. Glavincevski, R.T. Hemmings and
H.E. Henderson,
Inorganic Syntheses, Vol 19 (1979) 274

126 J.E. Drake, B.M. Glavincevski, R.T. Hemmings and
H.E. Henderson,
Inorganic Syntheses, Vol 20 (1980) 176

127 E. Hengge, H. Keller-Rudek, D. Koschel, U. Kruerke and
P. Merlet,
"Silicon"
Gmelin Handbook of Inorganic Chemistry, Vol B1 (1982)

128 G. Brauer,
Handbuch der Praparativen Chemie,
Vol 2, Enke, Stuttgart (1978) 160

129 C. Glidewell,
J. Chem. Soc. A. (1971) 823

130 W.C. Schumb and D.W. Robinson,
J. Am. Chem. Soc. 77 (1955) 5294

131 H. Burger,
Angew. Chem. Internat. Edit. 12, (1973) 474

132 A. Almenningen, K. Hedberg and R. Seip,
Acta Chem. Scand. 17, (1963) 2264

133 A. Almenningen, O. Bastiansen, V. Ewing, K. Hedberg and
M. Traetteberg,
Acta Chem. Scand. 17, (1963) 2455

134 C. Glidewell, D.W.H. Rankin, A.G. Robiette,
G.M. Sheldrick, B. Beagley and S. Cradock,
J. Chem. Soc. A. (1970) 315

135 W. Saak and S. Pohl,
Z. Anorg. Allg. Chem. 552, (1987) 186

136 J. Strouse, S.W. Layten and C.E. Strouse,
J. Am. Chem. Soc. 99, (1977) 562

137 M.J. Barrow, E.A.V. Ebsworth and M.M. Harding,
Acta. Cryst. B. 35 (1979) 2093

138 H. Burger,
Fortschr. Chem. Forsch. 9 (1967) 1

139 N. Wiberg, H. Schuster, A. Simon and K. Peters,
Angew. Chem. Int. Ed. Engl. 25 (1986) No1

140 H. Vahrenkamp and D. Wolters,
J. Organomet. Chem. 224 (1982) C17

141 R. Ball, M.J. Bennett, E.H. Brooks, W.A.G. Graham,
J. Hoyano and S.M. Illingworth,
Chem. Comm. (1970) 592

142 M. Don, M.G. Richmond, W.H. Watson and A. Nagl,
Acta Cryst. (1991) C47, 93

143 R.C. Ryan, C.U. Pittman, J.P. O'Conner and L.F. Dahl,
J. Organomet. Chem. 193 (1980), 247

144 H. Vahrenkamp and D. Wolters,
Organometallic. 1 (1982), 874

145 M.G. Richmond and J.K. Kochi,
Inorg. Chem. 25 (1986) 656

146 M.G. Richmond and J.K. Kochi,
Inorg. Chem. 25 (1986) 1334

147 W. Wojnowski, K. Peters, E.M. Peters and
H.G. von Schnering,
Z. Anorg. Allg. Chem. 525 (1985) 121

148 W. Wojnowski, W. Bochenska K. Peters, E.M. Peters and
H.G. von Schnering,
Z. Anorg. Allg. Chem. 533 (1986) 165

149 W.E. von Schklower, Y.T Strutschkow, L.E. Guselnikow,
W.W. Wolkowa and W.G. Awakyan,
Z. Anorg. Allg. Chem. 501 (1983) 153

150 C. Eaborn, P.B. Hitchcock, P.D. Lickiss and A.D. Taylor,
J. Organomet. Chem. 398 (1990) 59

151 C.H. Wei,
Inorg. Chem. Vol 8 (1969) 2384

152 V.G. Albano, D. Braga and S. Martinengo,
J. Chem. Soc. (Dalton Trans). (1986) 981

153 E. Lukevics, O. Pudova and R. Sturkovich,
"Molecular Structure of Organosilicon Compounds",
Ellis Horwood, Chichester, (1989)

154 K. Suwinska, G.J. Palenik and R. Gerdil,
Acta Crystallogr. 42C (1986) 615

155 T.A. Albright, K.A. Yee, J. Saillard, S. Kahlal,
J. Halet, J.S. Leigh and K.H. Whitmire,
Inorg. Chem. 30 (1991) 1179